PROTEINS AT INTERFACES

THE ADSORPTION OF HUMAN PLASMA ALBUMIN AND BOVINE PANCREAS RIBONUCLEASE ON POLYSTYRENE LATICES

W. NORDE

577.112:541.183

W. NORDE

PROTEINS AT INTERFACES

THE ADSORPTION OF HUMAN PLASMA ALBUMIN AND BOVINE PANCREAS RIBONUCLEASE ON POLYSTYRENE LATICES

(with a summary in Dutch)

PROEFSCHRIFT

TER VERKRIJGING VAN DE GRAAD
VAN DOCTOR IN DE LANDBOUWWETENSCHAPPEN
OP GEZAG VAN DE RECTOR MAGNIFICUS,
DR. IR. J. P. H. VAN DER WANT,
HOOGLERAAR IN DE VIROLOGIE,
IN HET OPENBAAR TE VERDEDIGEN
OP WOENSDAG 6 OKTOBER 1976
DES NAMIDDAGS TE VIER UUR
IN DE AULA
VAN DE LANDBOUWHOGESCHOOL TE WAGENINGEN

H. VEENMAN & ZONEN B.V.–WAGENINGEN – 1976

STELLINGEN

1.

De mate waarin een vanuit een oplossing adsorberend eiwitmolekuul zijn struktuur wijzigt, hangt veeleer af van de eigenschappen met betrekking tot zijn struktuur in die oplossing dan van de eigenschappen van het adsorbens.

Dit proefschrift, hoofdstukken 3, 4 en 6.

2.

Bij de adsorptie van eiwitten vanuit oplossingen vervullen de in de oplossing aanwezige ionen een belangrijke, doch door vele onderzoekers onvoldoende onderkende rol.

Dit proefschrift, hoofdstukken 3, 5 en 6.

3.

De specifieke komponent van de adsorptie vrije enthalpie van anionen is in het algemeen groter dan die van kationen. Op grond hiervan kan verklaard worden dat, in geval van adsorptie van ambivalente polyelektrolyten (bijvoorbeeld eiwitten), zelfs aan negatief geladen adsorbentia, de affiniteit van het adsorbens voor de anionogene groepen veelal groter is dan voor de kationogene groepen.

Dit proefschrift, hoofdstuk 5.

4.

De adsorptie van menselijk bloedplasma-albumine en van runderpancreasribonuclease vanuit hun waterige oplossingen aan negatief geladen polystreenoppervlakken wordt, onder zeer uiteenlopende omstandigheden, gedreven door entropietoename. Deze entropiewinst moet deels worden toegeschreven aan dehydratatie van het polystyreenoppervlak en deels aan dehydratatie van en/of struktuurveranderingen in de adsorberende eiwitmolekulen.

Dit proefschrift, hoofdstuk 6.

5.

De experimentele gegevens betreffende de dikte van geadsorbeerde lagen van runderserum-albumine aan silica, in kombinatie met die betreffende de geadsorbeerde hoeveelheden, gerapporteerd door MORRISSEY en STROMBERG, zijn niet in overeenstemming met hun uitspraken over de struktuur van de geadsorbeerde eiwitmolekulen.

B. W. MORRISSEY en R. R. STROMBERG,
J. Colloid Interface Sci. **46** 152–164 (1974)

6.

Het verdient aanbeveling om, in het onderzoek naar het mechanisme van de Ca^{2+} afhankelijke enzymatische degradatie van polyuronaten, zoals polygalacturonaat, niet *poly-* maar *oligo*-uronaten als substraat te kiezen.

R. KOHN,
Pure and Appl. Chem. **42** 371–397 (1975)

7.

De gegevens van SCHUFLE, CHIN-TSUNG HUANG en DROST-HANSEN met betrekking tot het elektrisch geleidingsvermogen van elektrolytoplossingen in glaskapillairen tonen aan dat hun meetresultaten niet op de juiste wijze verwerkt zijn. Om deze reden, maar ook vanwege enkele aanvechtbare en in hun interpretatie inkonsistente vooronderstellingen moet weinig waarde worden gehecht aan de door hen voorgestelde dikte van de gestruktureerde waterlaag.

J. A. SCHUFLE, CHIN-TSUNG HUANG en W. DROST-HANSEN,
J. Colloid Interface Sci. **54** 184–202 (1976)

8.

In het door JACROT, PFEIFFER en WITZ voorgestelde model voor het Bromegrass Mosaic Virus, dat gebruikt wordt ter beschrijving van pH- en temperatuurgeïnduceerde konformatieveranderingen van dit virus, komen mogelijke variaties in de struktuur van het virus-eiwit onvoldoende tot uiting.

B. JACROT, P. PFEIFFER en J. WITZ,
Symposium 'The assembly of regular viruses',
The Royal Society, London (1975)

P. PFEIFFER en L. HIRTH,
FEBS Letters **56** 144–148 (1975)

9.

In het licht van de resultaten verkregen door ZOLTEWICZ, OESTREICH en SALE met betrekking tot de dehalogenering van hetarylhalogenides met methoxide in methanol, is te verwachten dat bij de door BREDERECK, GOMPPER en HERLINGER gerapporteerde omzetting van 5-broompyrimidine in 5-methoxypyrimidine ook pyrimidine gevormd zal worden.

H. BREDERECK, R. GOMPPER en H. HERLINGER,
Chem. Ber. **91** 2832–2849 (1958)

J. A. ZOLTEWICZ, T. M. OESTREICH en A. A. SALE,
J. Amer. Chem. Soc. **97** 5889–5896 (1975)

10.

Op het terrein van de internationale wetgeving met betrekking tot additieven en contaminanten in levensmiddelen, bestaat er in vele gevallen een diskrepantie tussen de konsumentenbelangen enerzijds en de ekonomische belangen van ontwikkelingslanden anderzijds.

W. NORDE
Wageningen, 6 oktober 1976

VOORWOORD

Het verschijnen van dit proefschrift schenkt mij, na een aantal jaren wetenschappelijk werk, veel voldoening.

Bij deze gelegenheid zou ik willen benadrukken dat het voltooien van het promotieonderzoek, en daarmee de officiële afronding van mijn wetenschappelijke opleiding, slechts gerealiseerd kon worden dankzij de direkte of indirekte bijdrage van velen.

In de eerste plaats zijn daar mijn ouders die mijn opleiding mogelijk maakten en mij de vrijheid boden een onbezorgde studie en studietijd te beleven. Mijn dank aan jullie, vader en moeder, is groot.

De studiemogelijkheden aan de Landbouwhogeschool vormden een goede voedingsbodem voor mijn belangstelling voor de chemisch-biologische disciplines. Voor uw stimulerende invloed ben ik u, hoogleraren, lectoren en docenten van de Landbouwhogeschool, zeer erkentelijk.

Dat ik het in dit proefschrift beschreven onderzoek kon uitvoeren in het Laboratorium voor Fysische en Kolloidchemie beschouw ik als een gelukkige omstandigheid. Immers, de goede sfeer op deze afdeling schept een klimaat waarin op ontspannen wijze gewerkt en samengewerkt kan worden.

Hans Lyklema, door jouw heldere overdracht van de kennis der kolloidchemie is de fasegrens voor mij een boeiend schouwtoneel geworden. Ik voel het als een voorrecht onder jouw bezielende en kreatieve begeleiding mijn wetenschappelijk werk te mogen doen. Jouw betrokkenheid bij mijn bezigheden heb ik als veel meer dan dat van een promotor ervaren, vooral ook vanwege je belangstelling voor de mens achter de wetenschapper. Hiervoor, Hans, wens ik mijn dank en waardering uit te spreken.

Tijdens zijn verblijf als gastmedewerker heeft Kunio Furusawa een belangrijk aandeel in het onderzoek gehad. Dear Kunio, I remember our cooperation as valuable and pleasant. I am much indebted to you, especially for your advice regarding the production of well-defined polystyrene latices.

Joekje Eikelboom-Akkerman dank ik voor de nauwgezette assistentie bij een deel van de experimenten. Ook de studenten, die in het kader van hun ingenieursstudie aan het onderzoek hebben bijgedragen, ben ik zeer erkentelijk.

Brian Vincent, ik dank je voor de korrektie van de Engelse tekst en ook voor de opmerkingen van meer inhoudelijke aard, die je maakte als vriend en confrater in de kolloidchemie.

Bij het persklaar maken van het manuscript werd de zeer gewaardeerde medewerking ondervonden van Marian Heitkamp-Rijckaert, Henny van Beek en Simon Maasland, die op accurate wijze respektievelijk het type-, teken- en fotowerk voor hun rekening hebben genomen.

Tenslotte spreek ik de hoop uit dat de in dit proefschrift neergelegde bevindingen zullen bijdragen tot een betere kennis van het gedrag van eiwitten aan grensvlakken en dat de eventuele praktische relevantie van die kennis zich zal beperken tot zinvolle toepassingen.

ABBREVIATIONS

i.e.p.	isoelectric point
i.i.p.	isoionic point
L-A	liquid-air
L-L	liquid-liquid
PA	plasma albumin
	BPA bovine PA
	HPA human PA
PGA	polyglutamic acid
PL	polylysine
PS	polystyrene
RNase	ribonuclease
S-L	solid-liquid

superscripts:

ads	adsorbed state
protein ads	adsorbed protein layer
PS	polystyrene particle
PS/protein	protein covered polystyrene particle
sol	dissolved state

subscripts:

ads	adsorption
cd	charge distribution
dehydr PS	dehydration of the hydrophobic parts of the polystyrene surface
el	electrostatic
ion med	ionic medium effect
int	intrinsic
max	maximum
med	medium
prot	protonation
str pr	protein structure
titr	titration
vdW	van der Waals interaction

CONTENTS

1. INTRODUCTION

1.1. PROTEINS AT INTERFACES

Proteins in solution interact with almost any interface.

In nature, interactions between proteins and interfaces are of great importance. Already in the prebiotic stage of the genesis of terrestrial life accumulation of proteins (or protenoids) at interfaces may have played an essential role (OPARIN, 1964; FOX and DOSE, 1972). Also, in all the biological systems that have evolved since, interactions between proteins and interfaces have been widespread.

The most common and the most important biological interfaces that are known to contain physiologically active proteins are the biological membranes (i.e. the membranes of living cells and sub-cellular particles such as nuclei, mitochondria, chloroplasts, etc.). For example, glyco-proteins on the cell wall participate in controlling cellular aggregation (PESSAC and DEFENDI, 1972) and cellular growth (SCHNEBLI and BURGER, 1972); proteins of the reticulo-endothelial system are likely to be involved in phagocytosis (WILKINS, 1967); the cytochrome enzyme system for oxidative phosphorylation is bound to the mitochondrion membrane (GREEN and YOUNG, 1971) and membrane proteins of chloroplasts have been shown to mediate in energy transfer processes during photosynthesis (SYBESMA and VREDENBERG, 1963; 1964; ANDERSON, 1975).

The chemical structure of biological membranes is very complex. According to the classical Danielli-model (DANIELLI and DAVSON, 1935), biological membranes consist of an inner lipid layer on either side of which a layer of extrinsic proteins is attached. However, structures in which proteins are to some extent embedded in the lipid matrix have also been proposed (SINGER, 1971; SINGER and NICHOLSON, 1974). It may even be true that the ability of a membrane to alter its structure as needs be is essential for its different physiological functions (WOLMAN, 1970).

The biological importance of the adsorption of proteins at naturally occurring interfaces is further illustrated by the following examples.

It is now generally accepted that intravascular thrombosis is an interfacial process. It has been suggested that adsorption of proteins at the blood vessel wall facilitates the adhesion of platelets during thrombogenesis (see e.g. SALZMAN, 1971; STONER and SRINIVASAN, 1970).

Pancreatic lipases and phospholipases control the digestion of alimentary fats in the duodenum. Generally, these fats are insoluble in water; they are present as emulsified globules. Before the dissolved enzymes can exert their action they have to adsorb at the surface of these fatty globules (DESNUELLE, 1972).

In soil systems, the activity of extra-cellular enzymes may be altered as a result of their adsorption on clay particles (see e.g. KOBAYASHI and AOMINE,

1967). Hence, the microbial life in the soil may be affected by such adsorption processes. In addition, if this adsorption occurs irreversibly, the availability of proteins as a substrate for microorganisms decreases.

In a number of instances, when human intelligence endeavours to control nature, biological substances are brought into contact with non-biological substances. More specifically, any adsorption of proteins at non-biological interfaces may have significant consequences.

Various proteins may be used as emulsifiers and/or stabilizers in colloidal dispersions (see e.g. GRAHAM and PHILLIPS, 1974; 1975). Thus, proteins are often essential ingredients in sprays, cosmetics, pharmaceutics, food-stuffs and many other industrial products.

In biochemistry, adsorption of proteins to solid materials can be helpful in purification procedures (NISHIKAWA, 1975).

In various industrial and clinical procedures it is economically efficient to use enzymes that are insolubilized by attachment to a solid matrix (MOSBACH, 1971).

In serological tests immuno-proteins, adsorbed on solid particles, are used to improve the observation of agglutination after the addition of suitable antibodies. For example, a well-known standard procedure for the detection of rheumatoid factors in human serum involves the use of polystyrene coated with human γ-globulin (SINGER, 1961; 1974).

Finally, with the increasing use of synthetic biomedical materials as prostheses in, especially, cardiovascular surgery it is of vital importance to know how to control the interactions between serum proteins and these materials (see e.g. BRASH and LYMAN, 1971).

In view of the structure-function relation of proteins, in most, if not all, of the examples mentioned above, the question as to the three-dimensional structure of proteins at interfaces is of prime interest. Unfortunately, only a very limited number of techniques are available for the direct study of the structure of interfacial proteins in situ.

The structure (conformation) of a protein molecule is the net result of intramolecular interactions and interactions between the protein molecule and its environment. Therefore, it is reasonable to assume that the structure of proteins at interfaces may be different from that in bulk solution. Hence, structural perturbations in protein molecules may occur as a result of adsorption.

In studying the adsorption of proteins, it has to be realized that adsorption from solution is always a competitive process. When protein molecules adsorb, solvent (water) molecules and possibly other components (e.g. ions) must be displaced. In general, the interplay between all components in the system determines the mode of interaction between the protein and the interface and, consequently, the structure of the protein in the adsorbed layer.

A general discussion on the adsorption of proteins, especially in relation to their properties in solution, will be given in chapter 3.

1.2. Objectives of the present study

As illustrated above, the occurrence of proteins at interfaces is of great biological, medical and technological significance. Adsorption of proteins is also of considerable theoretical interest, e.g. a study of the structural changes in an adsorbed protein molecule may help in understanding the factors determining its structure in solution. For these reasons, proteins at interfaces have been the subject of a large number of studies.

On surveying the literature, it appears that the mechanism of protein adsorption is far from resolved. Indeed, because of the specific structure in aqueous solution of proteins, it is difficult to establish any principles governing protein adsorption. Moreover, the fact that many studies have been carried out with insufficiently defined systems has contributed to the confusion that exists regarding the interfacial behaviour of proteins.

The aim of the present study is, therefore, to gain more insight in the mechanism of the adsorption from solution of proteins at charged solid surfaces. To this end, special attention was paid to the characterization of all the components. In order to keep the system as simple as possible, the use of buffers was avoided. Thus, in adjusting the ionic strength only one kind of electrolyte, i.e. KNO_3, was used.

As it is recognized that the overall adsorption process has many facets, the problem was approached from various directions, that is, several parameters were investigated simultaneously, using various techniques.

The first part of this study was concerned with the preparation and characterization of well-defined interfaces. For this purpose negatively charged polystyrene latices were chosen. The density of charged groups at the polystyrene surface is considered to be fixed. The preparation procedure allows control of the charge density and, hence, the hydrophobicity of the polystyrene surface (Furusawa et al, 1972).

Human plasma albumin (HPA) and bovine pancreas ribonuclease (RNase) were chosen as the proteins to be adsorbed. These proteins are known to differ considerably with regard to their conformational stability in aqueous solution. The internal coherence in dissolved HPA molecules is much less than in dissolved RNase molecules (Tanford, 1967). Therefore, perturbation of the protein structure upon adsorption is more likely with HPA than with RNase.

The adsorption process was studied by determining the adsorption isotherms, by performing hydrogen ion titrations and electrophoretic measurements and by measuring enthalpies of adsorption. The electrostatic contributions to the interactions may be elucidated by varying the charge on the polystyrene surface and on the protein molecules and by varying the ionic strength of the medium. Entropic contributions accompanying, for example, the hydrophobic interactions may be revealed by varying the temperature.

Thus, an attempt was made to estimate the relative importance of each of the factors governing the adsorption from solution of HPA and RNase on negatively charged polystyrene surfaces.

2. POLYSTYRENE LATICES

2.1. INTRODUCTION

2.1.1. *General*

A dispersion of polymer particles in a liquid is referred to as a latex. These systems have found a large field of application. In industry, for example, they are used as fillers in paper and textiles and as film-forming material in emulsion paints. Moreover, latices also serve many scientific goals, such as

(a) the calibration of various instruments, e.g. ultracentrifuge, light scattering instruments and electron microscope.
(b) the determination of pore size of (biological) membranes and filters.
(c) serologic diagnostic tests, e.g. of rheumatoid arthritis and human pregnancy.
(d) stimulation of antibody production and purification of antibodies.
(e) studies of the reticulo – endothelial system.
(f) they are used as a model system in colloidal and adsorption studies.

With respect to these scientific applications monodispersity of the latex is generally desired and for colloidal investigations additional knowledge of its surface properties is required.

Aqueous polystyrene latices are usually prepared by emulsion or dispersion polymerization of styrene. The polymerization proceeds according to a free radical mechanism with the subsequent steps: decomposition of the initiator into free radicals, formation of a styrene monomer radical, growth of the polystyrene chain and chain transfer to different components in the system, termination of the polymerization either by combination or disproportionation.

2.1.2. *The mechanism of emulsion polymerization*

The starting materials in the preparation of polystyrene latices consist of styrene monomer, water, free radical initiator and usually one or more emulsifiers the concentrations of which are beyond their critical micelle concentrations.

The theory of emulsion polymerization has been extensively discussed by various authors (HARKINS, 1947; SMITH and EWART, 1948; BOVEY et al, 1955; FLORY, 1953, Ch. V; VAN DER HOFF, 1962; ALEXANDER and NAPPER, 1971). For styrene, the mechanism of emulsion polymerization postulated by HARKINS (1947) and evaluated quantitatively by SMITH and EWART (1948) is still accepted, although some aspects have been questioned (see e.g. VAN DER HOFF, 1967; ROE and BRASS, 1957 and ROE, 1968). According to this mechanism, in an agitated mixture of water, styrene monomer and emulsifier, the emulsifier is simultaneously present in three different states: (i) aggregated in micelles, (ii) molecularly dissolved in the aqueous phase and (iii) adsorbed at the water-styrene interface. The styrene monomer is also present at three loci: (i) in droplets emulsified in the aqueous phase, (ii) dissolved in the aqueous phase

and (iii) solubilized in the apolar interior of the emulsifier micelles. Most of the emulsifier and the monomer are present in the micelles and the droplets, respectively. The number of monomer droplets is many orders of magnitude less than the number of micelles in the system, so that the water-droplet area is negligibly small as compared to the micelle-water interface. Addition of a water-soluble initiator leads to the formation of free radicals in the aqueous phase, usually by decomposition. The rate of decomposition is enhanced by increasing the temperature. These radicals have no tendency to adsorb at the styrene-water interface nor to penetrate into the micelles. This applies especially if the radicals are negatively charged and the micelles are of an anionic emulsifier. Some of the radicals react with dissolved styrene monomer to form monomeric radicals and the polymerization continues in the aqueous phase until the oligostyrene radicals have become sufficiently surface active to enter the micelles. The oligomeric radicals are preferentially oriented with their polar end groups towards the aqueous phase. The hydrophobic end of the radical is in the interior of the micelle. It is here that the polymerization is propagated by the subsequent addition of styrene monomers. Thus, those micelles, containing an oligomer radical become growing polymer particles, stabilized by the polar end groups and by the emulsifying agent now adsorbed at the particle surface. The monomer consumed during the propagation is supplied by diffusion from the droplets via the aqueous phase to the polymerizing particles. The micelles that did not capture radicals disappear to furnish emulsifier for the stabilization of the growing polymer particles. The disappearance of the micelles, either by becoming polymer particles or by break-up, corresponds to the termination of the nucleation stage. The particle growth continues until the supply of radicals and/or monomer is exhausted. In order to obtain a monodispers latex, the nucleation stage must be short enough to minimize overlap of the nucleation stage with the growth stage, even though the particle size distribution narrows during the latter stage (VAN DER HOFF et al, 1956).

Although it has been usual in the past to use emulsifier in emulsion polymerization, its presence is not indispensable for the formation of polymer particles. If polymerization takes place in the absence of emulsifier, the styrene monomer is initially present at two loci: (i) dissolved in the aqueous phase and (ii) in droplets. The oligomeric radicals formed in the aqueous phase, at a critical chain length and concentration, will form aggregates in an analogous way to the micelles formed by soap molecules. Nuclei are thus formed in which the polymerization then proceeds in a similar way to that described above. Owing to the absence of added emulsifier, the growing polymer particles are only stabilized by the ionic end groups originating from the initiator. Since the nuclei contain a small number of chains, their surface charge densities are low. Because of this and their small size, some coalescence is likely to occur. Hence, the coagulation stage is important in controlling the particle size. According to GOODWIN et al (1973), polymerization in a medium of higher ionic strength leads to larger particles. The lower rate of polymerization as compared with

polymerization in the presence of added emulsifier, can be explained by this coalescence (DUNN, 1971). Although it has been stated by HARKINS (1952) that in the absence of emulsifier the latex will have a high degree of heterodispersity, KOTERA et al (1970a) described a method to prepare stable, monodisperse polystyrene latices without adding any emulsifying agent. Obviously, such 'clean' latices are particularly attractive as model substances.

2.1.3. *The polystyrene-water interface*

After completion of the polymerization, the aqueous phase of the latex may contain residual initiator, styrene monomer, emulsifier if any, and buffer compounds. Emulsifier and non-polymerized styrene are expected to be also adsorbed on the particle surface. If the latex is to be used as an adsorbent, these impurities should be removed from the particles in order to render the surface clean and well-defined.

The aqueous phase can be freed from its low-molecular weight solutes by dialysis. However, many investigators were unable to desorb detergent molecules completely from the particle surface, even by prolonged dialysis (e.g. FRYLING, 1963; BRODNYAN and KELLEY, 1965; FOREL et al, 1968). Only OTTEWILL and SHAW (1967a) have evidence for the complete removal of emulsifier from the particle by dialysis. VAN DEN HUL and VANDERHOFF (1968) applied an ion exchange technique to remove all ionic components from the surface. To avoid contamination of the latex by impurities from the ion exchange resins, the resins must be extensively purified, prior to use. However, even if no impurities can be extracted from the resins by rinsing with water, the absence of contamination of the particles by the resins is not fully guaranteed.

In latices prepared without emulsifier, only oligomers may be physically adsorbed at the particle surface (FURUSAWA et al, 1972). Since there is, in principle, no difference in the chemical constitution of an oligomer and a polymer of styrene, such oligomers are not considered as being 'foreign' material. In other words, their presence on the polystyrene surface is not regarded as contamination.

In the absence of other ionic substances, the latex surface charge stems from the ionic end groups of the polystyrene and oligostyrene molecules. The nature of these ionic end groups depends on the initiator used. The most common initiator is potassium persulphate, $K_2S_2O_8$. Sulphate radicals are formed, according to: $S_2O_8^{2-} \rightarrow 2\ SO_4^{\cdot-}$, leading to sulphate, $-OSO_4^-$, end groups. However, hydroxyl radicals can also be generated as has been shown by KOLTHOFF and MILLER (1951): $SO_4^{\cdot-} + H_2O \rightarrow HO\cdot + H^+ + SO_4^{2-}$. As these hydroxyl radicals presumably act similarly to the sulphate radicals in the polymerization process, this would result in hydroxyl end groups. If oxygen or an oxidizing agent is present in the reaction vessel the hydroxyl groups may be converted into carboxyl groups. The generation of hydroxyl groups by this so-called Kolthoff reaction is cooperative because it is favoured by lowering the pH (PALIT and MANDAL, 1968). The consequence of all of this is that, if no particular precautions are taken, the particle surface would be covered with

sulphate, hydroxyl and carboxyl groups.

In persulphate initiated polystyrene latices, prepared at 70°C under the exclusion of oxygen, VAN DEN HUL and VANDERHOFF (1970) showed that the latex surface charge is completely accounted for by strong acid groups. The same authors, as well as GHOSH et al (1964), determined the sum of the numbers of sulphate and hydroxyl end groups per polymer chain in the particles. For latices prepared in the pH region 2–8 the values for this total number did not differ significantly from two. The sulphate to hydroxyl ratio is very sensitive to pH, being maximal at neutral pH values. This indicates that reactions causing hydrophobic end groups, e.g. spontaneous thermal initiation via the Diels-Alder mechanism (MAYO, 1960), chain transfer and termination by disproportionation, occur at a relatively negligible rate in the polymerization process. The saturation concentration of molecularly dissolved styrene in the aqueous phase has been calculated to be about 4.6×10^{-3} M at 70°C (BOVEY and KOLTHOFF, 1950). Thus, from the values of the rate constants of the various reactions, given by MAYO (1968) and by VAN DER HOFF (1960), it can be deduced that thermal initiation and chain transfer reactions contribute only slightly to the end group formation, provided that not too low initiator concentrations are used. In addition, there is experimental evidence that termination occurs by combination rather than by disproportionation (see e.g. MAYO et al, 1951; OVERBERGER and FINESTONE, 1956).

Based on the mechanism of emulsion polymerization a higher $K_2S_2O_8$ concentration would result in shorter polystyrene chains. Hence, at constant particle size, the number of hydrophilic surface groups is expected to increase with the $K_2S_2O_8$ concentration. The degree of hydrophobicity of the latex surface may have far reaching consequences for the structure of the vicinal water. There appears to be evidence that hydrophobic as well as hydrophilic surfaces influence the structure of water in the layers adjacent to the interface.

Hydrogen bonding between the water molecules as well as dipolar interactions seem to govern the structure of liquid water in bulk. Based on these interactions different theories regarding the structure of liquid water have been postulated, the two main ones being the 'flickering cluster' theory and the 'network' theory (EISENBERG and KAUZMAN, 1969).

In the flickering cluster theory, hydrogen bonded water molecules are thought to form clusters of varying size in equilibrium with non-hydrogen bonded water molecules. Between these latter molecules there will still be dipole-dipole interactions (NÉMETHY and SCHERAGA, 1962a). It is assumed that the whole system is in dynamic equilibrium. The average lifetime of a molecule in a cluster is of the order of 10^{-11} seconds. Hence, the structure of liquid water can be considered as a continuous distribution of all possible cluster sizes in equilibrium. Based on this model HAGLER et al (1972) calculated an average cluster size of 11.2 molecules at 0°C in pure water.

In the network theory the structure is described in terms of an irregular network of water molecules interconnected by hydrogen bonds (BERNAL and FOWLER, 1933; POPLE, 1951). It is assumed that not all the possibilities for

hydrogen bond formation are utilized and that a continuous rearrangement of the hydrogen bonds takes place.

Hydrophilic surfaces are believed to favour the dipole-dipole interactions in the vicinal water (DROST-HANSEN, 1969). On the other hand, hydrophobic surfaces promote hydrogen bonding between the water molecules in the layers adjacent to the surface (DROST-HANSEN, 1969; NÉMETHY and SCHERAGA, 1962b). Thus, in terms of the cluster theory and the network theory, respectively, hydrophobic surfaces promote cluster formation or induce a stronger network in the vicinal water, whereas the opposite effect is caused by hydrophilic surfaces.

It will be clear that the density of the polar groups on the polystyrene surface, which is otherwise hydrophobic, may affect the structure of the vicinal water considerably. In addition, the counterions, especially those that are specifically adsorbed, contribute to the vicinal water structure.

Around ions and presumably also charged surface groups, three regions of water with different structure may be distinguished (FRANK and WEN, 1957): (i) an inner structure forming region of water molecules immobilized by polarization and electrostriction; (ii) an intermediate region in which the water molecules are more randomly organized than in bulk water and (iii) an outer region corresponding to bulk water. The net effect of an ion on the structure of the surrounding water depends very much on its charge and its radius. The inner region is the more extended the higher the electric field of the ion (i.e. the smaller the radius and the higher the charge). In the view of GURNEY (1953) there is a critical radius above which the electric field of the ion is too weak to have a net ordering effect (i.e. a net loss of entropy) on the surrounding water structure. Calculations by BERNAL and FOWLER (1933) reveal that for monovalent ions this critical radius is about 0.16 nm. Experimental results generally support the above considerations of ion-water interaction (see e.g. KAVANAU, 1964; HERTZ, 1970).

Needless to say, these features concerning the structure of water play an important role in the interfacial behaviour of biocolloids that possess themselves tertiary structures based on a delicate balance of among other things hydrophilic and hydrophobic interactions.

2.2. MATERIALS

The glassware used in this study was all Pyrex. It was cleaned thoroughly with chromic acid, diluted nitric acid and distilled water, consecutively. All chemicals used were of analytical grade. The water and the styrene monomer (Baker Chemicals N.V. – Deventer, the Netherlands) were vacuum-distilled, each from an all-Pyrex apparatus. $K_2S_2O_8$ (Baker Chemicals N.V.) was recrystallized from water and dried in a desiccator. All these procedures were carried out shortly before use. $K_2S_2O_8$ solutions of the desired concentrations were prepared immediately before use. $KHCO_3$ and KH_2PO_4, both from B.D.H. Ltd., were used without further purification.

2.3. EXPERIMENTAL

To ensure the entire absence of emulsifier on the latex surface and to avoid possible contamination of the surface due to a cleaning procedure with ion exchange resins (see section 2.1.3.), latices have been prepared using a modification of the method described by KOTERA et al (1970a). The modification concerns the way of agitation of the polymerizing system and the control of pH during the polymerization. The hydrodynamic conditions during the polymerization appear to be very important. In preliminary experiments it was shown that rotating the mixture results in more reproducible latices than is obtained by stirring. The negative surface charge of the latex is found to be considerably higher if the pH during polymerization is kept at neutral values, by adding $KHCO_3$ or KH_2PO_4 to the system (FURUSAWA et al, 1972). This probably results from a suppression of the Kolthoff reaction (see section 2.1.3.), i.e. an avoidance of the generation of hydroxyl radicals (cf. VAN DEN HUL and VANDERHOFF, 1970).

A number of experiments have been performed to characterize the latices with respect to their surface and electrical double layer properties.

Some latices (the L-series and C-3) have been prepared in duplicate or triplicate. Average values of their properties will be presented for these latices, since they seem to be reproducible.

2.3.1. *Preparation*

In a bottle of 250 cm^3 a mixture of 20 cm^3 styrene monomer and 175 cm^3 water or solutions of $KHCO_3$ and KH_2PO_4 in water were saturated with nitrogen at 70°C after which 5 cm^3 of a nitrogen-saturated $K_2S_2O_8$ solution was added. The bottles were glass-stoppered immediately, attached to a wheel rotating end over end with a speed of 40 r.p.m. in a waterbath thermostatted at 70°C. The polymerization was allowed to proceed over a period of at least 30 hours. The degree of conversion of styrene calculated from the dry weight content of the polystyrene latex and the initial weight percentage of styrene monomer, appeared to be always higher than 90%. Additional data on the polymerization conditions are given in table 2.1.

Some agglomerates, formed during the polymerization, were removed by filtering through Pyrex glass wool.

The latices, transferred to well-boiled Visking dialysis tubing, were dialyzed against water at a volume ratio of about 1:25, in order to remove low molecular weight substances. The dialysis was carried out at 40°C over a period of about 3 weeks, changing the water daily. Even so, after a period of one week, no increase in the conductivity of the dialysate could be detected.

2.3.2. *Particle size*

The dimensions of the latex particles were determined by electron microscopy. From the literature it is known that the average particle sizes obtained by electron microscopy are in good agreement with those from other methods, provided the particles are not exposed too long to the electron beam (LECLOUX

TABLE 2.1. Preparation of polystyrene latices.

sample	$c_{K_2S_2O_8} \times 10^4$ M	$c_{electrolyte} \times 10^2$ M	final pH	d_n nm	s $m^2\ g^{-1}$
L–1	3.10	–	3.4	494	11.6
L–2	12.40	–	2.9	513	11.1
L–3	21.70	–	2.5	501	11.4
		$KHCO_3$			
C–1	18.50	1.00	7.6	510	11.2
C–2	27.70	1.00	7.5	580	9.9
C–3	37.40	0.50	6.2	647	8.9
		KH_2PO_4			
P–1	29.30	0.50	7.4	650	8.7
P–2	36.90	0.50	7.8	600	9.6

et al, 1970; DAVIDSON and HALLER, 1973; COOKE and KERKER, 1973).

A drop of very diluted latex was allowed to evaporate on a poly (vinyl formal)-coated copper grid. Micrographs of at least three different areas of each grid were taken at magnifications of 26,300 or 33,300 using a Philips EM 300 electron microscope. All samples showed monodisperse spherical particles. An example of a micrograph is presented in figure 2.1. The micrographs were projected and at least 150 particles of each sample were sized. The diameters were calcuclated by comparison with the known dimensions of a carbon grating.

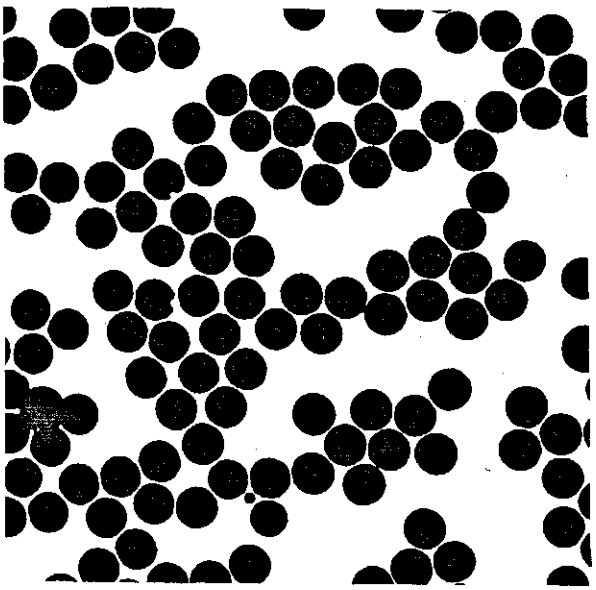

FIG. 2.1. Electron micrograph of polystyrene latex C-3.

The dispersity of the latex may be expressed through the uniformity coefficient U, defined as

$$U \equiv d_w/d_n \tag{2.1}$$

where d_w and d_n are the weight- and number-average particle diameter, respectively. d_w/d_n can be calculated from the individual particle diameters d_i, using

$$d_w/d_n = \{(\Sigma_i n_i d_i^6)/(\Sigma_i n_i d_i^3)\}^{1/3} / \{(\Sigma_i n_i d_i)/\Sigma_i n_i\} \quad (2.2.)$$

where n_i is the number of particles. For all the latices the size distributions are very narrow, with $U < 1.02$.

Because of the monodispersity, the specific surface area s (i.e. the surface area per gram polystyrene) may be calculated, using

$$s = 6/\rho d \quad (2.3.)$$

in which ρ is the density of polystyrene.

By means of pyknometry the densities of the polystyrene particles were found to be between 1.048 and 1.052 g cm^{-3}.

The experimental results of this section are summarized in the fifth and sixth column of table 2.1.

In accordance with the results of e.g. FURUSAWA et al (1972), GOODWIN et al (1973) and LAAKSONEN et al (1975) the presence of electrolyte in the polymerizing system leads to larger polystyrene particles.

No significant influence of the initiator concentration on the particle size can be observed; this is in distinction to the results obtained by KOTERA et al (1970a) and GOODWIN et al (1973). Both these authors agitated the polymerizing mixture by stirring. However, they report opposite effects of the initiator concentration on the particle size. This seems to support the importance of the rheological conditions during polymerization, mentioned earlier.

2.3.3. *Surface charge density and total sulphur content*

The negative surface charge of the latex particles originates from sulphate groups and possibly (although unlikely because of the N_2 atmosphere and, except for the L-series, the buffering) from carboxyl groups derived by oxidation of hydroxyl groups. If these acidic surface groups are neutralized with protons, they can be titrated with base. From the amount of base required to neutralize all the protons the number of negatively charged groups can be evaluated.

Samples of the latices have been treated with extensively purified Dowex ion exchange resins according to the method described by VAN DEN HUL and VANDERHOFF (1968). Thus, all charged surface groups were converted to the H^+ form. Every latex sample underwent this procedure three times; after each treatment about 100 cm^3 of the latex was titrated, under N_2, with diluted NaOH (2×10^{-3} or 10^{-2}M), both potentiometrically and conductometrically in the same titration vessel. The potentiometric measurements were performed with an Electrofact 36200 potentiometer using a glass electrode. The conductometric ones were carried out using a Philips conductivity meter PW 9501/01 equipped with a Philips conductivity cell PR 9515 (cell constant 0.02 cm^{-1}).

The equivalence points determined by both techniques were always very

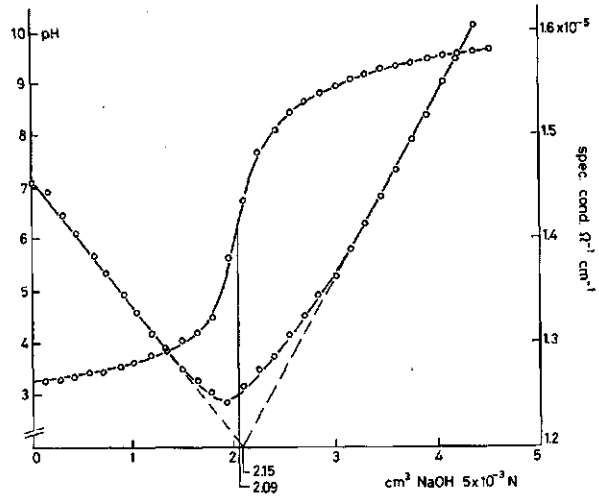

FIG. 2.2. Conductometric and potentiometric titration of latex C-3 after ion exchange.

close. By way of example the titration curves of latex C-3 are shown in figure 2.2. As can be judged from these curves, as well as from the titration curves of all the other latex samples, there is no indication for the occurrence of titratable groups other than strong acid ones. These groups certainly are $-OSO_3^-$ groups. A similar titration behaviour has been observed by VAN DEN HUL and VANDERHOFF (1970), who prepared their latex in N_2 atmosphere in rotating bottles too. However, GOODWIN et al (1973), STONE-MASUI and WATILLON (1975) and LAAKSONEN et al (1975) report the presence of surface carboxyl groups for latices that have been prepared in an N_2 atmosphere.

From the equivalence point, the titrated volume, the dry weight content and the specific surface area of the sample, the surface charge density, σ_0, is calculated. Its value after each of the three subsequent ion exchange treatments differed less than 5%, indicating attainment of complete exchange of the counter-ions of the latex. The results are presented in table 2.2.

To compare the number of $-OSO_3^-$ groups at the surface (i.e. titratable $-OSO_3^-$ groups) with the total number of $-OSO_3^-$ groups in the particles, the sulphur content of the latex was determined by X-ray fluorescence. Tablets were prepared from freeze-dried samples by compressing the material under a pressure of about 3×10^5 N m^{-2}. Measurements were made in duplicate for both sides of the tablets using a Philips 1130 X-ray fluorescence spectrometer. Polystyrene latices of known sulphur content and without sulphur were mixed in different proportions to obtain a calibration curve[1]. Data on the sulphur content are also given in table 2.2.

[1] Drs. H. J. van den Hul and J. W. Goodwin are kindly acknowledged for providing polystyrene latex samples with known sulphur content and sulphur free, respectively.

TABLE 2.2. Surface charge and sulphur content of the polystyrene latices.

sample	sulphur content % w/w × 10^2			σ_0 μC cm^{-2}		surface:bulk sulphur	
	before i.e.	(% recovery)	after i.e.	before i.e.	after i.e.	before i.e.	after i.e.
L–1	1.9	(77)	1.4	− 2.3	−1.0	0.45	0.27
L–2	3.4	(35)	2.5	− 4.6	−2.1	0.48	0.31
L–3	4.0	(23)	2.8	− 6.3	−3.0	0.57	0.39
C–1	9.0	(61)	7.5	− 8.4	−4.5	0.34	0.23
C–2	11.0	(52)	7.6	−17.2	−6.9	0.51	0.30
C–3	11.9	(40)	9.6	−15.5	−7.4	0.37	0.23
P–1	8.0	(34)	5.8	−15.7	−8.1	0.58	0.41
P–2	10.0	(34)	8.0	−15.0	−8.7	0.48	0.35

The recoveries of sulphur in the polystyrene, as percentages of sulphur added, are given in parentheses in the third column. Treatment of the latex with ion exchange resins causes losses of sulphur of up to 30%. It is assumed these losses are due to desorption of poly- and/or oligostyrene sulphates from the latex surface, which is more probable than removal from the interior of the particles. Hence, from the difference in sulphur content before and after ion exchange and from the titration data, the surface charge density before ion exchange can be found.

In each of the series the surface charge increases with the $S_2O_8^{2-}$ concentration. This is predicted from the mechanism of emulsion polymerization (see section 2.1.2.). Buffering the systems during polymerization leads to higher values of σ_0 (compare L-series with C- and P-series). As mentioned before, this is attributed to suppression of the Kolthoff reaction. The recoveries of sulphur values indicate that in the L-series relatively larger amounts of persulphate are lost through side-reactions or remain undissociated. Moreover, the pH decrease in the unbuffered L-series (see table 2.1.) points to the formation of sulphuric acid, as occurs in the Kolthoff reaction.

In view of the low surface volume: bulk volume ratio, the fractions of the total sulphur that are located at the surface are relatively high. This is an obvious consequence of the hydrophilic character of the sulphate groups.

2.3.4. *Number-average molecular weight of polystyrene molecules. Number of sulphate groups per polystyrene molecule*

The number-average molecular weight, M_n, of polystyrene molecules was determined in order to calculate the number of sulphate groups per polymer molecule. These experiments were restricted to non-ion exchanged latices of the L-series (no buffer added).

Freeze-dried samples of latices were dissolved in freshly distilled toluene after which the M_n value for the polymer molecules was determined by osmometry at 30°C. For each sample five or six dilutions were prepared in the concentration range 0.1–1.0% w/w. The osmotic rise, h, was measured, using

a Hallikainen automatic membrane osmometer, model 1361[1]. The membranes were of the type 'Ultracellar allerfeinst' (Sartorius). The osmotic pressure, Π,is calculated from the rise, according to

$$\Pi = hg/v_1 \tag{2.4.}$$

where g is the acceleration due to gravity and v_1 the specific volume of the solvent.

The relation between M_n and Π is given by

$$\Pi/RTc = 1/M_n + Bc + Cc^2 + \ldots\ldots \tag{2.5.}$$

where R is the gas constant, T the temperature in K, c the weight-concentration of solute (concentration in grams per unit volume), B and C the second and third virial coefficient, respectively.

Plots of h/c versus c are shown in figure 2.3. From these curves M_n and B are estimated; their values are collected in table 2.3.

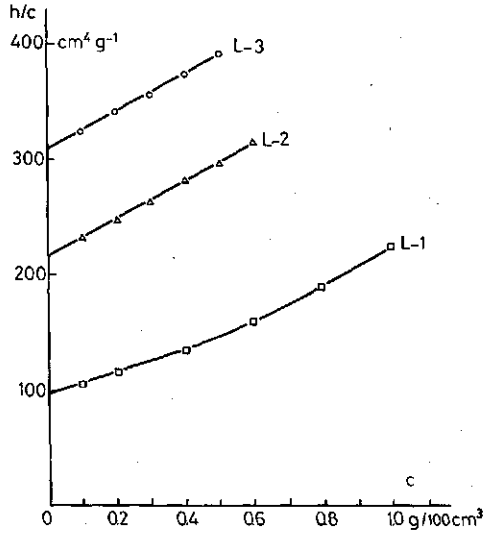

FIG. 2.3. Osmometric data for solutions of polystyrene (L-series) in toluene. $T = 30°C$.

If oligomers were present in the non-ion exchanged latex particles, then account should be taken of possible errors resulting from the transport of these relatively low molecular weight materials through the membrane. Thus, if the difference in surface charge before and after ion exchange were completely due to oligomers that, during the osmosis experiment, all permeate through the membrane and if the contribution of these oligomers to the mass of the particle

[1] The osmometric measurements were carried out in the Laboratory for Material Research, Technical University Twente, The Netherlands. The technical assistance of Mr. G. van de Ridder is kindly acknowledged.

TABLE 2.3. Number-average molecular weights and second virial coefficients for solutions of polystyrene in toluene at 30°C. Number of sulphate groups and hydroxyl groups per polystyrene molecule.
$v_1^{30°C} = 1.16\ cm^3\ g^{-1}$ $g = 981\ cm\ s^{-2}$

sample	$c_{K_2S_2O_8} \times 10^4$ M	M_n	$B \times 10^5$ mole $cm^3\ g^{-2}$	$-OSO_3^-$/ molecule	–OH/molecule
L-1	3.1	312,000 (260,000)	32	1.85 (1.54)	0.15 (0.46)
L-2	12.4	140,000 (122,000)	50	1.50 (1.31)	0.50 (0.69)
L-3	21.7	98,000 (86,000)	52	1.21 (1.07)	0.79 (0.93)

were negligible, M_n values of 260,000, 122,000 and 86,000 would be calculated for latex L-1, L-2 and L-3, respectively. In the table these values for M_n are given in parentheses.

The numbers of $-OSO_3^-$ groups per polystyrene molecule, calculated from the total sulphur content (table 2.2.) and M_n, are also presented in table 2.3. Again, the figures in parentheses stand for the case of oligomer leakage through the membranes. Assuming negligible contributions of chain transfer processes and thermal initiation (see section 2.1.3.), the sum of the number of $-OSO_3^-$ groups and –OH groups per polymer molecule should equal two (VAN DEN HUL and VANDERHOFF, 1970; GHOSH et al, 1964).

A decreasing number of $-OSO_3^-$ groups per molecule can be interpreted as an increasing number of –OH groups. Hence, it can be concluded that the generation of ·OH radicals increases progressively with $c_{K_2S_2O_8}$. This is consistent with the observed trend in the pH (table 2.1.). The ratio's of $-OSO_3^-$/ molecule: –OH/molecule are of the same order of magnitude as those found by VAN DEN HUL and VANDERHOFF (1970).

The values of the second virial coefficients show good agreement with those reported by HANSEN and HVIDT (1973), after correction for the difference in temperature using the FLORY-KRIGBAUM theory (FLORY, 1953, Ch. XII) of polymer solutions.

2.3.5. *Electrophoresis*

The movement of charged particles in an external electric field is referred to as electrophoresis. The electrophoretic mobility, that is the velocity, u, per unit field strenght, X, of a charged colloidal particle in a dispersion can be measured accurately. The conversion of the electrophoretic mobility into the electrokinetic or ζ-potential, that is the potential difference between the plane of shear and the bulk of the solution, is generally complicated by the effects of retardation and relaxation.

Extending the equations of VON SMOLUCHOWSKI (1903) and HÜCKEL (1924), HENRY (1931) derived an equation to calculate the ζ-potential of spheres in which he took only the retardation effect into account. Hitherto, the most complete derivation of the relationship between ζ-potential and electrophoretic

mobility, including both retardation and relaxation, has been presented by WIERSEMA (1964) and WIERSEMA et al (1966). This calculation is still based on several premises, of which the most important are spherical geometry, diffuse distribution of the counterions outside the plane of shear and non-conduction of the particles. In the case of polystyrene latices the first two conditions will be satisfied but there must be some doubt as to whether the last assumption is justified. For example, WRIGHT and JAMES (1973) found a considerable surface conductivity at the polystyrene-electrolyte solution interface. For a detailed discussion on the theory of electrophoresis and on the conversion of the electrophoretic mobility into the ζ-potential is referred to OVERBEEK and WIERSEMA (1967).

The electrophoretic mobilities of the polystyrene latices were determined at 25 °C at different pH values and in aqueous solutions of KNO_3 of different concentrations. The measurements were performed in a Rank Brothers microelectrophoresis apparatus using a cylindrical cell. The velocities of the particles were measured in dispersions of about 10^7 particles per cm^3 at the two depths in the cell where the net flow of the solvent is supposedly zero (VAN GILS and KRUIJT, 1936). At least 10 particles were timed in each direction of the electric field. The standard deviation for these 40 measurements was not usually more than 10%. The symmetry of the parabolically shaped streaming profile was checked at regular intervals. The strength of the electric field was calculated from the electrical current passing through the cell, the specific conductivity of the dispersion and the cross section of the cell (HUNTER and ALEXANDER, 1962). The specific conductivity was measured using a Philips conductivity meter PW 9501/01 equipped with a Philips conductivity cell PR 9510 (cell constant 0.76 cm^{-1}).

If possible, the ζ-potential was derived following the method of WIERSEMA (1964). However, at low electrolyte concentration, viz. 10^{-5} and 10^{-4} M KNO_3, the experimental mobilities exceed the maximal values predicted by WIERSEMA. This feature has been previously observed quite often (see e.g. OTTEWILL and SHAW, 1967b). In those cases the Henry equation was applied.

Based on the concepts of GOUY (1910) and CHAPMAN (1913) of the diffuse electrical double layer, LOEB et al (1961) performed calculations relating the potential and the charge at any point in the electrical double layer around a spherical particle. Using their tables, the charge density at the plane of shear was derived from the ζ-potential. As a first approximation the ζ-potential was put equal to the Stern-potential ψ_d, i.e. the plane of shear is thought to coincide with the outer Helmholtz plane. Hence, the charge density on the plane of shear equals σ_d. Because of electroneutrality

$$\sigma_0 + \sigma_m + \sigma_d = 0 \qquad (2.6.)$$

where σ_m is the surface charge density in the Stern layer (molecular condensor) due to the specific adsorption of counterions in this layer.

In the pH range 4 to 10 the mobilities of the latex particles in media of 10^{-2} M KNO_3 appeared to be essentially independent of pH. CLINT et al (1973) also

observed the independence of mobility on pH between pH 4.3 and pH 9 with polystyrene latex prepared using the same procedure. According to OTTEWILL and SHAW (1967b), the presence of carboxyl groups, having pK_a values between about 4.0 and 4.6 would cause a steady increase in the electrophoretic mobility up to pH 6. However, since in this study the electrophoretic mobility is not very sensitive to the surface charge σ_0, the independence of the ζ-potential on pH does not entirely rule out the presence of weak acid groups at the particle surface.

The effect of σ_0 on the electrophoretic mobility is tabulated in table 2.4. The value of σ_d, calculated from the ζ-potential may contain a systematic error, as will be indicated when discussing the effect of c_{KNO_3} on the ζ-potential. Still, it is obvious, as can be seen in figure 2.4., that at higher σ_0 values σ_m increases at about the same rate as σ_0, leading to a virtually constant value of σ_d. A similar feature has been observed by LIJKLEMA (1957) for the silver iodide-aqueous solution interface.

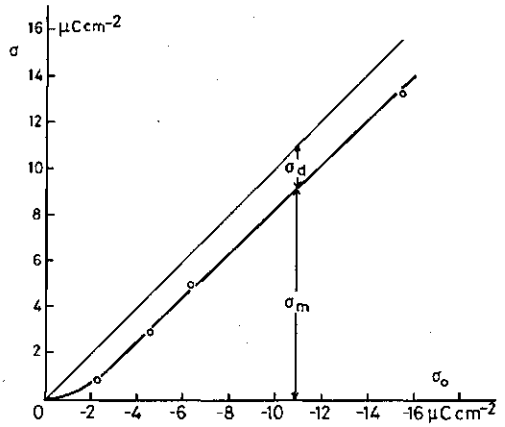

FIG. 2.4. Charge distribution over the regions inside (m) and outside (d) the plane of shear as a function of the surface charge of polystyrene latex. c_{KNO_3} = 0.05 M T = 25°C.

TABLE 2.4. Influence of latex surface charge on ζ-potentials of various polystyrene latices. T = 25°C.

sample	σ_0 μC cm^{-2}	c_{KNO_3} M	$u/X \times 10^4$ cm^2 V^{-1} s^{-1}	$\zeta^{Wiersema}$ mV	σ_d μC cm^{-2}	σ_m μC cm^{-2}
L-1	− 2.3	0.01	3.80 ± 0.19	−55	1.5	0.8
L-2	− 4.6	0.01	3.80 ± 0.31	−55	1.5	2.9
L-3	− 6.3	0.01	3.73 ± 0.42	−54	1.4	4.9
C-3	−15.5	0.01	5.52 ± 0.23	−75	2.3	13.2
L-1	− 2.3	0.05	2.96 ± 0.22	−36	2.0	0.3
C-3	−15.5	0.05	4.17 ± 0.22	−52	3.0	12.5

The increased shielding of the surface charge by the counterions explains the reduction of the ζ-potential with increasing c_{KNO_3}, as is shown for sample L-2 in table 2.5.

TABLE 2.5. Influence of the KNO_3 concentration on the ζ-potential of polystyrene latex L-2.
$\sigma_0 = -4.6\ \mu C\ cm^{-2}$ $d = 508$ nm $T = 25°C$

c_{KNO_3}	$u/X \times 10^4$ $cm^{-2}\ V^{-1}\ s^{-1}$	ζ^{Henry} mV	$\zeta^{Wiersema}$ mV	σ_d^{Henry} $\mu C\ cm^{-2}$	$\sigma_d^{Wiersma}$ $\mu C\ cm^{-2}$
10^{-5}	7.15 ± 1.30	−131		0.26	
10^{-4}	5.81 ± 0.17	− 90		0.34	
10^{-3}	4.70 ± 0.10	− 67	−78	0.61	0.80
10^{-2}	3.82 ± 0.31	− 50	−55	1.35	1.43
10^{-1}	2.70 ± 0.18	− 35	−32	2.77	2.53

The specific adsorption of K^+ ions and, hence, σ_m is expected to increase with increasing c_{KNO_3}. Since in this work σ_o is not greatly influenced by variations in c_{KNO_3}, σ_d should decrease with increasing c_{KNO_3}. However, the opposite effect is observed. Taking account of the visco-electric effect as considered by LYKLEMA and OVERBEEK (1961) leads to an increase in the ζ-potential at higher c_{KNO_3} values. This would imply an even stronger increase of σ_d with increasing c_{KNO_3}. The ζ-potentials reported by KOTERA et al (1970a; 1970b) tend to be somewhat lower than those in this study. The σ_d values calculated from their experimental data also increase with increasing electrolyte concentration. The causes underlying this inconsistency are not clear. They may be found in a wrong estimation of the retardation and/or relaxation effect, in a shifting of the plane of shear with varying c_{KNO_3}, in preferential adsorption of NO_3^- ions at the particle surface or in incorrect assumptions made in calculating the ζ-potential. Possibly, the latex surface is 'hairy' or porous due to the presence of loosely bound poly- and/or oligostyrene molecules, as was supposed in section 2.3.4. In that case a part of the surface charge (i.e. the charge determined by titration) will be located in a layer that is penetrated by the aqueous solution. This layer may shrink upon addition of electrolyte, causing an inwards shift of the plane of shear. Thus, an increase of σ_d with increasing c_{KNO_3} could result.

2.3.6. *Stability*

All the latices were stable against coagulation after preparation. Only the ion exchanged sample L-1 showed coagulation upon titration. According to the theory of DERJAGUIN and LANDAU (1939) and VERWEY and OVERBEEK (1948) (the DLVO theory), the coagulation concentration, c_c, for electrolytes (that is the minimum electrolyte concentration at which rapid coagulation occurs) serves as a means of quantifying the stability of an electrostatically stabilized dispersion. At the coagulation concentration (in moles dm^{-3}) for

symmetrical electrolytes, ψ_d can be estimated acoording to equation

$$c_c = \frac{49.66 \times \varepsilon^3 \times (kT)^5}{6.03 \times 10^{20} \times A^2 \times (ze)^6} \times \tanh^4 \left(\frac{ze\psi_d}{4kT}\right) \qquad (2.7.)$$

where ε is the dielectric constant of the solvent, k Boltzmann's constant, z the valency of the ions, e the elementary charge and A the Hamaker 'constant' for the system.

Equation (2.7.) refers to spherical particles. However, if the thickness of the double layer is small compared to the particle radius one may, to a first approximation, use the flat plate model. The value of ε of water in the region of the electrical double layer may differ considerably from that of bulk water. Also the value of A is uncertain. Moreover, equation (2.7.) is only a simplification. Nevertheless, ψ_d can be estimated rather well because of the 4th power dependence on the hyperbolic tangent term, which, to a first approximation, also implies a 4th power dependence on ψ_d at low values of ψ_d. For the same reason a given experimental error in c_c results in a relatively smaller uncertainty in ψ_d. For example, with the silver iodide system differences of up to 30% have been observed when comparing c_c values obtained by following the initial coagulation (kinetic method) and by judging the coagulation after several hours (static method), respectively (cf. KLOMPÉ, 1941 and REERINK and OVERBEEK, 1954). Such a difference leads to an uncertainty in ψ_d of about 7%. The c_c values obtained by the kinetic method are undoubtedly closer to the c_c values as defined in the DLVO theory and, where available, are to be preferred for use in equation (2.7.).

c_c values of the latex samples L-1 and C-3 for KNO_3, $Ba(NO_3)_2$ and $Mg(NO_3)_2$ were determined by a static method. Coagulation experiments using a Vitatron spectrophotometer, with a built-in stirring device, to follow the initial coagulation, appeared to be unsuitable for establishing c_c values for these latices.

In glass-stoppered tubes 5.0 cm^3 latex of ca. 0.2% w/w were mixed with 5.0 cm^3 electrolyte solution of various concentrations and the mixture was kept at 25°C in a thermostatted water bath. After two hours the tubes were turned end over end and replaced in the bath. After a total equilibration time of 18 hours the optical densities of the supernatants of the dispersions were measured against water at 540 nm in a Unicam SP 600 spectrophotometer using 1 mm optical cells. The optical densities were plotted against the electrolyte concentration. A typical example of such a plot is shown in figure 2.5. Extrapolation of the linear part of the sigmoidal curve to the abscissa yields an electrolyte concentration that is taken by us as the coagulation concentration.

To calculate ψ_d a value of 3×10^{-21} J was assigned to the Hamaker constant of polystyrene in water (EVANS and NAPPER, 1973).

Again, by means of the tables of LOEB et al (1961), the corresponding values of σ_d are obtained.

The results of the coagulation studies are presented in table 2.6.

The higher c_{KNO_3} required to coagulate sample C-3 (more negative σ_0) as

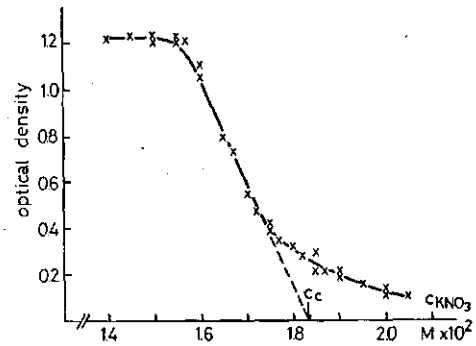

FIG. 2.5. Optical density of the supernatant of polystyrene latex C-3 as a function of c_{KNO_3}. The arrow indicates the derived coagulation concentration c_c. $T = 25°C$.

TABLE 2.6. Coagulation of polystyrene latices. $\varepsilon = 78.5$ $A = 3 \times 10^{-21}$ J $T = 25°C$

electrolyte	latex L-1 c_c M	$\sigma_0 = -2.3$ ψ_d mV	μC cm^{-2} σ_d μC cm^{-2}	latex C-3 c_c M	$\sigma_0 = -15.5$ ψ_d mV	μC cm^{-2} σ_d μC cm^{-2}
KNO_3	16.5×10^{-2}	−14.4	1.3	18.3×10^{-2}	−14.8	1.3
$Ba(NO_3)_2$	2.4×10^{-3}	−12.9	1.0	8.4×10^{-3}	− 9.8	0.4
$Mg(NO_3)_2$	2.2×10^{-3}	−12.7	1.0	1.0×10^{-3}	− 0.3	0.5

compared to L-1 is in agreement with expectation. However, the reasons for the opposite trend with respect to σ_0 observed using $Ba(NO_3)_2$ and $Mg(NO_3)_2$ as coagulants are obscure. If it were due to a strong increase in specific adsorption of Ba^{2+} and Mg^{2+} on the latex particle with increasing σ_0, then a lower ζ-potential for latices with higher σ_0 would result. From the literature there is no evidence for such behaviour; on the contrary, OTTEWILL and SHAW (1972) report larger electrophoretic mobilities of equally sized polystyrene latices with higher σ_0 in solutions of $Ba(NO_3)_2$. Perhaps, the coagulation by bivalent ions occurs partly as a result of bridging of $-OSO_3^-$ groups. If this were the case, it is conceivable that the c_c value for these ions is the smaller the higher the surface concentration of $-OSO_3^-$ groups.

The electrophoresis results for latex L-2 reveal a linear relationship between ζ and log c_{KNO_3}. Assuming an analogous relation, extrapolation of the ζ-potentials at c_{KNO_3} values of 10^{-2} and 5×10^{-2} M to the coagulation concentration yields ζ-potentials of −24 mV and −32 mV for sample L-1 and C-3, respectively. These values are much higher than those for ψ_d calculated from the c_c values for KNO_3.

CLINT et al (1973) investigated the influence of $c_{Ba(NO_3)_2}$ on the electrophoresis of a similarly prepared polystyrene latex with $\sigma_0 = -4.0$ μC cm^{-2}. At $c_{Ba(NO_3)_2} =$

20×10^{-3} M they calculated $\zeta = -13$ mV. This value agrees well with ψ_d of sample L-1 ($\sigma_0 = -2.3$ μC cm^{-2}) at the same $Ba(NO_3)_2$ concentration.

Finally, it should be mentioned that SMITHAM et al (1973) required very high NaCl concentrations to coagulate their polystyrene latices, including those prepared following the method of KOTERA et al (1970a). They provide evidence to indicate that these latices are stabilized by a combination of electrostatic and steric factors. In some way, the steric effects seem to be associated with carboxyl groups attached at the particle surface. In accordance with the results of GOODWIN et al (1973), but in distinction to other investigators (FURUSAWA et al, 1972; VAN DEN HUL and VANDERHOFF, 1970; CLINT et al, 1973; this thesis), SMITHAM et al demonstrated the presence of carboxyl groups for polystyrene latices prepared in the absence of O_2 and using $K_2S_2O_8$ as the initiator. Since in the present study the c_c values for KNO_3 are lower by a factor of three than those for NaCl in the study of SMITHAM et al, and since the influence of the valency of the counterions on the c_c values (see table 2.6.) shows the trend expected for electrostatically stabilized dispersions, there is no indication for steric hindrance to coagulation. Thus, with regard to the matter of the possible desorption of poly- and/or oligostyrene molecules from the latex particle surfaces (section 2.3.3.), the question whether the surface of the polystyrene particles is 'hairy' or smooth would seem to be an important issue.

2.4. SUMMARY OF THE MOST RELEVANT PROPERTIES OF THE POLYSTYRENE LATICES IN RELATION TO THEIR APPLICATION IN ADSORPTION EXPERIMENTS

With respect to the adsorption of proteins the chemical constitution as well as the electric properties of the polystyrene-water interface are considered to be of interest. Some of these properties are summarized in table 2.7.

For example, the degree of hydrophobicity of the particle surface, which affects the vicinal water structure (see section 2.1.3.) would govern to a large extent the part played, if any, by hydrophobic bonding in the adsorption process. In this connection, the density of the hydrophilic groups at the particle surface is an important variable. Because of the different kinds of interaction with the surrounding water and because of the possible specific interactions with the protein molecules, the nature of these groups should be known.

The surface charge of the latices is due to $-OSO_3^-$ groups (section 2.3.3.). Since these groups are monovalent and relatively large, they are expected to break the structure of the vicinal water, i.e. increase its entropy. The number of K^+ ions bound per unit area of polystyrene surface increases with σ_0 (section 2.3.5.). K^+ ions are also assumed to be structure-breakers (see e.g. KAVANAU, 1964). The –OH groups, possibly present at the surface of the polystyrene particles (section 2.3.5.), probably have only a slight effect on water structure (FRANK and WEN, 1957; D'ORAZIO and WOOD, 1963). Thus, in this sense, the hydrophobicity of the polystyrene surface decreases with increasing σ_0.

Proteins contain charged groups, usually unevenly distributed over the

molecule, and these will interact more or less specifically with the charged groups on the polystyrene particle surface. Therefore, electrostatic properties of the latex, such as σ_0 and ζ, in the presence of the protein are of great importance.

Treatment of the latices with ion exchange resins results in poly- and/or oligostyrene molecules being removed from the particles, giving rise to a corresponding reduction in σ_0 (section 2.3.3.). Anticipating the discussion of the experimental results to be described later, it is worth noting that the amounts of human plasma albumin adsorbed at the particle surface is lowered by about 25% for latices that have been ion exchanged. To avoid possible contaminations, all the latex samples used in the adsorption experiments described in the chapters 4, 5 and 6 have not been treated with ion exchange resins.

Samples L-1 and C-3 were used in most of the work.

TABLE 2.7. Some experimental data for the polystyrene latices that were used as substrates in the studies of protein adsorption.
$T = 25°C$.

sample	s	surface area/ charged group	σ_0	$c_{KNO_3} = 0.01$ M		$c_{KNO_3} = 0.05$ M	
				σ_m	ζ	σ_m	ζ
	$m^2\ g^{-1}$	nm^2	$\mu C\ cm^{-2}$	$\mu C\ cm^{-2}$	mV	$\mu C\ cm^{-2}$	mV
L–1	11.6	7.0	– 2.3	0.8	–55	0.3	–36
L–2	11.1	3.5	– 4.6	2.9	–55		
L–3	11.4	2.6	– 6.3	4.9	–54		
C–3	8.9	1.0	–15.5	13.2	–75	12.5	–52

3. THE BEHAVIOUR OF PROTEINS AT INTERFACES IN RELATION TO THEIR PROPERTIES IN SOLUTION. SOME GENERAL FEATURES

3.1. INTRODUCTION

Like all other macromolecules, proteins adsorb at almost any interface. Only a fraction of the segments of an adsorbed macromolecule is generally attached to the interface. This is reflected in the fact that the amount adsorbed considerably exceeds the amount that can be accomodated in a flat monolayer. For most synthetic macromolecules bound fractions in the range 0.2 to 0.4 have been reported (THIES, 1966; PEYSER et al, 1967; KILLMANN and ECKART, 1971; HERD et al 1971; FLEER et al, 1972; FOX et al, 1974). Usually this fraction diminishes with increasing amount adsorbed, indicating a change in the structure of the adsorbed layer (THIES, 1966; KILLMANN and ECKART, 1971).

Because of the high degree of polymerization the molecule has many contact points with the interface, even in the case of relatively small bound fractions. Statistically it is very improbable all the attached segments of one molecule would desorb simultaneously. Therefore, the adsorption of macromolecules is usually an irreversible process. Thus, the applicability of thermodynamic relationships, such as those of Gibbs and Clapeyron that are based on the attainment of equilibrium, becomes questionable. Apart from this there is the problem as to whether these equations should be applied to whole molecules or to segments.

Since, for an adsorbed polymer, exchange between attached and non-attached segments remains possible, it may take some considerable time (hours or days) before the adsorbed molecules attain their steady-state conformation.

In many respects proteins, which constitute a special category of natural macromolecules, differ from synthetic macromolecules. They are co-polymers of some twenty-two different possible amino acids, linked by peptide bonds. The amino acid residues, which, as side chains, occur in a specific sequence along the polypeptide chain, vary considerably in their polarity. Some of them contain acid or base groups. Therefore, dependent on the pH, protein molecules are either net positively or negatively charged. Due to intramolecular and intermolecular interactions, proteins in solution show very specific spatial arrangements (see section 3.2.) which govern their physiological activities. Generally, a protein molecule in solution contains parts with different degrees of order ranging from random coils to α-helix and β-sheet structures. For only a very small number of proteins has the structure been completely solved.

Because of the specific structures they adopt in solution, a general theory for the adsorption of proteins at interfaces is not possible at present. Only for the limiting cases of randomly coiled and rigid macromolecules have theories for their adsorption been given.

The theories for the adsorption of random coils all presuppose the attainment of equilibrium. These theories often involve many parameters (SILBERBERG, 1962a, b; 1967; 1968) or a few parameters of composite character (HOEVE, 1965; 1966; 1970; 1971). For these reasons experimental results of the adsorption of randomly coiled macromolecules are usually difficult to interpret in the light of these theories. No complete theory has yet emerged to take into account the effects of Coulombic interactions, as occurs with adsorbed polyelectrolytes, including proteins, although HESSELINK's work on polyelectrolyte adsorption may be mentioned in this respect (HESSELINK, 1972).

MILLER and BACH (1973) presented a theory for rigid macromolecules of any shape at interfaces. In their model the interface is assumed to exert an influence only on the first layer of adsorbed segments. This theory also contains many parameters. FRISCH and STILLINGER (1962) have given a theoretical treatment of the adsorption of rigid rod-like polyelectrolytes, oriented parallel to the interface.

For proteins, as a rule, the experimental adsorption isotherms show plateau levels of adsorption reached at low concentrations in solution and usually the adsorption is, at least partially, irreversible. As a consequence, the conformation of the adsorbed protein molecules is very dependent on their 'history'. In this respect relevant factors may be the protein concentration in the bulk solution from which they are adsorbed, the rate of diffusion to, and the rate of unfolding at, the interface. For this and other possible reasons it is difficult to compare protein adsorption data in the literature critically (see section 3.3.1.).

Although many experiments have been reported, much confusion exists concerning the mechanism of protein adsorption and about the structure of the adsorbed layer. Possible non-homogeneity of the conformations adopted by adsorbed protein molecules may very well lead to erroneous or ambiguous conclusions being drawn from experiments. Moreover, most of the experimental methods used for the conformational analysis of proteins in solution are not applicable to adsorbed layers without complications.

Whether or not changes in the conformation occur upon adsorption depends on the interplay between the forces governing adsorption and the forces controlling the protein conformation in solution. These forces may be of various kinds, viz. Coulombic, hydrogen bonding, hydrophobic bonding, all types of van der Waals interactions and chemical bonding. Lateral interactions between adsorbed macromolecules also have a direct effect on the conformations they adopt.

If, upon adsorption, the conformation of a protein changes, a concomitant effect on its physiological activity would be expected. However, even the binding of a protein molecule in its native conformation at an interface may render the active site(s) less accessible. Therefore, a change in the physiological activity is not necessarily the result of conformational changes.

The behaviour of proteins at interfaces of different nature have been extensively reviewed by a number of authors, e.g. JAMES and AUGENSTEIN (1966), BRASH and LYMAN (1971) and MILLER and BACH (1973).

3.2. Structure of proteins in aqueous solution with special attention to plasma albumin and ribonuclease

In this section the most important features of the interactions controlling the conformation of dissolved proteins will be considered. Because an aqueous medium is the natural habitat of dissolved protein molecules, the discussion will be restricted to proteins in aqueous solution.

The conformation of proteins is characterized by its primary, its secondary and its tertiary structure[1]. The secondary and tertiary structures are the net result of the intramolecular interactions in the protein molecule and the interactions of the protein with solvent molecules and other solute molecules, if present.

As many of these interactions tend to counter-balance one another, any one conformation may only be marginally more thermodynamically stable than any other. Therefore, the conformation of proteins is, as a rule, very sensitive to environmental factors influencing these interactions, e.g. pH, ionic strength and temperature. As compared to simple polyelectrolytes, conformational changes in protein molecules due to variations in environmental conditions tend to occur rather abruptly (see e.g. Lumry and Biltonen, 1969).

The various interactions that may contribute to the conformation of proteins will now be reviewed briefly.

a. *Coulombic interactions*

Coulombic interactions exert their influence over a relatively long range; the potential energy between two point charges is inversely proportional to their separation. For fixed charges in a medium, the Coulombic interaction may be reduced by increasing the ionic strength, as a result of the charge-shielding action of the counterions.

In its isoelectric state the net charge on a protein molecule is zero; the molecule carries as many positive as negative charges. If these charges are more or less evenly distributed over the molecule, the net Coulombic interaction in an isoelectric protein may be an attractive one and thus favour a compact structure. At pH values other than the isoelectric point (i.e.p.) there will be a surfeit of either positive or negative charges, resulting in an increase in the free energy of a compact conformation. This effect increases essentially as the square of the net charge on the protein molecule.

As it is energetically unfavourable to place isolated charges in the non-polar interior of a protein molecule, the charged groups tend to accumulate at its surface. Because of the low dielectric constant and the essential absence of hydration, oppositely charged groups in the interior of a protein molecule

[1] The *primary structure* of a protein is defined as the sequence in which the amino acids are linked together in a linear polypeptide chain. The *secondary structure* refers to the conformation the polypeptide backbone adopts (e.g. α-helix, β-structure and random coil). The *tertiary structure* refers to the manner in which folded segments of the polypeptide chain are mutually arranged in space to each other and to the mutual ordering of the side chains.

may form ion pairs. Also, charged groups of the same sign will repel each other more strongly. The difference in free energy between the charges at the surface of a molecule (i.e. exposed to the aqueous medium) and the non-polar interior determines whether or not location of charged groups in the interior of the protein favours a compact protein structure. The formation of ion pairs is sensitive to the *type* of electrolyte present in the system. For example, bivalent ions may form salt bridges between charged monovalent groups of the same sign in the interior of a protein molecule.

b. *Hydrogen bonding*

Hydrogen bonds are directional with a bond length of the order of a tenth of a nanometer.They are characterized by a negative enthalpy of formation of the order of 25 kJ $mole^{-1}$. Their strength decreases with increasing temperature.

With respect to proteins in aqueous solution different kinds of hydrogen bonds may be distinguished: (i) hydrogen bonds between peptide units in the polypeptide backbone, (ii) hydrogen bonds between side chain groups, for example a phenol-carboxylate bond and (iii) hydrogen bonds between groups of the protein and water molecules.

Since intramolecular hydrogen bonding competes with hydrogen bonding to water molecules, the overall contribution of hydrogen bonding to the protein structure is difficult to assess. In a compact conformation at least a part of the polypeptide backbone will reside in the low dielectric interior of the protein molecule, where the formation of hydrogen bonds is enhanced.

c. *Hydrophobic bonding*

The term hydrophobic bonding is used to describe the spontaneous aggregation of non-polar residues in an aqueous environment. This aggregation originates from the fact that water-water contacts are thermodynamically much more favourable than contacts between two non-polar groups or between a non-polar group and water, i.e. it is a question of non-polar groups tending to be rejected from an aqueous medium rather than being positively attracted to one another (see e.g. TANFORD, 1973). Thus, since it is not the non-polar groups that dislike the water, but the water that has antipathy of the non-polar groups, a better name for this phenomenon would be 'lipophobic bonding'.

Hydrophobic bonding involves the disruption of hydrogen bonds between water molecules (see section 2.1.3.). It is characterized, at least at 25 °C, by a relatively small, usually positive enthalpy change, a negative change in heat capacity and a large positive entropy change in the range of 6–50 J K^{-1} per bond (NÉMETHY and SCHERAGA, 1962c).

The importance of hydrophobic bonding for the structure of proteins has first recognized by KAUZMANN (1959). As protein molecules generally contain many non-polar amino acid residues, intramolecular aggregation of these side-chains is expected to occur in aqueous solution, stabilizing a compact protein structure. Indeed, burying of the non-polar residues in the interior of the protein molecules has been shown experimentally (see e.g. KENDREW, 1962; RICHARDS and WYCKOFF, 1971).

d. *Disulfide bonds*

Covalent disulfide bonds may be formed between two cysteine residues. As their formation results in intramolecular cross links, this in itself tends to lead to a more folded structure. However, their formation may very well interfere with other interactions favouring a compact structure. For example, to gain maximal benefit from hydrophobic bonds, hydrogen bonding, electrostatic interactions, etc., it is necessary that the interacting groups be within short-range of each other. Disulfide bonds may keep them apart. Therefore, it is impossible to assess in a quantitative way the contribution of disulfide bonds to the conformational stability of protein molecules.

In addition to the interactions discussed so far, other interactions such as the various kinds of van der Waals forces between parts of the molecule, hydration etc., may play a significant role. These interactions, taken together with considerations of the overall conformational entropy of the molecule, determine its actual conformation under given conditions.

The different interactions mentioned are not all independent of each other, as has been indicated several times.

Also the important role of the solvent is obvious. In this respect the unique properties of water having a high dielectric constant and a strong ability to form hydrogen bonds with appropriate groups of the protein molecule, must be stressed (cf. HAGLER et al, 1973).

From the foregoing it is evident that an experimental investigation to determine the separate contributions of the different types of interaction to the overall conformation would be very complicated, if possible at all.

3.2.1. *Plasma albumin*

The biological function of plasma albumin (PA) is concerned with the binding and transport of small molecules and ions. PA is able to bind these substances to a considerable extent (KLOTZ, 1953; FOSTER, 1960). Because of its relatively high level in the plasma, for example 4.2 and 2.9 grams per 100 cm^3 of human and bovine plasma, respectively (KOLB, 1964), albumin plays an important role in maintaining a given osmotic pressure and a constant pH in the blood. In addition, PA serves as a source of amino acids.

The amino acid compositions of PA extracted from different species appear to be rather similar and this is true in particular for PA of human and bovine origin, denoted as HPA and BPA, respectively (PHELPS and PUTNAM, 1960; STEINHARDT et al, 1971). Most of the information available in the literature in fact concerns BPA and HPA. The properties and features described in this section apply to these two kinds of albumin.

The detailed structure of the PA molecule in solution has not been finally settled, although many authors have found that several physical quantities (light scattering, sedimentation, diffusion, low angle X-ray scattering) are satisfactorily accounted for by assuming the molecule to be a prolate ellipsoid

of revolution. The actual values presented for the axial lengths depend on the method of measurement and to some extent also on the author. For example, RIDDIFORD and JENNINGS (1966) found major and minor axes of 11.6 and 2.7 nm, respectively, by low angle X-ray scattering, but SQUIRE et al (1968) report 14 and 4 nm from sedimentation and diffusion measurements. Systematic discrepancies, such as the lower values derived from X-ray analysis as compared to those obtained hydrodynamically may perhaps be due to the fact that one kind of measurement includes the water of hydration whilst the other does not (RIDDIFORD and JENNINGS, 1966; BRODERSEN et al, 1973).

PA consists of a single polypeptide chain of ca. 590 amino acid units and has a molecular weight of about 69,000. The amino acid composition is known (see e.g. SPAHR and EDSALL, 1964) but the sequence has not been established yet. There are indications that the distribution of the amino acids over the chain is rather uniform (BRAAM, 1972). The molecule contains 17 disulfide bonds, 18% of the amino acid residues are acidic, 10% contain an ε-amino group and 3.5% a phenolic hydroxyl group. Together with 3% imidazole and minor amounts of other dissociating groups, the ratio of these amino acids determines the number of charged groups per molecule, Z, as a function of pH.

The isoionic point, i.e. that pH at which the charge would be zero if no ions other than protons were bound, is about 5.5 (FOSTER and STERMAN, 1956) and it attains its isoelectric state in the pH region 4.3–4.8, the exact value depending on the ionic strength of the medium (AOKI and FOSTER, 1957a; 1957b).

The hydrophobicity of the protein, expressed in terms of the parameter proposed by BIGELOW (1967) amounts to 4.68 kJ per residue.

From viscosity measurements it is concluded that, at room temperature, PA in aqueous solution has a compact structure between pH 4.3 and 10.5, possessing an intrinsic viscosity of 3.7 $cm^3\ g^{-1}$ (TANFORD et al, 1955a; TANFORD and BUZZELL, 1956). Over this pH region about 55% of the molecule is in the α-helix form, the remainder of the molecule having a randomly coiled or an irregular structure (URNES and DOTY, 1961). From titration curves (TANFORD et al, 1955b) it may be deduced that, at an ionic strength of 0.03 M, unfolding sets in at Z values of about +20 and –40 charged groups per molecule. At higher ionic strengths higher values of Z are required to attain the same degree of unfolding.

However, the increase in the intrinsic viscosity with decreasing pH on the acid side of pH 4.3 down to 3.6 is only small. This reflects a reversible change in conformation, the so-called 'N-F transition', for which much other supporting experimental evidence has been collected (FOSTER, 1960). Besides the increase in viscosity, some other important features of the N-F transition are a marked reduction in the α-helix content (SOGAMI and FOSTER, 1968) and an increase in the electrostatic interaction (TANFORD et al, 1955b). The N-F transition may be explained by the model of FOSTER (1960). According to this model, the PA molecule consists of a single polypeptide chain comprising four compact subunits. In going from the N- to the F-conformation, the distance between the subunits increases as a consequence of the increasing electrostatic repulsion.

As a result of this expansion of the molecule hydrophobic areas between the subunits become exposed to the solvent, but ionic groups which hold the subunits together in the N-form become exposed too. VIJAI and FOSTER (1967) found that 40 carboxyl groups, which are masked in the N-form, become titratable in the F-form. The same authors suggested that in the N-conformation these carboxyl groups would form ion pairs with positively charged ε-amino groups.

Also between pH 7 and 9 the PA molecule undergoes a conformational change: the so-called 'neutral transition' (BRAAM, 1972). This change has been less extensively investigated than the N-F transition. There appears to be a number of analogies between the two transitions. For example, in both cases about 150 hydrogen atoms become available for exchange with deuterium (BENSON et al, 1964; BRYAN and NIELSEN, 1969) and histidine residues seem to be liberated from salt bridges (HARMSEN, 1971). However, the neutral transition is less drastic than the N-F transition: no increase in viscosity has been observed (TANFORD et al 1955a; TANFORD and BUZZELL, 1956) nor a change in the α-helix content (SOGAMI and FOSTER, 1968; HARMSEN, 1971).

For PA, in particular, it would seem that the conformation of the molecule is very sensitive to alterations in its environment; it may be called a 'nervous' molecule. This behaviour seems to underlie its many biological functions.

All proteins combine to a certain extent with both anions and cations, but PA is different from most other proteins in its unusually high ability to bind anions non-specifically (see e.g. SCATCHARD and YAP, 1964 and CARR, 1952). Binding of ions to proteins influences the effective dissociation constants of the various constituent acid and base groups (ARVIDSSON, 1972) and, obviously, also the electrophoretic behaviour.

Natural PA is known to contain 1–2.2 molecules of fatty acids per molecule (ROSSENEU-MOTREFF et al, 1970). These fatty acids appear to have a stabilizing effect on the structure of the albumin molecule (SOGAMI and FOSTER, 1968; ANDERSON, 1969).

Since PA does not contain a whole number (i.e. 0.7) of sulfhydryl groups per molecule (KOLTHOFF et al, 1957; ANDERSSON, 1966) it is assumed that two classes of albumin exist, viz. mercaptalbumin and non-mercaptalbumin. In non-mercaptalbumin the sulfhydryl group is blocked by cysteine or glutathione (ANDERSSON, 1966).

3.2.2. *Ribonuclease*

The ribonucleases (RNase's) constitute a class of enzymes that catalyze the hydrolytic cleavage of ribonucleic acids. The individual enzymes of only a few species have been isolated and studied in detail. For example, the amino acid composition and sequence of bovine RNase (SMYTH et al, 1963), porcine RNase (JACKSON and HIRS, 1970) and rat RNase (BEINTEMA and GRUBER, 1967) have been determined. Considerable differences in the primary structure were observed between these different RNases. Research on the structure of RNase has been mainly concentrated on bovine pancreas RNase. The discussion to be given in this section deals with this kind of RNase. For a detailed review on

bovine pancreas RNase the reader is referred to RICHARDS and WYCKOFF (1971).

RNase, having a molecular weight of 13,680, consists of 124 amino acids. In the A-form the amino acids are arranged in one polypeptide chain; in the S-form the polypeptide chain is cleaved between the 20th and 21st amino acid residue, but this has no major effect on the spatial structure.

RNase is one of the very few proteins for which the three-dimensional structure has been solved in detail. KARTHA et al (1967) were the first to determine the sequence of the peptide chain of RNase-A, using X-ray diffraction. Independently, WYCKOFF et al (1967; 1970), using the same technique, found the complete structure of RNase-S. DICKERSON and GEIS (1969) constructed stereodrawings of the α-carbon chains of RNase-A and RNase-S. That of RNase-A is depicted in figure 3.1., together with its amino acid sequence. In addition, RICHARDS and WYCKOFF (1971) have presented a very detailed stereopicture of RNase-S. The shape of the RNase molecule is more or less ellipsoidal with axial dimensions of 3.8, 2.8 and 2.2 nm, based on the X-ray structure.

According to BIGELOW (1971), the hydrophobicity parameter of RNase equals 3.57 kJ per residue. More detailed information about the hydrophobicity has been obtained by LEE and RICHARDS (1971) who calculated, from the coordinates of all non-hydrogen atoms given by WYCKOFF et al (1970), the accessibility for the solvent for each of these atoms in the RNase-S molecule. RICHARDS and WYCKOFF (1971) have given a plot of the total accessibility of each amino acid residue. This picture shows that the longer hydrophobic side chains are generally more deeply 'buried'. RICHARDS and WYCKOFF calculated that the total hydrosphere surface of 70 nm^2 is composed of 32 nm^2 carbon and sulphur and 38 nm^2 of nitrogen and oxygen. Thus, the surface may considered to be 45% hydrophobic.

RNase molecules contain 4 disulfide bonds. 9% of the amino acids contain a carboxyl group, 3% an imidazole and 13% an ε-amino or phenolic hydroxyl group. Together with some other ionizable groups, this results in an isoionic point of about 9.6 (TANFORD and HAUENSTEIN, 1956). For the i.e.p., values around 9.45 have been reported (see e.g. ANDERSON and ALBERTY, 1948), except for the case of phosphate containing media in which lower values were found.

Viscosity measurements at 25°C reveal that the RNase molecule does not unfold in the pH range 1–11. At ionic strengths from 0.05 to 0.25 M for the intrinsic viscosity a value between 3.3 and 3.5 $cm^3\ g^{-1}$ has been found in this pH region (BUZZELL and TANFORD, 1956). From titration data (TANFORD and HAUENSTEIN, 1956) it was concluded that, over the pH region quoted above, the molecule does not expand between Z values of about +16 (which is almost the maximal attainable positive charge) and −7 charged groups per molecule, the limits becoming closer at higher temperatures (HERMANS JR. and SCHERAGA, 1961; BRANDTS and HUNT, 1967).

According to PFLUMM and BEYCHOK (1969) in the compact form the secondary structure of RNase consists of 11.5% α-helix and 33% β-structure, the remainder of the molecule being more or less unordered. There are no indications of

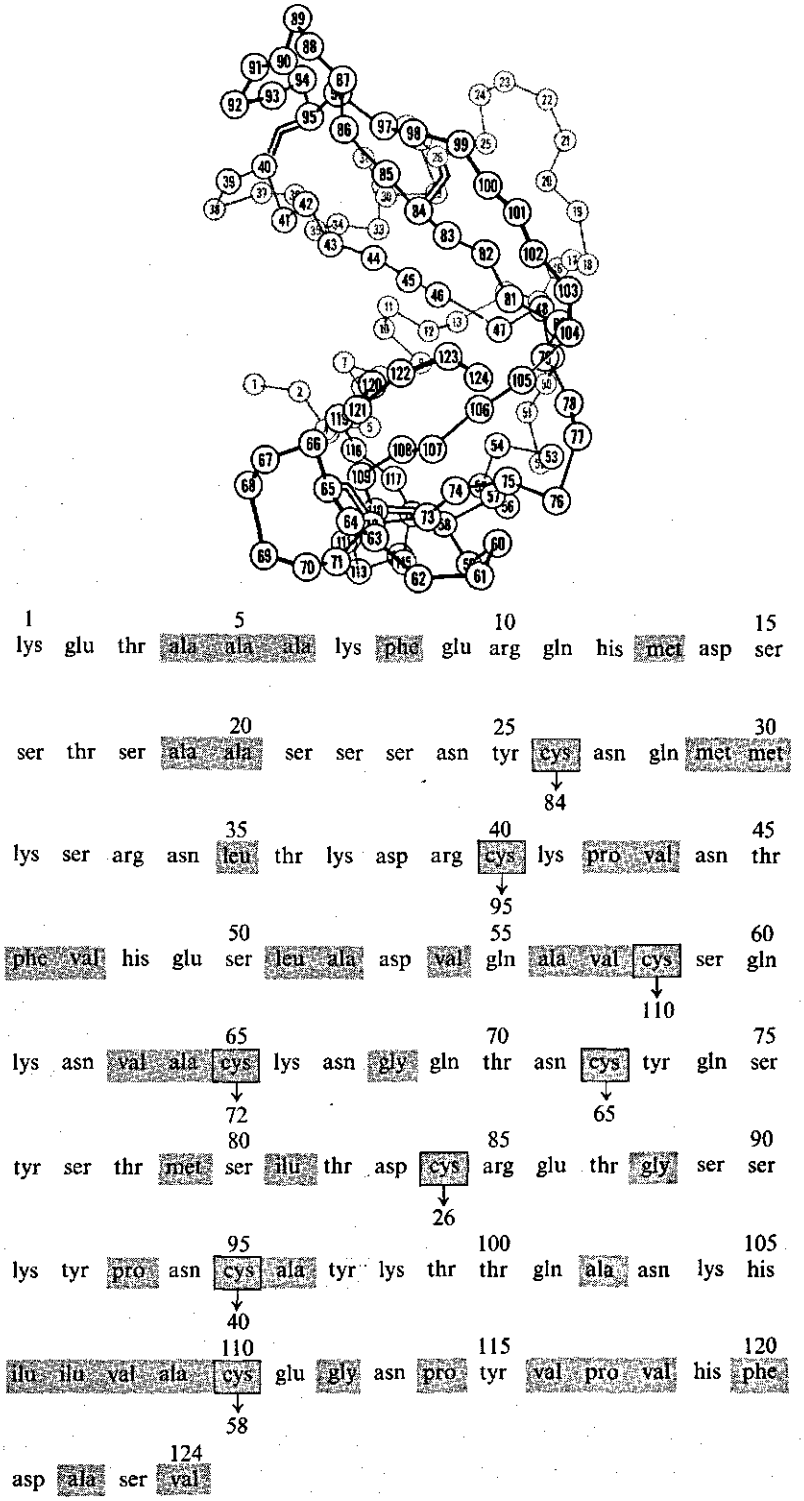

FIG. 3.1. Ribonuclease A. Stereodrawing of the α-carbon chain, together with the numbered amino acid residues. Hydrophobic residues are tinted grey. Cystein disulfide-bridge participants are outlined in black and their connections are indicated. (Drawing after DICKERSON and GEIS, 1969.)

pH-induced conformational changes within the limits of unfolding.

In solution RNase molecules are known to form, to some extent, dimers and higher aggregates. Dissociation of these aggregates can be achieved by adjusting the RNase solution to pH 6.5 and then heating at 62 °C for 10 minutes (FRUCHTER and CRESTFIELD, 1965).

3.2.3. *A comparison of some of the properties of plasma albumin and ribonuclease that may affect their behaviour at interfaces*

Some of the properties of PA and RNase that may be relevant to their adsorption behaviour are summarized in table 3.1.

The molecular volumes of RNase and PA differ by about a factor of five. From a consideration of the dimensions of the molecules, it would seem that in close-packed monolayers of these proteins in their native conformations at interfaces a larger amount of PA can be accomodated per unit area than of RNase, provided their orientation at the interface is not too different (e.g. one parallel and the other perpendicular).

At low surface coverages the rate of adsorption can expected to be controlled by translational diffusion. Under these conditions the rate of adsorption is

TABLE 3.1. Comparison of some properties of PA and RNase.

	PA	RNase
molecular weight	69,000	13,680
density (g cm^{-3})	1.35	1.42
shape	ellipsoid	ellipsoid
size (nm)	$11.6 \times 2.7 \times 2.7$	$3.8 \times 2.8 \times 2.2$
diffusion coefficient ($cm^2\ s^{-1}$)	0.70×10^{-6} [1]	1.07×10^{-6} [2]
isoelectric point (pH units)	4.2–5.0	ca. 9.5
isoionic point (pH units)	ca. 5.5	ca. 9.4
conformational stability towards pH	low	high
hydrophobicity (kJ per amino acid residue[3])	4.68	3.57

[1] according to KELLER et al, 1971.
[2] according to CREETH, 1958.
[3] according to BIGELOW, 1967.

somewhat higher for RNase, as it is proportional to the square root of the diffusion coefficient.

It has been suggested in the foregoing sections that the conformational stability of PA is less than that of RNase, at least with respect to changes in pH. TANFORD (1967), using the Debye-Hückel theory for impenetrable spherical particles, calculated the electrostatic free energies of both proteins at Z values where unfolding sets in. Quantitative comparison of the results, however, is of limited value because of the approximations involved. Nevertheless, the calculations reveal that the internal coherence in RNase is much greater than in PA. Thus, it is to be expected that the effect of pH on structural rearrangement upon

adsorption is greater with PA than with RNase.

Although, because of the complex structure of proteins, the degree of hydrophobicity as expressed in terms of BIGELOW's parameter may not fully represent the polar-non polar balance in the molecule, an increasing tendency to unfold at (hydrophobic) interfaces with increasing value of this parameter is to be expected. For example, such a trend has been observed for the adsorption of several proteins at the air-water interface (BIRDI, 1973).

3.3. EFFECT OF THE NATURE OF THE INTERFACE ON THE ADSORPTION OF PROTEINS

Obviously, the interfacial behaviour of a protein depends on its structure and its structural stability in the solution from which it is adsorbed as well as on the nature of the adsorbing interface. The adsorption experiments, that have been described in the literature, at a given interface have been performed using not only various proteins but also different conditions in the aqueous medium (e.g. type of electrolyte present, ionic strength, pH, etc.). Therefore, the effect of the nature of the interface is difficult to establish. Nevertheless, an attempt is made in the following sections to draw some general trends from these experiments as to how the nature of the interface controls adsorption. The discussion will primarily deal with solid-liquid interfaces.

3.3.1. *The solid-liquid (S-L) interface*

Aqueous interfaces with solid substrates may be broadly classified as being either hydrophobic or hydrophilic. A given solid surface may be heterogeneous, with both hydrophobic and hydrophilic sites.

As has been discussed already in section 2.1.3., it is believed that the structure of the water adjacent to both the adsorbent and the protein molecule is influenced by the local degree of hydrophobicity and also by the types of charged groups and ions present at and near their respective surfaces.

In view of these considerations, a strong dependency of the interfacial behaviour of proteins on the hydrophobicities of the surfaces involved would be expected. Also, the types of ionic groups and electrolytes present in the system are likely to affect the adsorption mechanism.

The adsorption of protein molecules, containing both hydrophobic and hydrophilic groups themselves, at a hydrophobic interface is governed to a large extent by hydrophobic bonding (the breakdown of ordered water structure at the hydrophobic surface); this type of bonding is characterized by a positive change in entropy.

At hydrophilic interfaces polar interactions seem to be of dominant importance.

Upon adsorption, protein molecules may change their conformation. This is more probable the higher the net charge on the protein molecule, since then the intramolecular Coulombic interactions progressively counteract a stable

folded conformation. The reduction in hydrophobic bonding between the amino acid residues in the folded interior of the dissolved molecule is more or less compensated for by placing these residues at the adsorbent surface, thus shielding them from contact with water.

The main available experimental work seems to support the ideas discussed above.

VROMAN (1967) found that the wettability of surfaces, i.e. glass and lucite, on which proteins had been adsorbed depends very much on the material of the adsorbent. The author concluded that with glass the protein interacts via hydrophilic bonds but with lucite via hydrophobic bonds. Also a definite effect of the hydrophobicity of the interface on the electrophoretic mobility of protein-covered particles has been observed (WILKINS and MYERS, 1970). Interaction of proteins with particles having hydrophobic surfaces leads to elevated positive mobilities, indicating preferential exposure of the cationic groups of the protein to the solvent.

Solutes that are known to influence polar interactions tend to have a stronger influence on the adsorption of proteins at hydrophilic interfaces than at hydrophobic ones. SHAPIRA (1959) found that RNase could be desorbed from glass by elution with electrolyte solutions above a certain minimum ionic strength. Later, HUMMEL and ANDERSON (1965) observed a decrease in the maximum adsorption of RNase on glass with increasing ionic strength. Moreover, MESSING (1969), investigating the adsorption of different proteins (among which RNase) on glass, was able to elute the proteins from the glass only by using a solution composed of acid and urea. From these studies MESSING suggested the occurrence of ionic interactions and hydrogen bonding between these proteins and the glass.

Investigations by MCLAREN (1954) and by HARTER and STOTZKY (1971) of the adsorption of various proteins on kaolinite and smectite revealed that adsorption of proteins is strongly influenced by the valency of the positive counterions associated with these clays. Both sets of authors point out that an ion exchange mechanism may be involved in the adsorption of proteins at these substrates. MCLAREN (1954) and ARMSTRONG and CHESTERS (1964) were able to desorb lysozyme from kaolinite and bentonite at high pH values or at high ionic strengths.

MACRITCHIE (1972) compared the adsorption of BPA on both a hydrophobic and a hydrophilic silica surface under otherwise similar conditions. He deduced that the free energy of adsorption at the hydrophilic interface is less negative in comparison to that for the hydrophobic interface. In the case of the hydrophilic interface the adsorption process approaches reversibility, the more so the further the pH of the system is removed from the i.e.p. of the protein. The amount adsorbed appeared to be higher on the hydrophobic silica. The author attributes this to aggregation of the protein at this particular surface.

DILLMAN and MILLER (1973) investigated the adsorption of albumin, γ-globulin and fibrinogen from bovine plasma on a series of polymer membranes,

both cationic and neutral. For all the proteins studied they distinguish two independent types of adsorption on these membranes, which occur simultaneously. One type is very sensitive to pH and NaCl concentration (type 1 adsorption). Desorption can be achieved by washing with 0.1 N NaOH. Type 1 adsorption of albumin appeared to increase linearly with the cation exchange capacity of the membrane. The other type of adsorption (type 2) is much less sensitive to pH and NaCl concentration. It is not influenced by the cation exchange capacity of the membrane. Type 1 adsorption is exothermic and type 2 endothermic. From these results DILLMAN and MILLER deduced that the interactions in type 1 adsorption are mainly of a polar nature, whereas type 2 is governed by hydrophobic interactions.

The adsorption of molecules, either charged or uncharged, at charged interfaces interferes with the composition of the electrical double layer. Hence, adsorption, desorption and reorientation of adsorbed molecules may cause alterations in the differential capacitance of the double layer. This differential capacitance, C, is defined as the change in surface charge density σ_0 per unit surface potential ψ_0: $C = \delta\sigma_0/\delta\psi_0$. In this way PAVLOVIC and MILLER (1971a), performing polarographic experiments with polyglutamic acid (PGA) and polylysine (PL) at mercury-water interfaces, studied schematically the role of charge-charge interactions in the adsorption process. (Strictly speaking, the interface between mercury and water is of the liquid-liquid type, but, because of the properties of mercury, it resembles in many respects a S-L interface). The authors concluded that, at a positively charged interface, completely ionized PGA adsorbs in a flat orientation (0.45 nm^2 per glutamic acid residue), whereas PGA subsequently desorbs at negative polarizations of the mercury surface. The area per residue of 25%-ionized PGA is about 0.15 nm^2, which is in accord with a helical structure or possibly some other 'non-flat' conformation. Upon charging the surface positively, the adsorbed molecules reorient to a flatter conformation. Neutral PL remains adsorbed even at high positive and negative surface charges. Positively charged PL shows some unspecified conformational changes at a negative mercury surface and it desorbs at positive surface charges.

Due to the more complicated structure of proteins as compared to polyamino acids, changes in the differential capacitance upon adsorption are more difficult to interpret. PAVLOVIC and MILLER (1971b) found that the relatively more polar parts of the RNase molecule are attached to the mercury surface. The adsorbed amount, ca. 1.14 $mg\,m^{-2}$, is roughly constant over a wide range of surface charge.

In passing it is worth noting here that, in interpreting charge-charge interactions between the interface and the adsorbing molecules, the mutual effect of the electric fields on the effective dissociation constants of the titratable acid and base groups of the adsorbing molecules and the adsorbent must be taken into account (section 5.3.3.).

Since Coulombic forces act over a relatively long distance, they may also influence the adsorption kinetics. Thus, the rate of adsorption is expected to be higher the greater the electrostatic attraction between the adsorbate and the interface. This suggestion is experimentally supported by MESSING (1969).

The conformational analysis of adsorbed proteins is very complicated and the interpretations given by different authors are rather controversial. For many systems the surface conformation of a protein is reported to be dependent on the protein concentration in bulk. This is plausible since at low bulk concentrations the rate of protein supply to the interface is relatively low in comparison with the rate of spreading and/or reorientation of the adsorbed molecules, resulting in conformational changes at the interface. Conversely, at high bulk concentrations, deformation of adsorbed molecules is less likely.

LYMAN et al (1968) used electron microscopy to study the adsorption of γ-globulin on silica surfaces. Although the γ-globulin molecules could not be distinguished individually, the authors observed different patterns of aggregation at low and high surface concentrations. From this study they suggest that surface denaturation of γ-globulin takes place at low concentrations but that adsorption in the natural conformation occurs at higher concentrations. The same authors studied, at the physiological pH, the adsorption of some plasma proteins (among which HPA) on a variety of uncharged, hydrophobic polymer surfaces by internal reflection infra-red spectroscopy and found only minor differences in the adsorbed amounts for the various substrates. They suggest the formation of complete monomolecular layers adsorbed from solutions ranging in concentration from less than 0.1 g dm^{-3} up to normal plasma levels.

In some cases two steps can be distinguished in the adsorption isotherms (BULL, 1956; ORESKES and SINGER, 1961; NORDE et al, 1972 and this thesis, ch. 4.). Such behaviour may be interpreted in the following ways: (i) the formation of a second layer in interaction with a probably unfolded first layer; (ii) side-on adsorption of the first molecules, whereafter additional adsorption in the end-on mode takes place on the uncovered areas; (iii) rearrangement of the adsorbed molecules from a parallel to a more perpendicular orientation at the interface by which a larger amount of protein can be accomodated per unit area of the adsorbent.

Using infra-red differential spectroscopy, MORRISSEY and STROMBERG (1974) found, for the adsorption of BPA and bovine prothrombine on a hydrophilic silica surface, that the fraction of attached segments of the proteins to be independent of the surface concentration. They concluded that for these systems no significant conformational changes are involved in the adsorption process, even at low concentrations of the proteins in solution.

MATHOT and ROTHEN (1969), performing ellipsometric measurements, recorded the increase of the thickness of the adsorbed layer with time on chromium coated slides in contact with a 0.05 g dm^{-3} γ-globulin solution. The globulin layer thickness appeared to grow linearly with time. A discontinuity occurred at about 7.5 nm; beyond this value adsorption continues at a lower rate. The inflection point may indicate completion of a first monolayer of γ-globulin.

A general feature of protein adsorption on both hydrophilic and hydrophobic interfaces is that the plateau value of the adsorption isotherm, plotted as a function of pH, passes through a maximum around the i.e.p. of the dissolved

protein under consideration (see e.g. McLAREN, 1954; BULL, 1956; HUMMEL and ANDERSON, 1965; BATEMAN and ADAMS, 1957; ARMSTRONG and CHESTERS, 1964; MACRITCHIE, 1972; MORRISSEY and STROMBERG, 1974; NORDE et al, 1972 and this thesis, ch. 4.). The effect of pH may be due to structural changes in the adsorbing protein molecules at pH values away from the i.e.p., to lateral repulsion between the adsorbed protein molecules or to a combination of these two processes. Unfolding and lateral repulsion are both favoured if there is a net charge on the protein molecule. The data reported in the literature do not allow any firm inference to be drawn as to which particular mode of adsorption dominates in any one case. In this connection it should be noted that the maximum amount of protein adsorbed is largely controlled by the properties of the protein in solution, notably its conformational stability, rather than by its affinity for the interface (LYKLEMA and NORDE, 1973).

3.3.2. *The liquid-liquid (L-L) and the liquid-air (L-A) interface*

Many aspects of protein adsorption discussed in section 3.3.1. also apply to the adsorption at L-L and L-A interfaces. However, an important difference between S-L interfaces on the one hand and L-L and L-A interfaces on the other concerns the fluidity of the interface and the possibility of non-polar residues of the adsorbed protein molecule being able to protrude into the non-polar phase. Therefore, the free energy decrease to be gained by unfolding an adsorbing molecule and thus exposing its non-polar groups to the non-polar phase, may be greater at liquid interfaces than at solid interfaces. In fact, because at L-A and L-L interfaces both phases are penetrable, these types of interfaces constitute ideal 'solvents' for macromolecules containing both polar and non-polar groups.

Since in the determination of the adsorption isotherms changes in surface area must be avoided, very few techniques are available for the case of liquid interfaces. As a consequence, only a limited number of such determinations have been done (see e.g. KHAÏAT and MILLER, 1969; ADAMS et al, 1971; YAMASHITA and BULL, 1967; 1972; PHILLIPS et al. 1972). Some of these authors report relatively large amounts adsorbed. This may be the result of a salting-out effect in the aqueous phase, since in these cases the aqueous phase contained high electrolyte concentrations.

An advantage of investigating the adsorption at liquid interfaces is the possibility of measuring the interfacial pressure built up by the adsorbed layer. However, measurement of the interfacial pressure does not in general lead to a value for the amount adsorbed. If a macromolecule is adsorbed with only a fraction of its segments attached to the interface, the question arises as to what extent these segments and the segments in the loops contribute to the interfacial pressure.

For the adsorption of BPA at liquid interfaces, it has been found that the interfacial pressure increases with increasing interfacial tension of the clean interface (GHOSH and BULL, 1963), as is to be expected theoretically (MILLER and BACH, 1973).

From a comparison of the behaviour of lysozyme, BPA and β-casein at an L-A interface, EVANS et al (1970) concluded that the rate of adsorption and the tendency to unfold at the interface increases with decreasing stability of the tertiary structure in solution.

MUSSELWHITE and KITCHENER (1967) estimated the limiting thickness of an isolated lamella formed from solutions of BPA to be ca. 3.5 nm. As it was assumed that the lamella consists of two layers of BPA a considerable degree of flattening of the molecules must occur upon adsorption.

If it is assumed that only the segments attached to the interface are responsible for the interfacial pressure, the degree of coverage of the interface by these segments may be directly related to the pressure (BÖHM, 1974). Thus, for some polyelectrolytes and proteins a decrease of surface coverage with increasing molecular charge has been observed (CUMPER and ALEXANDER, 1950; MILLER and KATCHALSKY, 1957; JAFFÉ and RUYSSCHAERT, 1964; BÖHM, 1974). This effect is probably due to the low affinity of charged groups for these uncharged hydrophobic interfaces. If, in addition, the adsorbed amount is determined independently, the number of bound segments per adsorbed molecule can be computed. From this quantity conclusions regarding the statistics of the segment distribution may be drawn. The values for the bound fractions estimated by BÖHM (1974) for partially esterified polymethacrylic acid at paraffin oil-water interfaces tend to increase with increasing molecular charge. This indicates that a change in the molecular conformation at the interface is enhanced by increasing the charge on the molecules.

3.3.3. *Concluding remarks*

Although the foregoing discussion is by no means complete, it nevertheless illustrates the complex nature of protein adsorption. In spite of this, some trends concerning the effect of the nature of the interface on the adsorption may be recognized. In summarizing these it can be said that with hydrophilic surfaces polar interactions, and with hydrophobic surfaces non-polar interactions, play a dominant role. Consequently, at hydrophobic interfaces protein molecules are more tightly bound. Usually, the amount of protein adsorbed in the plateau region is a maximum near the i.e.p. of the protein, the effect of pH being less pronounced at hydrophobic interfaces. Both on hydrophobic and hydrophilic interfaces, at pH values not too far from the i.e.p. and under conditions of sturated adsorption, the structure of proteins does not seem to be affected severely by adsorption. In general, the tendency to change the structure upon adsorption increases with decreasing conformational stability of the protein in solution. Especially, a large contribution from intramolecular hydrophobic interaction to the conformational stability of the protein in solution enhances the probability of structural rearrangement at the interface. However, until direct techniques become available enabling us to observe proteins at interfaces, the detailed elucidation of the structure of adsorbed protein molecules under different conditions remains a difficult problem.

4. THE ADSORPTION OF HUMAN PLASMA ALBUMIN AND BOVINE PANCREAS RIBONUCLEASE AT POLYSTYRENE-WATER INTERFACES

4.1. INTRODUCTION

Some general features of the adsorption of macromolecules and, in particular, of dissolved protein molecules have been discussed in the previous chapter. That discussion was based on theoretical considerations and experimental data available in the literature.

This chapter is concerned with experimental studies of the amount of HPA and RNase adsorbed from solution onto polystyrene surfaces (section 4.3.). The variables in these experiments are the pH (i.e. the net charge of the proteins), the surface charge density of the polystyrene particles, the electrolyte (KNO_3) concentration and the temperature. In addition, a discussion is given on the weight fraction of the protein in the first layer adjacent to the polystyrene surface, i.e. the bound fraction (section 4.4.) and the thickness of the adsorbed layer (section 4.5.), both as a function of the plateau levels of adsroption.

From the amount adsorbed, the bound fraction and the thickness, an impression of the sructure of the adsorbed layer can be obtained. However, since these quantities have not been determined independently, the values obtained for them do not constitute a firm basis for a quantitative evaluation of the structure of the adsorbed layer.

In the interpretation of the experimental data, the question as to whether or not the protein molecules undergo structural changes upon adsorption will be a central point of discussion.

4.2. MATERIALS

The polystyrene latices have been described in chapter 2.

Electrophoretically pure HPA and crystalline RNase from bovine pancreas (5 × crystallized, protease-free, salt-free and roughly chromatographed to increase the 'A' fraction (HIRS et al, 1953)) were purchased from Sigma Chemical Company. Without further purification, HPA contains 1–2.2 moles of fatty acids per mole protein (cf. section 3.2.1.). HPA and RNase were stored in a desiccator at ca. –5°C. Aqueous solutions of the proteins were prepared and dialyzed for two days at 4°C against a ca. 100-fold excess amount of water, which was refreshed after one day. The protein solutions were kept at 4°C and they were discarded if their age exceeded one week. Prior to use the solutions of RNase were adjusted to pH 6.5 and heated for 10 minutes at 62°C to break up any possible aggregates (FRUCHTER and CRESTFIELD, 1965).

All chemicals used were of analytical grade. The water was distilled and the cyclohexane vacuum-distilled from an all-Pyrex apparatus, shortly before use.

4.3. Adsorption isotherms. Effects of the charge of the protein and the polystyrene surface, the electrolyte concentration and the temperature

The charge of the polystyrene surface can be varied in a controlled way by varying the polymerization conditions (see section 2.3.3.). The charge of the protein molecules can be controlled by adjusting the pH of the medium (see section 5.4.2.). A study of the adsorption of proteins on polystyrene latices under different conditions of charge may provide insight into the electrostatic component of the interaction between the adsorbing protein molecules and the polystyrene surface. If Coulombic and/or other electrostatic interactions play a role in the adsorption process, the adsorbed amounts would be expected to depend on the ionic strength of the medium. For this reason, experiments were performed at two ionic strengths, viz. 0.01 M KNO_3 and 0.05 M KNO_3. Adsorption isotherms were determined at 5 °C, 22 °C and 37 °C.

4.3.1. *Experimental procedure*

1.00 cm^3 of polystyrene latex, with a total surface area of about 0.5 m^2, was added to 3.50 cm^3 of protein solution of various concentrations in glass-stoppered vials of 5 cm^3. Prior to mixing, both solutions were brought to the same pH and c_{KNO_3}, without using buffers. The vials were rotated end over end for about 16 hours. The suspensions were then centrifuged for 30 minutes at 20,000 *g*. For the clear supernatant as well as for the protein solution, the protein concentration was determined according to the method to be described in section 4.3.1.1. From the difference in the protein concentration before and after adsorption the amount of protein adsorbed per unit area of the polystyrene was calculated.

In these experiments, the temperature was kept constant during all manipulations up to the decantation of the supernatant obtained by centrifugation.

4.3.1.1. Determination of the protein concentration

The protein concentrations in the stock solutions were determined spectrophotometrically using the extinction coefficients $E^{1\ cm}_{0.1\%\ HPA} = 0.530$ at 279 nm (Steinhardt et al, 1971) and $E^{1\ cm}_{0.1\%\ RNase} = 0.710$ at 278 nm (Sage and Singer, 1962). The concentrations in these solutions were also determined by the micro-biuret method, described by Itzhaki and Gill (1964). The results obtained using these two methods always agreed within 5% in a non-systematic way.

After adsorption, for most of the suspensions the residual concentration of dissolved protein was too low to apply succesfully either of the two methods mentioned above. Moreover, in the supernatant, obtained by precipitating the protein-covered polystyrene particles, traces of styrene, oligo- or polystyrene may have been present, which would interfere in the spectrophotometric determination of the protein. For this reason, the protein concentrations in the supernatants were determined according to a modification of the method of

LOWRY (1951), developed further by ROOZEN (1967). In contrast to the procedure described by ROOZEN, immediately after mixing the protein and the reagents, the solutions were thermostatted for 3 hours at 25 °C to standardize the effect of temperature. In each series of protein determinations standard samples were included for the construction of a calibration curve.

4.3.2. *Results and discussion*

Examples of adsorption isotherms are given in figure 4.1. (HPA series) and figure 4.2. (RNase series). In these figures the amount of protein adsorbed, Γ_p (expressed in mg m^{-2}), is plotted against the concentration of protein in solution, c_p, after adsorption.

If an adsorption isotherm is well-described by a certain isotherm equation, it may seem logical to interpret the adsorption data in terms of the theory underlying this equation. However, such an interpretation only holds if the

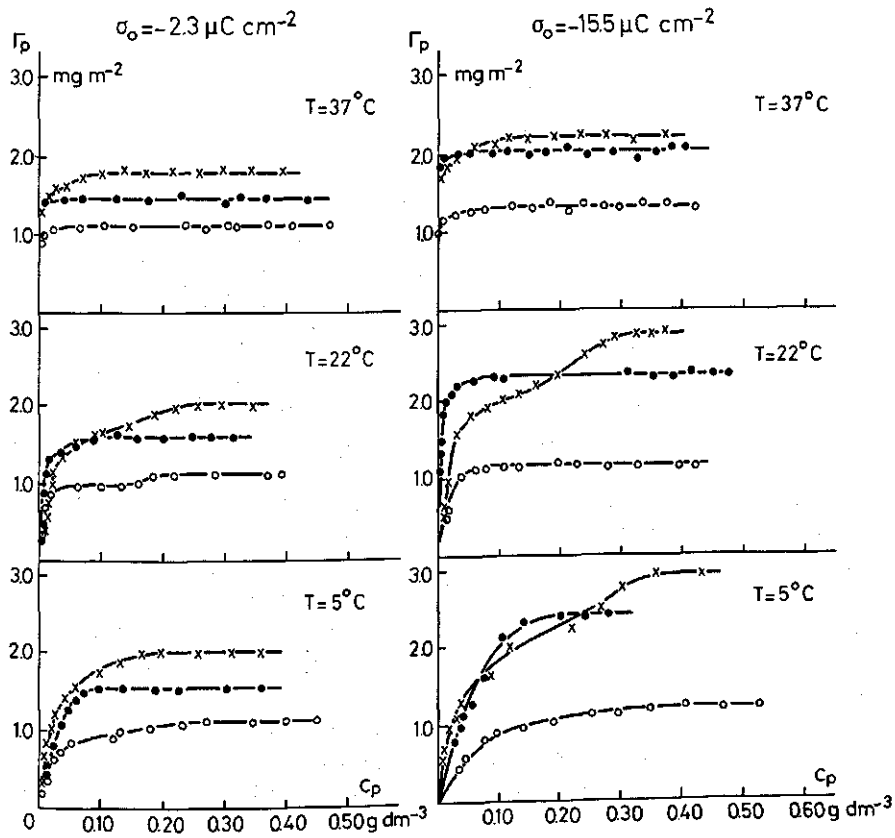

FIG. 4.1. Examples of adsorption isotherms for HPA on polystyrene latices. • pH 4.0 × pH 4.7 O pH 7.0. c_{KNO_3} = 0.05 M.

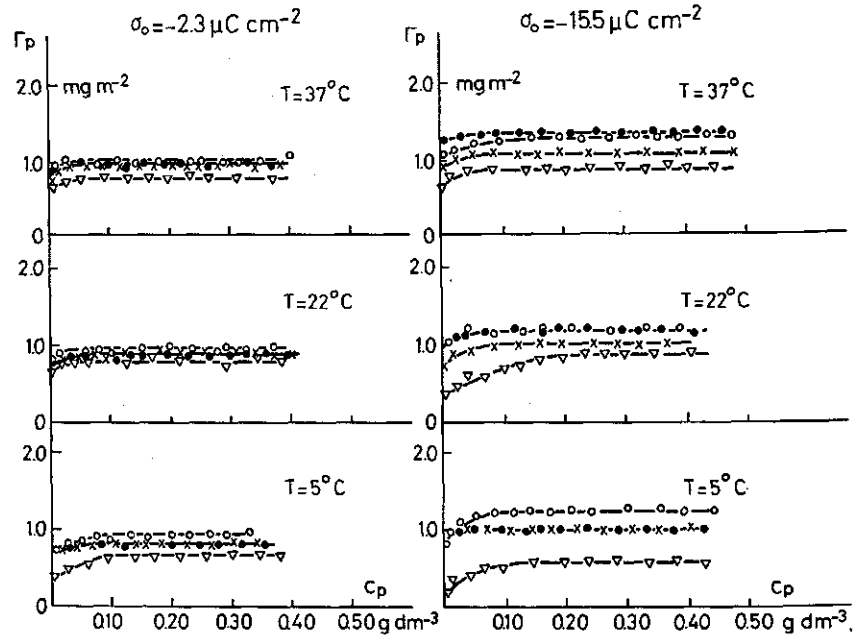

FIG. 4.2. Examples of adsorption isotherms for RNase on polystyrene latices. • pH 4.0 ○ pH 7.0 × pH 9.3 ▽ pH 11.0. $c_{KNO_3} = 0.05$ M.

premises of the theory are realized in the experiment. For this reason it would be incorrect to use the Langmuir theory to analyze the adsorption isotherms (cf. ORESKES and SINGER, 1961), even though the experimental data can be fitted to Langmuir isotherms (one- or two-step versions), because the adsorption of polymers, in general, does not correspond to the premises of the Langmuir theory. A similar reservation applies to the Scatchard theory (cf. DEŽELIĆ et al, 1971), which is phenomenologically identical to the Langmuir theory. The basic assumptions in these theories, applied to adsorption from solution (i.e. competitive adsorption of solute and solvent molecules) are: reversible physical adsorption, independence of the molar Gibbs free energy of adsorption of the degree of coverage of the adsorbent by adsorbates and ideal behaviour of the solution and the adsorbate. For the systems currently studied, it will appear in the forthcoming discussion that none of these premises is usually met, except for the fact that the adsorption is mostly physical. In view of the discussion in section 3.1., HPA and RNase in this respect do not differ from other biopolymers.

To date adsorption theories have only been developed for uncharged, random-coil polymers (SILBERBERG, 1962a, b; 1967; 1968; HOEVE, 1965; 1966; 1970; 1971). Therefore, the adsorption isotherms for HPA and RNase can only be analyzed semi-quantitatively.

For both HPA and RNase the adsorption is highly irreversible with respect

to dilution. As a consequence, the amount of protein adsorbed is influenced by the kinetics of adsorption, i.e. by the rates of arrival and structural rearrangements. The adsorption isotherms are expected to have a high-affinity character. It may be anticipated that the isotherms intersect the ordinate-axis at a value > 0.6 mg m^{-2}. This figure is arrived at by taking 0.3 nm^2 per amino acid residue (YAMASHITA and BULL, 1967); the amount of protein accomodated in a completely spread flat monolayer then amounts to ca. 0.55 mg m^{-2}. Such high-affinity isotherms are indeed found with RNase, but not with HPA, except at 37 °C. Apparently, for some unknown reason, bare polystyrene surface co-exists with dissolved HPA molecules, in spite of the irreversibility of the adsorption. The adsorption isotherms at 5 °C for HPA at different polystyrene surfaces, determined by DEŽELIĆ et al (1971), show the same phenomenon.

Also contrary to RNase, the adsorption isotherms for HPA sometimes show a distinct step; in other cases the curves are smooth. In view of the irreversibility of the adsorption process, the inflection points in the isotherms probably reflect structural rearrangements of the adsorbed protein molecules rather than formation of a second layer of protein molecules (NORDE and LYKLEMA, 1975). In this connection it is noted that CHATTORAJ and BULL (1959) have observed discontinuities as a function of c_p in the electrophoretic mobilities of BPA and ovalbumin on different substrates. One of these irregularities coincides with steps in the adsorption isotherms occuring around similar values for c_p as observed in figure 4.1.

All the adsorption isotherms, both for HPA and RNase, attain plateau values. In this respect these proteins differ from randomly coiled macromolecules for which the adsorbed amount theoretically and often experimentally is an continuously increasing function of the concentration in solution. Such an increase is only possible if specific intramolecular interactions are absent. It constitutes a principal point of distinction between proteins and randomly coiled polymers.

In view of the following discussion, it should be borne in mind that different parts of the adsorption isotherms reflect different interactions.

The initial parts, i.e. those at very low surface coverage, are mainly determined by the protein-polystyrene interaction, because at low coverage there is little or no limitation of the amount adsorbed as a result of packing or crowding on the surface.

On the other hand, the part of the isotherm in the region approaching the plateau reflects the lateral interactions between the adsorbed protein molecules.

Obviously, the platform values reflect adsorption saturation.

4.3.2.1. Effect of charge

Upon adsorption of HPA and RNase, a small change of pH is observed. The reason for this will be explained in chapter 5. The values for the pH of adsorption refer to those before adsorption occurs.

Under all the conditions tested experimentally, RNase shows a high affinity for the polystyrene surface. The same is observed for the adsorption of HPA at 37°C. For sake of clarity, the experimental values for Γ_p at $c_p = 0$ are not indicated in figures 4.1. and 4.2. At 5°C and 22°C the initial parts of the isotherms for HPA directly reflect the net Coulombic interactions between the protein molecules and the polystyrene surface. As can be seen in figure 4.3., at fixed ionic strength and temperature, the initial slopes of the isotherms tend to increase with increasing charge difference between the surface and the adsorbate.

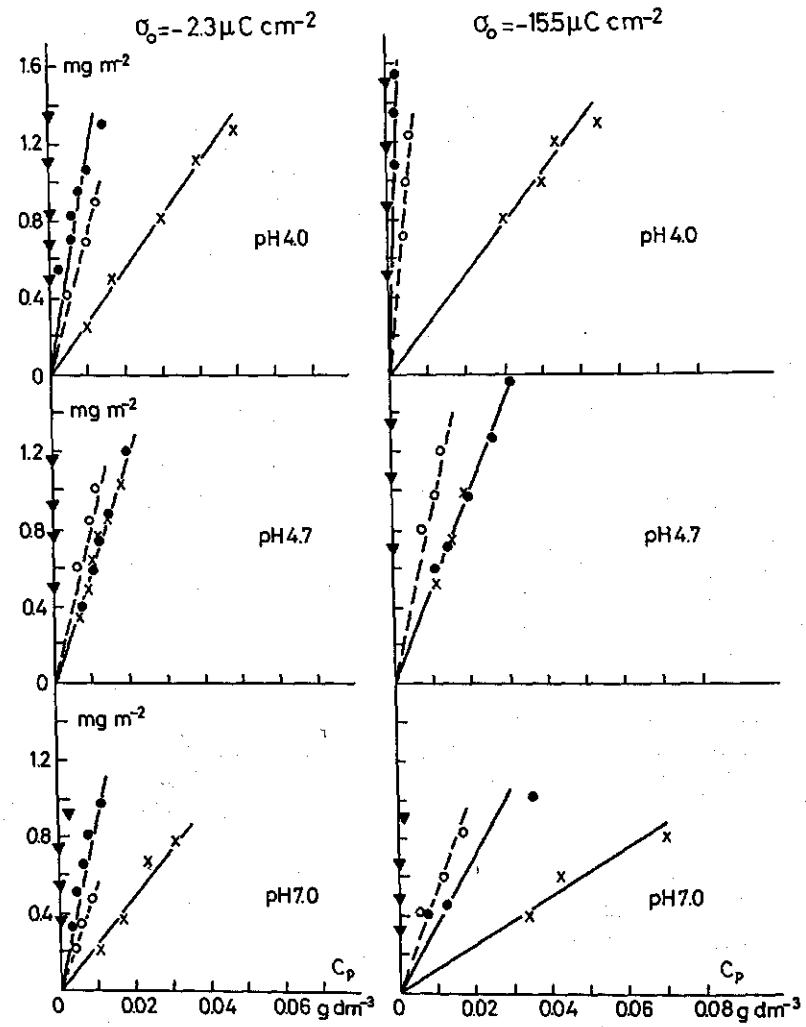

FIG. 4.3. Initial parts of the adsorption isotherms for HPA on polystyrene latices.
solid lines: $c_{KNO_3} = 0.05$ M × 5°C • 22°C ▼37°C
dashed lines: $c_{KNO_3} = 0.01$ M O 22°C

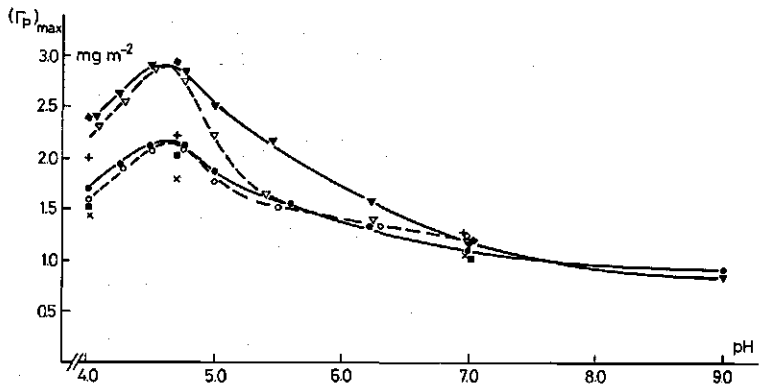

FIG. 4.4. Adsorption of HPA on polystyrene latices. Plateau values.
solid lines: $c_{KNO_3} = 0.05$ M $T = 22°C$ ▼ $\sigma_0 = -15.5$ μC cm^{-2} ● $\sigma_0 = -2.3$ μC cm^{-2}
dashed lines: $c_{KNO_3} = 0.01$ M $T = 22°C$ ▽ $\sigma_0 = -15.5$ μC cm^{-2} ○ $\sigma_0 = -2.3$ μC cm^{-2}
◆ $c_{KNO_3} = 0.05$ M $T = 5°C$ $\sigma_0 = -15.5$ μC cm^{-2}
■ $c_{KNO_3} = 0.05$ M $T = 5°C$ $\sigma_0 = -2.3$ μC cm^{-2}
+ $c_{KNO_3} = 0.05$ M $T = 37°C$ $\sigma_0 = -15.5$ μC cm^{-2}
× $c_{KNO_3} = 0.05$ M $T = 37°C$ $\sigma_0 = -2.3$ μC cm^{-2}

In figures 4.4. (HPA series) and 4.5. (RNase series) curves are given showing the effects of pH and σ_0 on the plateau adsorption, $(\Gamma_p)_{max}$.

The adsorption of these proteins is 'semi-reversible' towards pH. On changing the pH away from the value where $(\Gamma_p)_{max}$ is maximal very little desorption occurs. However, a change of the pH towards that value leads to additional adsorption up to ca. 80% of the amounts that adsorb in the direct experiments.

Both for HPA and RNase, $(\Gamma_p)_{max}$ is greater the more negatively charged

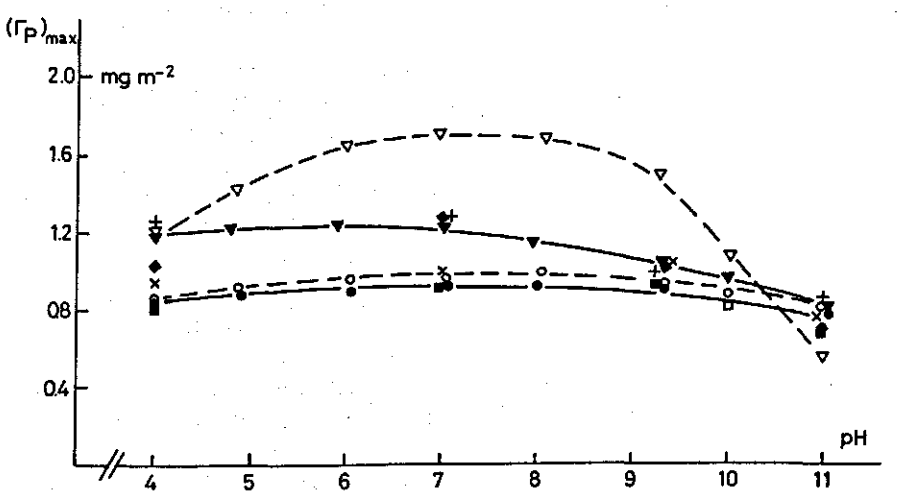

FIG. 4.5. Adsorption of RNase on polystyrene latices. Plateau values. Symbols as in figure 4.4.

the polystyrene surface, even at pH values > i.e.p. where both the surface and the protein bear a negative charge. The fact that with HPA $(\Gamma_p)_{max}$ is virtually unaffected by variation in σ_0 between -2.3 and -6.3 μC cm^{-2}, suggests that in this region σ_0 is low compared to the charge density in that part of the protein close to the polystyrene surface (LYKLEMA and NORDE, 1973). The effect of pH on $(\Gamma_p)_{max}$ will be discussed for HPA and RNase, separately.

With HPA, $(\Gamma_p)_{max}$ vs. pH is more or less symmetrical with respect to the i.e.p. of the protein in solution (figure 4.4.). This indicates that the maximum adsorbed amount is determined by the charge on the dissolved HPA molecule, either directly or indirectly. A direct effect of charge could be that the HPA molecules become less densily packed the further the pH is from the i.e.p. because of intermolecular electrostatic repulsion between the adsorbed molecules. An indirect effect of charge could lie in the conformational stability of the dissolved HPA molecule as a function of pH (cf. section 3.2.1.). The dependence of $(\Gamma_p)_{max}$ on pH would then be explicable in terms of structural alteration, in order to increase the contact between the protein molecules and the polystyrene surface, which proceeds progressively with increasing distance from the i.e.p. Such a mechanism can only be operative if the rearrangements in the protein molecule, upon adsorption, occur at a comparable rate or is faster than the arrival of the protein molecules at the interface. As an alternative, one could also consider the possibility that around the i.e.p. the ellipsoidally shaped HPA molecule adsorbs more or less end-on but becomes, on the average, increasingly tilted on moving further from the i.e.p. In this picture, the molecule would adsorb without reconformation.

Based on the molecular weight and the dimensions of the dissolved HPA molecules (table 3.1.) and assuming a layer of hydration of 0.5 nm around the molecules, a complete monolayer of molecules adsorbed end-on would correspond to an adsorbed amount of 8.4 mg m^{-2}. Considering the values for $(\Gamma_p)_{max}$ as a function of pH (figure 4.4.), an end-on orientation of the adsorbed HPA molecules seems to be very improbable.

In a similar way, for a complete monolayer of side-on adsorbed HPA molecules a surface concentration of 2.5 mg m^{-2} is calculated. Allowing for an uncertainty of 10–20% in the calculation, mainly because of the uncertainties in the hydrodynamic dimensions of the HPA molecules, such a side-on orientation of the molecules at the interface could well explain the adsorbed amounts around the i.e.p., especially at high σ_0 and at 5°C and 22°C. However, the fact that $(\Gamma_p)_{max}$ at the i.e.p. depends on σ_0 suggests that the conformations of the adsorbed HPA molecules are not exactly the same as in solution. The smaller adsorbed amounts at pH values further from the i.e.p. must then be accounted for by increasing lateral electrostatic repulsion and/or progressive spreading at the interface. Some evidence to discriminate between these two explanations may be obtained by considering the lateral interaction between the adsorbed molecules as a function of pH.

The concentration of protein in solution at which 90% of the plateau adsorption has been attained, $c_p^{90\%}$, can serve as a relative measure of the lateral

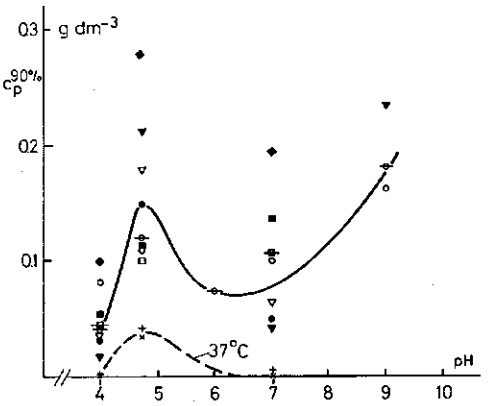

FIG. 4.6. Adsorption of HPA on polystyrene latices. Concentration of HPA in bulk solution at which 90% of the plateau adsorption has been reached. Open symbols 0.01 M KNO_3; filled symbols 0.05 M KNO_3.
$\sigma_0 = -2.3\ \mu C\ cm^{-2}$ □ 5°C ○ 22°C × 37°C
$\sigma_0 = -4.6\ \mu C\ cm^{-2}$ –○– 22°C
$\sigma_0 = -6.3\ \mu C\ cm^{-2}$ –□– 22°C
$\sigma_0 = -15.5\ \mu C\ cm^{-2}$ ◇ 5°C ▽ 22°C + 37°C

interaction between the protein molecules in the adsorbed state. Values for $c_p^{90\%}$, obtained at various conditions, are plotted against pH in figure 4.6. Although these data scatter considerably, they allow the conclusion that $c_p^{90\%}$ continuously increases with increasing pH (the 'baseline'), superimposed on which a maximum occurs around the i.e.p. The schape of the baseline indicates that the net electrostatic repulsion is not the only contribution to the lateral interaction, since in that case a pseudoparabola with its apex at the i.e.p. ought to be found. It would seem that the lateral interaction is also related to the extent of interaction between the HPA molecules and the polystyrene surface. This finding argues against a conformation of the adsorbed HPA molecules that is independent of the pH.

The maximum of the functionality $c_p^{90\%}$(pH) at the i.e.p. is also indicative of different adsorption mechanisms in the region of, and far away from, the i.e.p. It is remarkable that the maximum occurs at a pH value where the net charge on the HPA molecules is practically zero. It suggests that it is not the total charge but the way in which the charge is distributed over the molecule, that dominates the lateral interaction. From dielectric studies it has been deduced that the native HPA molecule has a net dipole moment in the direction of its short axis (VAN DER DRIFT, 1972). If, at the i.e.p., HPA molecules are adsorbed side-on in an unperturbed state, the dipoles, in parallel orientation, repel each other strongly. When the adsorbing molecules become flattened, the lateral distance between the dipoles increases and the repulsion is reduced. Thus, the analysis of $c_p^{90\%}$(pH) is not in conflict with the hypothesis that the decreasing values for $(\Gamma_p)_{max}$ at pH values far from the i.e.p. is due to pro-

gressive rearrangements in HPA molecules rather than to increasing distances between them and assuming that they adsorb in the same conformation at all pH's.

In the pH range studied, the HPA molecules do not become completely unfolded, i.e. with all amino acids in contact with the adsorbent, since in that case the amount adsorbed would approach ca. 0.6 mg m^{-2}.

With RNase the effect of pH on $(\Gamma_p)_{max}$ is much less pronounced than with HPA (cf. NORDE and LYKLEMA, 1975). The curves for $(\Gamma_p)_{max}$ vs. pH tend to pass through a maximum at neutral pH values. A similar trend has been observed by KHAÏAT and MILLER (1969) for the adsorption of RNase at an air-water interface and at a condensed lecithin monolayer. At pH 11 $(\Gamma_p)_{max}$ is significantly smaller than at lower pH values. Only for the adsorption on latex C-3 ($\sigma_0 = -15.5$ μC cm^{-2}) in media of 0.01 M ionic strength, is $(\Gamma_p)_{max}$ strongly dependent on the pH.

The quantity of RNase that can be accomodated in monolayers of close-packed molecules adsorbed in an unperturbed state ranges between 1.2 and 1.9 mg m^{-2}. These values allow for a hydration layer of 0.5 nm around the RNase molecules.

By analogy with the discussion for HPA, it seems that over the whole pH range the RNase molecules adsorbed on latex L-1 ($\sigma_0 = -2.3$ μC cm^{-2}) are either partially perturbed or do not form a complete monolayer. However, the latter situation seems unlikely since in that case $(\Gamma_p)_{max}$ would be expected to be dependent on the charge of the protein (i.e. pH) to a larger extent than is observed experimentally.

Except at high pH values, the maximum amounts adsorbed on latex C-3 could be explained by a complete monlayer of RNase molecules of unperturbed dimensions, which, for the case of adsorption at 0.01 M ionic strength, undergo different degrees of tilting on changing the pH. However, these experiments do not confirm the reality of this picture of the adsorbed layer (see also section 4.3.2.2.).

4.3.2.2. Effect of ionic strength

The effect of the ionic strength, in these cases c_{KNO_3}, on the adsorption isotherms of HPA and RNase has been tested at 22°C, using latices L-1 and C-3 as the adsorbents. Experiments have been performed at concentrations of KNO_3 of 0.01 M and 0.05 M.

Upon increasing c_{KNO_3} from 0.01 M to 0.05 M, the electrokinetic potential (= ζ-potential) of the polystyrene particles is reduced by some 30% (see table 2.4.). The effect of c_{KNO_3} on the ζ-potential of the dissolved HPA and RNase molecules can be observed by comparing the corresponding curves in figures 5.12. and 5.13., respectively.

For HPA, at pH < ca. 5, ζ is less positive and, at pH > ca. 5, less negative at higher c_{KNO_3}.

The affinity between the HPA molecules and the polystyrene surface, as judged from the initial slopes of the isotherms, seems to be governed by the overall Coulombic interactions (see section 4.3.2.1.). Therefore, it would be expected that, on increasing c_{KNO_3} from 0.01 to 0.05 M, at pH < 5 the affinity between HPA and the polystyrene surface would decrease, whereas it would increase at pH > 5. However, in figure 4.3. it can be seen that the effects of c_{KNO_3}, experimentally found, are not in line with these predictions. It suggests that the electrolyte primarily exerts its influence on the adsorption process in a different way, for example by affecting the conformational stability of the protein and/or by being taken up in the adsorbed layer (see section 5.5.2.).

At all pH values, over the range considered, the ζ-potential for RNase is more negative at 0.05 M KNO_3 as compared to 0.01 M KNO_3. Because the adsorption isotherms for RNase all show a high-affinity character, no satisfactory definite conclusions concerning the effect of c_{KNO_3} on the affinity of the RNase molecules for the polystyrene surface can be drawn from them.

The curves in figure 4.4. show that in the region of the isoelectric point the maximum amount of adsorbed HPA is not significantly influenced by c_{KNO_3}. However, at other pH values $(\Gamma_p)_{max}$ increases with increasing c_{KNO_3}, except at relatively high pH values (pH $\geq$ 7) where the c_{KNO_3} seems again to have little effect. TANFORD et al (1955b) and TANFORD and BUZZELL (1956) reported that the conformational stability of dissolved PA towards the pH of the medium increases with increasing ionic strength (see also section 3.2.1.). Hence, the the larger values for $(\Gamma_p)_{max}$ at higher c_{KNO_3} can be explained in terms of a lesser extent of conformational changes in HPA molecules adsorbed at pH's far from the i.e.p.

Figure 4.5. shows that the amount of RNase maximally adsorbed on latex L-1 is essentially the same in media of 0.01 M and 0.05 M KNO_3. The adsorbed layer at this surface probably consists of partially perturbed RNase molecules (section 4.3.2.1.). Hence, it is concluded that, over the pH range studied, the conformational stability of the RNase molecule does nog change very much on varying c_{KNO_3} between 0.01 and 0.05 M. This conclusion is consistent with the conclusion of BUZZEL and TANFORD (1956), that the molecular dimensions of dissolved RNase as a function of pH are not substantially influenced by variations in the ionic strength (see also section 3.2.2.).

The causes underlying the effect of c_{KNO_3} on $(\Gamma_p)_{max}$ for RNase at the surface of latex C-3 are not clear. In view of the previously mentioned influence of the ionic strength on the structure of the dissolved RNase molecule, it is not plausible to assume that the difference in $(\Gamma_p)_{max}$, occuring at neutral pH values, is due to larger conformational changes in media of higher salt concentration. The

possibility, already suggested in section 4.3.2.1., that the different values for $(\Gamma_p)_{max}$ reflect different orientations of RNase molecules of the same dimensions, seems more likely. Alternatively, the relative large amounts adsorbed may be the result of a certain degree of association of RNase molecules at the interface, which, in view of the irreversibility of the adsorption process, is not lowered upon dilution.

4.3.2.3. Effect of temperature

The adsorption of HPA and RNase on the polystyrene latices L-1 and C-3, each containing 0.05 M KNO_3, have been studied at 5°C, 22°C and 37°C.

The initial parts of the adsorption isotherms for HPA are strongly temperature dependent (figure 4.3.). Both at pH < i.e.p. and pH > i.e.p. the initial slopes steepen continuously with increasing temperature. In the region of the i.e.p. no difference could be observed between the initial slopes at 5°C and 22°C, but on raising the temperature to 37°C the initial slope increases.
According to the equation of Clausius-Clapeyron

$$\left(\frac{\delta \ln c_p}{\delta T}\right)_{\Gamma_p} = -\frac{\Delta H_{ads}}{RT^2} \qquad (4.1.)$$

increased adsorption at higher temperatures implies a positive enthalpy of adsorption, ΔH_{ads}, and, hence, a substantial entropic contribution to the Gibbs free energy of adsorption. This conclusion, however, is questionable since application of equation (4.1.) requires (i) reversibility and (ii) isosteric conditions. As mentioned before, the adsorption process is irreversible. Also, the assumption of isosteric conditions, which implies that at a given amount adsorbed the conformation of the adsorbed protein layer is independent of the temperature, seems to be unjustifiable.

Still, the different effects of temperature on the initial adsorption point to different adsorption mechanisms at the isoelectric pH and the other pH values, respectively. This is in agreement with the concept of different extents of structural alterations in the adsorbing HPA molecules. This picture has been put forward as the most plausible explanation for the dependence of $(\Gamma_p)_{max}$ on pH (section 4.3.2.1.).

According to the above reasoning, the effects of temperature on the initial slopes leads to the expectation that the maximum amount of isoelectric HPA adsorbed is essentially the same at 5°C and 22°C, but that it is significantly lower at 37°C. In figure 4.4. it can be seen that this expectation is confirmed by the experiments.

With RNase no significant effect of temperature, either on the initial slopes or on the platform values of the isotherms, could be observed. It suggests that the dimensions of the adsorbed RNase molecules are not affected very much by variations in the temperature of adsorption between 5°C and 37°C.

4.3.3. *Concluding remarks*

The isotherms for the adsorption of HPA and RNase at differently charged polystyrene surfaces contain several interesting features, although some of them are difficult to understand. Interpretation in terms of a Langmuir-plot or on the basis of the theories for homopolymer adsorption would obscure several subtleties and hence must be regarded as too crude.

Bearing in mind that the adsorption mechanism is different at low and high surface coverage, it is not surprising that transitions can occur in the range of intermediate adsorptions. These transitions are probably responsible for the inflection points, or steps, that are sometimes observed in the isotherms for HPA (figure 4.1.).

There are also several reports in the literature, for the adsorption of PA and other proteins at various interfaces, where $(\Gamma_p)_{max}$ is found to be maximal in the isoelectric region of the protein under consideration (see section 3.3.1.). The fact that this trend is independent of the nature of the adsorbent supports the present idea that the decrease of the amount adsorbed with increasing distance from the i.e.p. is due to a property of the protein molecule itself. The experimental data, obtained in this study, indicate that the conformational stability of the HPA molecule, i.e. its internal coherence, is one of the main molecular properties determining the maximum adsorption at the polystyrene surface. At the i.e.p., where an equal number of positively and negatively charged groups are present in the protein molecule, the molecular structure is expected to be relatively most stable (cf. section 3.2.). The fact that for RNase $(\Gamma_p)_{max}$ is less sensitive to the pH may then be explained by the greater conformational stability of RNase with respect to pH (BUZZELL and TANFORD, 1956).

The reason for the lower plateau value of adsorption when using latex L-1 ($\sigma_0 = -2.3$ μC cm $^{-2}$) as compared to latex C-3 ($\sigma_0 = -15.5$ μC cm^{-2}), observed both with HPA and RNase (figures 4.4. and 4.5.), is not clear-cut. This effect may be due to differences in charge density and/or hydrophobicity of the latex surface.

The influence of temperature on the initial adsorption of HPA (figure 4.3.) suggests that, at least outside the isoelectric region, entropic factors dominate the interaction between HPA and the polystyrene surface (section 4.3.2.3.). This feature agrees with the observation, made both with HPA and RNase, that the adsorption is not directly governed by the overall Coulombic interaction between the protein molecule and the polystyrene particle.

According to DEŽELIĆ and DEŽELIĆ (1970), HPA retains its immunochemical activity against specific antibodies after adsorption at polystyrene surfaces at pH ca. 8.0. In spite of this, these authors also conclude that the adsorbing HPA molecules change their conformation (DEŽELIĆ et al, 1971). Apparently, either the conformation of the HPA molecules is not very crucial with respect to its immunochemical activity or the physiologically active site does not change appreciably.

In the present study it was found that after adsorption from solutions over the pH range 4 to 11, the enzymatic activity of RNase is reduced almost to zero. Conformational changes and/or inaccessibility of the active site for the substrate (= ribonucleic acid) are the most probable causes underlying this effect.

4.4. Bound fraction

The bound fraction v_p is defined as the fraction of the adsorbed protein that is in actual contact with the surface. Generally, it depends on the amount adsorbed, Γ_p, and the degree of coverage, θ_s, of the adsorbent surface by the first layer

$$v_p = \frac{M_s}{A_s N_{Av}} \times \frac{\theta_s}{\Gamma_p} \tag{4.2.}$$

where M_s is the average molecular weight of the sements of the protein attached to the polystyrene surface, A_s the average interfacial area per attached segment and N_{Av} Avogadro's number. Substituting in equation (4.2.) for M_s, A_s and N_{Av} values of 100 g mole $^{-1}$, 0.30 nm^2 and 6.03 $\times$ 10^{23} mole^{-1}, respectively, yields

$$v_p = \theta_s/1.819\ \Gamma_p \tag{4.3.}$$

in which Γ_p is expressed in mg m^{-2}.

The following discussion will be limited to plateau levels of adsorption.

The low values of $(\Gamma_p)_{max}$ for both HPA and RNase have been attributed to adsorption of partially perturbed molecules in a complete layer (section 4.3.2.). Since this perturbation is the result of the protein molecules rearranging themselves in order to increase their contact with the polystyrene surface, θ_s is expected to increase with increasing extent of these rearrangements.

For adsorption of unperturbed molecules of BPA and bovine prothrombin at silica surfaces, Morrissey and Stromberg (1974) reported that a fraction of ca. 0.11 of the carboxyl groups is bound at the silica surface. The molecular size and shape are very similar between these two proteins. Based on the molecular dimensions of (B)PA, mentioned in table 3.1., a side-on orientation of molecules adsorbed in their unperturbed states leads to $v_p = 0.11$ if the fraction of the molecule within a distance of 0.55 nm from the adsorbent surface is regarded as bound. By analogy, in an end-on orientation this distance amounts to 2.40 nm. Hence, the results of Morrissey and Stromberg strongly suggest that the protein molecules are adsorbed side-on. Since in a complete monolayer of side-on oriented native molecules of BPA, or bovine prothrombin, ca. 2.5 mg m^{-2} can be accomodated, the corresponding degree of coverage of the adsorbent surface by bound segments is, according to equation (4.3.), ca. 0.50.

In the present experiments the plateau levels of adsorption of HPA and RNase

at polystyrene surfaces have been interpreted in terms of a complete monolayer of molecules that are more or less spread out. In view of the foregoing, for the adsorption of both HPA and RNase $\theta_s = 0.50$ has been assumed at those values of $(\Gamma_p)_{max}$ that are equal or exceed the value that can be accounted for by a complete monolayer of side-on adsorbed molecules in their unperturbed states, i.e. $(\Gamma_p)_{max} = 2.50$ mg m^{-2} for HPA and $(\Gamma_p)_{max} = 1.20$ mg m^{-2} for RNase. On the other hand, complete coverage of the polystyrene by completely unfolded protein molecules is characterized by $\theta_s = 1.00$, $v_p = 1.00$ and $(\Gamma_p)_{max} = 0.55$ mg m^{-2} ($A_s = 0.30$ nm^2 and $M_s = 100$ g mole^{-1}). As a first approximation, the values for θ_s at intermediate values of $(\Gamma_p)_{max}$ are estimated by linear interpolation between $\theta_s = 0.50$ and $\theta_s = 1.00$.

Thus, using equation (4.3.), v_p can be calculated as a function of $(\Gamma_p)_{max}$. The results for HPA and RNase are shown in graphical form in figure 4.7. According to equation (4.3.), at a given value of $(\Gamma_p)_{max}$, v_p is proportional to θ_s. In view of the way θ_s has been estimated as a function of $(\Gamma_p)_{max}$, the uncertainty in θ_s and, hence, in v_p may be of the order of ca. 25%.

As v_p represents the fraction of the protein in the first layer adjacent to the polystyrene surface, the curves in figure 4.7. may give some information on the effect of $(\Gamma_p)_{max}$ on the distribution of the segments of the protein in the adsorbed layer.

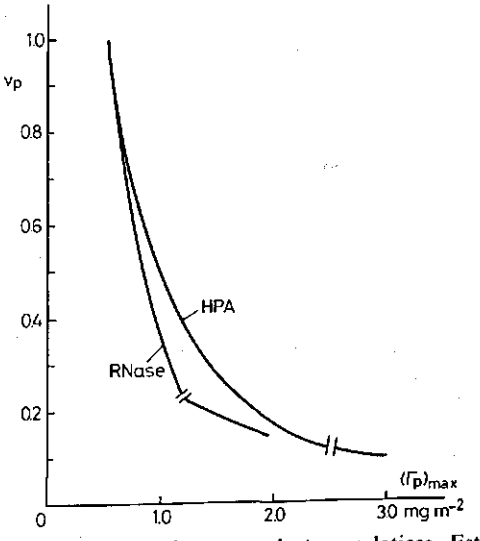

FIG. 4.7. Adsorption of HPA and RNase on polystyrene latices. Estimate of the bound fraction as a function of the maximum adsorbed amount. The break in the curve corresponds to the attainment of a complete monolayer of side-on adsorbed unperturbed protein molecules.

4.5. Thickness and fraction of the adsorbed layer occupied by the protein

It is obvious that, at a given amount of protein adsorbed, the thickness of the adsorbed layer is directly related to its structure. The question whether or not structural changes in HPA and RNase molecules occur upon adsorption at polystyrene surfaces has been discussed in section 4.3.

If the protein molecules are adsorbed in their unperturbed states, the thickness of the adsorbed layer may be approximated on the basis of the dimensions of the molecules in solution (see table 3.1.) and their orientation at the interface. However, if adsorbing protein molecules undergo structural alterations the thickness of the layer is much more difficult to estimate, since the modes of these alterations are not directly known. In this regard, two extreme situations for the adsorbed layer may be distinguished:

(i) The adsorbed layer is completely made up of protein, i.e. the volume fraction of the protein in this layer equals unity. In this case, the thickness of the adsorbed layer follows from the amount adsorbed and the density of the protein in the adsorbed state.

(ii) The adsorbed protein molecule assumes a very loose structure. It is adsorbed in a conformation as is generally assumed for randomly coiled polymers. Trains of segments are attached at the adsorbent surface, and, when relatively large amounts are adsorbed, long loops and tails protrude into the solution (see e.g. Fleer et al, 1972). Hence, the volume fraction of the protein in the adsorbed layer is small. Obviously, in this case the adsorbed layer is much thicker than it would be in the case of a compact structure of the adsorbed protein molecules.

For the adsorption of HPA and RNase on polystyrene latices, the probability of a compact or loose structure of the adsorbed layer will be discussed on the basis of the following considerations.

Some experimental data plead against the existence of a loose structure of HPA molecules adsorbed at pH values outside the isoelectric region. Firstly, from hydrogen ion titrations with HPA (to be discussed in section 5.3.3.), it is concluded that the distance between the average position of the carboxyl groups (i.e. the *polar* glutamic acid and aspartic acid residues) in the adsorbed protein molecules and the polystyrene surface is reduced at the lower plateau levels of adsorption that are obtained on moving the pH away from the i.e.p. of HPA. This finding would suggest a flattening of the adsorbed protein molecules rather than unfolding into a loose structure. Secondly, as mentioned in section 4.3.3., in spite of indications for some degree of structural changes, Deželić and Deželić (1970) observed physiological activity of HPA adsorbed on polystyrene latex at pH 8. Physiological activity would only be expected if the compact conformation of HPA in solution is more or less retained after adsorption. Thirdly, Musselwhite and Kitchener (1967), who investigated the adsorption of BPA at air-water interfaces, found that the adsorbed protein layer tends to be thinner the further the pH of adsorption is removed from the i.e.p. At pH 7,

for a film, consisting of two protein layers enclosing a hydration layer, a limiting thickness of 3.5 nm was recorded.

These examples provide convincing evidence that, at least with regard to the present study, the conformational changes induced by the adsorption do not greatly destroy the compactness of the HPA molecules. Even so, the average position of the carboxyl groups in the HPA molecules adsorbed at pH values away from the i.e.p. and the thickness of the BPA film at pH 7 suggest a flattening of the protein molecule and, hence, an increased volume fraction of the protein in the adsorbed layer.

It is known that the internal coherence in RNase is much greater than in HPA (see section 3.2.3.). Therefore, also for RNase it is assumed that decreased plateau levels of adsorption correspond to a smaller thickness of the adsorbed layer.

Moreover, preliminary ellipsometric measurements[1] with both HPA and RNase seem to point to a decreasing thickness of the adsorbed layer with decreasing amount adsorbed.

In view of the foregoing discussion, it would seem that, at adsorption saturation, the volume fraction ϕ_p of HPA and RNase in the various layers on the

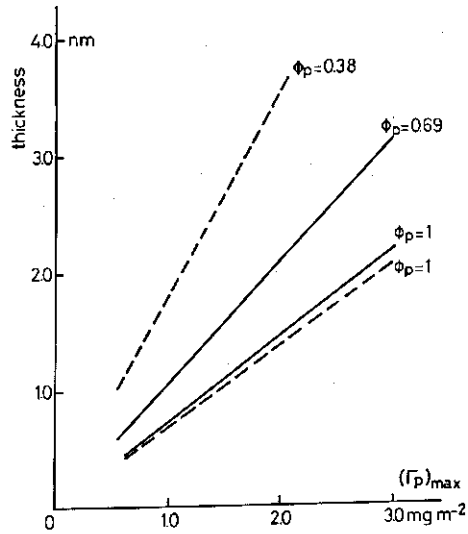

FIG. 4.8. Adsorption of HPA and RNase on polystyrene latices. Estimate of the thickness of the adsorbed layer as a function of the maximum adsorbed amount at various volume fractions of the protein in the adsorbed layer. —— HPA – – – RNase

[1] These experiments were performed at the Laboratory of Cardiobiochemistry, University of Leyden, The Netherlands. Drs. P. A. Cuypers and W. Th. Hermens are kindly acknowledged for their help and advice.

polystyrene latices varies between unity and that of a layer of side-on oriented unperturbed molecules (i.e. $\phi_p = 0.69$ for HPA and $\phi_p = 0.38$ for RNase). The corresponding ranges for the thickness of the protein layers are shown as a function of $(\Gamma_p)_{max}$ in figure 4.8. For both cases the density of the protein in the adsorbed state is taken equal to that in the dissolved state.

In the sections 4.3.2. and 4.3.3. it has been concluded that, under most conditions investigated, RNase undergoes little or no conformational changes upon adsorption. Thus, on the basis of the above semi-quantitative arguments, it can be concluded that ϕ_p in adsorbed layers of RNase tends to be lower than in adsorbed layers of HPA.

4.6. Summary

The amounts of HPA and RNase adsorbed at negatively charged polystyrene surfaces have been determined (figures 4.1.–4.5.). The adsorption has been studied under different conditions of charge on both the adsorbate and adsorbent, ionic strength (0.01 M and 0.05 M KNO_3) and temperature (5°C, 22°C and 37°C).

In section 4.3. it has been shown that the mode of adsorption depends very much on the properties of the protein in solution. Especially with HPA, the accumulated evidence strongly points to a certain amount of conformational alteration of the protein upon adsorption at the polystyrene surface. The extent of this alteration increases with decreasing conformational stability of the dissolved molecule (i.e. with increasing net charge, with decreasing ionic strength and with increasing temperature). In the case of RNase less insight has been obtained regarding structural changes in the adsorbing molecules. In general, the maximum amount of RNase adsorbed is not so sensitive to variations in the pH, the ionic strength and the temperature. The differences in adsorption behaviour between HPA and RNase can, for a great part, be traced to the fact that dissolved RNase does not adapt its structure to environmental changes as readily as HPA.

Judging from the shapes of the initial parts of the isotherms, at all conditions tested RNase shows a high affinity towards the polystyrene surfaces. The affinity between HPA and the polystyrene surface appears to be influenced by Coulombic interactions, viz. the initial slopes steepen with increasing charge difference (figure 4.3.). Nevertheless, adsorption still occurs with HPA when the adsorbate and the adsorbent are both negatively charged. It indicates that the adsorption is not governed by Coulombic interactions. The effect of temperature, shown in figure 4.3., suggests that away from the isoelectric region where the adsorbed molecules are assumed to have changed their conformation to a relatively large extent, the binding between HPA and the polystyrene surface is characterized by a net entropy gain. Hydrophobic bonding and/or increased mobility inside the protein molecule may be largely responsible for this entropy gain.

Both for HPA and RNase the plateau levels of adsorption increase with increasing charge density at the polystyrene surface. It is not clear whether this should be ascribed to an electrostatic or a hydrophobic effect.

Based on the concept of conformational changes upon adsorption, rather than the formation of an incomplete layer of unperturbed protein molecules, the weight fraction of the protein in the first layer adjacent to the polystyrene surface has been estimated as a function of the maximum amount adsorbed (section 4.4.). Some data available in the literature have been used for this purpose. The bound fraction of protein rises with decreasing plateau level of adsorption, as indicated in figure 4.7.

Section 4.5. is concerned with the thickness of the adsorbed layer. This thickness has been approximated on the basis of considerations regarding the volume fraction of the protein in the adsorbed layer. It appears plausible that, after conformational alterations, the adsorbed molecules retain a compact structure. Finally, the general conclusion is made that in the adsorbed layers of RNase relatively more protein-void space exists than in the case of HPA.

5. ELECTROSTATIC ASPECTS OF THE ADSORPTION

5.1. INTRODUCTION

Charged polystyrene particles and charged protein molecules in solution are both surrounded by counterions. In the case of the polystyrene latex it has been shown in section 2.3.5. that a fraction of the counterions are specifically adsorbed at the polystyrene surface, the remainder being distributed in a diffuse layer. In general, protein molecules also bind ions to a greater or lesser extent. The unusually high ability of PA to bind anions has already been mentioned in section 3.2.1. By analogy with the specifically adsorbed ions at the polystyrene surface, the ions bound to the protein are defined here as those causing the difference between the charge titratable with hydrogen ions and the electrokinetic charge of the protein molecule. Thus, the ions bound in the interior of the protein molecule as well as those that are located in the shear layer are referred to as 'bound'. Hence, the electrokinetic charge of the protein is solely balanced by counterions in the diffuse layer.

After adsorption of protein molecules onto the polystyrene particles, the electrical double layers of the protein molecules and the polystyrene particles overlap each other. As a consequence, the amounts and the distributions of the ions in both the diffuse and the non-diffuse parts of these layers will undergo alterations. Simultaneously, the interacting electric fields may affect the dissociation of the titratable groups of the adsorbed protein molecules and those at the polystyrene surface. Together with other effects, due to specific interactions of different kinds between reactive groups of the protein molecule and the latex surface, this may result in a change in the relation between the net proton charge Z_H and the pH for both the protein and the latex.

In view of the obvious importance of electrostatic aspects of the interactions, hydrogen ion titrations and electrophoresis measurements of polystyrene latices, dissolved HPA and RNase and of HPA and RNase adsorbed on the polystyrene particles have been performed. The most important variables in these experiments are the pH (the charge of the protein) and the surface charge of the polystyrene. Because they reflect different types of interaction, insight into the electrostatic contributions is, in turn, useful in the elucidation of the mechanism of protein adsorption.

5.2. MATERIALS

The polystyrene latices indicated by L-1 and C-3 were used in this study. Their surface charge densities amount to -2.3 and -15.5 $\mu C\ cm^{-2}$, respectively. A detailed description of their properties and features has been given in chapter 2.

The solution of HPA and RNase were prepared as described in section 4.2. All other chemicals used were of analytical grade. The water was distilled from an all-Pyrex apparatus.

5.3. Hydrogen ion titration

Like all proteins, HPA and RNase contain a variety of acidic and basic groups. The net proton charge on a protein molecule in equilibrium with a solution is reflected in its hydrogen ion titration curve, showing Z_H of the protein as a function of pH. From the titration curves the number of dissociating groups of various kinds, together with their dissociation constants, can be accurately estimated. Such analyses have been made by Tanford et al (1955b) for BPA and by Tanford and Hauenstein (1956) for RNase. In both cases the authors obtained good agreement between the number of groups found by titration and that predicted from the amino acid content. Table 5.1. summarizes the results of these investigations.

Table 5.1. Titratable groups and their dissociation constants (comprising the intrinsic and the medium term), $K_{int+med}$, in BPA and RNase. $T = 25°C$.

group	BPA, mol. wt. = 69,000 number	$pK_{int+med}$	RNase, mol. wt. = 13,680 number	$pK_{int+med}$
α-carboxyl	1	3.8	1	3.75
β-, γ-carboxyl	105	4.0	10.2	4.0–4.7
imidazole	17	6.9	4	6.5
α-amino	1	7.8	1	7.8
ε-amino	60	9.8	10	10.2
phenolic OH	20	10.4	3	9.95
			3	inaccessible
guanidyl	23	>12	4	≥12

Tanford et al (1955b) pointed out that the titration behaviour of HPA is only slightly different from that of BPA. This has been confirmed by Steinhardt et al (1971).

5.3.1. *Theory*

As a rule, the titration curves of proteins do not coincide with the titrations of the contributing functional groups in their free state. The main reason for this must be Coulombic interactions, but location in a hydrophobic region of the protein molecule and involvement in hydrogen bonding would also affect the dissociation constant of the group under consideration.

As a first step, the Gibbs free energy of dissociation ΔG of a hydrogen ion from any particular group can be split up into an intrinsic, a medium and an electrostatic term

$$\Delta G = \Delta G_{int} + \Delta G_{med} + \Delta G_{el} \qquad (5.1.)$$

The intrinsic contribution should equal the Gibbs free energy of dissociation of the isolated group at an infinitely low concentration in water. The medium term includes all environmental effects and interactions of the group with other groups. The electrostatic contribution represents the amount of reversible isothermal work required to remove a hydrogen ion, after dissociating, from the immediate vicinity of the charged protein molecule to infinity.

Apart from being involved in specific short-range interactions with titratable groups of the protein molecule, similar to formation of ion pairs, the charged polystyrene surface is expected to influence the dissociation of functional groups in adsorbed protein molecules by changing the medium and the electric field. Moreover, lateral interactions between and conformational alterations, if any, in the adsorbed protein molecules may contribute to changes in the titration behaviour of the proteins as a result of adsorption.

The apparent dissociation constant of any one class of groups is related to the pH through

$$pK_{aj} = pH + \log [(1-\alpha_j)/\alpha_j] \tag{5.2.}$$

where pK_{aj} is the negative log of the apparent dissociation constant of the n_j groups of class j and α_j their degree of dissociation. Writing pK_{aj} in terms of the Gibbs free energy of dissociation results in

$$pK_{aj} = 0.434\,(\Delta G_{int} + \Delta G_{med} + \Delta G_{el})/RT \tag{5.3.}$$

Combining equations (5.2.) and (5.3.) yields the formula

$$pH = 0.434\,(\Delta G_{int} + \Delta G_{med} + \Delta G_{el})/RT - \log [(1-\alpha_j)/\alpha_j] \tag{5.4.}$$

After introducing the intrinsic dissociation constant, K_{ij}, equation (5.4.) may be modified to read

$$pH = pK_{ij} - \log [(1-\alpha_j)/\alpha_j] + 0.434\,(\Delta G_{med} + \Delta G_{el})/RT \tag{5.5.}$$

Equation (5.5.) will be used in the analysis of the variation in the titration behaviour of a protein, arising from adsorption.

If equal Z_H values for the dissolved and for the adsorbed protein molecules implies the same degree of dissociation of the jth class of groups in both states, then subtraction of equation (5.5.) applied to an adsorbed protein molecule from the same equation applied to a dissolved one, gives

$$\begin{aligned}(pH^{ads} - pH^{sol})_{Z_H} &= 0.434(\Delta G^{ads}_{med} - \Delta G^{sol}_{med})/RT + \\ &+ 0.434(\Delta G^{ads}_{el} - \Delta G^{sol}_{el})/RT\end{aligned} \tag{5.6}$$

The subscript Z_H implies that this quantity is constant.

Since ΔG_{el} can be expressed by

$$\Delta G_{el} = -F\psi \tag{5.7.}$$

where F is the Faraday constant and ψ the electrostatic potential at the place of the dissociating group, equation (5.6.) may be written as

$$\begin{aligned}(pH^{ads} - pH^{sol})_{Z_H} &= 0.434(\Delta G^{ads}_{med} - \Delta G^{sol}_{med})/RT - \\ &- 0.434F(\psi^{ads} - \psi^{sol})/RT\end{aligned} \tag{5.8.}$$

If the condition for obtaining equation (5.6.) is satisfied, equation (5.8.) may be used in interpreting the variations in the titration curves of a protein upon adsorption.

5.3.2. *Experimental procedure*

Prior to mixing, the polystyrene latices and the protein solutions were adjusted to 0.05 M KNO_3 and to the desired pH (see table 5.2.). 50 cm^3 of polystyrene latex (ca. 8% w/w) were mixed with 25 cm^3 of protein solution in glass-stoppered 100 cm^3-flasks. The concentration of the protein was chosen in such a way as to ensure adsorption saturation (see section 4.3.2.). Thus, HPA solutions of ca. 9.0 g dm^{-3} and RNase solutions of ca. 4.5 g dm^{-3} were used. In these experiments, the adsorption was allowed to take place at room temperature and under conditions similar to those mentioned in section 4.3.1. After centrifugation at 25 °C, the protein concentration in the clear supernatant was determined according to the method described in section 4.3.1.1. The sediment was redispersed in a 30 cm^3 aqueous solution of 0.05 M KNO_3 and rotated end over end for two hours. The pH of the dispersion, thus obtained, did not differ significantly from the pH of the dispersion directly after adsorption. The dispersion was then centrifuged again. No protein could be detected in the supernatant which implies that the protein molecules are adsorbed irreversibly (cf. section 4.3.2.). The sediment was redispersed in 7.0 cm^3 0.05 M KNO_3 aqueous solution and kept in a glass-stoppered vial at 3 °C until it was used for titration. Blank samples, containing no protein but otherwise identical, were subjected to the same analysis. The titrations were performed within three days of preparing the samples.

5 cm^3 of each of these samples, as well as 5 cm^3 of HPA and RNase in 0.05 M KNO_3 aqueous solution, were titrated[1]. The titrations were carried out at 25 °C under argon gas using 0.07579 M NaOH or 0.07579 M HCl as the titrant. The titrant was added at constant time intervals by means of a high precision microburette. The time intervals were chosen in such a way that, before the next addition, equilibrium was reached. In the samples containing adsorbed protein, equilibrium usually was obtained at a slower rate than in the other samples. The time intervals were set at two minutes and one minute, respectively. Just before each addition ten pH readings were taken and averaged.

To obtain maximum reproducibility the titration device was completely automated. A detailed description of it has been given by VAN OS et al (1972).

The samples were titrated in both directions of pH, according to the scheme presented in table 5.2.

The values for the pH of adsorption in table 5.2. refer to the pH before mixing. The pH of the dispersion changes upon adsorption of protein, as was mentioned in section 4.3.2.1. The reasons underlying this feature will be discussed in the following section.

[1] Thanks are due to the Department of Biophysical Chemistry of the University of Nijmegen, The Netherlands, for granting the facilities to perform the titration experiments.

TABLE 5.2. Scheme of the titration experiments. $c_{KNO_3} = 0.05$ M $T = 25°C$

sample	pH of adsorption	titration over approximate pH region	
HPA adsorbed on polystyrene latices L–1 and C–3	3.6	4 → 8	8 → 4
	4.0	4 → 8	8 → 4
	4.6	4.6 → 8	8 → 4
		4.6 → 4	4 → 8
HPA adsorbed on polystyrene latex L–1	7.3	7.3 → 4	4 → 8
HPA adsorbed on polystyrene latex C–3	8.0	8 → 4	4 → 8
RNase absorbed on plystyrene latices L–1 and C–3	4.0	4 → 11	11 → 4
	7.0	7 → 11	11 → 4
		7 → 4	4 → 11
	9.3	9.3 → 11	11 → 4
		9.3 → 4	4 → 11
	11.0	11 → 4	4 → 11
polystyrene latices L–1 and C–3		3 → 11	11 → 3
HPA in solution		4 → 8.5	8.5→ 4
RNase in solution		4 → 11	11 → 4

5.3.3. *Results and discussion*

The amounts of HPA and RNase adsorbed on both latices are given in table 5.3. They agree well with the plateau values of the corresponding isotherms shown in section 4.3.2. (figures 4.4. and 4.5.), where the surface area of polystyrene present per unit volume is about five times as less.

Since the protein molecules appear to be adsorbed irreversibly, virtually no dissolved protein would have been present in the samples prepared for titration. According to the experimental results concerning the reversibility of the adsorption with respect to the pH (see section 4.3.2.1.), it is noted here that the amounts of protein adsorbed do not significantly change upon varying the pH of the samples during the titration experiments.

TABLE 5.3. Amounts (mg m^{-2}) of HPA and RNase adsorbed on polystyrene latices L–1 and C–3, under the conditions of the titration experiments (see text). $c_{KNO_3} = 0.05$ M $T = 22°C$

pH of adsorption	HPA		pH of adsorption	RNase	
	latex L–1	latex C–3		latex L–1	latex C–3
3.6	1.46	2.12	4.0	0.86	1.21
4.0	1.70	2.35	7.0	0.91	1.21
4.6	2.21	2.88	9.3	0.89	1.05
7.3	1.06		11.0	0.78	0.80
8.0		0.97			

From the amount of acid or base added to the sample and the concomitant change in the pH, $\Delta Z_H/\Delta pH$ can be calculated. To do this properly, corrections should be made for the amount of acid or base required to bring about corresponding pH changes in the blank samples. These amounts are negligible in the pH range 4–10.

The bare polystyrene surfaces do not contain a significant amount of groups titratable between pH 3 and 11. This may be expected since the latex surface charge arises from strong $-OSO_3^-$ groups. The intrinsic dissociation constant of these groups may be compared with that of benzene sulphonic acid, viz. ca. 2.0×10^{-1} M at 25°C.

Upon protein adsorption the permittivity at the polystyrene surface reduces and, hence, the sulphate groups at this surface may associate with cations, as described by the equation derived by FUOSS (1958)

$$\ln K_{ass} = \ln K^{o}_{ass} - \frac{z_+ z_- e^2}{4\pi\varepsilon\varepsilon_0 akT} \qquad (5.9.)$$

where K^o_{ass} is the non-Coulombic contribution to the association constant, z_+ and z_- the valencies of the associating positive and negative ions, e the elementary charge, $\varepsilon\varepsilon_0$ the permittivity of the medium, a the distance of closest approach between the ions and where kT has its usual meaning.

The ions in solution available for association with the sulphate groups at the latex surface are K^+ and H^+. The relative extent to which either ion is involved in the association with those sulphate groups is determined by the concentrations of K^+ and H^+ in bulk solution, according to

$$\frac{-OSO_3^-K^+}{-OSO_3^-H^+} = K_H^K \times \frac{c_{K^+}}{c_{H^+}} \qquad (5.10.)$$

in which K_H^K is the equilibrium constant (= selectivity coefficient) for the exchange equilibrium where, at the latex surface, H^+ is displaced by K^+.

In the systems currently studied $c_{K+} = 5 \times 10^{-2}$ M and c_{H+} is given by the pH ($c_{H+} \leq 10^{-4}$ M). Ion exchange studies in non-aqueous solvents of low permittivites using sulphonated polystyrene resins like Dowex 50 and Amberlite IR – 120 suggest that the selectivity coefficient K_H^K of these resins is in the order of 10^0 (GABLE and STROBEL, 1956; SAKAKI and KAKIHANA, 1953; BODAMER and KUNIN, 1953). By analogy, for the $-OSO_3^-$ groups at the protein-covered polystyrene surface a comparable value for K_H^K may be assumed. However, in this way K_H^K may be underestimated for these particular systems, since the larger K^+ ion, having a greater polarizability, is more likely to be transferred from the aqueous solution to the non-aqueous environment of the protein-covered polystyrene surface. Hence, in view of the large $c_{K+}:c_{H+}$ ratio, the contribution of H^+ to the neutralization of $-OSO_3^-$ groups at the polystyrene surface, after protein adsorption, is negligible.

The experimental results are recorded in the form of differential titration curves in figures 5.1. and 5.2. The titration of all the samples appeared to be

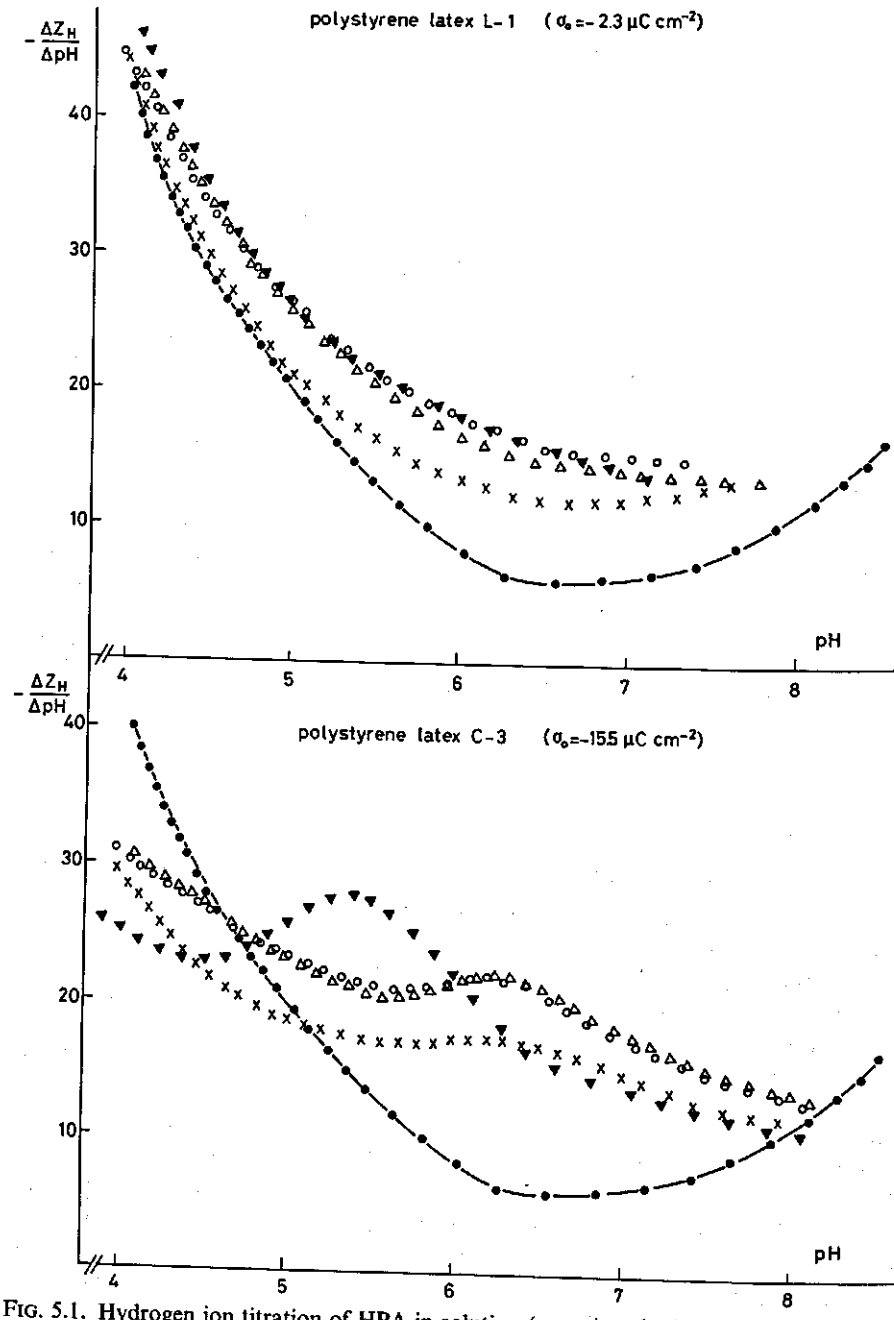

FIG. 5.1. Hydrogen ion titration of HPA in solution (—●—) and adsorbed on polystyrene latices. Experimental results. pH of adsorption 3.6 (○) 4.0 (△) 4.6 (×) and 7.3 or 8.0 (▼). c_{KNO_3} = 0.05 M T = 25°C.

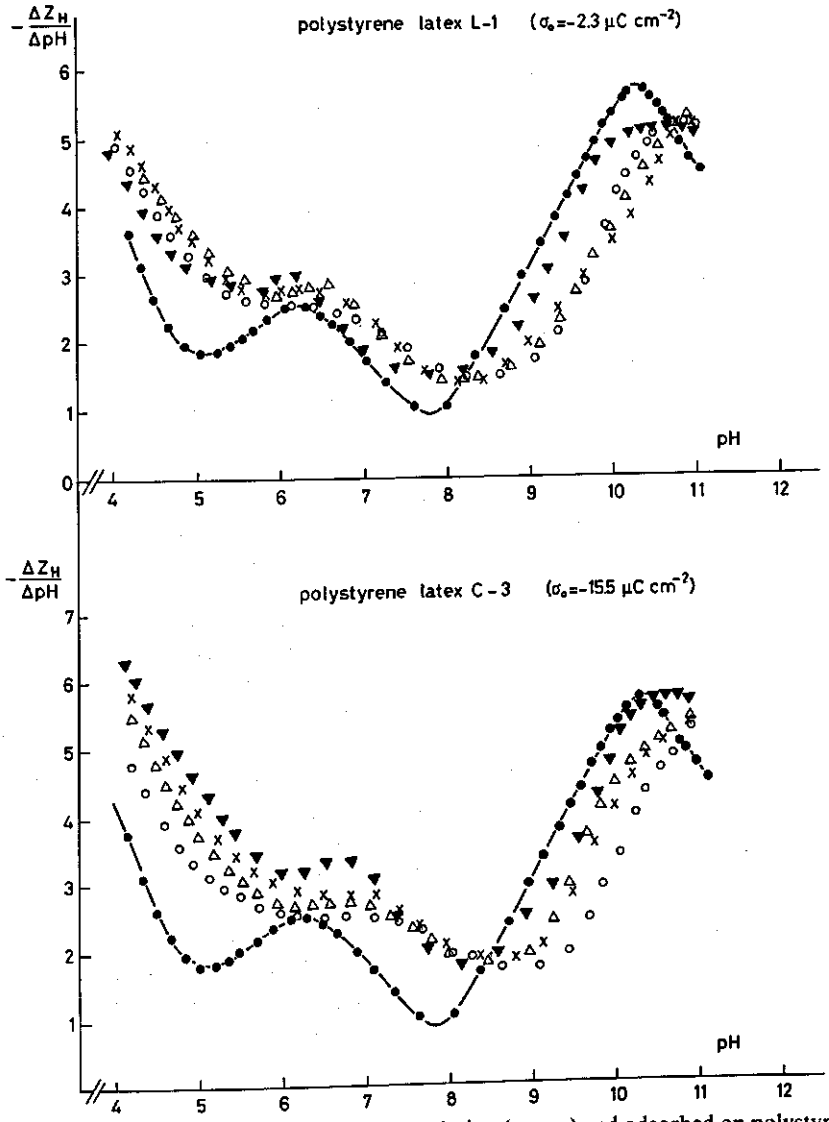

FIG. 5.2. Hydrogen ion titration of RNase in solution (—●—) and adsorbed on polystyrene latices. Experimental results. pH of adsorption 4.0 (○) 7.0 (△) 9.3 (×) and 11.0 (▼). c_{KNO_3} = 0.05 M T = 25°C.

reversible within one unit of Z_H. It can be seen that the titration behaviour of both HPA and RNase is drastically influenced by the adsorption at the polystyrene surface.

From the differential titration curves the integral ones (Z_H vs. pH) can be constructed, provided that Z_H at one point of this curve is known. The net

proton charge of a protein molecule is practically zero at its isoionic point (i.i.p.). Since for a protein in solution the i.i.p. is known, one can use this point as the reference point to construct the integral titration curve. At an ionic strength of 0.05 M, HPA and RNase attain their isoionic states at pH values of about 5.5 and 9.6, respectively (see section 3.2.3.). However, as a result of adsorption, the i.i.p.'s for both proteins shift in an undetermined way. Therefore, the reference point for the titration curve for adsorbed proteins must be established in a different way. In the present study, it has been estimated from the changes in pH that were observed upon adsorption.

In separate adsorption experiments with systems of identical composition as those used in the titrations, the change in pH upon adsorption was investigated as a function of the pH of adsorption. The results are shown in figure 5.3. At most pH values a positive change of pH due to the adsorption was observed, indicating a decreased degree of dissociation of the groups titrated over the pH region considered. This feature will be emphasized when discussing the integral titration curves Z_H (pH). At the pH of adsorption where ΔpH equals zero, from now on denoted as $pH_{r(eference)}$, no net uptake by, nor net release of protons from, the adsorbing protein molecules occurs, provided no surface groups of the polystyrene particles are protonated at that particular pH value. For HPA adsorbed on polystyrene latices L-1 and C-3 the values of pH_r, as estimated from figure 5.3., are ca. 7.3 and ca. 8.0, respectively. The same figure shows that for RNase pH_r amounts to ca. 11.0 for both polystyrene latices. If upon adsorption the pH does not vary, the Z_H value of the adsorbed protein molecule is equal to that of the protein molecule in solution. In this way, a reference point for the integral titration curves was established. It should be borne in mind that the conformation of the protein molecules at the interface, as well as the protein-polystyrene surface interactions, may depend on the pH of adsorption (cf. section 4.3.2.1.). Therefore, the value of Z_H for a protein molecule initially adsorbed from a solution at a pH $\neq$ pH_r, but which is then brought to pH_r, does not necessarily coincide with Z_H of the protein molecule in a solution of pH = pH_r. Hence, accurate location of the integral titration curves is only possible for the cases of dissolved protein and protein adsorbed at pH_r, but, so far, not for the cases where the pH does change upon adsorption.

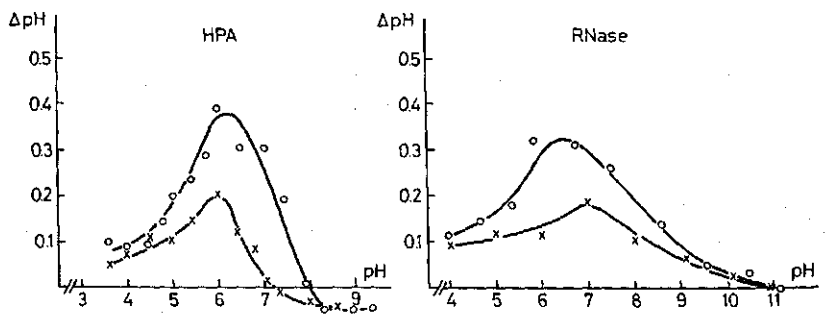

FIG. 5.3. Variation of pH due to the adsorption of HPA and RNase on polystyrene latices L-1 (×) and C-3 (○). c_{KNO_3} = 0.05 M T = 22°C.

5.3.3.1. Reciprocal differential titration curves: $\Delta pH/\Delta Z_H$ vs. Z_H

The occurrence of inflection points in the integral titration curves Z_H (pH) indicates distinct regions over which the different classes of groups are titrated. The values for Z_H at which these inflection points occur can be estimated much more accurately from the reciprocal differential titration curves $\Delta pH/\Delta Z_H$ (Z_H) than from the integral titration curves Z_H (pH).

Figures 5.4. and 5.5. show the reciprocal differential titration curves for the HPA series and the RNase series, respectively. For sake of clarity, in the cases of the adsorbed proteins the experimental points are given only.

In the curve for HPA in solution a maximum at $Z_H = -7.0$ is observed. Based on the data for HPA given in table 5.1. this maximum approximates to the completion of titration of a class of 108 negative groups. This class consists of 106 carboxyl groups of HPA itself and probably 2 carboxyl groups of fatty acids bound to this protein. At more negative Z_H values, i.e. at higher pH values, the other kinds of groups are titrated in the order of their pK values (see table 5.1.).

The curves for HPA adsorbed at pH_r do not show a maximum at a Z_H value of about -7. Therefore, in the adsorbed state the dissociation of the carboxyl and the imidazole groups overlap each other to a large extent. This becomes especially clear in the case of adsorption on latex C-3 which has the more negative surface charge.

In spite of the above considerations, the curves for HPA adsorbed at pH $\neq pH_r$ are presented on the basis of a common intersection point of the integral titration curves Z_H (pH) at pH_r. As each point $\Delta pH/\Delta Z_H$ represents an experimental determination, the possible error in the reciprocal differential titration curves, introduced by assuming such a common intersection point, implies an uncertainty with respect to the position of the curve along the abscissa. From these curves it is also evident that the titration regions of the carboxyl groups and the imidazole groups cannot be distinguished.

In figure 5.5. it is shown that the reciprocal differential titration curve for dissolved RNase comprises two maxima. Using the data for RNase given in table 5.1. it can be deduced that the maximum at $Z_H = 8$ reflects the completion of the titration of the 11 carboxyl groups. The region between the maximum at $Z_H = 8$ and the one at $Z_H = 3$ represents the titration of 5 groups, viz. 4 imidazole and 1 α-amino group. At more negative Z_H values the more basic groups are titrated, the titration regions of the ε-amino and the phenolic groups overlapping each other.

As for HPA, the positions of the reciprocal differential titration curves for RNase are *chosen* on the basis of a common intersection point of the integral titration curves Z_H (pH) at pH_r. Doing so, for the curve for RNase adsorbed at pH 11.0 ($= pH_r$) the real position is obtained, whereas the positions of the curves for RNase adsorbed at pH $\neq pH_r$ are uncertain with respect to the abscissa.

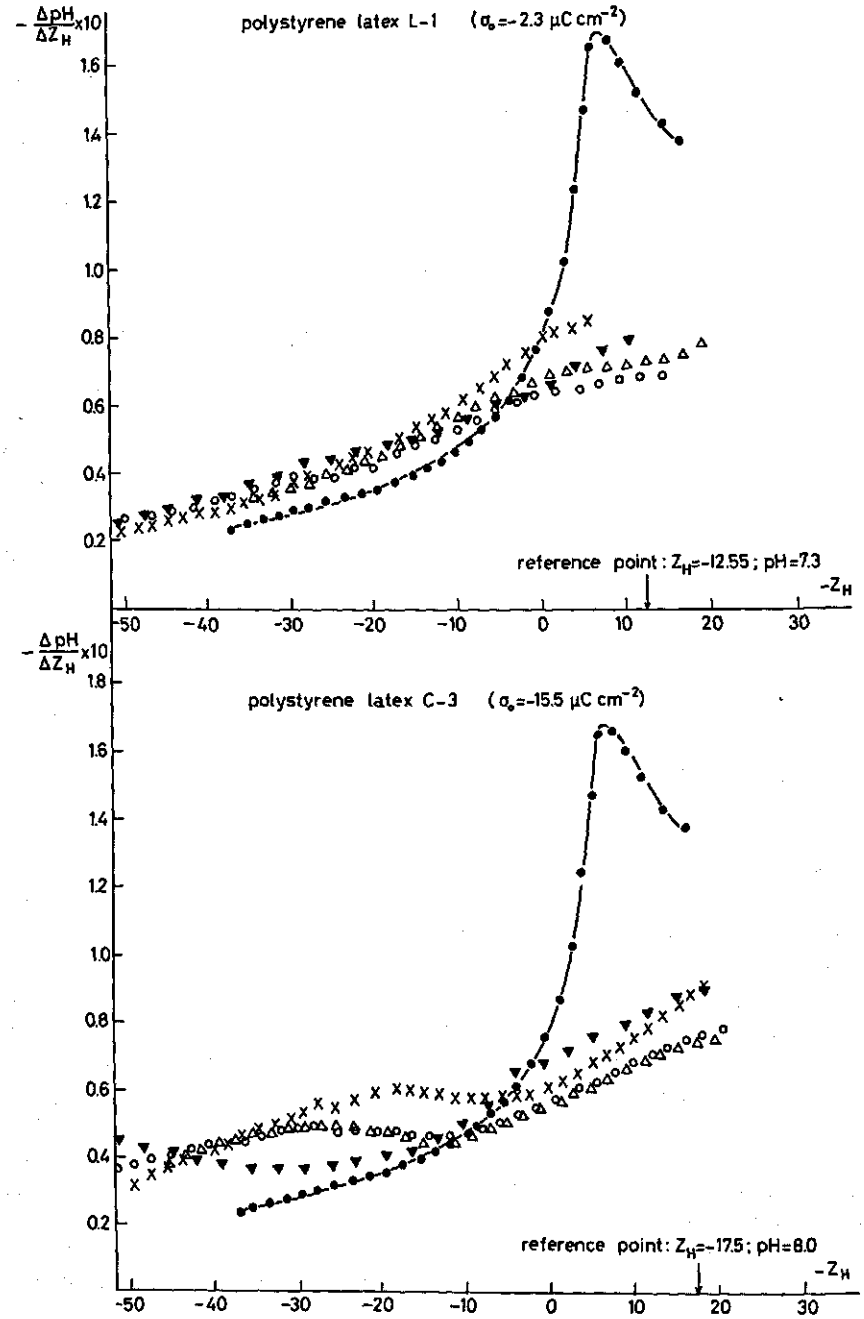

FIG. 5.4. Reciprocal differential titration curves for HPA in solution (—●—) and adsorbed on polystyrene latices. pH of adsorption 3.6 (○) 4.0 (△) 4.6 (×) and 7.3 or 8.0 (▼). c_{KNO_3} = 0.05 M T = 25°C.

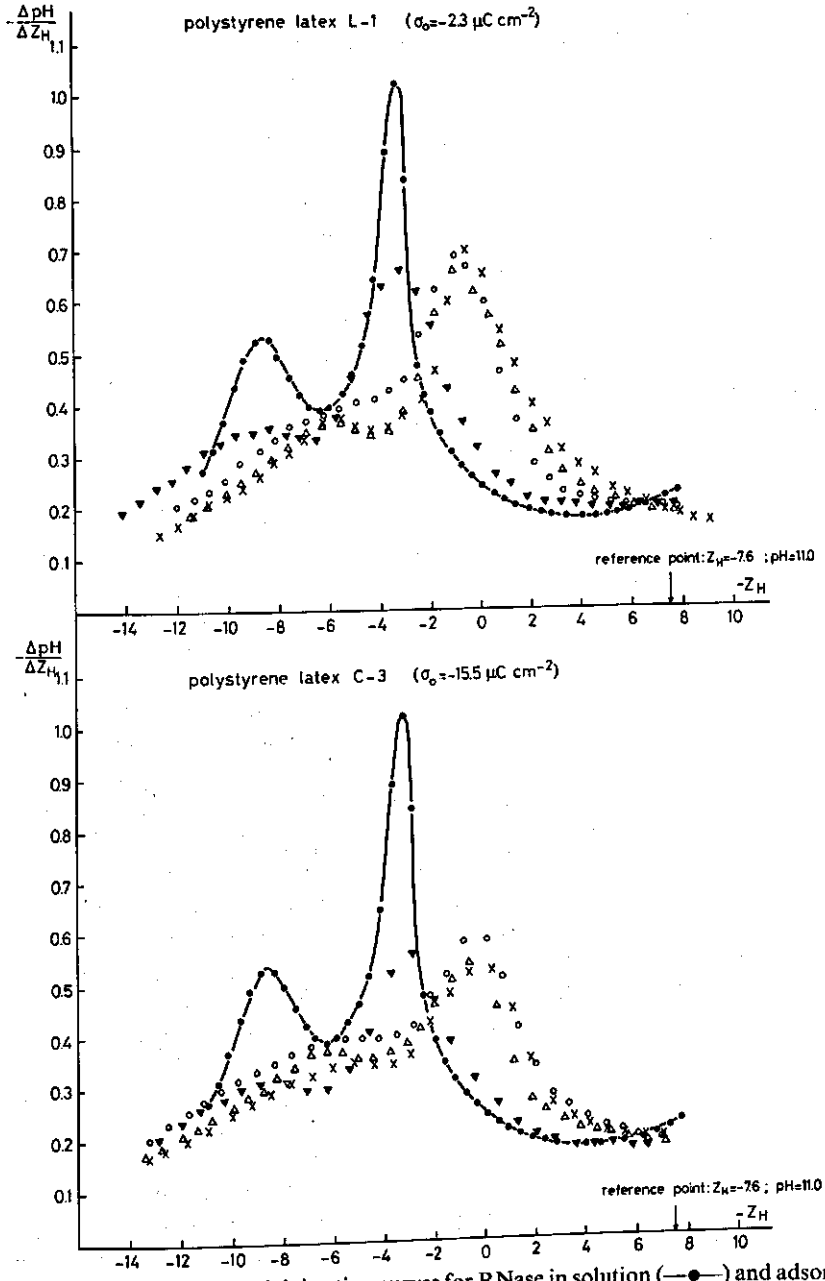

FIG. 5.5. Reciprocal differential titration curves for RNase in solution (—●—) and adsorbed on polystyrene latices. pH of adsorption 4.0 (○) 7.0 (△) 9.3 (×) and 11.0 (▼). c_{KNO_3} = 0.05 M T = 25°C.

Comparing the reciprocal differential titration curves for adsorbed RNase, thus obtained, with the one for dissolved RNase, it is observed that, as a result of adsorption, for most cases the maxima are shifted and, for all cases, they are much less pronounced. The left-hand maximum, separating the titration region of the carboxyl groups and the titration region of the imidazole and α-amino groups, is diminished almost completely. Hence, the titration regions of these classes of groups are much less distinct in adsorbed RNase than in dissolved RNase. Nevertheless, these titration regions do not overlap each other to the same extent as they do in adsorbed HPA.

For RNase adsorbed at pH 11.0, 9.3 and 7.0 a shallow maximum can still be observed at the place where it would be expected, namely at 5 Z_H units to the left of the right-hand peak. Although for RNase adsorbed from a solution of pH 4.0 the left-hand maximum is barely discernible, it is judged to be located 4.0 to 4.5 Z_H units away from the right-hand maximum. These findings indicate that in a RNase molecule adsorbed at pH 11.0, 9.3 or 7.0, four imidazole and one α-amino group are titratable, just as in the dissolved RNase, whereas in the case of adsorption from a solution of pH 4.0 10–20% of these groups seem to be unavailable for titration. Probably, the reasons for this reduced number of groups available for titration must be sought in interactions between these groups and the polystyrene surface. Ion pair bonding is the most likely type of interaction preventing the titration of interacting groups.

According to table 5.1. the pK values of the imidazole and the α-amino groups in dissolved RNase are 6.5 and 7.8, respectively. Hence, at pH 11.0 and 9.3 virtually all these groups are dissociated. At pH 7.0 most of the imidazole and only a small fraction of the α-amino groups are dissociated, whereas at pH 4.0 both the imidazole and the α-amino groups are protonated. Formation of ion pairs between the negative sulphate groups at the polystyrene surface and groups of the adsorbed RNase molecules, is only expected to occur when the RNase molecule is adsorbed from solutions having pH values where the groups, participating in the ion pairs, are not dissociated. For these resaons, ion pairing of some of the positively charged imidazole groups, rather than the α-amino groups, with the negatively charged groups at the polystyrene surface, has been assumed to be the reason for the smaller number of groups titratable in the class consisting of imidazole and α-amino groups, as is observed for RNase adsorbed at pH 4.0.

As with dissolved RNase, the reciprocal differential titration curves for RNase adsorbed from a solution of pH 11.0 (= pH_r) show maxima at $Z_H = 8$ and $Z_H = 3$. Since the positions of these curves are fixed, it is concluded that, at least up to pH 11.0, for RNase adsorbed at pH 11.0, the sequence in the titration regions of the different classes of groups is not changed as a result of adsorption.

If, for RNase adsorbed at pH $\neq$ pH_r, the sequence of the titration regions does not change either, the maxima in the corresponding reciprocal differential

titration curves, in their *absolute* positions, should occur at $Z_H = 3$ and $Z_H = 8$ as well, unless a different number of carboxyl groups and/or imidazole and α-amino groups are titrated.

As has been discussed earlier, for RNase adsorbed at pH 9.3 and pH 7.0 all imidazole and α-amino groups are titrated in a distinct region. For the RNase molecule adsorbed at pH 4.0 0.5–1.0 groups in the class consisting of imidazole and α-amino groups appeared to be unavailable for titration.

For RNase molecules dissolved at pH 11.0, 9.3 or 7.0 virtually all the carboxyl groups are dissociated. Therefore, in the cases of adsorption at pH 9.3 and pH 7.0 the titration behaviour of these groups would be similar to that for the case of adsorption at pH 11.0. This implies that for RNase adsorbed at pH 9.3 and pH 7.0 all carboxyl groups are dissociated when the RNase molecule has reached a Z_H value of ca. 8 units.

For RNase dissolved at pH 4.0, about half of the carboxyl groups are dissociated. If, upon adsorption at pH4.0, dissociation of the protonated carboxyl groups is blocked or they only dissociate at exceptionally high pH values, the titration region of the imidazole and the α-amino groups and, consequently, that of the ε-amino and the phenolic groups, would shift to more positive values of Z_H. Figure 5.5. reveals that the maxima in the reciprocal differential titration curves of RNase adsorbed at pH 4.0, pH 7.0 and pH 9.3, all having the same reference point with respect to their positions along the abscissa, occur at values of Z_H that nearly coincide. Hence, it seems logical to conclude that the dissociation of the carboxyl groups in the RNase molecules adsorbed at pH 4.0 takes place over the same trajectory of Z_H as for the RNase molecules adsorbed at pH 9.3 and 7.0.

Having established this, the curves shown in figure 5.5. may be transposed along the abscissa to their absolute positions. Hence, in each case the real value for Z_H at pH 11.0 ($= pH_r$) can be read off from the abscissa. These values are collected in table 5.4.

In view of the close relative positions of the right-hand maxima in the reciprocal differenrial titration curves in their absolute positions, the finding that for RNase adsorbed at pH $\neq pH_r$ the real Z_H at pH 11.0 has shifted to less negative values, has been ascribed to a smaller number of ε-amino and/or phenolic groups dissociated at pH 11.0. The reduction in this number, thus calculated, is presented in table 5.4. For RNase adsorbed from solutions at pH 4.0., the effect of adsorption on the dissociation of the imidazole groups, estimated from the distance between the two maxima, has been taken into account.

Thus, in contrast to adsorption at pH 11.0, at other pH values for adsorption some ε-amino and/or phenolic groups are found to be protected from dissociation up to pH 11.0. The number of these groups protected appears to be virtually independent of the pH of adsorption. The number is somewhat higher in the case of adsorption at the more negatively charged polystyrene surface (latex C-3), indicating the involvement of the negatively charged sulphate groups.

TABLE 5.4. Real values for Z_H at pH = 11.0 and values for the number of groups in the class consisting of ε-amino and phenolic groups that are protected from dissociation up to pH 11.0, as a result of adsorption.
RNase series $c_{KNO_3} = 0.05$ M $T = 25°C$

sample	pH of adsorption	$Z_H^{pH=11.0}$	number of groups protected for dissociation
RNase dissolved		-7.6	
RNase adsorbed on latex L-1	4.0	-4.9	2.0
	7.0	-5.4	2.2
	9.3	-5.1	2.5
	11.0	-7.6	0.0
RNase adsorbed on latex C-3	4.0	-4.0	2.8
	7.0	-4.6	3.0
	9.3	-4.9	2.7
	11.0	-7.6	0.0

Referring to the earlier discussion on the titration of the imidazole groups, formation of ion pairs between groups in the RNase molecule and groups at the polystyrene surface is the most likely reason for a change in the number of groups that are detectable by titration. In their protonated form, the phenolic groups are uncharged and the ε-amino groups bear a positive charge. Therefore, the reduction in the number of groups, in the class consisting of ε-amino and phenolic groups, that are available for titration is assumed to be due to the formation of ion pairs between the ε-amino groups and the negatively charged sulphate groups at the polystyrene surface.

At pH 4.0 and pH 7.0 virtually none, at pH 9.3 only a small fraction and at pH 11.0 nearly all, of the 10 ε-amino groups in the dissolved RNase molecule are dissociated. The protonated ε-amino groups still present in the molecule dissolved at pH 11.0 may, upon adsorption at that pH, form ion pairs with the polystyrene surface. Hence, the number of ε-amino groups that are protected from titration up to pH 11.0 (see table 5.4.) is considered to be equal to the *extra* number of these groups involved in ion pairs, i.e. taking the number of ion pairs formed upon adsorption at pH 11.0 as the reference point.

The finding that for RNase molecules adsorbed from solution at pH 4.0, 7.0 and 9.3 the number of ε-amino groups ion-paired with a given polystyrene surface is approximately constant, suggests more or less similar orientations of the RNase molecules at the interface at these pH values. As has been suggested in section 4.3.2.1. the same conclusion may be drawn from the fact that the amount of RNase adsorbed, appears to be virtually constant over the considered pH region (see figure 4.5. and table 5.3.).

5.3.3.2. Integral titration curves: Z_H vs. pH

Having estimated the number of groups in the adsorbed RNase molecule that are not available for titration, the absolute value of Z_H as a function of pH can now be established.

As with RNase, so also in the case of adsorbed HPA a fraction of the positively charged groups may be blocked with regard to dissociation. In view of the fact that the reference point in the HPA series has been fixed at pH values of 7.3 and 8.0 for the low and high charged latex, respectively, any interaction of ε-amino groups with the polystyrene surface does not affect the positioning of the differential titration curves of adsorbed HPA. However, unlike at pH 3.6, 4.0 and 4.6, for HPA dissolved at pH 7.3 and pH 8.0 the imidazole groups are almost completely and the α-amino groups are partly dissociated. This difference in the degree of dissociation of these groups in the dissolved state may lead to a different number of the groups being involved in ion pair bonds with the sulphate groups at the polystyrene surface. If so, for HPA molecules adsorbed from solution at pH 3.6, 4.0 or 4.6, the absolute value of Z_H at the pH of the reference point would be more positive than was in fact assumed when positioning their reciprocal differential titration curves, as indicated in figure 5.4. Unfortunately, the titration data for HPA do not allow quantitative corrections in this respect. Based on the fractions of the positively charged groups in the RNase molecule becoming, after adsorption, involved in ion pairs, the number of ion-paired imidazole groups in a HPA molecule adsorbed at pH 3.6, 4.0 or 4.6 is estimated to be of the order of 3–5.

The integral titration curves Z_H (pH) are presented in figure 5.6. (HPA series) and in figure 5.7. (RNase series). The ones for the proteins in the dissolved state in aqueous solutions of 0.05 M KNO_3 agree rather well with titration curves for HPA or BPA (TANFORD et al, 1955b; STEINHARDT et al, 1971) and for RNase (TANFORD and HAUENSTEIN, 1956), reported in literature. No data on the titration of adsorbed proteins with protons seem to be available in the literature.

As a general trend, the dissociation of the functional groups appears to be reduced as a result of adsorption. Both for HPA and RNase the effect is most pronounced in the titration regions of the carboxyl groups. For RNase, the titration behaviour of the phenolic and the ε-amino groups is not significantly affected, apart from the fraction of these groups that is supposed to be ion-paired to the polystyrene surface. The effect of adsorption on the dissociation of the phenolic and the ε-amino groups in the HPA molecule cannot be analyzed, since the titration curves do not extend to the pK values of these groups. However, the shapes of the integral titration curves for the HPA series extrapolated to the region where the phenolic and ε-amino groups are titrated ($Z_H < -22$) give the impression that the dissociation of these groups is slightly enhanced by adsorption.

The effects of adsorption on the titration curves may be interpreted in terms of the theory presented in section 5.3.1. It should be realized, however, that application of equation (5.6.) or equation (5.8.) to real systems is not straightforward, especially in the case of overlapping titration regions of different classes of groups (e.g. carboxyl and imidazole groups in adsorbed HPA).

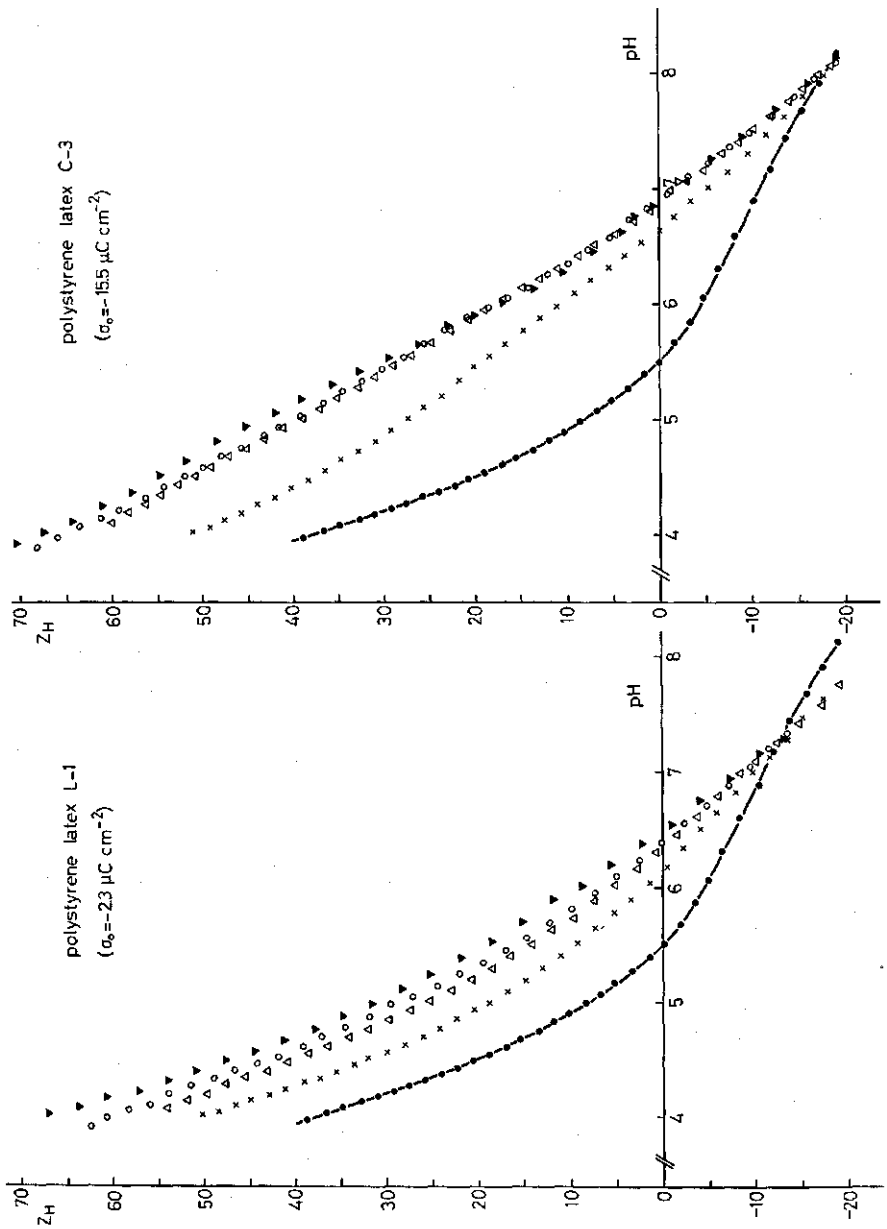

FIG. 5.6. Integral titration curves for HPA in solution (—●—) and adsorbed on polystyrene latices. pH of adsorption 3.6 (○) 4.0 (△) 4.6 (×) and 7.3 or 8.0 (▼). c_{KNO_3} = 0.05 M T = 25°C.

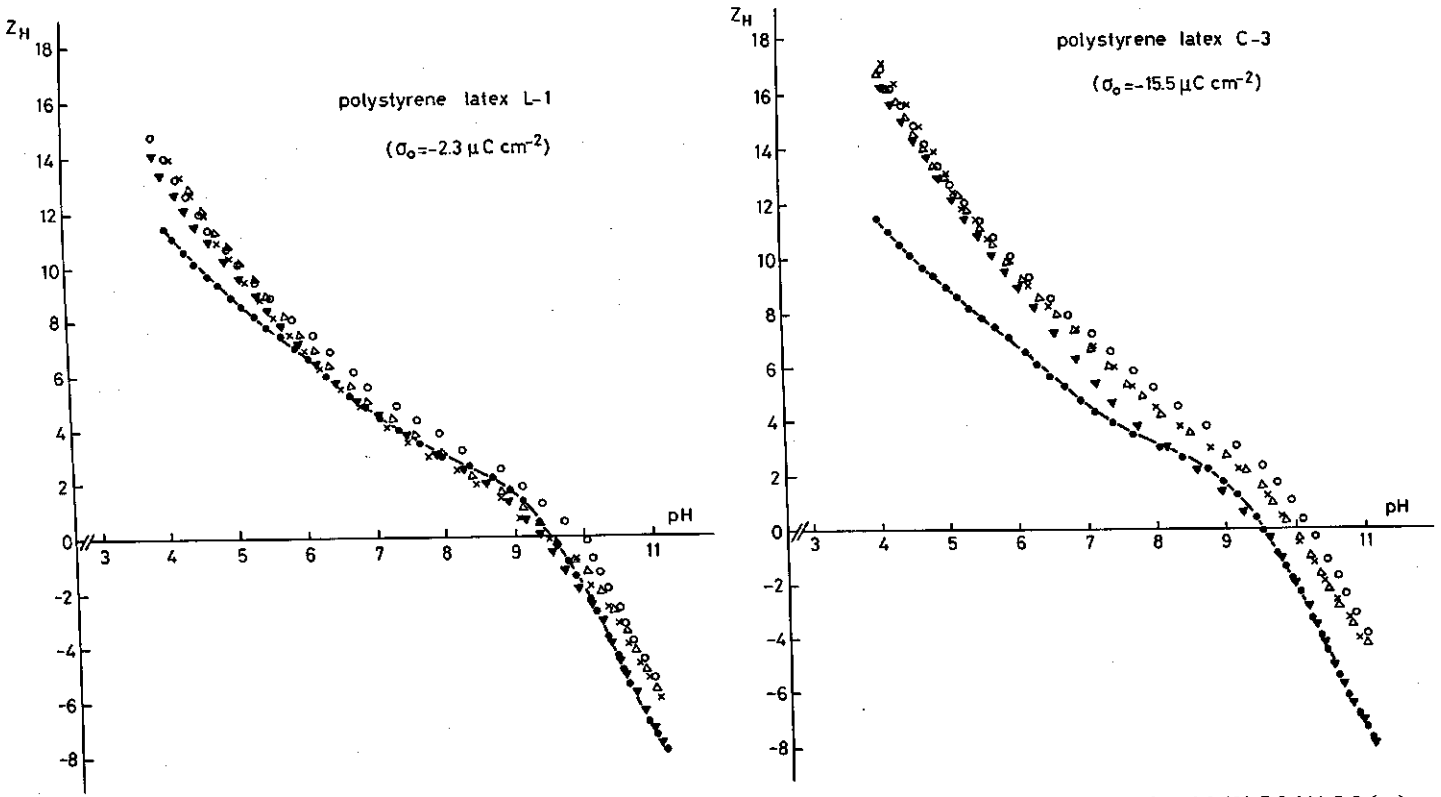

FIG. 5.7. Integral titration curves for RNase in solution (—●—) and adsorbed on polystyrene latices. pH of adsorption 4.0 (○) 7.0 (△) 9.3 (×) and 11.0 (▼). c_{KNO_3} = 0.05 M T = 25°C.

The negative electric field at the polystyrene surface lowers the electrostatic potential, ψ, at the sites of dissociating groups near this surface and, hence, tends to increase ΔG_{el}. The influence of the polystyrene surface on ΔG_{med} is not clear. If it were to lead to the titratable groups only being in a more hydrophobic environment, then an increase of ΔG_{med} would result. Lateral interactions between the adsorbed protein molecules would also affect ΔG_{el} and ΔG_{med}. However, because the interaction between the adsorbed protein molecules and the polystyrene surface is stronger than that between adjacent protein molecules in the adsorbed layer, the influence of the polystyrene surface on the titration behaviour is expected to be larger than that due to lateral interactions between neighbouring protein molecules.

In the light of these considerations it is evident that it is not easy to account for all the possible changes in the orientations and interactions of the relevant groups during the adsorption process. Therefore, the contribution, due to each of these changes, to the experimental value of $(pH^{ads} - pH^{sol})_{Z_H}$ is difficult to establish.

By comparing the integral titration curves of a given protein adsorbed at latex L-1 and C-3, respectively, and correcting for the groups assumed to be involved in ion pair formation with the polystyrene surface, it can be deduced that for both proteins the negative electric field at the polystyrene surface is the dominant contribution to the shift in the titration curves. If medium effects are negligibly small as compared to electrostatic effects, then the shifts in the titration curves at a constant value of Z_H, $(pH^{ads} - pH^{sol})_{Z_H}$, should be proportional to $-(\psi^{ads} - \psi^{sol})$, according to equation (5.8.). The value for $(\psi^{ads} - \psi^{sol})$ represents the difference in the mean electrostatic potential of a group, titrated at the considered value of Z_H, in the adsorbed and the dissolved state, respectively.

Thus, assuming the electric field at the polystyrene surface to be the dominant factor underlying the effect of adsorption on the titration behaviour, it seems that, in the case of adsorbed HPA and RNase molecules, on average the carboxyl groups are located closer to the polystyrene surface than the other titratable groups. This feature may explain the increasing overlap of the titration regions of the carboxyl and the imidazole groups upon titration. Apparently, in spite of their negative charges, carboxyl groups are adsorbed preferentially at the negatively charged polystyrene surface. This preference may arise from the generally weaker hydration of anions as compared to cations (NANCOLLAS, 1966), as a result of which the anions are more easily accomodated at the hydrophobic polystyrene surface. Also cations, present in the electrical double layer, may screen the interaction between the negative charges at the polystyrene surface and those of the adsorbed protein molecules.

If, for the phenolic and ε-amino groups in HPA the small negative value for $(pH^{ads} - pH^{sol})_{Z_H}$, as indicated in figure 5.6., is real, then this might be due to the accumulation of positively charged groups at a relatively large distance from the polystyrene surface, i.e. at the aqueous side of the adsorbed protein

molecules. Also, environmental changes, that could occur as a result of changes in the molecular conformation during the adsorption process, may stimulate deprotonation of the groups under consideration.

After correction for the different numbers of groups available for titration, no pronounced effect in the case of RNase of the pH of adsorption on the titration behaviour is observed. In the case of HPA the titration curves of the protein adsorbed at pH 4.6 differ substantially from those adsorbed at other pH values studied, these being positioned close to each other. Adsorption of HPA from a solution at pH 4.6, in which the molecules virtually attain their isoelectric state, leads to relatively small changes in the titration behaviour of the protein.

As has been discussed above, for the carboxyl groups the change in the titration behaviour is primarily due to electrostatic effects. Neglecting medium effects, for both proteins at each pH of adsorption, and using equation (5.8.), $(\psi^{ads} - \psi^{sol})$ has been calculated from $(pH^{ads} - pH^{sol})_{Z_H}$ at a Z_H value where only carboxyl groups are titrated. The Z_H values for the dissolved HPA and RNase molecules, corresponding to pH 4.0, has been chosen in these calculations. The results are given in table 5.5.

The values for $(\psi^{ads} - \psi^{sol})$ obtained for the HPA series indicate that the average location of the carboxyl groups in the adsorbed molecules depends on the pH of adsorption. As a rule, the greater the net charge of the HPA molecules before adsorption, the nearer the carboxyl groups become located to the polystyrene surface.

For the RNase series, on the other hand, the values for $(\psi^{ads} - \psi^{sol})$ would suggest that the orientation of the protein molecules at the interface is not very sensitive to the net charge they have in the corresponding solution from which they are adsorbed.

These results support the ideas concerning the effect of the pH of adsorption on structural changes in the adsorbed HPA and RNase molecules suggested from the experiments described in chapter 4.

TABLE 5.5. Changes in the pH and the calculated average electrostatic potential (mV) as a result of adsorption, at a constant value of Z_H.
HPA: $Z_H = 37.5$ RNase: $Z_H = 11.6$
For further conditions see text.

HPA					RNase				
pH of adsorption	$(pH^{ads} - pH^{sol})_{Z_H}$		$(\psi^{ads} - \psi^{sol})$		pH of adsorption	$(pH^{ads} - pH^{sol})_{Z_H}$		$(\psi^{ads} - \psi^{sol})$	
	L-1	C-3	L-1	C-3		L-1	C-3	L-1	C-3
3.6	0.66	1.10	-39	-65	4.0	0.64	1.40	-38	-83
4.0	0.58	1.08	-34	-64	7.0	0.70	1.40	-41	-83
4.6	0.31	0.49	-18	-29	9.3	0.64	1.40	-38	-83
7.3	0.77		-46		11.0	0.52	1.29	-31	-76
8.0		1.22		-72					

5.4. ELECTROPHORESIS

As has been discussed in section 2.3.5. information may be obtained from electrophoretic experiments concerning the electrical double layer, namely the electrokinetic potential (= ζ-potential) and the electrokinetic charge.

Changes in the ζ-potential of the protein as a result of adsorption have often been explained in terms of redistribution of the charged groups in the protein molecule, i.e. variations in the type of the charged groups exposed towards the aqueous phase (see e.g. CHATTORAJ and BULL, 1959, and WILKINS and MYERS, 1970). However, this kind of conclusion cannot be drawn unambiguously without more information being available on the role of the electrolyte in the adsorption process. A joint study of the electrokinetic charges of the polystyrene particles and the protein molecules before and after adsorption together with the change in net proton charge of the adsorbing protein molecules, gives a more complete picture of the charge distribution in the adsorbed protein, thereby accounting for the role of the electrolyte in the adsorption process.

5.4.1. *Experimental procedure*

The protein-covered polystyrene particles used in the electrophoretic measuremtents were prepared under the conditions mentioned in section 4.3.1., using protein concentrations that ensure adsorption saturation. After separating the protein-covered particles from the protein solution by centrifugation, they were redispersed to a concentration of about 10^7 particles per cm^3. At this concentration the buffering capacity of the adsorbed protein is too small to maintain a constant pH in solution. Therefore, the system was buffered by means of an acetate-veronal buffer following MICHAELIS (1931); KNO_3 was used to adjust the ionic strength. The pH of the dispersion was chosen to be equal to that of the system directly after adsorption.

In the buffered dispersions, having ionic strenghts of 0.01 M and 0.05 M, the combined molarity of sodium acetate and sodium veronal (sodium 5,5 diethyl barbiturate) amounted to 0.57×10^{-2} M and the KNO_3 concentration to 0.43×10^{-2} M and 4.43×10^{-2} M, respectively. Desorption of the proteins upon changing the composition of the aqueous phase could not be detected.

Samples of the bare latex particles, using solutions of KNO_3 instead of protein, were similarly prepared.

The electrophoretic mobilities of the bare and the protein-covered particles were determined using a Rank Brothers microelectrophoresis apparatus, according to the procedure described in section 2.3.5.

Solutions (7.5 g dm^{-3}) of HPA and RNase were prepared in the same buffers as described above. These solutions were dialyzed for 48 hours at 4°C against the corresponding buffer in the volume ratio of 1:20. After dialysis there is usually a difference in electrolyte concentration between the protein solution and the dialysate, due to a Donnan equilibrium.

Electrophoretic mobilities of the dissolved protein molecules were determined by measuring the displacement of the boundary between the protein solution and the dialysate, caused by a known, applied electric field. A Kern-Aarau L.K. 30 apparatus, equipped with a micro-Tiselius cell and an interferometric optical system to observe the boundary, was used for these measurements.

The solutions were de-gassed just before filling the cell. The boundary between the protein solution and the dialysate was observed according to the method of LABHART and STAUB (1947). The number of lines in the interference pattern depends on the difference in refractive index between the protein solution and the dialysate. For the solutions used in this study the number of lines amounts to twenty. The closer the parallel lines are, the larger is the gradient of refractive index and, hence, the gradient of protein concentration.

The measurements were performed at ca. 25°C. The applied electric field was chosen such that the boundary could be traced for a period of 45–120 minutes. In order to avoid disturbances of the boundary by thermal convection, the product of the electric current and the voltage (= Joule-heat evolved per unit of time) was always kept less than 200 mJ s^{-1}.

The interference pattern was recorded photographically at regular time intervals. During the electrophoresis the interference pattern does not stay completely symmetrical due to small gradients in the electric field in the boundary zone. The middle line in the pattern corresponds to the location in the cell where the protein concentration is reduced to half its value in the bulk solution. Therefore, the middle line was considered to represent the movement of the boundary.

Dividing the electrophoretic velocity, u, by the strength of the electric field, X, which is calculated as described in section 2.3.5., yields the electrophoretic mobility, u/X, of the protein. The data obtained from the descending boundary were used in the derivation of the ζ-potential, because at the ascending boundary anomilies in the electrophoretic mobilities may occur, due to a gradient of protein concentration at this boundary (LONGSWORTH and MACINNES, 1940).

5.4.2. *Results and discussion*

u/X is plotted against pH in figures 5.8.–5.10. For the bare and the protein-covered polystyrene particles the standard deviation for each determination of u/X is in the range of 5–10%. The standard deviation for u/X determined for the dissolved proteins is about 2–5%.

The electrophoretic mobilities of the bare particles in the buffered media are constant over the pH range 4–11. The same has been observed for polystyrene latex in 0.01 M KNO_3 solutions (section 2.3.5.). Moreover, their values do not differ significantly from those in aqueous solutions of KNO_3 of the same ionic strength (cf. table 2.4.).

With respect to the conversion of mobility to ζ-potential, the geometry of the particle should be considered. The bare and the protein-covered polystyrene particles are spherical, whereas the dissolved HPA and RNase molecules have

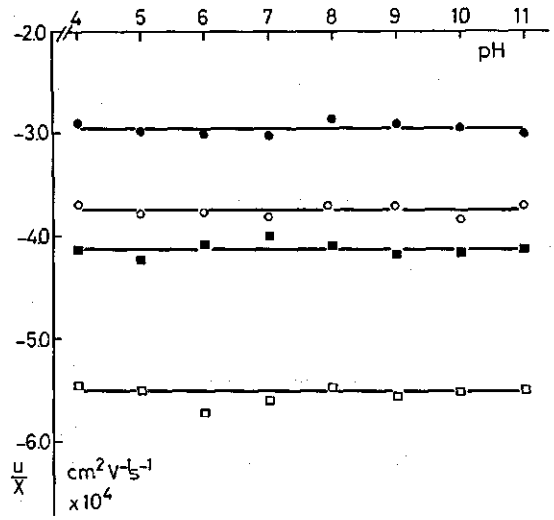

FIG. 5.8. Electrophoretic mobilities of polystyrene latices L-1 (○) and C-3 (□) in acetate-veronal-KNO_3 buffers. Open symbols ionic strength 0.01 M; filled symbols ionic strength 0.05 M. $T = 25°C$.

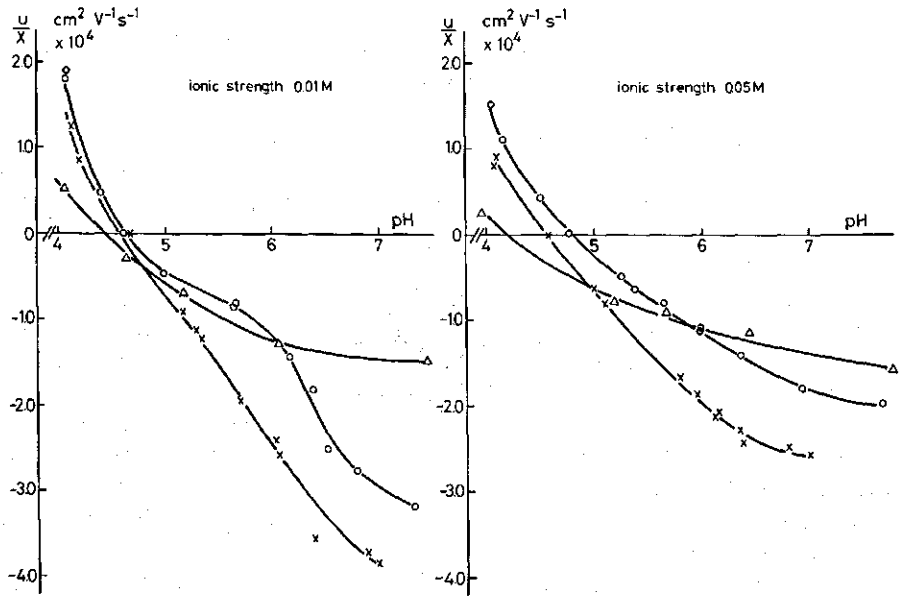

FIG. 5.9. Electrophoretic mobilities of HPA in solution (△) and adsorbed on polystyrene latices L-1 (○) and C-3 (×). Medium: veronal-acetate-KNO_3 buffer. $T = 25°C$.

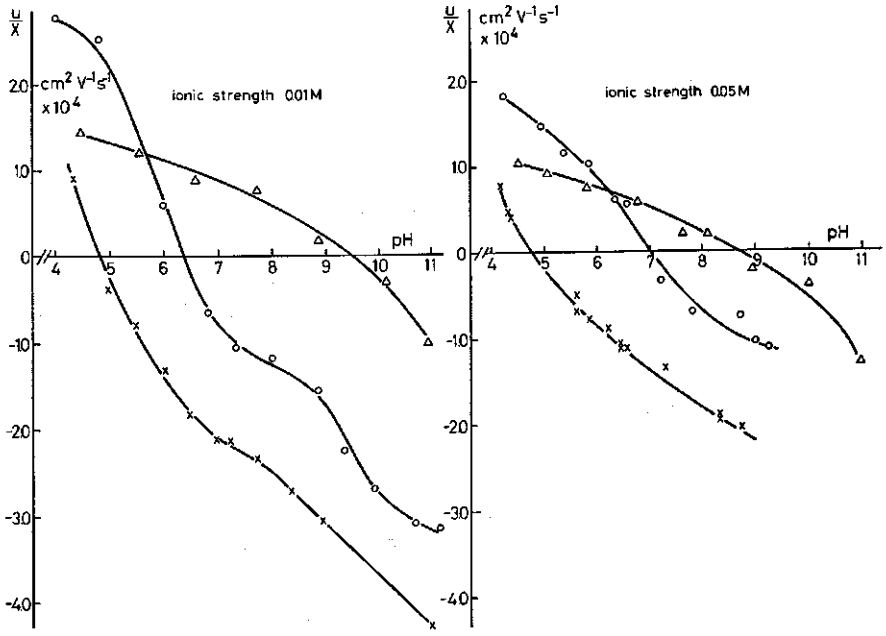

FIG. 5.10. Electrophoretic mobilities of RNase in solution (△) and adsorbed on polystyrene latices L-1 (○) and C-3 (×). Medium: veronal-acetate-KNO_3 buffer. $T = 25°C$.

a more or less ellipsoidal shape (see section 3.2.3.). However, unlike for spheres and cylinders, for ellipsoids no theory has yet been developed relating ζ-potential to mobility. The geometry of the HPA molecule resembles a cylinder rather than a sphere; the reverse is true for RNase.

The ζ-potentials of the bare and the protein-covered polystyrene particles, as well as those of the dissolved RNase molecules, have been calculated according to the theory of WIERSEMA (1964) and WIERSEMA et al (1966). The ζ-potentials of the dissolved HPA molecules have been calculated using the formula for cylinders, derived by ABRAMSON et al (1942). In this treatment relaxation effects are not taken into account. The conditions for the HPA molecule in aqueous solutions of 0.05 M ionic strength are such, that, for the values of the electrophoretic mobilities measured, relaxation effects are practically negligible. Application of ABRAMSON's formula does not, therefore, introduce significant errors on this account.

The radii of the protein-covered particles are obtained by adding the thickness of the adsorbed protein layer, including a hydration layer of 0.5 nm, to the radius of the polystyrene particle. Values for the latter are given in table 2.1. and for the thickness of the adsorbed protein layer the average of the two values given in figure 4.8. was taken. The dimensions of the modified shapes of the dissolved protein molecules are based on their molecular volumes, which have been reported in section 3.2.3., to which a hydration layer of 0.5 nm is

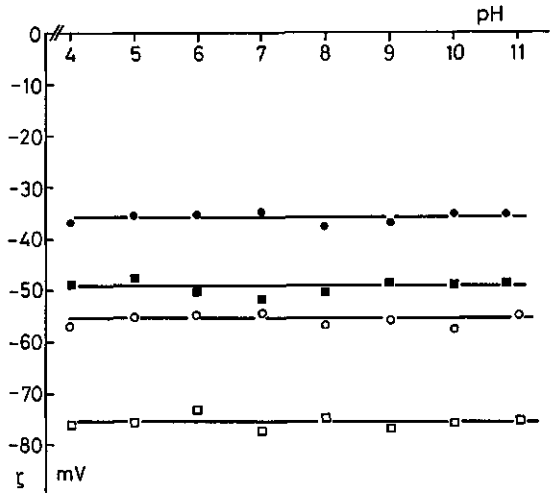

FIG. 5.11. Electrokinetic potentials of polystyrene latices L-1 (○) and C-3 (□) in acetate-veronal-KNO_3 buffers. Open symbols ionic strength 0.01 M; filled symbols ionic strength 0.05 M. $T = 25°C$.

added. Thus, the RNase molecule is approximated to a sphere with a radius of 2.08 nm and the HPA molecule to a cylinder with a length of 13.20 nm and a radius of 1.89 nm. However, the values calculated for the ζ-potentials of the proteins are not very dependent on the molecular dimensions.

Curves representing the ζ-potentials as a function of pH are shown in the figures 5.11.–5.13. Due to the negative charge of the polystyrene surface one would expect the ζ-potentials of the protein-covered particles to be more negative than those of the dissolved proteins. This is not a matter of course, however,

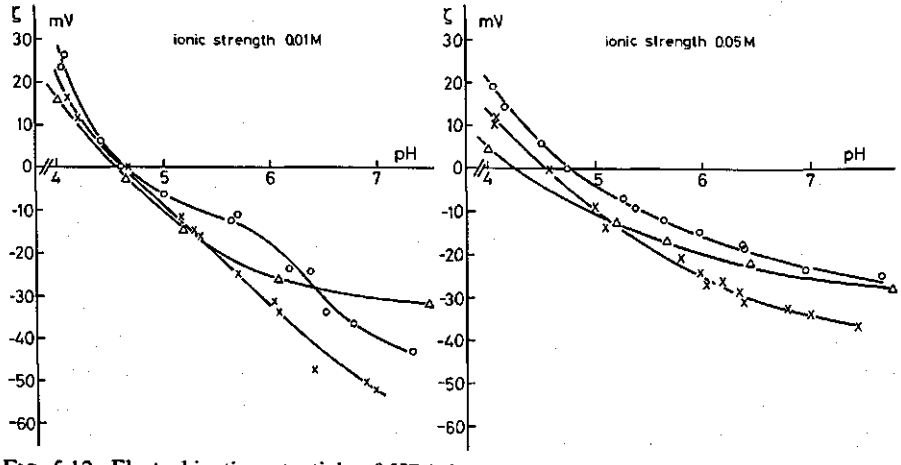

FIG. 5.12. Electrokinetic potentials of HPA in solution (△) and adsorbed on polystyrene latices L-1 (○) and C-3 (×). Medium: veronal-acetate-KNO_3 buffer. $T = 25°C$.

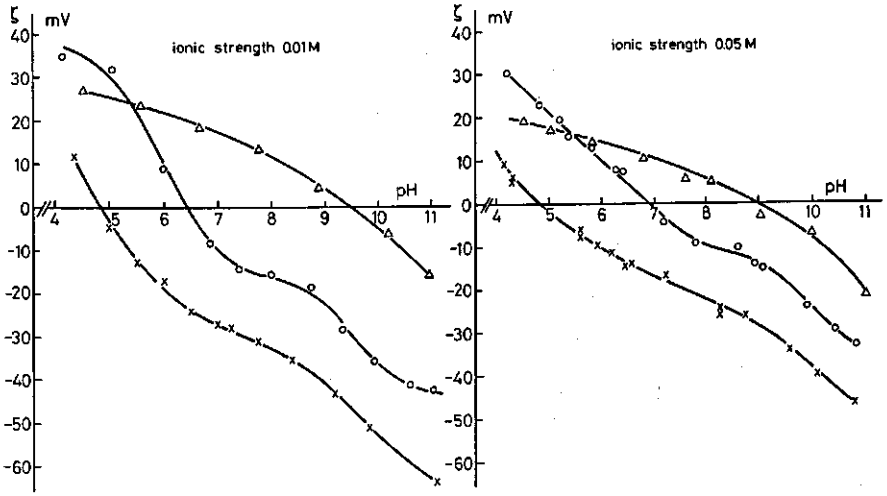

FIG. 5.13. Electrokinetic potentials of RNase in solution (Δ) and adsorbed on polystyrene latices L-1 (O) and C-3 (×). Medium: veronal-acetate-KNO_3 buffer. $T = 25°C$.

since changes in the net proton charge of the protein molecules and possible changes in the number of specifically adsorbed and bound ions to both the polystyrene particles and the proteins can occur upon adsorption. For example, in the case of HPA, the differences in ζ (pH) between the dissolved molecules and the covered particles are relatively small. However, adsorption on the more negatively charged polystyrene particles (C-3) does render the ζ-potential more negative. In the curves for RNase, the influence of the negatively charged polystyrene surface is clearly recognized. It is remarkable that both for HPA and RNase the difference between ζ (pH) for the protein-covered particles and the dissolved protein molecules is less negative or even positive at lower pH values.

The decrease of ζ (pH) with increasing ionic strength can be attributed to the charge shielding action of electrolytes.

Instead of comparing ζ-potentials it is more instructive to compare electrokinetic charges before and after the adsorption process. This provides information concerning the uptake or exclusion of ions in or from the electrokinetic units. Such comparisons have been made only in media of 0.05 M ionic strength, since titration data in 0.01 M KNO_3 are not available. Moreover, the composition of the buffered medium of ionic strength 0.01 M may differ too much from a 0.01 M KNO_3 solution for a reasonable comparison between titration data and electrophoresis measurements to be made. At ionic strength 0.05 M such a comparison may be more valid.

The electrokinetic charges are derived from the ζ-potentials by interpolation of the tables of LOEB, WIERSEMA and OVERBEEK (1961). These tables refer to spherical particles. They have been used for dissolved HPA as well, since the

charge-potential relation for cylindrical particles, elaborated by ABRAMSON et al (1942) is valid only for potentials much less than 25 mV. In the present calculations the dissolved HPA molecule is assumed to be a sphere having a radius of 3.82 nm. Contrary to the calculation of electrokinetic *potential* calculation of electrokinetic *charge* depends critically on the dimensions assumed for the molecule.

The ζ-potentials from which the electrokinetic charges have been calculated were taken from the ζ (pH) curves. The results for HPA and RNase are presented in table 5.6.

The second column in table 5.6. contains the net number of electrokinetically measurable groups, Z_{ek}, in the dissolved protein molecules. The difference between Z_H and Z_{ek} is attributed to ions bound to the protein molecules. Curves for Z_H and Z_{ek}, as a function of pH, are shown in figures 5.14. and 5.15. for HPA and RNase, respectively. The trend is that Z_{ek} is more negative than Z_H, indicating preferential binding of anions onto the native molecules. This binding is particularly large with HPA (cf. section 3.2.1.).

The electrokinetic charge per unit area, σ_d in table 5.6., corresponds to that at the plane of shear around the bare or the protein-covered polystyrene particles. The sub-index '*d*' indicates the plane of shear. Thus, σ_d^{PS} and $\sigma_d^{PS/protein}$ represent the electrokinetic charge per unit area of the bare and the protein-covered polystyrene particles, respectively. The quantity $\sigma_d^{protein\ ads}$ is the contribution of the adsorbed protein to $\sigma_d^{PS/protein}$ for the case where the number of ions bound to the protein does not change upon adsorption. The change of Z_H in the adsorbing protein molecules (see section 5.3.3.2.) has been accounted for in the calculation of $\sigma_d^{protein\ ads}$. ΔZ_H can be derived from the titration curves presented in figures 5.6. and 5.7., taking into account the variation of the pH due to adsorption (figure 5.3.). As has been mentioned in section 5.3.3.2., allowance has to be made for a relatively small uncertainty in the integral titration curves for the adsorbed HPA molecules along the ordinate. Thus, ΔZ_H values are obtained for those pH values at which the titration experiments have been performed. For other pH values ΔZ_H has been estimated by interpolation. The amounts of protein adsorbed per unit area of polystyrene, which are needed in the calculations of $\sigma_d^{protein\ ads}$, are given in section 4.3.2.1.

Because of the requirement of overall electroneutrality, any difference between $\sigma_d^{PS/protein}$ and $(\sigma_d^{protein\ ads} + \sigma_d^{PS})$, from here on denoted as $(\Delta\sigma_d)_{ads}$, must be balanced by an uptake or exclusion of charge on the protein-covered particles. It is presumed that this occurs by the transfer to or from solution of mobile ions during the adsorption process. Curves, representing $(\Delta\sigma_d)_{ads}$ as a function of pH have been constructed. For HPA they are shown in figure 5.16. and for RNase in figure 5.17. The values of the electrokinetic charges may contain considerable errors (see section 2.3.5.). However, because of the fact that the calculations refer to systems of equal ionic strengths, i.e. 0.05 M, at least any trends in the curves for $(\Delta\sigma_d)_{ads}$ versus pH may be considered to be realistic.

Qualitatively, the variation of $(\Delta\sigma_d)_{ads}$ with pH is more or less the same for both proteins. Adsorption at low pH leads to ions being incorporated and/or

TABLE 5.6. Electrokinetic charges of HPA molecules, RNase molecules and polystyrene particles before and after adsorption.
Ionic strength = 0.05 M $T = 25°C$

		polystyrene latex L–1 $\sigma_d^{PS} = 2.0$ μC cm^{-2}					polystyrene latex C–3 $\sigma_d^{PS} = 3.0$ μC cm^{-2}			
	pH	Z_{ek}	ΔZ_H	ads. amount × 10^{-12} molec. cm^{-2}	$\sigma_d^{protein\ ads}$ μC cm^{-2}	$\sigma_d^{PS/protein}$ μC cm^{-2}	ΔZ_H	ads. amount × 10^{-12} molec. cm^{-2}	$\sigma_d^{protein\ ads}$ μC cm^{-2}	$\sigma_d^{PS/protein}$ μC cm^{-2}
HPA	4.0	2.9	17.2	1.48	–4.8	–1.1	23.5	2.04	–8.6	–0.8
	4.25	0.0	13.7	1.70	–3.7	–0.6	20.5	2.28	–7.5	–0.4
	4.6	– 1.5	10.1	1.92	–2.6	–0.2	16.0	2.50	–5.8	0.1
	5.0	– 6.0	7.7	1.63	–0.5	0.2	12.5	2.19	–2.3	0.5
	5.5	– 9.0	5.4	1.37	0.8	0.5	9.4	1.83	–0.1	0.9
	6.0	–11.6	3.5	1.24	1.6	0.7	6.4	1.52	1.3	1.3
	6.5	–13.8	1.9	1.11	2.1	1.0	4.8	1.26	1.8	1.5
	7.0	–15.4	0.6	0.99	2.4	1.2	2.8	1.02	2.1	1.7
	7.3	–16.2	0.0	0.92	2.4	1.3				
	7.5	–16.6					1.1	0.90	2.2	1.9
	8.0	–18.0					0.0	0.84	2.4	2.1
RNase	4.0	6.8	2.6	3.77	–5.7	–1.7	5.4	5.31	–10.4	–0.6
	5.0	5.4	1.2	3.86	–4.1	–1.1	3.8	5.39	– 7.9	0.1
	6.0	4.1	0.4	3.99	–2.9	–0.6	2.6	5.35	– 5.7	0.6
	7.0	2.9	0.0	3.99	–1.9	0.1	1.6	5.31	– 3.8	0.9
	8.0	1.7	0.0	3.99	–1.1	0.5	1.2	5.13	– 2.4	1.2
	9.0	0.1	0.0	3.95	–0.1	0.7	0.8	4.82	– 0.7	1.5
	9.3	–0.4	0.0	3.90	0.3	0.9	0.6	4.61	– 0.2	1.7
	10.0	–2.0	0.0	3.68	1.2	1.3	0.3	4.21	1.1	2.0
	11.0	–6.2	0.0	3.42	3.4	1.8	0.0	3.51	3.5	2.8

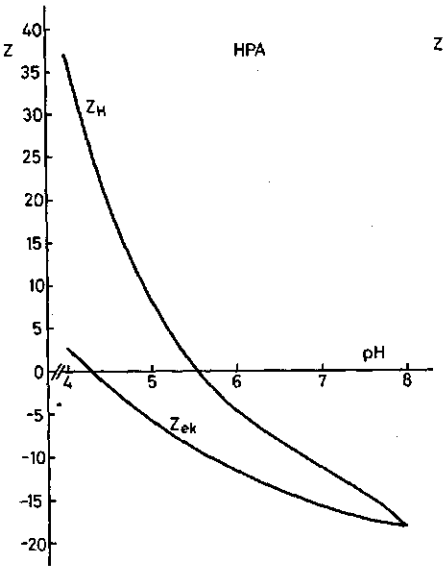

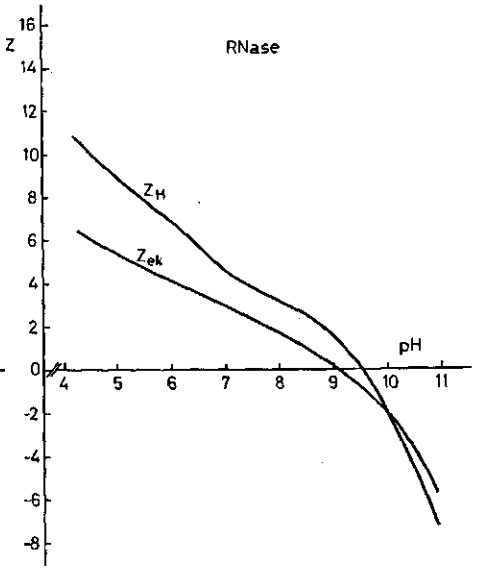

FIGS. 5.14. and 5.15. Net proton charge, Z_H, and electrokinetic charge charge, Z_{ek}, of dissolved HPA and RNase. Ionic strength 0.05 M $T = 25°C$.

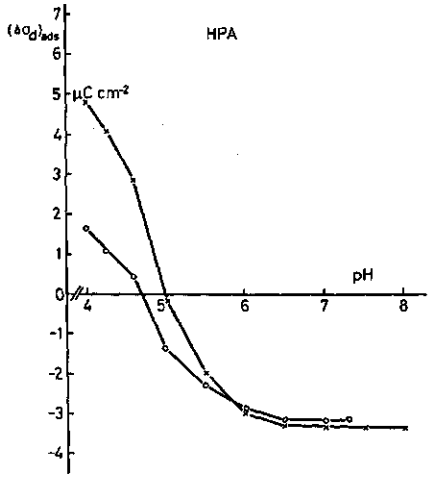

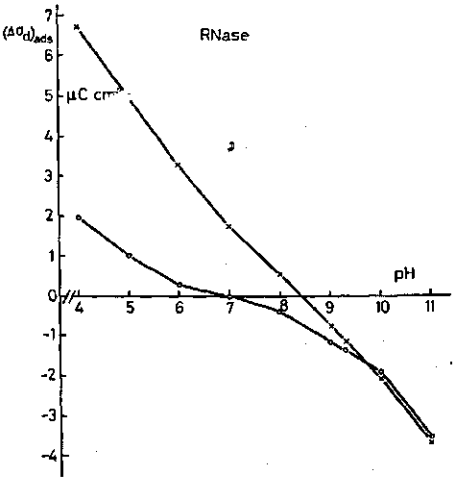

FIGS. 5.16. and 5.17. Contribution from the inclusion and/or expulsion of mobile ions to the electrokinetic charge of polystyrene particles of latices L-1 (O) and C-3 (×) covered with HPA and RNase. Ionic strength 0.05 M $T = 25°C$.

expelled, resulting in a positive value for $(\Delta\sigma_d)_{ads}$. Adsorption at higher pH values results in a negative value for $(\Delta\sigma_d)_{ads}$.

The effect of the charge of the polystyrene surface on ΔZ_H (see figure 5.6. and 5.7.) is clearly reflected by the variation of $(\Delta\sigma_d)_{ads}$ with pH.

In section 5.5.2. the ionic composition of $(\Delta\sigma_d)_{ads}$ will be analyzed semi-quantitatively.

5.5. The role of charged groups in the adsorption process

5.5.1. *A simple model for a protein layer adsorbed at a charged interface*

In order to undertake any electrostatic analysis of the adsorption process, a picture of the interface, before and after adsorption, is required.

One of the major questions in this respect concerns the position of the $-OSO_3^-$ groups, which the negative charge of the polystyrene surface has been ascribed to (section 2.3.3.). No evidence has been obtained as to the exact positions of

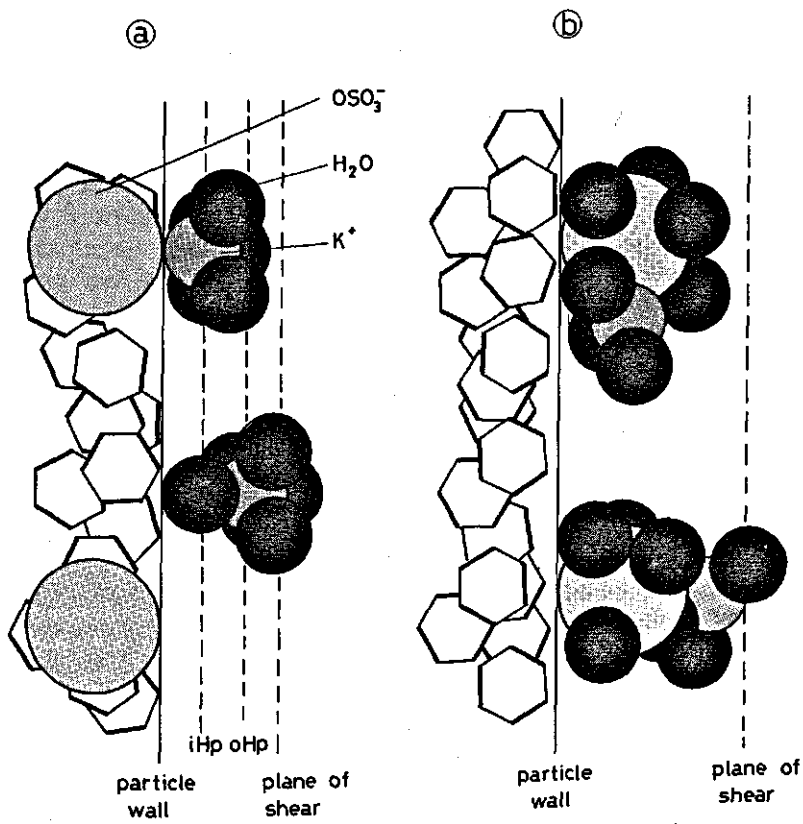

FIG. 5.18. Schematic representation of two possible structures of the polystyrene-aqueous solution interface. a. Sulphate end groups located within the particle wall; b. Sulphate end groups protruding into the solution. The assumed molecular radii (nm) are: OSO_3^- 0.29; K^+ 0.133; H_2O 0.138.

these groups, viz. to what extent are they incorporated in the polystyrene chains or do they protrude into the aqueous solution? Two extreme situations are schematically depicted in figure 5.18.

In case (a) the specifically adsorbed counterions are considered to be located between the particle wall and the shear plane. The latter may be identified with the outer Helmholtz plane. In case (b) the specifically adsorbed ions within the shear plane are not necessarily located on the bulk solution side of the $-OSO_3^-$ groups, but may reside in the same plane.

The ions and the water dipoles in the layers adjacent to the polystyrene surface will be strongly oriented, leading to a low dielectric constant in the region between the plane of shear and the particle wall.

Upon adsorption at the polystyrene surface, a part of the protein molecule may penetrate between the $-OSO_3^-$ groups of the particle, which may partially reside outside the surface, to adhere to the polystyrene particle. In this respect, the charge density and the hydrophobicity of the polystyrene surface are important properties. For latices L-1 and C-3 these properties are discussed in section 2.4. (table 2.7.).

As for dissolved protein molecules, the polar (charged) groups of the adsorbed protein molecules that are located at the interface with the aqueous solution may protrude more or less into this solution.

During the adsorption process the protein molecules may undergo some structural changes, but, referring to the discussion given in section 4.5., there are no indications that the adsorbed protein molecules adopt a conformation that would allow considerable penetration by water molecules and ions.

On the basis of the above considerations and assuming that, at adsorption saturation, the polystyrene surface is completely covered by the protein (see section 4.3.2.), a model for the adsorbed layer has been constructed in which three regions are distinguished. This model, shown in figure 5.19., has been used in the following discussion concerning the charge distribution in, and electrostatic potential across, the adsorbed layer.

In the inner region 1, $0 < x \leq m$, adjacent to the polystyrene surface, any ions trapped between the adsorbed protein molecules and the particle wall are accomodated. The thickness of region 1 is considered to be somewhat less than that of the immobile layer around the bare polystyrene particles. For case (a), figure 5.18., a thickness of 0.30 nm and for case (b) a thickness of 0.60 nm has been assumed for region 1. The thickness of the outer region 3, $p \leq x \leq d$, has been chosen to equal to the sum of that of the hydration layer around the protein-covered particles and the distance over which the charged groups of the protein protrude into the solution. In this way a value of 0.70 nm was assumed for the thickness of region 3. The thickness of the middle region 2, $m \leq x \leq p$, can be obtained from the thickness of the protein layer, less that for region 1. The thicknesses of the adsorbed layers of HPA and RNase were discussed in section 4.5. (figure 4.8.).

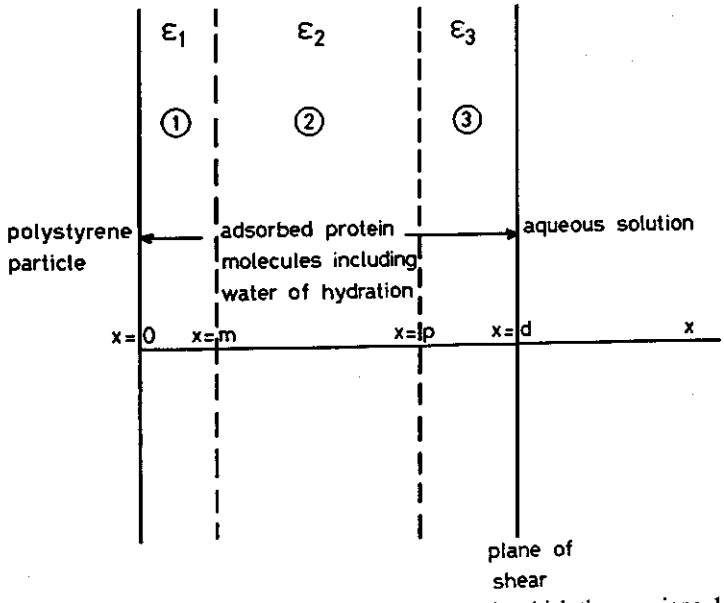

FIG. 5.19. Model of a layer of adsorbed protein molecules in which three regions, 1, 2 and 3, are distinguished. Further explanation is given in the text.

5.5.2. *Charge distribution in, and electrostatic potential across, the adsorbed layer*

Before adsorption takes place the electrokinetic charge of the polystyrene particle is compensated by the charge within its shear plane. After adsorption consideration must be given to region 1 in the model for the adsorbed protein layer, which corresponds to the interior of the protein-covered particle. Because of the low dielectric constant, the occurrence of a net charge in this region is energetically unfavourable. A fraction of the *positively* charged groups of the adsorbed protein molecules forms ion pairs with the $-OSO_3^-$ groups of the polystyrene surface (sections 5.3.3.1. and 5.3.3.2.), leading to charge compensation at this surface. On the other hand, the titration experiments revealed that the average position of the *negatively* charged carboxyl groups of the adsorbed protein molecules also tend to be relatively close to the polystyrene surface. However, the uptake of cations or the expulsion of anions, in or from region 1, during adsorption, provides one possibility of counterbalancing the effect of these groups in region 1. Region 2 is also characterized by a low dielectric constant. In this region the absence of isolated charged groups is assumed, by analogy with the interior of protein molecules dissolved in an aqueous medium. Oppositely charged groups, occurring in ion pairs, may be present in this region, however. Thus, the charge density, ρ, in region 2 is assumed to be zero. In region 3, for which the dielectric constant is assumed to be considerably higher than for region 1 or 2, the net charge, $\sigma_3^{PS/protein}$, follows from the balance between the electric charge $\sigma_d^{PS/protein}$, the charge of the polystyrene surface

titratable with protons, σ_0^{PS}, and the net charge in region 1 due to the presence of ions and charged groups of the protein molecules, $\sigma_1^{PS/protein}$

$$\sigma_0^{PS} + \sigma_1^{PS/protein} + \sigma_3^{PS/protein} + \sigma_d^{PS/protein} = 0 \qquad (5.11.)$$

With respect to the location of the negatively charged groups of the polystyrene particles, the real situation probably is somewhere between the extreme cases (a) and (b), described in the previous section and depicted in figure 5.18. As a first approxomation, the surface charge of the polystyrene is taken to be located at $x = 0$, coinciding with the particle wall.

In region 1 (thickness 0.45 nm) and also in region 3 (thickness 0.70 nm) it is assumed that a homogeneous distribution of charge is approached. (N.B. Assuming a variation of $\rho(x)$ with x, would leave us with unknown parameters in the forthcoming equations for the electrostatic potential across the adsorbed layer.) As mentioned before, it is assumed in region 2 that $\rho = 0$. As a matter of fact, the distributions of charge assumed in the various regions cannot be totally realistic because of the necessary continuity in $\rho(x)$ at $x = m$ and $x = p$.

In order to obtain an impression of the amounts of charge in the regions 1 and 3, it is instructive to determine how the electrostatic potential across the adsorbed layer varies with the charge in these regions.

At any point in an electrical double layer the charge per unit area can be related to the potential gradient, using Gauss' theorem from the theory of electrostatics,

$$\iiint \rho \, dV = \varepsilon_0 \iint (\vec{D} \cdot \overrightarrow{dO}) \qquad (5.12.)$$

where ρ is the charge density in the volume V, ε_0 the permittivity of free space, $\vec{D}$ the dielectric displacement and $\overrightarrow{dO}$ the surface vector. The left-hand term is integrated over a closed volume, the right-hand term over the surface, O, of that volume. In the medium, having a dielectric constant ε, at any point x in the electric field the scalar product $(\vec{D} \cdot \overrightarrow{dO})$ equals $\varepsilon(d\psi/dx)_x \times dO$. Hence, for the total charge in the volume, expressed per unit area of its enclosing surface located at a distance x from the charged surface the following equation holds

$$\sigma_x = \varepsilon\varepsilon_0(d\psi/dx)_x \qquad (5.13.)^1$$

To find $\psi(x)$ across the adsorbed layer, the three regions are treated separately, beginning with region 3, $p \leq x \leq d$. Applying equation (5.13.) for $x = d$ and $x = p$, yields

$$\left.\begin{aligned} &(d\psi/dx)_{x=d} = \sigma_d/\varepsilon_0\varepsilon_3 \\ &\text{and} \\ &(d\psi/dx)_{x=p} = (\sigma_d + \sigma_3)/\varepsilon_0\varepsilon_3 \end{aligned}\right\} \qquad (5.14.)$$

Equation (5.14.) are the boundary conditions for solving $\psi(x)$ across $p \geq x \geq d$.

[1] Here, as well as in the following equations in this section, the superscripts, as used in equation (5.11.), are omitted.

It is assumed that $\psi_d (\equiv \psi_{x=d})$ is identical to $\zeta^{PS/protein}$. The following expression is then found

$$\psi(x) = \psi_d - \frac{d}{2\varepsilon_0\varepsilon_3}\left[2\sigma_d+\sigma_3\left(\frac{d}{d-p}\right)\right] + \frac{1}{\varepsilon_0\varepsilon_3}\left[\sigma_d+\sigma_3\left(\frac{d}{d-p}\right)\right]x - \frac{1}{2\varepsilon_0\varepsilon_3}\left[\frac{\sigma_3}{(d-p)}\right]x^2 \qquad (5.15.)$$

Since region 2 is free of charge, it may be treated as a parallel plate condenser for which the capacitance C is given by

$$C = (\sigma_3+\sigma_d) / (\psi_p-\psi_m) = \varepsilon_0\varepsilon_2/(p-m) \qquad (5.16.)$$

It follows that $\psi(x)$ drops linearly across region 2. $\psi(x)$ is found using $\psi_p \equiv \psi_{x=p}$, which can be calculated by means of equation (5.15.). Then, across region 2

$$\psi(x) = \psi_p + \frac{1}{\varepsilon_0\varepsilon_2}\left[\sigma_3+\sigma_d\right](x-p) \qquad (5.17.)$$

The expression for $\psi(x)$ across region 1, $0 < x \leq m$, is found in a way analogous to that for region 3. $\psi_m (\equiv \psi_{x=m})$ can be calculated using equation (5.17.). The equation for the potential across region 1 reads

$$\psi(x) = \psi_m - \frac{m}{2\varepsilon_0\varepsilon_1}\left[-\sigma_0+\sigma_3+\sigma_d\right] + \frac{1}{\varepsilon_0\varepsilon_1}\left[-\sigma_0\right]x - \frac{1}{2\varepsilon_0\varepsilon_1}\left[\frac{\sigma_1}{m}\right]x^2 \qquad (5.18.)$$

The values for ε, to be assigned to the different regions are not clear-cut. The permittivity of the interior of the adsorbed protein layer (regions 1 and 2) may be of the same order of magnitude as that of a protein molecule in aqueous solution. A value of 5 is ascribed to both ε_1 and ε_2. In region 3 the water molecules are expected to be oriented more strongly than in bulk water. Therefore, the permittivity in region 3 should lie between that of a completely rigid aqueous medium ($\varepsilon \approx 4$) and that of bulk liquid water ($\varepsilon = 78.5$). For ε_3 a value of 15 is taken. The possible errors in the values chosen for ε_1, ε_2 and ε_3 may be in the order of 100%. Moreover, local differences in ε may exist, due to the heterogeneous chemical composition of proteins and due to the presence of water molecules and ions in the possible inter-protein voids in the adsorbed layer.

$\psi(x)$ across the adsorbed layer may now be calculated as a function of σ_1. For example, curves for $\psi(x)$ at various values of σ_1 are shown in figure 5.20. for a few cases. It would be unrealistic to assume that in the adsorbed layer $\psi(x)$ reaches a very large value. Therefore, even allowing for the uncertainties in the choice of the parameters, it is evident that σ_0 must be balanced to a large extent by counter charge in the region $0 < x \leq m$. Values for σ_1 and σ_3, corresponding to $\psi_m = -100$ mV, are presented in table 5.7. The calculations of σ_1 and σ_3 are performed at two values of $(p-m)$. For the parameter p the limiting thicknesses of the adsorbed layer, as indicated in figure 4.8., are taken.

In the case of HPA the differences between the values of σ_1 and, hence, be-

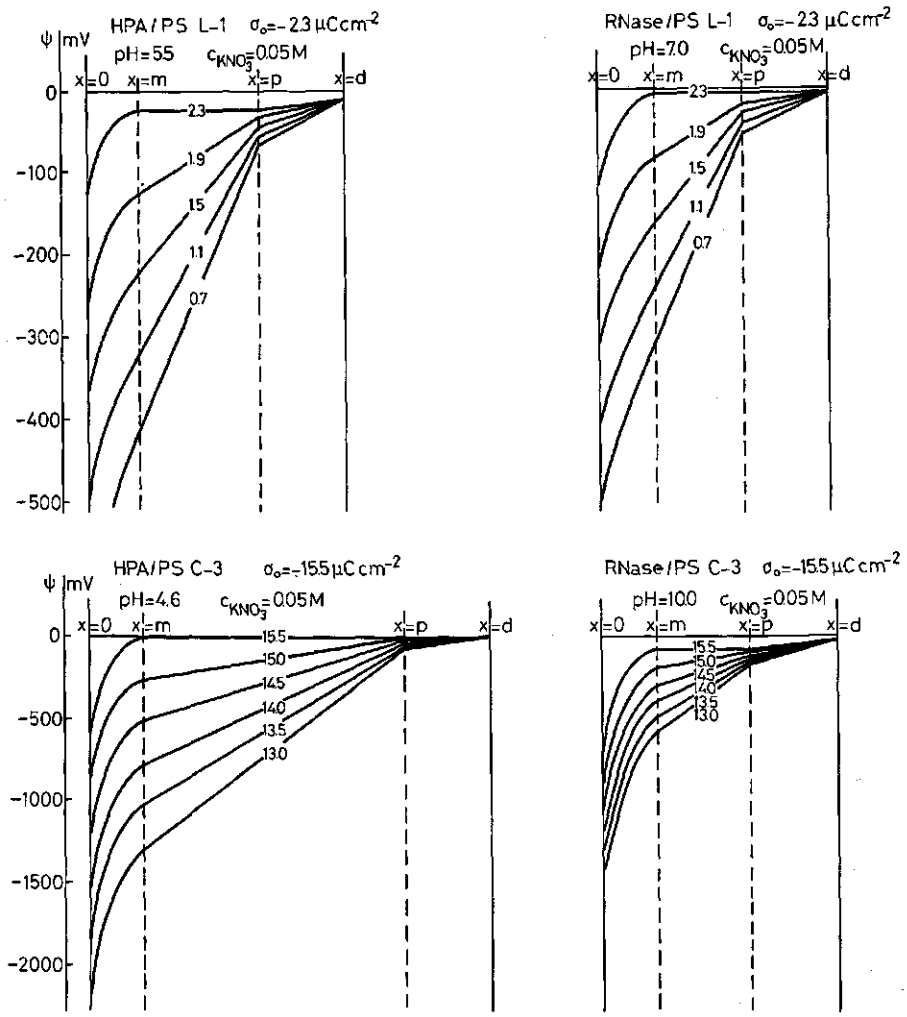

FIG. 5.20. Electrostatic potential across layers of HPA and RNase adsorbed on polystyrene latices L-1 and C-3. Curves are shown for different charge densities in $0 < x \leq m$ (values in $\mu C\ cm^{-2}$ inserted in the corresponding curves).

tween those of σ_3, obtained at the two values of $(p-m)$, are much smaller than in the case of RNase. In the first place, this is simply due to the closer values of $(p-m)$ for the adsorbed HPA layers. Also, the variation of σ_1 and σ_3 with $(p-m)$ is larger at smaller $(p-m)$ and at more negative σ_d (i.e. at more positive ψ_d). This may be seen from the equations (5.11.), (5.15.) and (5.17.), from which it follows that

$$\frac{\delta \sigma_1}{\delta(p-m)} = \frac{-\frac{\varepsilon_0}{\varepsilon_2}\psi_m + \frac{\varepsilon_0}{\varepsilon_2}\psi_d - \frac{d-p}{2\varepsilon_2\varepsilon_3}\sigma_d}{\left(\frac{d-p}{2\varepsilon_3} + \frac{p-m}{\varepsilon_2}\right)^2} \qquad (5.19.)$$

TABLE 5.7. Distribution of charge ($\mu C\ cm^{-2}$) over the adsorbed layer, calculated for $\psi_m = -100$ mV.
$c_{KNO_3} = 0.05\ M$ $T = 25°C$

		polystyrene latex L–1 $\sigma_0 = -2.3\ \mu C\ cm^{-2}$							polystyrene latex C–3 $\sigma_0 = -15.5\ \mu C\ cm^{-2}$						
	pH	σ_d	(p-m) nm	σ_1	σ_3	(p-m) nm	σ_1	σ_3	σ_d	(p-m) nm	σ_1	σ_3	(p-m) nm	σ_1	σ_3
HPA	4.0	–1.1	1.40	1.9	1.5	0.82	1.6	1.8	–0.8	2.08	15.2	1.1	1.29	15.1	1.2
	4.25	–0.6	1.65	2.0	1.0	0.99	1.8	1.2	–0.4	2.37	15.3	0.6	1.49	15.2	0.7
	4.6	–0.2	1.83	2.1	0.4	1.12	1.9	0.5	0.1	2.64	15.4	0.1	1.67	15.3	0.2
	5.0	0.2	1.54	2.1	0.1	0.92	1.9	0.2	0.5	2.27	15.4	–0.4	1.42	15.3	–0.3
	5.5	0.5	1.25	2.0	–0.3	0.72	1.9	–0.1	0.9	1.81	15.4	–0.8	1.11	15.3	–0.7
	6.0	0.7	1.08	2.0	–0.5	0.60	1.9	–0.3	1.3	1.44	15.4	–1.2	0.85	15.3	–1.1
	6.5	1.0	0.89	2.1	–0.7	0.47	1.9	–0.6	1.5	1.11	15.4	–1.4	0.62	15.3	–1.4
	7.0	1.2	0.75	2.0	–0.9	0.37	1.8	–0.7	1.7	0.81	15.4	–1.7	0.41	15.4	–1.6
	7.3	1.3	0.68	2.0	–1.0	0.32	1.7	–0.7							
	7.5														
	8.0								1.9	0.65	15.5	–1.9	0.31	15.4	–1.9
									2.1	0.59	15.5	–2.0	0.27	15.4	–2.0
RNase	4.0	–1.7	1.12	1.7	2.3	0.15	–0.5	4.5	–0.6	1.76	15.2	0.9	0.40	14.4	1.8
	5.0	–1.1	1.16	1.8	1.6	0.17	0.0	3.4	0.1	1.78	15.3	0.1	0.40	14.6	0.8
	6.0	–0.6	1.21	1.9	1.0	0.19	0.4	2.4	0.6	1.76	15.3	–0.4	0.40	14.8	0.2
	7.0	0.1	1.21	2.0	0.2	0.19	1.0	1.2	0.9	1.76	15.4	–0.8	0.40	15.0	–0.4
	8.0	0.5	1.21	2.0	–0.3	0.19	1.2	0.6	1.2	1.67	15.4	–1.1	0.36	15.0	–0.7
	9.0	0.7	1.20	2.1	–0.5	0.18	1.2	0.4	1.5	1.54	15.5	–1.4	0.31	15.2	–1.2
	9.3	0.9	1.16	2.1	–0.7	0.17	1.4	0.0	1.7	1.45	15.4	–1.6	0.28	15.2	–1.3
	10.0	1.3	1.07	2.2	–1.1	0.13	1.6	–0.6	2.0	1.29	15.5	–2.0	0.22	15.4	–1.9
	11.0	1.8	0.98	2.3	–1.8	0.10	2.0	–1.6	2.8	1.01	15.6	–2.9	0.11	16.0	–3.2

At given conditions, the variation of ψ_m with σ_1 is given by

$$\frac{\delta \psi_m}{\delta \sigma_1} = \frac{p-m}{\varepsilon_0 \varepsilon_2} + \frac{d-p}{2\varepsilon_0 \varepsilon_3} \qquad (5.20.)$$

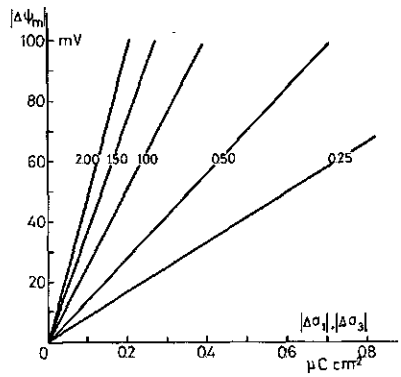

FIG. 5.21. Variation of ψ_m as a function of the charge distribution over the adsorbed protein layer. The values, inserted in the curves, refer to the thickness (nm) of the region $m \leq x \leq p$ of the adsorbed layer.

After having substituted the values for ε_2, ε_3 and $(d-p)$, mentioned above, equation (5.20.) is represented graphically for various values of $(p-m)$ in figure 5.21. Thus, the possible errors in σ_1 and σ_3 due to mis-judging ψ_m can be estimated from this figure.

The values for σ_1 and σ_3 used in subsequent calculations are the average of those given in table 5.8.

σ_1 and σ_3 originate from any charged groups of the protein molecules themselves and from any ions present in the regions 1 and 3, respectively. The distribution of the net proton charge of the adsorbed protein molecules may be roughly estimated from the titration data and the corresponding amounts of protein adsorbed. Based on the fraction of the ε-amino groups of the adsorbed RNase molecule that is supposed to be involved in ion pair formation with negatively charged groups at the polystyrene surface (see section 5.3.3.1.), for both HPA and RNase the percentage of the positively charged groups participating in such ion pairs is assumed to be ca. 20% for latex L-1 and ca. 30% for latex C-3. With respect to the position of the carboxyl groups of the adsorbed protein molecules, calculations have been made for different fractions being located in region 1, viz. 30%, 40%, 50%, 60% and 70%. Having distributed the net proton charge of the adsorbed protein over the regions 1 and 3, the contribution of ions to σ_1 and σ_3 can be calculated.

Any ions bound to the protein molecules in solution will still, after adsorption, contribute to σ_1 and σ_3. In section 5.4.2. values for $(\Delta\sigma_d)_{ads}$ have been calculated, indicating that mobile ions are also involved in the adsorption

process. In order to evaluate the distribution of $-(\Delta\sigma_d)_{ads}$ (i.e. the net change in the charge due to ionic effects upon adsorption) over region 1, $\Delta\sigma_1$, and over region 3, $\Delta\sigma_3$, the fraction of the charge due to ions bound to the dissolved protein molecules that will, after adsorption, reside in region 1, must be known. Calculations have been performed for different values of this fraction. In the case of RNase the fractions chosen were 15% and 30% and for HPA, because of its relatively high affinity for anions, 25% and 50% were chosen.

The values for $\Delta\sigma_1$ and $\Delta\sigma_3$ thus obtained under these different conditions, are represented graphically as a function of the pH of adsorption in figures 5.22. and 5.23. The following conclusions are reached. $\Delta\sigma_1$ and $\Delta\sigma_3$ are strongly affected by the values taken for the contributions of the net proton charge of the adsorbed protein molecules and of the charge bound to the adsorbing molecules. However, for each system, general trends for the dependence of $\Delta\sigma_1$ and $\Delta\sigma_3$ on the pH of adsorption emerge. As a rule, for both proteins, adsorbed on both latices, $\Delta\sigma_1$ is positive and $\Delta\sigma_3$ is negative. For RNase $\Delta\sigma_1$ increases with increasing pH. For HPA, $\Delta\sigma_1$ passes through a maximum in the region of pH were a maximum amount of protein is adsorbed (see figure 4.4.). Expressed per adsorbed protein molecule, for both HPA and RNase, the charge effects in region 1, due to the transfer to or from solution of mobile ions, tend to increase with increasing pH. Qualitatively, this feature is easily explained by realizing that, at higher pH's, an increasing number of negatively charged carboxyl groups and a decreasing number of positively charged groups of the protein molecules lie in region 1, where the charge of the polystyrene surface is compensated almost completely (see table 5.7.). In region 3 of the adsorbed layers of both proteins, the charge effects caused by the transfer of mobile ions, again expressed per adsorbed protein molecule, tend to be less negative at higher pH values.

One may consider whether there are any indications as to what extent the values taken for the numbers of the different charged groups in region 1 are real.

From the discussion on the effect of the pH on the titration behaviour of the adsorbed protein molecules (section 5.3.3.2.) it can be argued that the fraction of the carboxyl groups of HPA located near the polystyrene surface is minimal in the case of adsorption from its isoelectric solution. If, at a pH of adsorption of 4.6, say 30% of the carboxyl groups become located in region 1, then this figure may increase to 40%–50% when adsorption occurs at pH 4.0, and may be even as high as about 70% at pH 7.3 and pH 8.0. The experimental results with RNase do not indicate a significant effect of the pH of adsorption on the fraction of carboxyl groups that are located near the polystyrene surface. As compared to the figures given for HPA, for RNase this fraction may be about 40%.

With respect to the ions bound to the dissolved protein molecules, there is no information regarding the number present in region 1, after adsorption. Considering the repulsive electrostatic interactions that would otherwise result, one might expect that the bound anions prefer to become located in the

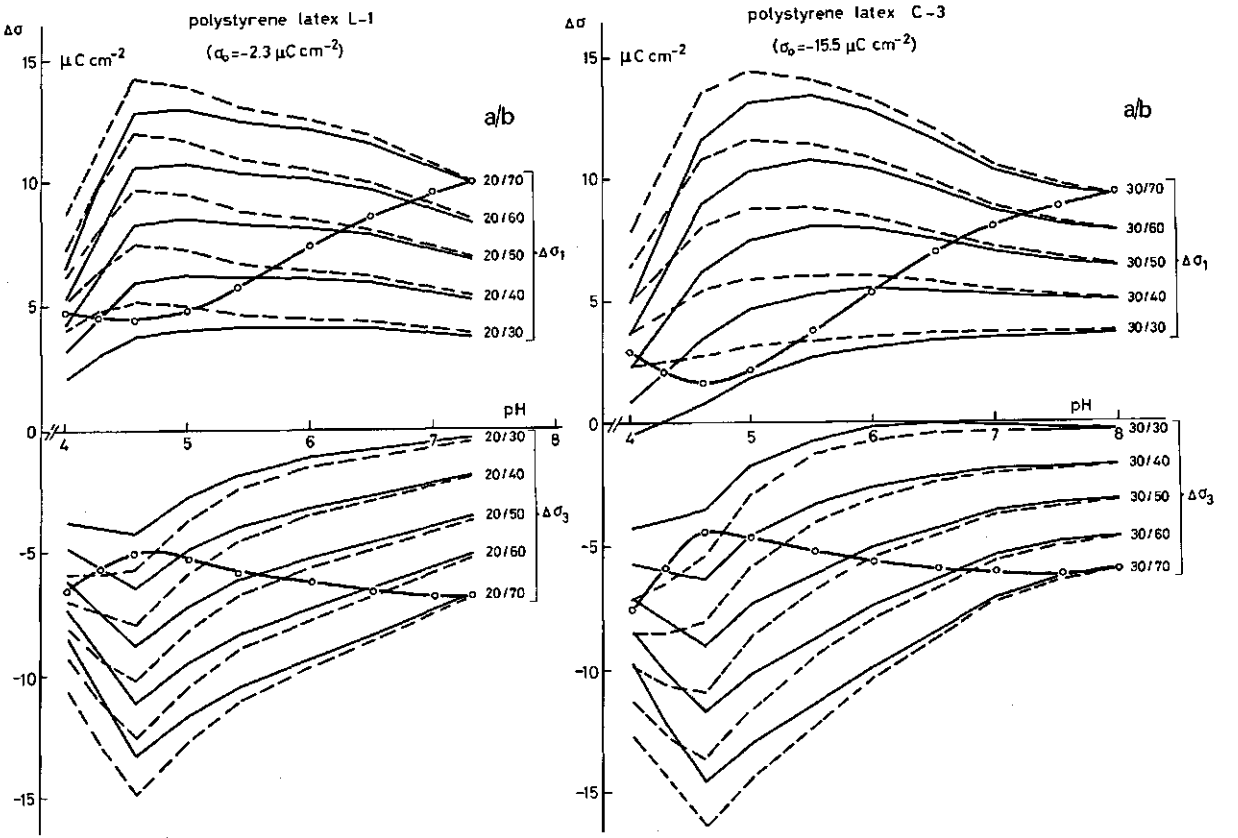

FIG. 5.22. Contribution from the inclusion and/or expulsion of mobile ions to the charge densities in the regions $0 < x \leq m$ and $p \leq x \leq d$ in layers of HPA molecules adsorbed on polystyrene latices. Ionic strength 0.05 M $T = 25°C$
Values calculated for 25% (——) and 50% (– – –) of the ions bound to the dissolved HPA molecule arriving in region $0 < x \leq m$. *a/b* refers to the fractions of, respectively, positively and negatively charged groups of the adsorbed HPA molecule residing in region $0 < x \leq m$. —O— trends of $\Delta\sigma_1$ and $\Delta\sigma_3$ as a function of pH (see text).

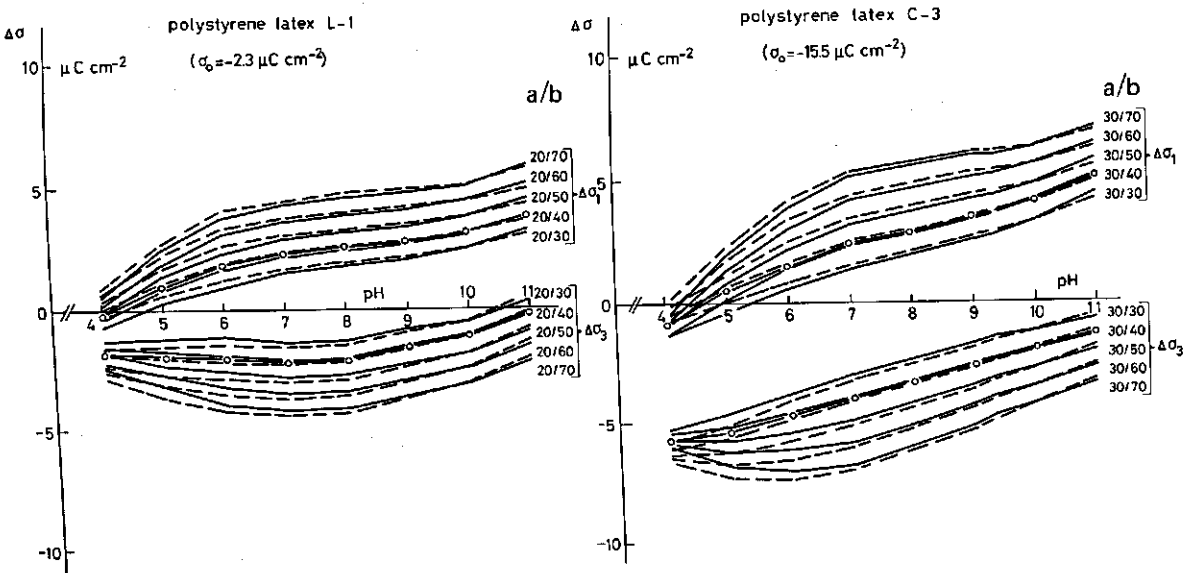

FIG. 5.23. Contribution from the inclusion and/or expulsion of mobile ions to the charge densities in the regions $0 < x \leq m$ and $p \leq x \leq d$ in layers of RNase molecules adsorbed on polystyrene latices. Ionic strength 0.05 M $T = 25°C$. Values calculated for 15% (——) and 30% (– – –) of the ions bound to the dissolved RNase molecule arriving in region $0 < x \leq m$. *a/b* as in figure 5.22.
—O— trends of $\Delta\sigma_1$ and $\Delta\sigma_3$ as a function of pH (see text).

aqueous side of the adsorbed layer. On the other hand, bound cations would preferentially stay closer to the polystyrene surface. The extent to which the position of these ions in the adsorbed layer is determined by electrostatic interactions alone, depends on the chemical affinity of the protein and the polystyrene surface for both kinds of ions.

At the acid side of the isoionic point, i.e. at positive values for Z_H, the type of ions bound to the dissolved protein will primarily be anions. Because the chemical affinity of the protein, especially HPA, for anions is higher than for cations, on the alkaline side of the isoionic point both anions and cations are expected to be bound to the dissolved protein molecules (cf. figures 5.14. and 5.15.). In this case, redistribution of anions and cations bound to the adsorbing protein molecules may occur. As a consequence, the assumption that, after adsorption, a fraction of the *net* bound charge will reside in region 1 may be unrealistic. The occurrence of such ionic redistribution is more likely the more weakly the ions are bound to the protein. In view of their different affinities for the proteins, the bound cations are expected to be more mobile than the bound anions.

Because of the many uncertainties concerning the distribution of charged groups over the adsorbed layer, it is difficult to determine the *real* values for $\Delta\sigma_1$ and $\Delta\sigma_3$. Nevertheless, the trends of $\Delta\sigma_1$ and $\Delta\sigma_3$, as a function of pH, may be distilled from the discussion given above. These trends are indicated in the figures 5.22. and 5.23.

A *positive* value for $\Delta\sigma_1$ points to the incorporation of cations (i.e. K^+) in region 1. At pH values where the charge bound to the dissolved protein mainly consists of anions, a *negative* value for $\Delta\sigma_3$ presumably results from the binding of anions (i.e. NO_3^-) in region 3. At higher pH, a negative value for $\Delta\sigma_3$ may, together with binding of anions, be the result of liberation of cations that were bound to the dissolved protein molecules.

It should be emphasized that the redistribution of ions in the adsorption process plays an important role in the thermodynamics of the process. In the next chapter this matter will be discussed in more detail.

5.6. Summary

In this chapter an attempt has been made to analyze the changes in charge distribution resulting from adsorption of HPA and RNase from aqueous solutions of ionic strength 0.05 M onto polystyrene surfaces of different surface charge density. For this purpose, both the bare polystyrene particles and the dissolved protein molecules, as well as the protein-covered polystyrene particles, were subjected to hydrogen ion titrations and to electrophoresis.

The variation of the net proton charge with pH, $\Delta Z_H/\Delta pH$, as a function of pH (figures 5.1. and 5.2.), is obtained directly from the titration experiments,

discussed in section 5.3. To derive the integral titration curve, Z_H(pH), one point of this curve must be known. For the dissolved protein molecules the isoionic point ($Z_H \approx 0$) has been taken as the reference point. When the proteins are adsorbed at the pH value pH_r, where the pH does not change after adsorption, Z_H(pH) may be derived, since a constant pH implies that the Z_H value for the molecule is not affected by adsorption. However, when the proteins are adsorbed at other pH values, Z_H(pH) cannot be established unequivocally. For these systems $\Delta pH/\Delta Z_H$ is plotted against Z_H (i.e. the reciprocal differential titration curve) where the position of the curves along the Z_H-axis is based on the assumption of a common intersection point for Z_H(pH) for the adsorbed and dissolved protein molecules at pH_r (figures 5.4. and 5.5.). The reciprocal differential titration curves for RNase reveal that a fraction of the positively charged groups in the adsorbing protein molecule is blocked, i.e. cannot be titrated. For adsorption on polystyrene latex L-1 this fraction amounts to ca. 20% and for latex C-3 to ca. 30%. Ion pair formation between these positively charged groups and the negatively charged sulphate groups at the polystyrene surface is considered to be the cause of this blocking. From this analysis the absolute location of the reciprocal differential titration curves and, hence, of the integral titration curves can be found. The integral titration curves for RNase are shown in figure 5.7. The absolute position of the titration curves for HPA adsorbed at $pH \neq pH_r$ cannot be derived from the experimental data. The integral titration curves for HPA (figure 5.6.) are located assuming a common intersection point at pH_r. The uncertainty along the Z_H-axis in the curves for HPA adsorbed at $pH \neq pH_r$ is estimated to amount to 3–5 Z_H units.

Apart from those groups blocked with regard to titration, in both HPA and RNase, it is the titration behaviour of the carboxyl groups that is most affected by the adsorption process. Because, at constant pH, the dissociation of the carboxyl groups decreases with increasing negative charge at the polystyrene surface, these effects have been primarily assigned to the negative electric field around the polystyrene particle. It is concluded that a relatively large number of carboxyl groups are located close to the polystyrene surface. Consequently, as a result of adsorption, the titration regions of the carboxyl groups and the imidazole and α-amino groups more or less overlap each other.

For HPA, the effect of adsorption on the titration behaviour increases with increasing net charge on the protein molecule in solution. This would suggest that the conformation of the adsorbed HPA molecules depends on their net charge in solution (cf. section 4.3.2.1.). The fraction of the carboxyl groups of the protein molecule that is located near the polystyrene surface seems to be minimal in case of adsorption from the isoelectric solution. For adsorbed RNase no significant effect of the molecular charge on the titration behaviour can be observed.

The electrophoresis of the different systems is discussed in section 5.4. From the electrophoretic mobilities (figures 5.8. –5.10) the electrokinetic potentials (= ζ-potentials) have been derived (figures 5.11.–5.13.). For the HPA-covered polystyrene particles the influence of the negatively charged polystyrene

surface on ζ(pH) is much less than for the RNase-covered particles. Except perhaps at low pH values, it can be said that the ζ-potentials of the protein-covered particles are lower than those of the corresponding dissolved protein molecules at the same pH. In all cases, adsorption at a more negatively charged surface (latex C-3) results in a more negative value for the ζ-potential.

At various pH values, the ζ-potential, interpolated from the ζ(pH) curve, is converted into the electrokinetic charge (table 5.6.). Based on the requirement of overall electroneutrality, analysis of the electrokinetic charges, whilst accounting for the change in net proton charge of the protein, indicates that charge effects due to the redistribution of mobile ions are involved in the adsorption process (figure 5.16. and 5.17.). For both proteins, adsorbed at both latices, these effects are similar, viz. a net uptake from solution of negative charge at low pH and of positive charge at high pH.

In section 5.5. the location of the ions participating in the adsorption process is analyzed in a semi-quantitative way. This analysis is based on a model for the adsorbed protein layer described in section 5.5.1. In spite of the many uncertainties in the assumptions involved, it seems reasonable to conclude that during the adsorption of protein molecules positive charge is taken up close to the polystyrene surface, whereas in the aqueous side of the adsorbed layer negative charge is bound (figures 5.22. and 5.23.). It would seem that this charge effect in the region near the polystyrene surface is mainly due to the uptake of cations from solution. The charge effect in the aqueous side of the protein layer would be due to the binding of anions from solution and, at relatively high pH (pH > i.e.p.), possibly also to liberation of cations from the adsorbing protein molecules.

6. THERMODYNAMIC ANALYSIS

6.1. Introduction

In the previous chapters the complexity of the adsorption of HPA and RNase at the polystyrene surface has been indicated. The factors governing the mutual interactions between the polystyrene surface and the adsorbing protein molecules as well as those responsible for the structure of the protein molecule in solution, influence the overall adsorption process.

The aim of this chapter is to estimate, from a thermodynamic standpoint, the relative importance of the roles played by these various factors.

For the adsorption process to occur spontaneously, the Gibbs free energy of adsorption ΔG_{ads} must be negative. At a given temperature, T, ΔG_{ads} can be expressed as

$$\Delta G_{ads} = \Delta H_{ads} - T\Delta S_{ads} \qquad (6.1.)$$

where ΔH_{ads} and ΔS_{ads} are, respectively, the net changes in enthalpy and entropy involved in the adsorption process. The terms can be evaluated e.g. per unit surface area of adsorbent or per mole adsorbed protein. Equation (6.1.) shows that a negative value for ΔH_{ads} and a positive value for ΔS_{ads} give rise to a negative value for ΔG_{ads} and, hence, favour the adsorption process.

Because of the irreversibility of the adsorption of HPA and RNase at polystyrene surfaces (see section 4.3.2.) and the probable non-isosteric conditions, the differential enthalpy that is obtained from measuring adsorption isotherms at different temperatures is not identical to the net adsorption enthalpy, denoted above as ΔH_{ads}. Since the adsorption proceeds under isobaric conditions, ΔH_{ads} can be determined directly by calorimetry (section 6.3.).

Also because of the irreversibility, ΔG_{ads} cannot be readily derived from the adsorption isotherms.

If ΔG_{ads} is unknown, then ΔS_{ads} cannot be obtained using equation (6.1.). Moveover, in view of the many possible conformational and configurational changes that the polymer molecules and solvent molecules may undergo in the adsorption process, it is obvious that a direct, statistical calculation of ΔS_{ads} is virtually impossible.

Any variations in the spatial configuration of the molecules participating in the adsorption process will also result in a net change in the apparent heat capacity, ${}^{\phi}C_P$[1], of the dispersion. $(\Delta^{\phi}C_P)_{ads}$ equals the temperature coefficient of ΔH_{ads} (at constant pressure P)

$$(\Delta^{\phi}C_P)_{ads} = \{\delta(\Delta H_{ads})/\delta T\}_P \qquad (6.2a.)$$

[1] ${}^{\phi}C_P$ of a system equals the sum of the heat capacities of the constituting components together with the contributions due to their interactions.

Obviously, in this equation $(\Delta^{\phi}C_P)_{ads}$ and ΔH_{ads} refer to the same amounts of substances. Unless otherwise stated, these quantities will be quoted per unit area of the adsorbent surface. If $(\Delta^{\phi}C_P)_{ads}$ were expressed per unit mass of protein adsorbed and ΔH_{ads} per unit area of adsorbent, equation (6.2a.) would have to be modified as follows

$$(\Delta^{\phi}C_P)_{ads} \times \Gamma_p = \{\delta(\Delta H_{ads})/\delta T\}_P \qquad (6.2b.)$$

where Γ_p is the amount of protein adsorbed in units of mass per unit area.

According to EVERETT (1957) the configurational part of the heat capacity can be written as the product of two factors

$$C_P^{config} = (\delta H/\delta\xi)_{T,P} \times (\delta\xi/\delta T)_P \qquad (6.3.)$$

where ξ is an ordering parameter whose value increases with decreasing configurational entropy of the system. ξ usually decreases with increasing temperatemperature: $(\delta\xi/\delta T)$ is negative. C_P^{config} itself is always positive and, hence, $(\delta H/\delta\xi)_{T,P}$ must be negative. In general, upon increasing the structure (i.e. order) $\delta H/\delta\xi$ will become more negative and $\delta\xi/\delta T$ less negative. Thus the two factors tend to compensate one another.

$(\Delta^{\phi}C_P)_{ads}$ may be interpreted in terms of the change in the configurational heat capacity of the system that result from the adsorption process. A positive value for $(\Delta^{\phi}C_P)_{ads}$ then implies that either both factors of the right-hand term of equation (6.3.) acquire more negative values or that the positive shift in one of the factors is overcompensated by the negative shift in the other.

In aqueous media, changes in ${}^{\phi}C_P$ are mostly discussed in terms of changes in water structure, notably the number and the strength of the hydrogen bonds. For example, the large negative value for $\Delta^{\phi}C_P$ observed for systems showing hydrophobic bonding points to the fact that the hydrogen bonds between the water molecules surrounding non-polar solutes are more labile than they are in pure water.

In this chapter microcalorimetric determinations of ΔH_{ads} will be described. ΔH_{ads} has been determined as a function of pH, surface charge of the polystyrene, concentration of KNO_3 and temperature. An attempt will be made to analyze the experimental data in terms of the contributions made by each of the various factors that are known to be involved in the adsorption process. Because knowledge of these factors exists only on a qualitative or semi-quantitative basis, a detailed interpretation of the results is not yet possible.

The analysis of ΔH_{ads} allows us to obtain an impression of how the various variables tested influence the adsorption process. In this way it is hoped that it may give some clues to solving the mechanism of protein adsorption.

6.2. Materials

The preparations of the polystyrene latices and the solutions of HPA and RNase have been described in sections 2.3. and 4.2., respectively.

All other chemicals used were of analytical grade. The water was distilled from an all-Pyrex apparatus.

6.3. Calorimetry

Calorimetry is the measurement of heat changes. Based on their mode of operation, calorimeters may be classified in two types, (i) the adiabatic type and (ii) the conduction type. The ideal adiabatic calorimeter is completely insulated from its surroundings so that the heat evolved is totally retained in the calorimeter. On the other hand, the ideal conduction calorimeter is perfectly connected 'thermally' to a surrounding heat sink to which the heat evolved in the reaction vessel is completely transferred. As the ideal heat sink is of infinite capacity, there is no final change in temperature of the calorimeter resulting from the process under investigation.

In this study the measurements were performed using a LKB 10700-2 batch microcalorimeter (LKB-Produkter AB, S-161 25 Bromma 1, Sweden). This instrument is of the conduction type. In its construction the twin principle has been adopted. Wadsö (1968) gives full details of the design and the operational procedure of this microcalorimeter. In our instrument the vessels are made of 18 carat gold.

The heat exchange between the vessels and the heat sink takes place through thermopiles. The arrangement of the thermopiles is such that the differential heat exchange is proportional to the voltage-time integral. The voltage signal was, after amplification by a Keithley 150 B Microvolt Ammeter (Keithley Instruments, Inc., Cleveland, Ohio, U.S.A.), recorded by a Servogor RE 512 recorder, fitted with a 'ball and disc' type integrator.

6.3.1. *Experimental procedure*

After the polystyrene latex and the protein solution had been both adjusted to the same KNO_3 concentration and pH, they were mutually dialyzed for two days against an aqueous solution of KNO_3 of identical concentration and pH. In this way it is ensured that the components that can pass the dialysis menbrane (i.e. water molecules and ions) are in thermodynamic equilibrium, prior to protein adsorption.

The thermostats of the microcalorimeter were set and the temperature of the room was adjusted to a constant value a few degrees centigrade below the temperature of the calorimeter.

The reaction vessel, which consists of two communicating compartments, was charged with polystyrene latex and protein solution in the same proportions as applied in the titration experiments (see section 5.3.2.), i.e. 4.0 cm^3

polystyrene latex (ca. 8% w/w) in one compartment and 2.0 cm^3 protein solution (ca. 9.0 grams HPA per dm^3 or 4.5 grams RNase per dm^3) in the other. Hence, after mixing the components, saturation adsorption is expected to be reached (see figures 4.1. and 4.2. and table 5.3.). The reference vessel contained 4.0 cm^3 dialysate in place of polystyrene latex.

After the vessels had reached thermal equilibrium with the heat sink, the components were mixed by rotating the vessels and the voltage signal from the thermopiles was recorded. Subsequent rotations did not show additional heat effects, except for a very small differential heat due to friction. This indicates that complete mixing of the components was achieved after the first rotation.

Each experiment was preceded and followed by a calibration procedure, as described by WADSÖ (1968). From these, the calibration constant (amount of heat per chosen unit area below the voltage-time curve) was obtained. The calibration experiments were performed while the vessels were charged with the components.

In order to obtain the heat of adsorption it is necessary to correct for the heats of dilution of the protein solution and the polystyrene latex. As the voltage-time integral reflects the difference between the amounts of heat evolved in the reaction vessel and the reference vessel, each containing the same protein concentration, the heat of dilution of the protein solution is automatically accounted for.The heat of dilution of the latex was established in a separate experiment, where the reaction vessel contained 4.0 cm^3 latex and 2.0 cm^3 dialysate and the reference vessel 4.0 cm^3 and 2.0 cm^3 dialysate. The heat of dilution of the polystyrene latex is very small relative to the heat of adsorption.

Prior to each measurement the vessels were thoroughly cleaned. The cleaning procedure consisted of rinsing several times with water, ethanol, toluene and ethanol, respectively. Then, the vessels were dried over air stream. Before charging, the vessels were rinsed with the dialysate and dried again.

6.3.2. *Results and discussion*

The heat of adsorption q_{ads} (= enthalpy of adsorption ΔH_{ads}) is expressed per unit area of polystyrene surface. It is to be noted again that ΔH_{ads} refers to adsorption saturation (N.B. The equilibrium concentration of protein was determined occasionally and was found to be in accordance with the plateau values given in the figures 4.4. and 4.5.). At fixed protein concentration but variable polystyrene content, ΔH_{ads} varies proportionally with the area of the adsorbing interface, as expected.

Figure 6.1. shows ΔH_{ads}(pH) for HPA at polystyrene surfaces of different surface charge, σ_0, and at different concentrations of KNO_3, c_{KNO_3}. In figure 6.2. the temperature dependence of ΔH_{ads}(pH) for HPA adsorbed on latices L-1 and C-3 is given. The corresponding graphs for RNase are collected in figures 6.3. and 6.4.

If ΔH_{ads} is determined purely by the overall electrostatic interaction between the protein molecules and the negatively charged polystyrene surface, then it

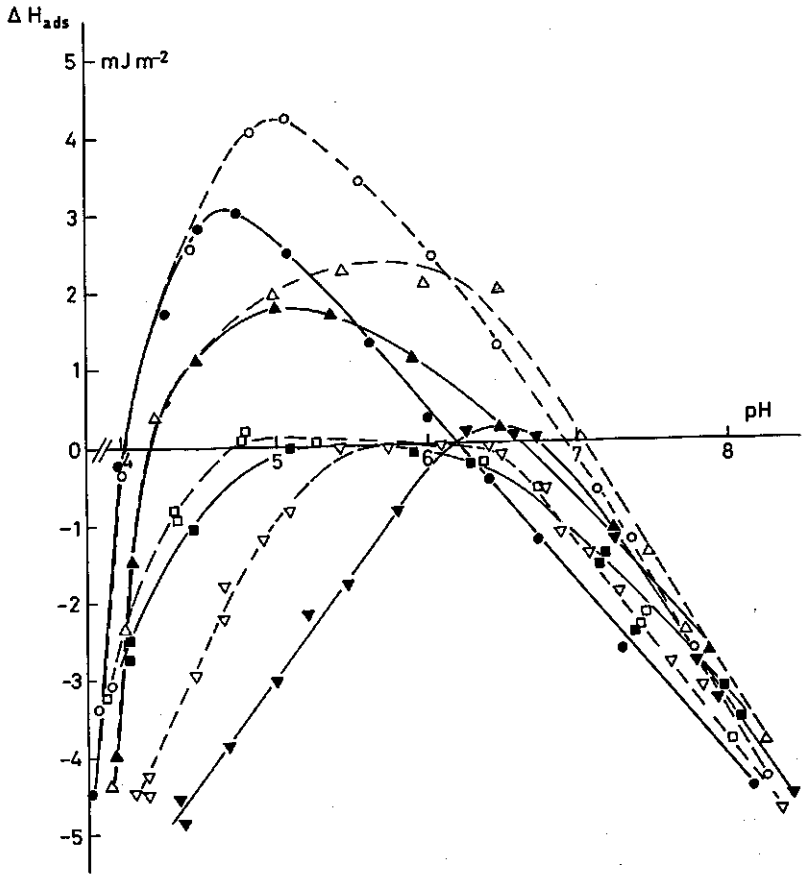

FIG. 6.1. Enthalpy of adsorption of HPA on polystyrene latices.
○ $\sigma_0 = -15.5\ \mu C\ cm^{-2}$ △ $\sigma_0 = -6.3\ \mu C\ cm^{-2}$ □ $\sigma_0 = -4.6\ \mu C\ cm^{-2}$
▽ $\sigma_0 = -2.3\ \mu C\ cm^{-2}$. Open symbols 0.01 M KNO_3; filled symbols 0.05 M KNO_3.
$T = 25°C$.

should become more endothermic (i.e. more positive) with increasing pH. However, neither with HPA (cf. NORDE and LYKLEMA, 1972 and NORDE et al, 1972) nor with RNase was an increase of ΔH_{ads} with pH found. The observed trends are more complex, reflecting the compounding of several contributions to ΔH_{ads} resulting from adsorption of the protein.

All the curves for ΔH_{ads}(pH) pass through a maximum. Upon increasing σ_0 this maximum becomes more positive and its position shifts to lower pH values. If, at a given σ_0, the shape of the curve for ΔH_{ads} (pH) could be explained in terms of alterations in the protein structure, the maximum in the curve would be expected at that pH where $(\Gamma_p)_{max}$ (pH) also reaches a maximum value (see figures 4.4. and 4.5.). Such a coincidence is not generally found; this is best illustrated for the case of HPA adsorbed at a polystyrene surface having a rela-

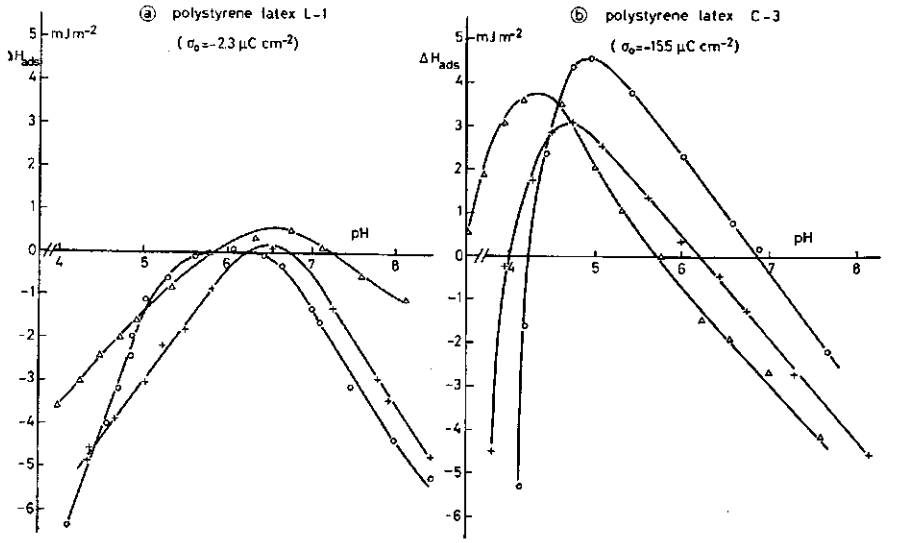

FIG. 6.2. Enthalpy of adsorption of HPA on polystyrene latices at various temperatures. △ 9°C + 25°C ○ 37°C c_{KNO_3} = 0.05 M.

tively low σ_0. Hence, also other factors (to be discussed later) contribute to ΔH_{ads}.

Unlike the case for RNase, ΔH_{ads} (pH) for HPA is significantly affected by c_{KNO_3}. The influence of the electrolyte depends in a systematic, but still somewhat complex, way on σ_0 and pH. In the case of adsorption of HPA at a polystyrene surface of small σ_0, the part of the curve on the acid side of the maximum is relatively most affected by changes in c_{KNO_3}. However, using latices of large σ_0 the effect of KNO_3 is more pronounced on the alkaline side, although at sufficiently high pH the effect diminishes.

The adsorption process is spontaneous, hence $\Delta G_{ads} < 0$. It is concluded that in the region where $\Delta H_{ads} > 0$ (and possibly also beyond it) a positive value for ΔS_{ads} must therefore be the reason for the negative value for ΔG_{ads}. It is recalled here that the temperature dependence of the isotherms for HPA (figure 4.3.) also suggests that the entropy gain is the driving force for the adsorption, at least at low surface coverage. Several factors could contribute to ΔS_{ads}, e.g. hydrophobic bonding, changes in the state of hydration of ions concomitant with the transfer to or from solution of these ions (section 5.5.2.) and structural changes in the adsorbing protein molecules. The feature, observed both with HPA (figure 6.2.) and RNase (figure 6.4), that $(\Delta^{\phi}C_P)_{ads}$ depends on both the pH and σ_0 underlines the complexity of the adsorption process.

As a consequence of the lack of understanding of the adsorption mechanism, prediction of ΔH_{ads} by a priori reasoning does not seem possible at this stage. It, therefore, appears more fruitful to examine which contributions to ΔH_{ads}

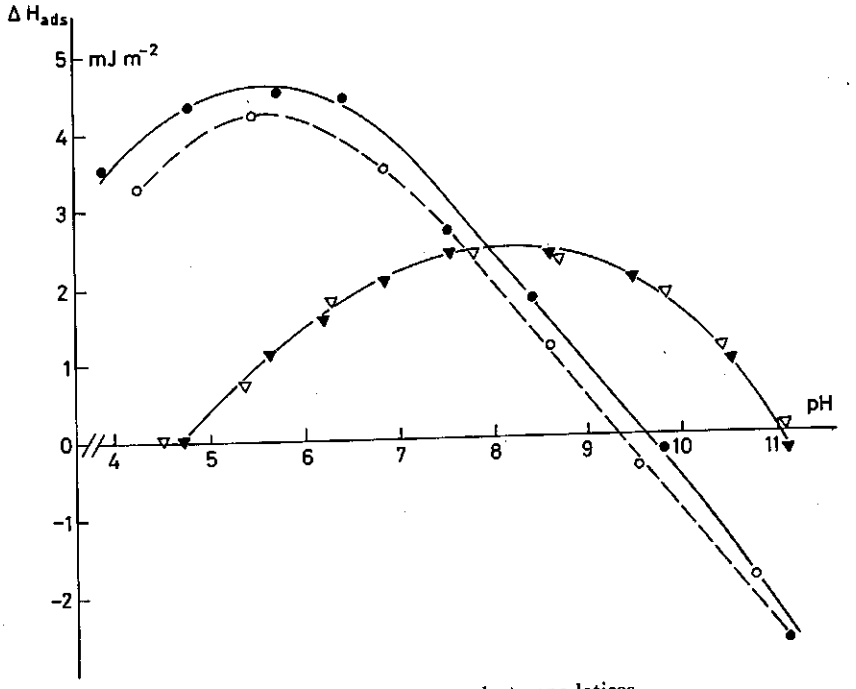

FIG. 6.3. Enthalpy of adsorption of RNase on polystyrene latices.
○ $\sigma_0 = -15.5$ μC cm^{-2} ▽ $\sigma_0 = -2.3$ μC cm^{-2}. Open symbols 0.01 M KNO_3; filled symbols 0.05 M KNO_3. $T = 25$°C.

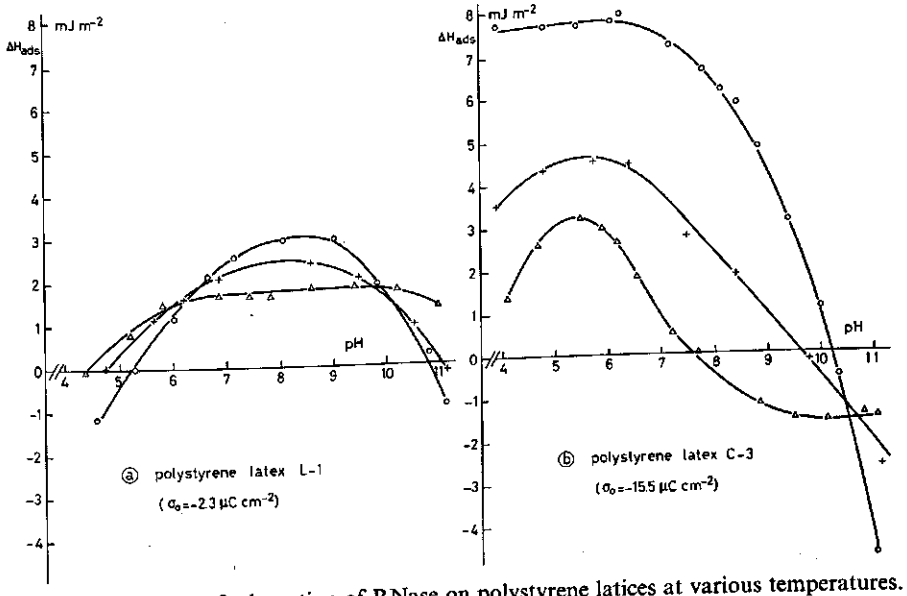

FIG. 6.4. Enthalpy of adsorption of RNase on polystyrene latices at various temperatures.
△ 9°C + 25°C ○ 37°C. $c_{KNO_3} = 0.05$ M.

one can reasonably estimate, and then to subtract the sum of these contributions from the experimental value of ΔH_{ads}. The term that is left is, as we shall discuss later, related to the enthalpy change accompanying the structural alterations in the protein molecule upon adsorption.

Since the electrostatic aspects of the adsorption process have been analyzed at 25 °C and at $c_{KNO_3} = 0.05$ M (see chapter 5), the analysis of ΔH_{ads} will be confined to these conditions.

6.3.2.1. Titration effect

In chapter 5 the effect of adsorption on the net proton charge of HPA and RNase was discussed. The number of protons taken up per adsorbing protein molecule can be estimated from the titration curves (figures 5.6. and 5.7.), taking into account any changes in pH that occur upon adsorption (figure 5.3.).

Since the systems do not contain any additional buffer, essentially all the protons taken up by the adsorbing protein molecules are provided by the protein molecules that remain in solution. Therefore, the decrease of protons in solutions, as calculated from the change in pH upon adsorption, is negligible.

With both the proteins studied the protonation of the adsorbed molecules is most pronounced in the region of Z_H where the carboxyl groups are titrated. In section 5.3.3.2. it was concluded that the average position of the carboxyl groups in the adsorbed protein layer is more close to the polystyrene surface than those of the other classes of titratable groups. In fact, a high percentage of the carboxyl groups of the adsorbed protein may reside in region 1 of the model proposed in section 5.5.1. In this region the conditions (the medium and the electric field) are essentially different from those in solution. As far as the thermodynamic functions of state are concerned, the protonation accompanying the adsorption process can be considered to occur in two consecutive steps: protonation of the protein molecule in the dissolved state followed by adsorption of the protonated protein molecule at the polystyrene surface. For the moment only the protonation occurring in solution is considered. In sections 6.3.2.2. and 6.3.2.3. the effects due to the different conditions between the adsorbed and the dissolved state will be taken into consideration.

The variations in the thermodynamic quantities resulting from the protonation (or deprotonation) of dissolved protein molecules mainly stem from electrostatic interactions and from hydration effects of the ionic groups involved (cf. CRESCENZI et al, 1972; 1973; DELBEN et al, 1972).

Using equation (5.4.) the Gibbs free energy of protonation, ΔG_{prot}, for each class j of groups of the protein can be derived from the hydrogen ion titration curve. ΔH_{prot} can either be determined directly by titration calorimetry or may be calculated from hydrogen ion titrations at different temperatures, according to the van 't Hoff equation

$$\delta \ln \{ [\text{protein-H}^+] / [\text{protein}] [\text{H}^+] \} = (\Delta H_{prot}/R) \delta T^{-1} \qquad (6.4.)$$

At constant Z_H, equation (6.4.) can be converted into

$$(\Delta H_{prot})_{Z_H} = -2.303\ R(\delta pH/\delta T^{-1})_{Z_H} \qquad (6.5.)$$

(N.B. The term $\delta \ln \{ [\text{protein-H}^+]/[\text{protein}] \}_{Z_H}$ equals zero.)

For about 10 carboxylic acid groups of BPA that are protonated in the isoionic region, LOVRIEN and STURTEVANT (1971) found, calorimetrically, an enthalpy of -5.9 ± 1.3 kJ mole^{-1}. In the literature no data on titration calorimetry over a wider region of Z_H of PA (either HPA or BPA) are available.

Based on hydrogen ion titrations with BPA at 5°C and 25°C, TANFORD et al (1955b) calculated $(\Delta H_{prot})_{Z_H}$ as a function of Z_H. For the carboxyl groups they found values between 0 and -8.5 kJ mole^{-1}, for the imidazole groups a value of about -27 kJ mole^{-1} and ca. -50 kJ mole^{-1} was found in the region where the ε-amino and the phenolic groups are titrated. Combining these values with the values for ΔG_{prot}, one obtaines values for ΔS_{prot} of about $+60$ J K^{-1} mole^{-1}, $+40$ J K^{-1} mole^{-1} and $+30$ J K^{-1} mole^{-1} for the carboxyl groups, the imidazole groups and the phenolic groups, respectively.

In view of the large similarity in titration behaviour between HPA and BPA (TANFORD et al, 1955b; STEINHARDT et al, 1971), the values mentioned above may apply to HPA as well.

The variations of the characteristic thermodynamic functions resulting from the protonation of the adsorbing protein molecules will be compensated, more or less, by the variations resulting from the deprotonation of the protein molecules remaining in solution. The overall enthalpy change of these protonations and deprotonations, denoted as ΔH_{titr}, can be estimated from ΔZ_H for the adsorbing and the non-adsorbing protein molecules and drom ΔH_{prot} (Z_H). Values for ΔZ_H for the adsorbing molecules are given in table 5.6. From these values and from the amounts of protein adsorbed and dissolved, respectively, ΔZ_H for the molecules in solution can be calculated. The values for ΔH_{prot} are taken from TANFORD et al (1955b). Curves for ΔH_{titr} (pH), thus estimated, are shown in figure 6.5. The contribution from ΔH_{titr} to ΔH_{ads} is relatively small,

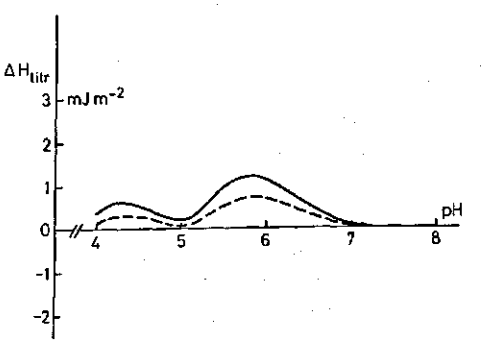

FIG. 6.5. Adsorption of HPA on polystyrene latices. Estimates of the enthalpy of the titration effect. – – – latex L-1 ($\sigma_0 = -2.3$ μC cm^{-2}); —— latex C-3 ($\sigma_0 = -15.5$ μC cm^{-2}). $c_{KNO_3} = 0.05$ M $T = 25$°C.

even in the case of adsorption at polystyrene latex C-3 for which the largest values for ΔZ_H are found.

In the case of RNase, no values for ΔH_{prot}, obtained by any method, seem to be reported in the literature. It is therefore assumed that also in the case of RNase adsorption ΔH_{titr} makes only a very small contribution to ΔH_{ads} (ΔH_{titr} (pH) 0–1 mJ m^{-2}).

6.3.2.2. Changes in the distribution of charge

In section 5.5.2. it was illustrated that protein adsorption is accompanied by a redistribution of charge, implying the overlap of electric fields.

For a flat plate model, the thermodynamic functions of state for a given distribution of charge over a region between $x = x_1$ and $x = x_2$, having a dielectric constant ε, are expressed by the following equations (BÖTTCHER, 1973).

$$G_{cd} = \frac{\varepsilon_0 \varepsilon}{2} \int_{x_1}^{x_2} \left(\frac{\delta\psi}{\delta x}\right)^2 dx \tag{6.6.}$$

$$H_{cd} = \frac{\varepsilon_0 \{\varepsilon + T(\delta\varepsilon/\delta T)_P\}}{2} \int_{x_1}^{x_2} \left(\frac{\delta\psi}{\delta x}\right)^2 dx \tag{6.7.}$$

and, hence

$$S_{cd} = \frac{\varepsilon_0 (\delta\varepsilon/\delta T)_p}{2} \int_{x_1}^{x_2} \left(\frac{\delta\psi}{\delta x}\right)^2 dx \tag{6.8.}$$

In these equations, G_{cd}, H_{cd} and S_{cd} refer to one unit surface area. By calculating the values of these properties of state for the systems before and after adsorption, the changes resulting from the overlap of electric fields upon adsorption may be obtained.

In the model for the adsorbed protein layer, proposed in section 5.5.1., various regions having different charge densities were distinguished (section 5.5.2.). For each of these regions the strength of the electric field, $\delta\psi/\delta x$, can be obtained by differentiating the potential, expressed in the equations (5.15.), (5.17.) and (5.18.), with respect to x.

The charge density in the shear layer (thickness 0.45 nm) of the bare polystyrene particle is assumed to be homogeneously distributed (i.e. analogous to region 1 of the adsorbed layer). The surface charge is taken to be located at $x = 0$, coinciding with the particle wall.

The electrokinetic charge of each protein molecule in solution is assumed firstly to be located in a peripheral sheet (thickness 0.70 nm) around the molecule, and secondly to be homogeneously distributed (cf. region 3 for the adsorbed protein layer). The inner core of the protein is considered to be neutral.

The following expressions are then obtained for $\delta\psi/\delta x$ within the shear region

a. for the bare polystyrene particles:

$$\delta\psi/\delta x = -\frac{1}{\varepsilon\varepsilon_0}\{\sigma_0 + (\sigma_m/d)\,x\} \tag{6.9.}$$

b. for the dissolved protein molecules:

$$\delta\psi/\delta x = \frac{1}{\varepsilon\varepsilon_0}\frac{\sigma_d}{d}x \tag{6.10.}$$

where d is the thickness of the shear layer in each case. σ_0, σ_m and σ_d are the surface charge densities at $x = 0$, across the shear layer and at $x = d$, respectively.

For the diffuse part of the electrical double layer (i.e. the part outside the plane of shear) $\delta\psi/\delta x$ follows from the theory of GOUY (1910) and CHAPMAN (1913). At relatively small values for $\psi(x)$, $\delta\psi/\delta x$ is given approximately by

$$\delta\psi/\delta x = -\psi_d \varkappa \exp[-\varkappa x] \tag{6.11.}$$

where ψ_d ($\equiv \zeta$) is the potential at the shear plane ($x = 0$) and $\varkappa$ is the reciprocal Debye length. $\varkappa$ is defined by the relation

$$\varkappa^2 = (\sum_i c_i z_i^2 F^2)/\varepsilon\varepsilon_0 RT \tag{6.12.}$$

where c_i and z_i are the bulk concentration (i.e. at the point where $\psi = 0$) and the valency, respectively, of ionic species i.

The temperature dependence of the dielectric constant, $\delta\varepsilon/\delta T$, is itself a function of ε. By interpolating the data for pairs of values for ε and $\delta\varepsilon/\delta T$, reported in the literature (Handbook of Chemistry and Physics, 1972–1973, 53rd ed. CRC, pp E43-E46), the following combinations of ε and $\delta\varepsilon/\delta T$, at 25 °C, were chosen: $\varepsilon = 5$, $\delta\varepsilon/\delta T = -0.012\ \mathrm{K}^{-1}$ for regions 1 and 2 of the adsorbed protein layer; $\varepsilon = 15$, $\delta\varepsilon/\delta T = -0.055\ \mathrm{K}^{-1}$ for the peripheral regions of the adsorbed protein layer and the dissolved protein molecules; $\varepsilon = 78.5$, $\delta\varepsilon/\delta T = -0.361\ \mathrm{K}^{-1}$ for the diffuse part of the double layer.

In the case of latex C-3 in particular, the charge distributions in the shear layer around the bare particles and in region 1 of the protein-covered particles contribute in a major way to the thermodynamic state functions of the complete charge distributions around the bare and in the protein-covered particles, respectively. Therefore, assuming the dielectric properties of region 1 to be constant, ΔH_{cd} has been calculated for different combinations of ε and $\delta\varepsilon/\delta T$ in the shear layer around the bare particles, viz. for $\varepsilon = 5$, $\delta\varepsilon/\delta T = -0.012\ \mathrm{K}^{-1}$; $\varepsilon = 8$, $\delta\varepsilon/\delta T = -0.023\ \mathrm{K}^{-1}$; $\varepsilon = 10$, $\delta\varepsilon/\delta T = -0.032\ \mathrm{K}^{-1}$ and for $\varepsilon = 15$, $\delta\varepsilon/\delta T = -0.055\ \mathrm{K}^{-1}$. Curves for ΔH_{cd} (pH), thus calculated, are shown in the figures 6.6. and 6.7. ΔH_{cd} appears to be very little dependent on pH. The effect of σ_0 on ΔH_{cd} is very sensitive to the difference between the dielectric properties of region 1 and those of the shear layer around the bare polystyrene particles.

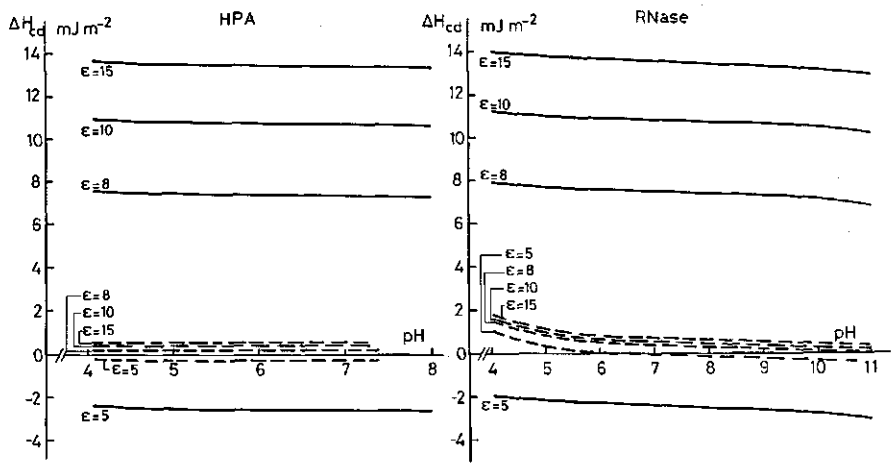

FIGS. 6.6. and 6.7. Adsorption of HPA and RNase on polystyrene latices. Estimates of the enthalpy of the redistribution of charge for different values of the dielectric constant ε in the shear layer around the bare polystyrene particles (see text). – – – latex L-1 ($\sigma_0 = -2.3$ μC cm^{-2}); —— latex C-3 ($\sigma_0 = -15.5$ μC cm^{-2}). $c_{KNO_3} = 0.05$ M $T = 25$°C.

6.3.2.3. Ionic medium effect

The redistribution of charge due to protein adsorption involves the transfer of ions from the aqueous to the proteinaceous medium (see section 5.5.2.). This change in the medium of the transferred ions is referred to as the *ionic medium effect*. It is virtually a chemical contribution in distinction to the electrical contribution due to the field overlap, as discussed in the previous section.

The changes in the thermodynamic quantities arising from the ionic medium effect may be compared with those observed for the transfer of ions from water to non-aqueous solvents. ABRAHAM (1973) reports on the thermodynamics of transfer of single ions from water to various non-aqueous solvents. He finds that the values for the Gibbs free energy of transfer are positive and amount to, at most, a few percent of the Gibbs free energy of dehydration of these ions (NANCOLLAS, 1966). Therefore, it would seem that ion transfer is accompanied only by structural changes in the hydration water, rather than by dehydration of the ions.

It has been shown by ABRAHAM that for chaotropic ions, as a rule, both the enthalpy and the entropy of transfer are negative. For the transfer of K^+ the enthalpy and the entropy were found to lie between -7 and -26 kJ mole^{-1} and between –42 and –92 J K^{-1} mole^{-1}, respectively. The ions considered by ABRAHAM do not include NO_3^-, but one might expect that the values for this anion would be of the same order as those for ClO_4^- (MILLERO, 1971), viz. an enthalpy between –1 and –40 kJ mole^{-1} and an entropy between –47 and –131 J K^{-1} mole^{-1}. It remains difficult, however, to arrive at a good approximation for the changes in thermodynamic quantities resulting from the ionic medium effect that accompanies protein adsorption.

The ionic medium effect involved in protein adsorption is calculated from the estimates of $\Delta\sigma_1$ (pH) and $\Delta\sigma_3$ (pH) (figures 5.22. and 5.23.), assuming that the positive value for $\Delta\sigma_1$ results from the uptake of K^+ and the negative value for $\Delta\sigma_3$ from the uptake of NO_3^-. In the discussion given in section 5.5.2., it was shown that accurate determination of $\Delta\sigma_1$ and $\Delta\sigma_3$ is not possible but that, nevertheless, the trends in the variations of these quantities with the pH of adsorption may be real. Consequently, the same applies for the ionic medium effect.

The enthalpy change attributable to the ionic medium effect, $\Delta H_{ion\ med}$, will be discussed further in section 6.3.2.7.

Since structural changes in the hydration layer of the ions are involved, the transfer of ions from water to non-aqueous media would affect ${}^{\phi}C_P$. According to FRANK and WEN (1957) such a transfer process increases ${}^{\phi}C_P$ for the system; the effect is greater the more chaotropic the nature of the transferred ions. Similarly, it is to be expected that the ionic medium effect accompanying protein adsorption makes a positive contribution to $(\Delta^{\phi}C_P)_{ads}$.

6.3.2.4. Dehydration of the hydrophobic parts of the polystyrene surface

In sections 4.3.2.3. and 4.3.3. the likelihood of hydrophobic interactions between the adsorbed molecules of HPA and RNase and the polystyrene surface was emphasized. In this section only the contribution from the dehydration of the polystyrene surface to the net hydrophobic interaction will be discussed. The part contributed by the adsorbing protein molecules will be considered in section 6.3.2.6.

As was mentioned in section 3.2c., the most characteristic features of hydrophobic bonding are a large positive entropy change and a marked decrease in the heat capacity. The change in the enthalpy due to hydrophobic interaction is relatively small. It stems mainly from changes in the interaction between water molecules, notably the number and/or strength of the hydrogen bonds.

The changes in the thermodynamic quantities due to the dehydration of a polystyrene surface that does not contain any hydrophillic groups can be considered to be comparable with those due to the dehydration of ethyl benzene. The effects observed upon dissolution of ethyl benzene in water, at 25°C, are: $\Delta H = 1.63$ kJ mole^{-1}, $\Delta S = -91.2$ J K^{-1} mole^{-1} and $\Delta^{\phi}C_P = 293$ J K^{-1} mole^{-1} (NÉMETHY and SCHERAGA, 1962b). These authors assume that the first layer of hydration water contains 25 moles of water per mole ethyl benzene. The first layer of hydration of one square meter polystyrene surface consists of about 10^{19} water molecules. Based on these figures, the dehydration of a hydrophobic polystyrene surface involves an enthalpy change, $\Delta H_{dehydr\ PS}$, of about -1 mJ m^{-2} and an entropy change, $\Delta S_{dehydr\ PS}$, of about $+50$ mJ K^{-1} m^{-2}.

It is noted again that, due to the presence of hydrophilic groups, only a part of the surface of the polystyrene particles used in this study can be regarded as

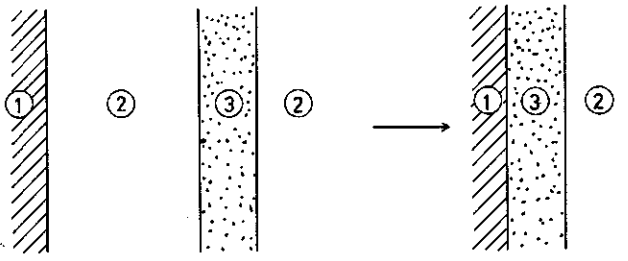

FIG. 6.8. Adsorption of a film of adsorbate 3 from a medium 2 onto a substrate 1. Model used for calculating the van der Waals interaction between the polystyrene particle and the adsorbed protein layer.

being hydrophobic. The hydrophobicity decreases with increasing σ_0 (section 2.4.). In view of this, the values taken for $\Delta H_{dehydr\ PS}$ are -0.9 mJ m^{-2} and -0.5 mJ m^{-2} for the latices L-1 and C-3, respectively. As it has been supposed that, in the pH range studied, for both latices adsorption saturation with HPA and RNase reflects the formation of a complete monolayer, the values for $\Delta H_{dehydr\ PS}$ are considered to be independent of pH.

6.3.2.5. Van der Waals interactions between the adsorbed protein film and the polystyrene particle

In order to calculate the variations in the thermodynamic state properties that accompany the protein adsorption process, two hypothetic steps may be distinguished: (i) the association of the protein molecules and the molecular deformations that lead to a protein film, and (ii) the transfer of this protein film from the solution onto the polystyrene surface.

In this section the change in van der Waals energy, ΔU_{vdW}, of the second step only will be considered. The contributions from the first step will be accounted for in section 6.3.2.6.

Based on the model shown in figure 6.8. and applying the theory for two semi-infinite plates (HAMAKER, 1937; DE BOER, 1936), neglecting retardation effects, ΔU_{vdW} is given by

$$\Delta U_{vdW} = -(A_{12(3)} - A_{22(3)})/12\pi d^2 \qquad (6.13.)$$

where $A_{12(3)}$ and $A_{22(3)}$, respectively, are the Hamaker constants for the polystyrene (1) – aqueous medium (2) and the medium (2) – medium (2) interaction, the interacting materials being separated by the protein film (3) and where d is the distance of separation (= thickness of the adsorbed film).

By substituting the relations (VISSER, 1972)

$$\left.\begin{aligned} A_{12(3)} &= A_{12} + A_{33} - A_{13} - A_{23} \\ A_{22(3)} &= A_{22} + A_{33} - 2A_{23} \end{aligned}\right\} \qquad (6.14.)$$

and by applying Berthelot's principle (BERTHELOT, 1898), that leads to the expression

$$A_{12} = \sqrt{A_{11}\, A_{22}} \tag{6.15.}$$

the numerator of equation (6.14.) can be re-expressed as follows

$$A_{12(3)} - A_{22(3)} = \sqrt{A_{11(2)}} \times \sqrt{A_{33(2)}} \tag{6.16.}$$

For $A_{11(2)}$ a value of 3×10^{-21} J (EVANS and NAPPER, 1973) and for $A_{33(2)}$ a value of 5×10^{-21} J (SRIVASTAVA, 1966) are taken. In this way, for adsorbed protein layers, having a thickness of 1–3 nm, ΔU_{vdW} is calculated to lie in the range -0.01 to -0.10 mJ m^{-2}. It is evident that, even allowing for an uncertainty of a factor of two or three in the Hamaker constants, ΔU_{vdW} ($\simeq H_{vdW}$) only contributes slightly to the net enthalpy of adsorption.

6.3.2.6. Changes in the structure of the protein molecule

The most important aspects of the structural alterations to proteins resulting from adsorption are: (i) variation in the number and the kind of amino acid residues exposed to the aqueous solvent, (ii) changes in van der Waals interactions in, and also between, adsorbed protein molecules, (iii) change in the number of ion pairs in the apolar regions of the protein molecule and, consequently, a change in the number of charged groups at the aqueous side of the protein molecule, (iv) disruption/formation of hydrogen bonds between peptide units and, possibly, between the side chains as well as a variation in the number of peptide-water and side chain-water hydrogen bonds, (v) change in the internal mobility of the polypeptide chain and perhaps of the side chains and (vi) interactions between specific groups of the polystyrene surface and the protein molecule. These effects are considered in turn below,

(i) As a result of the requirements of minimal exposure of hydrophobic groups and maximal exposure of hydrophilic groups to the aqueous medium, the periphery of native protein molecules in solution is relatively hydrophilic. Nevertheless, because of the action of other forces governing the structure of the protein molecule in solution (see section 3.2.) complete removal of the hydrophobic residues from contact with water is generally not possible. Hence, upon adsorption of a native protein molecule, hydrophobic patches at its surface are likely to become attached to the adsorbing interface. The removal of the hydration water results in a considerable increase in entropy. The enthalpy effect involved is relatively small and the heat capacity of the system decreases (cf. section 6.3.2.4.).

The tendency of a protein molecule to unfold at a given surface is expected to be great if the relative importance of intramolecular hydrophobic interactions, as a factor stabilizing the conformation in solution, is small. Obviously, the change in hydrophobic interactions resulting from structural alterations in the protein molecule depends on whether a greater or lesser number of hydrophobic residues come into contact with water. This question cannot generally be answered.

(ii) Due to changes in the interatomic distances that accompany structural perturbations of a protein molecule the intramolecular van der Waals interactions will be affected. The van der Waals interaction between adsorbed protein molecules depends on the mode of adsorption, including the molecular conformations. In general, also a variation in the types of groups of the protein that interact with the solvent molecules occurs.

The overall magnitude of these changes in van der Waals interactions is not known.

(iii) For energetic reasons, oppositely charged ions in the apolar interior of the protein molecule tend to form ion pairs (cf. section 3.2a.). At the aqueous surface of the dissolved protein molecule the ionic groups are hydrated. Hence, the variations in the thermodynamic quantities, due to the transfer of ionic groups from the interior to the aqueous surface, or vice versa, mainly depend on the extent of ion pair formation and disruption in the interior of the protein molecule and on the state of hydration at the surface. Since the effect of adsorption on the micro-environment of the various ionic groups is completely unknown, the changes in the thermodynamic quantities cannot be predicted.

(iv) With proteins the number of available possibilities for hydrogen bonding between peptide units (N–H$\cdots$O=C) is far greater than between side chains. Hence, with respect to the conformational stability of the protein molecule, the first type of hydrogen bond plays a more important role.

The most detailed approach to the contribution of peptide-peptide hydrogen bonding to protein stability is probably that of KRESHECK and KLOTZ (1969). These authors considered simple amide molecules (N-methyl.acetamide) to mimic peptide- peptide interaction in protein molecules (see figure 6.9.). They found that the stability of the hydrogen bonds between the amides largely depends on the environmental conditions. From their results KRESHECK and KLOTZ deduced the following thermodynamic data for the states of the amide groups in water and carbon tetrachloride, at 25°C:

hydrogen bonded		non-hydrogen bonded	
$(\text{N–H}\cdots\text{O=C})_{CCl_4}$	$\rightarrow$	$(\text{N–H, O=C})_{CCl_4}$	$\Delta H = +21.3$ kJ mole^{-1}
			$\Delta S = +37.6$ J K^{-1} mole^{-1}
			$\Delta G = +10.0$ kJ mole^{-1}
$(\text{N–H}\cdots\text{O=C})_{CCl_4}$	$\rightarrow$	$(\text{N–H, O=C})_{H_2O}$	$\Delta H = -11.3$ kJ mole^{-1}
			$\Delta S = -14.0$ J K^{-1} mole^{-1}
			$\Delta G = -7.1$ kJ mole^{-1}
$(\text{N–H}\cdots\text{O=C})_{H_2O}$	$\rightarrow$	$(\text{N–H, O=C})_{H_2O}$	$\Delta H = 0$ kJ mole^{-1}
			$\Delta S = +42$ J K^{-1} mole^{-1}
			$\Delta G = -13$ kJ mole^{-1}

From these data one may conclude that peptide units in the apolar interior of the protein tend to form hydrogen bonds, whereas they do not at the aqueous protein surface. Moreover, disruption of a peptide-peptide hydrogen bond in the interior and the consecutive exposure of the peptide units to an aqueous

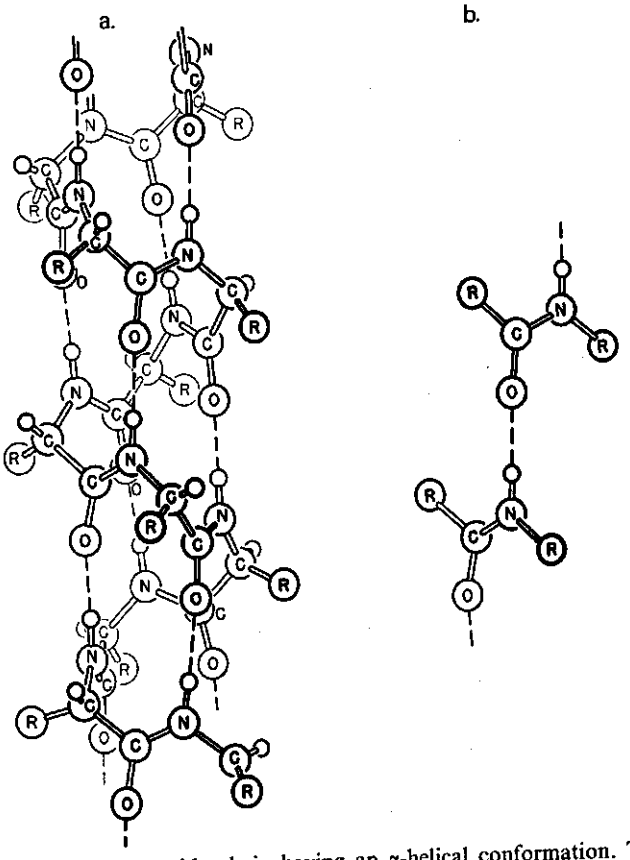

FIG.6.9. a. Part of a polypeptide chain having an α-helical conformation. The α-helix is stabilized by peptide-peptide hydrogen bonds. (Drawing after COREY and PAULING, 1956). b. N-methyl acetamide molecules interacting via hydrogen bonds. The interaction between these molecules may mimic the interaction between peptide groups in a polypeptide chain (KRESHECK and KLOTZ, 1969).

solvent (where the peptide units may form hydrogen bonds with the water molecules) would be thermodynamically favoured.

(v) The conformation of a polypeptide chain, i.e. its secundary (e.g. α-helix) and its tertiary structure are the result of the mutual action of the factors discussed in section 3.2.

It may be readily understood that breaking of hydrogen bonds, ion pairs, hydrophobic bonds, etc., leads to an increase in the rotational degree of freedom of the polypeptide backbone and possibly the side chains. In this respect, the α-helical structure depicted in figure 6.9a. may serve as an illustration.

From classical mechanics it follows that the enthalpy gain associated with an increase of one degree of rotational freedom equals 0.5 RT ($\approx$ 1.24 kJ, at 25°C) per mole of bonds. However, for a polymeric chain, even in a random

coil conformation, entirely free rotation about the bonds in the chain is not possible. According to BRANDTS (1969) the best estimates of the entropy change in proteins resulting from the increased rotational motion due to unfolding are in the range $+8$ to $+25$ J K^{-1} per mole of unfolded amino acid residues. In the same article, BRANDTS reasons that the non-hydrophobic rotational contributions to $\Delta^{\phi}C_P$ amounts to about a maximum of $+17$ J K^{-1} per mole unfolded amino acid residues.

The changes in the thermodynamic quantities reported for the disruption of hydrogen bonds between the amide molecules (see (iv)) already contain a contribution from increased rotational freedom. See figure 6.9b. In a polypeptide chain a larger number of bonds are affected by the disruption of a hydrogen bond between peptide units. Whether this leads to a larger increase in rotational flexibility per broken hydrogen bond depends on the resulting restrictions of rotation about the bonds in the polymeric chain.

The actual attachment of the protein molecule to the polystyrene surface reduces the overall rotational motion within the molecule. The rotational flexibility along the polypeptide chain is restrained by the fact that each adsorbed molecule is attached to the surface via many segments. As was discussed in section 4.4., the fraction of attached segments is likely to increase with increasing structural perturbation (i.e. decreasing amount adsorbed).

(vi) In section 5.3.3. evidence was obtained for the formation of ion pairs between the $-NH_3^+$ groups of the protein and $-OSO_3^-$ groups of the polystyrene surface. Also, the π-electrons in the benzene rings of the polystyrene may be involved in interactions with specific groups of the protein molecule. For similar reasons as discussed in section (iii) above, the changes in the thermodynamic quantities are unknown.

Each of the effects discussed in (i) – (vi) is directly related to structural alterations resulting from adsorption of the protein molecules. As yet, it is impossible to give a detailed analysis of the conformation of the adsorbed protein layer. Therefore, we consider for the present the sum of enthalpy changes considered in (i) – (vi), denoted as $\Delta H_{str\ pr}$, to be unknown. Even if there is no change in the protein structure resulting from adsorption, this does not imply that $\Delta H_{str\ pr}$ is zero. In that case $\Delta H_{str\ pr}$ is determined by the possible dehydration of hydrophobic areas of the protein molecule that bind to the polystyrene surface, by van der Waals interactions between adsorbed protein molecules and by specific interactions between the protein molecule and the polystyrene surface.

In order to assess $\Delta H_{str\ pr}$, in the next section the enthalpy contributions originating from the factors discussed in sections 6.3.2.1. to 6.3.2.5. will be evaluated. The difference between the sum of these enthalpies and the experimentally obtained adsorption enthalpy will then be put equal to $\Delta H_{str\ pr}$. Thus, $\Delta H_{str\ pr}$ consists of the contributions made by the factors mentioned under (i) – (vi), but it contains also the enthalpy contributions from possible additional factors that may have been overlooked. The accuracy of $\Delta H_{str\ pr}$ depends on the quality

of the model considerations underlying the calculations of the various enthalpy contributions.

6.3.2.7. Analysis of the adsorption enthalpy

For each of the systems under investigation it has been shown that the contributions to ΔH_{ads} made by ΔH_{titr}, $\Delta H_{dehydr\ PS}$ and ΔH_{vdW} are relatively small. The contribution from ΔH_{cd} is small in the case of adsorption on latex L-1 ($\sigma_0 = -2.3\ \mu C\ cm^{-2}$), but it may be quite large for latex C-3 ($\sigma_0 = -15.5\ \mu C\ cm^{-2}$). Allowing the value of ε for the shear layer around the bare polystyrene particle to be an adjustable parameter results in the value calculated for ΔH_{cd} varying over a wide range (see figures 6.6. and 6.7.).

Since $\Delta H_{dehydr\ PS}$ is not, and ΔH_{cd} and ΔH_{vdW} are only slightly dependent on pH, the variation of ΔH_{ads} (pH) is almost exclusively determined by the dependence of ΔH_{titr}, $\Delta H_{ion\ med}$ and $\Delta H_{str\ pr}$ on pH.

Both with HPA and RNase, the shape of the curves for $(\Gamma_p)_{max}$ vs. pH, at 0.05 M KNO_3, are qualitatively similar for the two latices (figures 4.4. and 4.5.). It seems plausible, therefore, that, for each protein, the variation of $\Delta H_{str\ pr}$ with pH is also more or less the same for the two polystyrene surfaces. Such a similarity between $\Delta H_{str\ pr}$ (pH) for the two latices may be reached by adjusting the molar enthalpy due to the uptake of mobile ions from solution (the ionic medium effect).

Because of the larger susceptibility of HPA molecules to variations in the pH, ΔH_{ads} (pH) measured with this protein is analyzed first.

Taking an enthalpy change of $-5\ RT$ per mole of ions transferred from solution to the adsorbed protein layer leads to a variation of $\Delta H_{ion\ med}$ with pH in such a way that the requirement of similarity between the curves for $\Delta H_{str\ pr}$ is reasonably met. Moreover, the value of $-5\ RT$ (≈ -12.4 kJ $mole^{-1}$, at 298 K) is in the range of the molar enthalpies reported for the transfer of K^+ and NO_3^- from water to non-aqueous media (see section 6.3.2.3.).

For both polystyrene surfaces the shape of the curve for $\Delta H_{str\ pr}$ (pH), thus obtained, shows a minimum in the isoelectric region. This minimum is more pronounced if $\Delta H_{str\ pr}$ is expressed per adsorbed HPA molecule. It is recalled that in the isoelectric region $(\Gamma_p)_{max}$ (pH) attains a maximum value (figure 4.4.). The coincidence of minimal $\Delta H_{str\ pr}$ and maximal $(\Gamma_p)_{max}$ supports the conclusion put forward in chapter 4, where the decrease in $(\Gamma_p)_{max}$ was assigned to progressive structural perturbation of the adsorbing HPA molecules.

Finally, the value of ΔH_{cd} (pH) is based on the condition that the values for $\Delta H_{str\ pr}$ (pH) are comparable for both latices. Thus, a value of 6.5 for ε in the shear layer around the bare polystyrene particles has been deduced. This value is to be compared with those found for water at the silver iodide surface ($\varepsilon = 8 \pm 1.6$, VINCENT et al, 1971) and at the mercury surface ($\varepsilon = 6$, BOCKRIS et al, 1963). These low values for ε point to a virtually fixed orientation of the water molecules at those interfaces, since in the absence of orientation polarizations ε for water would amount to ca. 4.2 (HASTED, 1973).

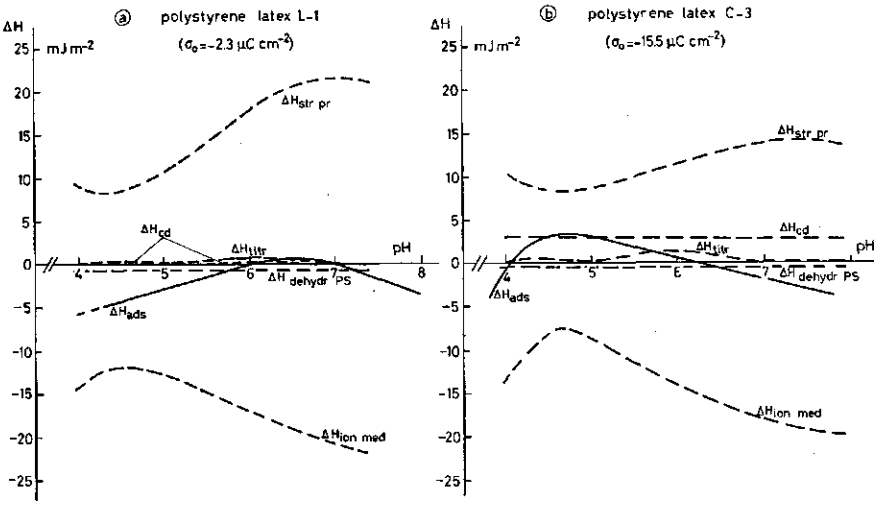

FIG. 6.10. Adsorption of HPA on polystyrene latices. Resolution of the overall enthalpy of adsorption ΔH_{ads} (——) into its constituents (– – –). c_{KNO_3} = 0.05 M T = 25°C.

The results of the above considerations are graphically represented in figure 6.10., where the constituents of ΔH_{ads} (pH) are shown.

Based on the model for the adsorbed protein layer there is, in the case of RNase adsorption, no reason for assuming other values for the molar enthalpies due to the medium change of the mobile ions than those evaluated for the adsorption of HPA. Obviously, the value of ε for the shear region around the bare polystyrene particles can also be assumed to be the same.

For RNase, the composition of ΔH_{ads} (pH) is shown in figure 6.11. The contribution of the titration effect has not been taken into account, but there is ample reason to assume that, as with HPA, ΔH_{titr} is very small in comparison with $\Delta H_{ion\ med}$ and $\Delta H_{str\ pr}$ (see section 6.3.2.1.).

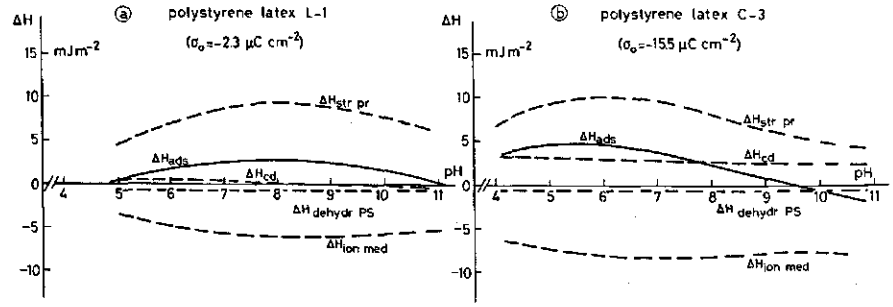

FIG. 6.11. Adsorption of RNase on polystyrene latices. Resolution of the overall enthalpy of adsorption ΔH_{ads} (——) into its constituents (– – –). c_{KNO_3} = 0.05 M T = 25°C.

It is remarkable that both for HPA and RNase $\Delta H_{str\ pr}$ is positive. In section 6.3.2.6. the complex nature of $\Delta H_{str\ pr}$ was emphasized. The contributions to $\Delta H_{str\ pr}$ from the various factors involved (see section 6.3.2.6., sections (i)–(vi)), will, in general, be different for various proteins. Therefore, a positive value for $\Delta H_{str\ pr}$ is not necessarily a general feature of protein adsorption.

6.3.2.8. Variation of $\Delta H_{str\ pr}$ with the amount of protein adsorbed. Comparison of HPA and RNase

$\Delta H_{str\ pr}$ is directly influenced by structural changes in the adsorbing protein molecules. It was concluded in chapter 4 that the variation of $(\Gamma_p)_{max}$ with pH reflects the extent of structural alteration in the adsorbed molecules. Hence, a direct correlation between $\Delta H_{str\ pr}$ (expressed per unit mass of protein) and $(\Gamma_p)_{max}$ is to be anticipated. Indeed, both with HPA and RNase such a correlation is observed (figure 6.12.), although the trends of $\Delta H_{str\ pr}$ with $(\Gamma_p)_{max}$ are strikingly different for the two proteins. Because of the intricate nature of $\Delta H_{str\ pr}$, indicated above, these different trends are not surprising. For the same reason, the value of $\Delta H_{str\ pr}$ can, by itself, not be used as a general measure for the extent of structural rearrangement.

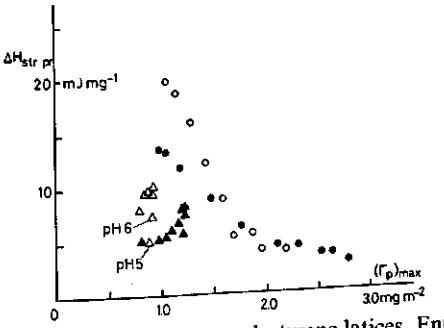

FIG. 6.12. Adsorption of HPA and RNase on polystyrene latices. Enthalpy changes due to structural alterations in the adsorbing protein molecules, $\Delta H_{str\ pr}$, as a function of the plateau value of the adsorption isotherms, $(\Gamma_p)_{max}$. ○ HPA △ RNase. Open symbols $\sigma_0 = -2.3\,\mu C$ cm^{-2}; filled symbols $\sigma_0 = -15.5\,\mu C\ cm^{-2}$. $c_{KNO_3} = 0.05$ M $T = 25°C$.

Another difference between HPA and RNase lies in the effect of the polystyrene surface charge, σ_0, on $\Delta H_{str\ pr}$. In this regard, it should be remembered that the results for RNase are based on parameters that were evaluated for the adsorption of HPA (section 6.3.2.7.). For example, the effect of σ_0 on $\Delta H_{str\ pr}$ for RNase could be eliminated by taking a somewhat smaller value for the dielectric constant of region 1 of the adsorbed RNase layer. On the other hand, a less positive value for $\Delta H_{str\ pr}$ in the case of adsorption at a more negatively charged polystyrene surface may be realistic, because of ion pair formation between positively charged groups of the protein and $-OSO_3^-$ groups of the polystyrene (section 5.3.3.). If so, the influence of σ_0 on $\Delta H_{str\ pr}$ would propor-

tionally decrease with increasing $(\Gamma_p)_{max}$. σ_0 would then affect $\Delta H_{str\ pr}$ of HPA in a qualitatively similar way. Indeed, at low values of $(\Gamma_p)_{max}$, such an influence of σ_0 is observed, but it decreases more rapidly with increasing $(\Gamma_p)_{max}$ than expected in this case.

The rather deviating values for $\Delta H_{str\ pr}$ observed for RNase at low pH (especially in the case of latex L-1) may result from the fact that, under these conditions, the charge distribution in the adsorbed layer and, hence, ΔH_{cd} and $\Delta H_{ion\ med}$ are relatively largely influenced by the layer thickness (see table 5.7.). Thus, if it is assumed that the value for σ_1 is more positive and for σ_3 more negative than the respective averages of the values given in table 5.7. (which implies the assumption of a thicker adsorbed layer), then the deviation of $\Delta H_{str\ pr}$ at low pH is reduced. This finding is in agreement with the suggestion that in adsorbed layers of RNase the protein volume fraction is relatively small (section 4.5., last paragraph).

Altogether, the unambiguous correlation between $\Delta H_{str\ pr}$ and $(\Gamma_p)_{max}$, as observed with HPA and RNase, strongly suggests that different extents of structural changes underlie the variation in the amount of protein adsorbed (cf. section 4.3.2.).

6.3.3. *Concluding remarks concerning the effects of charge, electrolyte concentration and temperature on the adsorption enthalpy*

The interpretation of the experimental adsorption enthalpy, as presented in this chapter, should be considered as a first approximation. Its limitation is mainly determined by the validity of the model of the adsorbed layer and the assumed distribution of charge in this layer (see sections 5.5.1. and 5.5.2.). The values calculated for the enthalpies pertaining to the ionic medium effect and to the changes in the distribution of charge directly depend on that model.

In the estimations of the various constituent terms in ΔH_{ads} reasonable values for the adjustable parameters have been taken. It results that, both for HPA and RNase, the least accessible constituent, $\Delta H_{str\ pr}$, shows an unambiguous correlation with the amount of protein adsorbed, $(\Gamma_p)_{max}$ (figure 6.12.). This finding supports the conclusion, made in chapter 4, that a decrease in $(\Gamma_p)_{max}$ is due to increasing structural changes in the adsorbed protein molecules. Therefore, the assumptions made regarding the model for the adsorbed layer and the distribution of charge therein are in that respect self-consistent.

In section 6.3.2. a preliminary discussion of the effects of various variables on ΔH_{ads} was given. Having analyzed ΔH_{ads}, it is now possible to discuss in some more detail how ΔH_{ads} depends on these variables.

6.3.3.1. pH of adsorption and charge density of the polystyrene surface

Figures 6.10. and 6.11. show that $\Delta H_{ion\ med}$ and $\Delta H_{str\ pr}$ are the constituents most susceptible to the pH of adsorption. However, the effect of the pH on these enthalpies is quite different for the two proteins.

For HPA, $\Delta H_{str\ pr}$ (pH) attains a minimum and $\Delta H_{ion\ med}$ (pH) a maximum value in the isoelectric region, where $(\Gamma_p)_{max}$ (pH) is also maximal. If $\Delta H_{str\ pr}$ and $\Delta H_{ion\ med}$ are expressed per unit mass of adsorbed protein, the effect of pH on these quantities is much more pronounced.

It was explained in section 6.3.2.8. that the variation of $\Delta H_{str\ pr}$ with pH may be related directly to the extent of rearrangement of the adsorbed molecules. The same reasoning also underlies the dependence of $\Delta H_{ion\ med}$ on pH. It has been deduced from the hydrogen ion titration curves (figure 5.6.) that, at values for the pH of adsorption where the adsorbed HPA molecules are supposed to be perturbed to a larger extent, a larger fraction of the (negatively charged) carboxyl groups is located near the polystyrene surface. As a consequence, the amount of mobile ions incorporated in the adsorbed protein layer and, hence, $\Delta H_{ion\ med}$, are minimal at the isoelectric point. The shape of the curve for ΔH_{ads} (pH) is essentially determined by the shapes of the curves for $\Delta H_{ion\ med}$ (pH) and $\Delta H_{str\ pr}$ (pH). Since the curves for these two constituents show opposite trends, the maximum in the curve for ΔH_{ads}(pH) does not necessarily occur in the isoelectric region.

Variation of the surface charge of the latex has its impact on all the constituent terms considered. In an absolute sense the effects of σ_0 on ΔH_{titr} and $\Delta H_{dehydr\ PS}$ are very small. Also $\Delta H_{ion\ med}$ appears to be insentitive to σ_0, except in the isoelectric region. ΔH_{cd} becomes more positive upon increasing σ_0. The resultant of these effects would render the adsorption of HPA more endothermic with increasing negative values for σ_0 (compare figures 6.10a. and 6.10b.). Such a dependence of ΔH_{ads} on σ_0 has been found at pH < ca. 6. The observation that at the more extreme pH values the influence of σ_0 diminishes or reverses (at the alkaline side) can be explained by the larger variation of $\Delta H_{ion\ med}$ with pH at higher σ_0 and by the differences in $\Delta H_{str\ pr}$ occuring at pH > ca. 6. The effect of σ_0 on the shape of the curve for $\Delta H_{ion\ med}$ (pH) also underlies the shift in the maximum of the experimental curve for ΔH_{ads} (pH) along the pH-axis.

With RNase $(\Gamma_p)_{max}$ varies much less with pH as compared to HPA. This feature is reflected in the smaller variation of $\Delta H_{str\ pr}$ (expressed per unit mass of adsorbed protein) with pH. Contrary to what has been deduced for HPA, in the case of the adsorption of RNase $\Delta H_{str\ pr}$ becomes more positive with increasing $(\Gamma_p)_{max}$ (figure 6.12.). In sections 6.3.2.6. and 6.3.2.8. it was pointed out that the dependence of $\Delta H_{str\ pr}$ on pH largely depends on the exact microenvironmental changes in the adsorbing molecules.

As a result of the relatively small tendency of the adsorbing RNase molecules to conformational changes, the hydrogen ion titration behaviour of this protein is only slightly dependent on the pH of adsorption (figure 5.7.). Consequently, the influence of the pH on $\Delta H_{ion\ med}$ is small.

Because the same model for the adsorbed protein layer is assumed for both proteins, then for RNase the influence of σ_0 on $\Delta H_{dehydr\ PS}$ is equal to, and that for ΔH_{cd} is very similar to, those influences observed with HPA. Also with RNase the effect of σ_0 on $\Delta H_{ion\ med}$ is relatively small. The sum of these consti-

tuents becomes more positive at higher σ_0. The curve for $\Delta H_{str\ pr}$ (pH) is affected by σ_0 in the same way as the curve for $(\Gamma_p)_{max}$(pH) (see figure 4.5.), viz. its maximum shifts to lower pH values with increasing negative σ_0. This behaviour is reflected in the shape of the curves for ΔH_{ads}(pH). The observation that, at alkaline pH values, ΔH_{ads} (pH) is more negative with the higher charged polystyrene surface can be attributed to the influence of σ_0 on $\Delta H_{str\ pr}$ in that pH region.

6.3.3.2. Electrolyte concentration

Since the analysis of ΔH_{ads} has been performed at only one concentration of KNO_3, i.e. $c_{KNO_3} = 0.05$ M, the influence of c_{KNO_3} on ΔH_{ads} cannot be readily analyzed. The fact, however, that, in the case of HPA, ΔH_{ads} (pH) is much more affected by c_{KNO_3} than in the case of RNase (compare figures 6.1. and 6.3.) suggests that the structural rearrangement is especially susceptible to c_{KNO_3}. The influence of c_{KNO_3} on structural changes agrees with the interpretation of the effect of c_{KNO_3} on the adsorption isotherms for HPA, as set out in section 4.3.2.2. The reason(s) for the different ways c_{KNO_3} affects ΔH_{ads} (pH) at different values of σ_0 requires further analysis.

ΔH_{ads} for the adsorption of RNase on latex C-3 is very little influenced by c_{KNO_3}. Therefore, it is likely that the dependence of $(\Gamma_p)_{max}$ on c_{KNO_3}, observed with this latex (figure 4.5.), must be ascribed to different orientations of the adsorbed RNase molecules rather than to different extents of structural perturbation.

6.3.3.3. Temperature

As with the effect of electrolyte concentration, the effect of temperature on ΔH_{ads} does not directly follow from the analysis of ΔH_{ads}. However, from data that are available in the literature, the sensitivity of the various constituent terms of ΔH_{ads} to the temperature may be deduced in a qualitative way.

The enthalpy contributions that are most sensitive to the temperature are $\Delta H_{dehydr\ PS}$, $\Delta H_{ion\ med}$ and $\Delta H_{str\ pr}$.

As mentioned in section 6.3.2.4., dehydration of the hydrophobic polystyrene surface is characterized by a negative value for $\Delta^{\phi}C_P$.

The ionic medium effect, i.e. the uptake into the adsorbed protein layer of the chaotropic ions K^+ and NO_3^-, is accompanied by an increase in ${}^{\phi}C_P$ (see section 6.3.2.3.).

Due to the many factors involved, the change in ${}^{\phi}C_P$ caused by structural changes in the protein molecule cannot be predicted. An increasing degree of motional freedom in the protein molecule would increase ${}^{\phi}C_P$ (BRANDTS, 1969). Hence, the disruption of intramolecular hydrogen bonds and ion pairs (as may occur during structural alteration) and the attachment of the protein molecule to the adsorbent influence ${}^{\phi}C_P$ in opposite senses. Moreover, the net hydrophobic interaction in the adsorbing protein molecule and, consequently, its contribution to ${}^{\phi}C_P$, are not known.

The change in ${}^{\phi}C_P$ of the system due to the overall adsorption process,

$(\Delta^{\phi}C_P)_{ads}$, is the resultant of the $\Delta^{\phi}C_P$'s for each of the constituents. In view of the foregoing discussion it is not surprising that, for a given protein, $(\Delta^{\phi}C_P)_{ads}$ depends on both the pH of adsorption and on σ_0.

In the case of adsorption of HPA on latex L-1 ($\sigma_0 = -2.3\ \mu C\ cm^{-2}$) $(\Delta^{\phi}C_P)_{ads}$, as derived from ΔH_{ads} (pH) at 9°C and 25°C, is negative over the entire pH region investigated (figure 6.2a.). Probably, the dehydration of the hydrophobic polystyrene surface is the dominant contribution to $(\Delta^{\phi}C_P)_{ads}$. The curve for ΔH_{ads} (pH) at 37°C shows anomalous behaviour between pH 4.5 and 5.8. In this connection it is recalled that, especially in the isoelectric region, $(\Gamma_P)_{max}$ at 37°C is lower than at 25°C or 9°C (see figure 4.4.). This effect was explained earlier by a larger extent of conformational perturbation at 37°C.

The influence of σ_0 on $(\Delta^{\phi}C_P)_{ads}$ can be observed by comparing figures 6.2a. and 6.2b. Adsorption on latex C-3 ($\sigma_0 = -15.5\ \mu C\ cm^{-2}$) causes a decrease in ${}^{\phi}C_P$ only at pH values < ca. 4.7; at higher pH values $(\Delta^{\phi}C_P)_{ads}$ is positive. Upon increasing σ_0 from $-2.3\ \mu C\ cm^{-2}$ to $-15.5\ \mu C\ cm^{-2}$ the polystyrene surface becomes much less hydrophobic. Therefore, the rise in $(\Delta^{\phi}C_P)_{ads}$ at pH > ca. 4.7, found with latex C-3, may well be due to overcompensation of the negative $(\Delta^{\phi}C_P)_{dehydr\ PS}$ by the positive $(\Delta^{\phi}C_P)_{ion\ med}$.

Because of the lack of knowledge on the structural changes in the adsorbing HPA molecules, the effect of σ_0 on $(\Delta^{\phi}C_P)_{str\ pr}$ has not been considered.

For RNase the variation of ΔH_{ads} (pH) with temperature differs considerably from that observed with HPA. The adsorption of RNase on latex L-1 involves a negative change in ${}^{\phi}C_P$ only at pH < ca. 6.3 and pH > ca. 10.0. At intermediate pH values, $(\Delta^{\phi}C_P)_{ads}$ is positive (figure 6.4a.). Apparently, in the pH region 6.3–10.0 the negative value for $(\Delta^{\phi}C_P)_{dehydr\ PS}$ is overcompensated by the sum of $(\Delta^{\phi}C_P)_{ion\ med}$ and $(\Delta^{\phi}C_P)_{str\ pr}$, whereas it is the other way round outside this region.

Figure 6.11a. shows that the curve for $\Delta H_{ion\ med}$ (pH) passes through a broad maximum at pH values where $(\Delta^{\phi}C_P)_{ads}$ is positive. As $\Delta H_{ion\ med}$ reflects changes in the structure of hydration water around the transferred ions (cf. section 6.3.2.3.), maximum positive values for $(\Delta^{\phi}C_P)_{ion\ med}$ may be expected in the same pH region.

It may be recalled that for RNase adsorbed on latex L-1 the variation of $(\Gamma_P)_{max}$ with pH is only small (see figure 4.5.). Therefore, it is probable that the conformation of the adsorbed RNase molecules is only slightly affected by the pH of adsorption, if at all. Nevertheless, if these conformational changes, however small in extent, imply a change in the exposure of hydrophobic residues of the protein molecule to the aqueous solution, ${}^{\phi}C_P$ would change considerably. Less exposure of hydrophobic residues with decreasing $(\Gamma_P)_{max}$ would contribute to the observed dependence of $(\Delta^{\phi}C_P)_{ads}$ on the pH of adsorption. For the reasons discussed before, reliable estimates of the values for $(\Delta^{\phi}C_P)_{str\ pr}$ cannot be given.

According to the curves for $\Delta H_{ion\ med}$ (pH) the ionic medium effects involved in the adsorption of RNase on latex L-1 are smaller than in the adsorption of

HPA on the same latex. This would favour a less positive value for $(\Delta^{\phi}C_P)_{ads}$ for RNase. However, the experiments reveal that with RNase $(\Delta^{\phi}C_P)_{ads}$ tends to be more positive. The reasons for this effect must be sought in (i) less hydrophobic interaction (less dehydration of the polystyrene surface) in the case of RNase adsorption, and/or (ii) a more positive (or less negative) value for $(\Delta^{\phi}C_P)_{str\ pr}$ for the adsorbing RNase molecules. The first possibility agrees with the suggestion that the adsorbed RNase layer contains a larger fraction of protein-void volume than the HPA layer (section 4.5., last paragraph). Regarding the second possibility, the experimental results do not yet allow one to draw any definite conclusions.

The more positive value for $(\Delta^{\phi}C_P)_{ads}$ in the case of RNase adsorbed on latex C-3 (figure 6.4b.) as compared to latex L-1 (figure 6.4a.) may be explained by the same arguments as were given for the adsorption of HPA, viz. decreasing hydrophobicity of the latex surface. Also the somewhat larger ionic medium effect with latex C-3 would contribute to a positive shift of $(\Delta^{\phi}C_P)_{ads}$. Further, $(\Delta^{\phi}C_P)_{ads}$ (pH) for the adsorption of RNase on latex C-3 can be interpreted along the same lines as for the adsorption of this protein on latex L-1. Disregarding the absolute values, the curves for $\Delta H_{ion\ med}$ (pH) of RNase are very similar for the two latices. Hence, more of less similar variations of $(\Delta^{\phi}C_P)_{ion\ med}$ with pH are expected. Unlike the case with latex L-1, for latex C-3 the decrease in $(\Gamma_P)_{max}$ is more marked at alkaline than at acid pH values (see figure 4.5.). Thus, the increasing structural changes that occur in the protein molecules adsorbed under alkaline conditions may be reflected in a more negative value for $(\Delta^{\phi}C_P)_{str\ pr}$, which, in turn, is (partly) responsible for the negative value of $(\Delta^{\phi}C_P)_{ads}$ found in this pH region. Moreover, a larger fraction of the polystyrene surface may become dehydrated as the extent of spreading of the RNase molecules increases.

In conclusion it can be said that the mechanisms proposed for the adsorption of HPA and RNase from aqueous solution onto different polystyrene surfaces are broadly consistent with the effect of temperature on ΔH_{ads} for these proteins.

6.3.4. *Further thermodynamic considerations. Gibbs free energy and entropy of protein adsorption*

The observation that, on diluting the system or on changing the pH, the HPA and RNase molecules do not readily desorb from the polystyrene surface (section 4.3.2.), implies a large negative value for ΔG_{ads} per adsorbed protein molecule.

In order to determine whether the various factors hitherto distinguished promote or inhibit the adsorption of the protein, the contribution to ΔG_{ads}, made by each of them, must be known. To that end, the following remarks may be made.

1. Titration effect. Referring to section 6.3.2.1., the titration effect is the net result of the protonation and the deprotonation of protein molecules in solution. Since, essentially, all the protons taken up by the adsorbing protein molecules

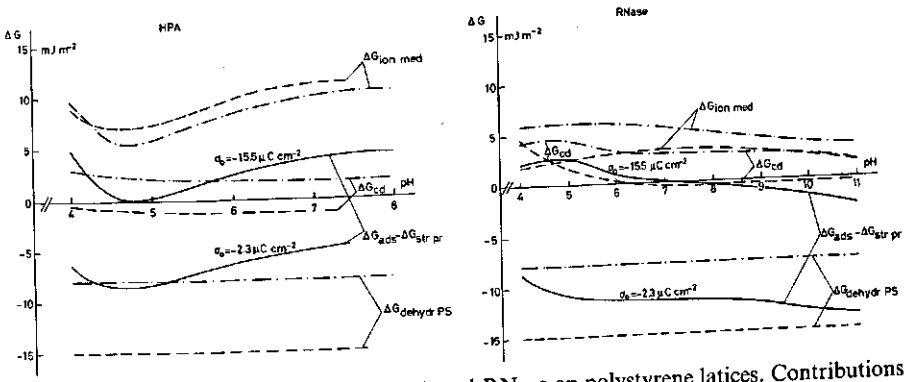

FIGS. 6.13. and 6.14. Adsorption of HPA and RNase on polystyrene latices. Contributions of some constituents to the net Gibbs free energy of adsorption, ΔG_{ads}. The sum of these contributions equals ($\Delta G_{ads} - \Delta G_{str\ pr}$). – – – latex L-1 ($\sigma_0 = -2.3$ μC cm^{-2}); —·— latex C-3 ($\sigma_0 = -15.5$ μC cm^{-2}). $c_{KNO_3} = 0.05$ M $T = 25$°C.

are provided by the molecules that remain in solution, the contribution from ΔG_{titr} to ΔG_{ads} is very small.

2. Changes in the distribution of charge. ΔG_{cd} can be calculated using equation (6.6.). Curves for ΔG_{cd} (pH), obtained under the same conditions at which ΔH_{cd} (pH) has been evaluated, are shown in figures 6.13. and 6.14.

3. Ionic medium effect. As a result of the relatively large loss of entropy of the hydration water, the transfer of ions from an aqueous to a non-aqueous medium is highly endergonic (ABRAHAM, 1973).

The average values for the Gibbs free energy of transfer of K^+ and ClO_4^- (comparable with NO_3^-) from water to different non-aqueous solvents, as reported by ABRAHAM, may, as a first approximation, be taken to be an estimate of $\Delta G_{ion\ med}$. Thus, values of 4.0 kJ mole^{-1} and 10.5 kJ mole^{-1} are attributed to the Gibbs free energy of transfer of, respectively, K^+ and NO_3^- from the aqueous to the proteinaceous environment.

$\Delta G_{ion\ med}$ (pH) per unit area of polystyrene surface or, for that matter, per adsorbed protein molecule can be estimated by interpolation in figures 5.22. and 5.23. (cf. section 6.3.2.3.). Values for $\Delta G_{ion\ med}$ (pH), thus obtained, are graphically presented in figures 6.13. and 6.14.

4. Dehydration of the polystyrene surface. Based on the data given for the dissolution of ethyl benzene in water (section 6.3.2.4.), for a completely hydrophobic polystyrene surface $\Delta G_{dehydr\ PS}$ would amount to ca. –17 mJ m^{-2}. In view of the fraction of the surfaces of latex L-1 ($\sigma_0 = -2.3$ μC cm^{-2}) and latex C-3 ($\sigma_0 =$ –15.5 μC cm^{-2}) covered by hydrophilic groups, the values for $\Delta G_{dehydr\ PS}$ considered in this work are –15 mJ m^{-2} and –8 mJ m^{-2}, respectively.

5. Van der Waals interactions between the protein film and the polystyrene particles. Because $T\Delta S_{vdW} \approx 0$, $\Delta G_{vdW} \approx \Delta H_{vdW}$. Hence, ΔG_{vdW} does not contribute considerably to ΔG_{ads} (see section 6.2.2.5.).

6. Structural changes in the adsorbing protein molecules. The factors, mentioned

in section 6.3.2.6. may all contribute to $\Delta G_{str\ pr}$. $\Delta H_{str\ pr}$ was in fact evaluated without any detailed knowledge of those factors. Because of this, no reliable prediction of $\Delta S_{str\ pr}$ and, hence, of $\Delta G_{str\ pr}$ can be given.

From the discussion of these various factors (*1–6*) it follows that dehydration of the hydrophobic parts of the polystyrene surface is an important effect in favour of protein adsorption. The negative value for $\Delta G_{dehydr\ PS}$ is almost entirely due to an entropy increase. The contribution of this factor decreases with increasing surface charge of the polystyrene particle.

The ionic medium effect and, in the case of adsorption at a polystyrene surface bearing a high negative charge (latex C-3), the changes in the distribution of charge oppose the adsorption process.

The contributions to ΔG_{ads} due to the titration effect and to the van der Waals interaction between the polystyrene surface and the adsorbed protein film are negligible.

Based on the data given above, values for $(\Delta G_{titr} + \Delta G_{ion\ med} + \Delta G_{cd} + \Delta G_{dehydr\ PS} + \Delta G_{vdW}) = (\Delta G_{ads} - \Delta G_{str\ pr})$ have been estimated. The curves for $(\Delta G_{ads} - \Delta G_{str\ pr})$ as a function of pH are shown in figures 6.13. (HPA series) and 6.14. (RNase series). In addition, in figure 6.15. $(\Delta G_{ads} - \Delta G_{str\ pr})$, expressed per unit mass of adsorbed protein, is plotted against $(\Gamma_p)_{max}$. Allowing for the uncertainties in the estimated constituents, for both proteins it appears that $(\Delta G_{ads} - \Delta G_{str\ pr})$ becomes more positive with increasing negative surface charge of the latex.

In the case of adsorption of HPA and RNase at latex C-3 positive values for $(\Delta G_{ads} - \Delta G_{str\ pr})$ are calculated. Since the adsorption of both proteins occurs irreversibly, ΔG_{ads} must acquire relatively large negative values, say, of the order of – 100 kJ mole^{-1}. It follows that $\Delta G_{str\ pr}$ is negative.

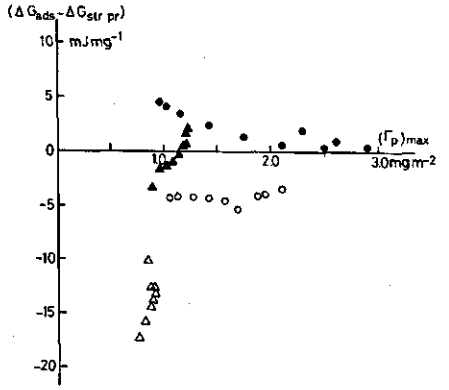

FIG. 6.15. Adsorption of HPA and RNase on polystyrene latices. $(\Delta G_{ads} - \Delta G_{str\ pr})$ as a function of the plateau value of the adsorption isotherms, $(\Gamma_p)_{max}$. ○ HPA △ RNase. Open symbols $\sigma_0 = -2.3\ \mu C\ cm^{-2}$; filled symbols $\sigma_0 = -15.5\ \mu C\ cm^{-2}$. $c_{KNO_3} = 0.05$ M $T = 25°C$.

In section 6.3.2.7. it was concluded that $\Delta H_{str\ pr}$ is positive. Hence, $\Delta S_{str\ pr}$ must be positive. This increase of entropy, together with a positive $\Delta S_{dehydr\ PS}$, is apparently the driving 'force' for the adsorption of the proteins.

In order to trace the source(s) of $\Delta S_{str\ pr}$ the factors (i) – (vi), mentioned in section 6.3.2.6., have to be re-examined. It emerges that the entropy gain most probably stems from the dehydration of the hydrophobic parts of the adsorbing protein molecules that possibly rearrange their structure and/or the increased rotational freedom due to this structural rearrangement upon adsorption. The proportions in which these factors contribute to $\Delta S_{str\ pr}$ are not yet known. Based on the values, mentioned in section 6.3.2.6., section (iii), the entropy gain from increased rotational freedom due to complete unfolding of a protein in aqueous *solution* lies in the range between $+0.07$ and $+0.25$ mJ K^{-1} mg^{-1}. At 298 K this would imply contributions to $\Delta G_{str\ pr}$ of -22 to -68 mJ mg^{-1}. As a matter of fact, with both proteins the lowest values for $(\Gamma_p)_{max}$ are in the range between 0.7 and 0.9 mg m^{-2}, which indicates that complete unfolding does not occur. Moreover, the rotational flexibility is restricted by the attachment of various segments to the polystyrene surface. Nevertheless, it should be realized that the positive value for $\Delta S_{str\ pr}$ may largely be due to increased rotational freedom in the protein molecule.

For both HPA and RNase, it is improbable that, at a given value of $(\Gamma_p)_{max}$ in figure 6.15., a difference in $\Delta G_{str\ pr}$ fully accounts for the variation of (ΔG_{ads} – $\Delta G_{str\ pr}$) with σ_0 of the polystyrene. ΔG_{ads} is less negative using latex C-3, as compared to L-1. In other words, the affinity between the protein and the polystyrene surface decreases with increasing surface charge density. This is primarily due to a less negative value for $\Delta G_{dehydr\ PS}$ and more positive values for ΔG_{cd}. For the adsorption of RNase $\Delta G_{ion\ med}$ (per mg) is also more positive in the case of latex C-3 than for latex L-1, but for HPA the opposite effect is observed.

Under conditions where a large number of ions are taken up upon adsorption (e.g. the adsorption of HPA at pH > ca. 7), the positive term ($\Delta S_{dehydr\ PS}$ + $\Delta S_{str\ pr}$) is largely opposed by the negative term, $\Delta S_{ion\ med}$. In these cases, however, the adsorption process is also favoured by a negative ΔH_{ads} (see figure 6.1.).

On the basis of the interpretation given here, the following general remarks concerning protein adsorption may be made.

In the absence of interactions between specific groups of the protein and the polystyrene surface, the properties of the bare interface influence ΔG_{ads} mainly through the contributions $\Delta G_{dehydr\ adsorbent}$, $\Delta G_{ion\ med}$ and ΔG_{cd}. The affinity between the interface and the protein decreases with decreasing hydrophobicity of the interface. In this way, relatively weak adsorption of proteins at hydrophilic interfaces (which does not necessarily imply smaller adsorbed amounts) is conceivable (see section 3.3.1.). The influences of the surface charge density and the electrokinetic charge density are more complex. The effects due to these properties can be traced by evaluating ΔG_{cd} and $\Delta G_{ion\ med}$ for a given set of model parameters (see the sections 5.5.1., 5.5.2., 6.3.2.2. and 6.3.2.3.). In most cases, the affinity decreases on increasing the (negative) surface charge.

For a given value of ε_1 and ψ_m in the model for the adsorbed protein layer (sections 5.5.1. and 5.5.2.), ΔG_{cd} is essentially determined by the properties of the bare interface, viz. its surface charge density and dielectric constant of the shear layer (section 6.3.2.2.). Hence, under these conditions, the influence of the protein on ΔG_{ads} is exerted mainly through $\Delta G_{str\ pr}$ and $\Delta G_{ion\ med}$. If interactions between specific groups of the protein and the interface do not play a dominant role, then it is primarily the properties of the protein that determines $\Delta G_{str\ pr}$. At constant electrokinetic charge density of the bare interface and at a given composition of the medium, $\Delta G_{ion\ med}$ is affected only by the distribution of the charged groups of the adsorbed protein molecules, which, in turn, controls the number of mobile ions taken up upon adsorption of the protein. This distribution is directly related to changes in the structure of the protein concomitant with adsorption. Thus, under the conditions mentioned above, ($\Delta G_{str\ pr}$ + $\Delta G_{ion\ med}$) is determined by the properties of the protein and not by those of the interface. Hence, the mode of adsorption, i.e. the structure of the adsorbed protein layer, is a characteristic function of the conformational properties of the proteinrather than of the nature, viz. the hydrophobicity and the surface charge, of the interface.

Variation of the electrokinetic charge density of the bare interface may lead to a different structure for the adsorbed protein layer, as a result of attaining an optimal value for ($\Delta G_{str\ pr}$ + $\Delta G_{ion\ med}$).

Any structural changes in the adsorbing protein molecule are less favourable (i.e. involves a less negative value for $\Delta G_{str\ pr}$) the more stable the conformation of the protein in solution is. This is reflected by the feature, generally observed for the adsorption of proteins, that maximal conformational stability of the protein in solution corresponds with a maximum value for the adsorption saturation (see section 3.3.1., last paragraph). By way of illustration, one may point to the differences between HPA and RNase concerning the effect of the pH of adsorption on $(\Gamma_p)_{max}$ (section 4.3.2.1., figures 4.4. and 4.5.) and on the hydrogen ion titration behaviour (section 5.3.3., figures 5.6. and 5.7.).

6.4. Summary

In this chapter the results obtained for the enthalpy of adsorption, ΔH_{ads}, of HPA and RNase at different polystyrene surfaces, using a microcalorimeter, are presented and discussed. ΔH_{ads} was measured at constant proportions of protein and polystyrene, corresponding to plateau values of the adsorption isotherms. The variables in these experiments were the pH, σ_0, c_{KNO_3} and T.

An attempt has been made to analyze ΔH_{ads} in terms of the different contributions that are known to be involved. To this end, the following factors are considered: a. *titration* (section 6.3.2.1.), b. *redistribution of charge* (section 6.3.2.2.), c. *ionic medium effect* (section 6.3.2.3.), d. *dehydration of the hydrophobic part of the polystyrene surface* (section 6.3.2.4.), e. *van der Waals interaction between the polystyrene particle and the adsorbed protein layer* (section

6.3.2.5.) and f. *differences in the structure of the adsorbed and the dissolved protein molecule* (section 6.3.2.6.).

The analysis of ΔH_{ads}, as a function of pH, has been carried out for the adsorption of HPA and RNase on polystyrene latices L-1 ($\sigma_0 = -2.3$ μC cm^{-2}) and C-3 ($\sigma_0 = -15.5$ μC cm^{-2}) at 0.05 M KNO_3 and 25°C.

The enthalpies due to the factors a.–e. are estimated on the basis of the model for the adsorbed protein layer and the assumed distribution of charge therein (sections 5.5.1. and 5.5.2.). The enthalpy arising from the last-mentioned factor, the structural change in the protein upon adsorption, is the least accessible one. This factor may comprise (i) variation in the number and the kind of amino acid residues exposed to the aqueous solution, (ii) change in the van der Waals interactions, internal and between adsorbed protein molecules, (iii) variation in the number of ion pairs, (iv) variation in the number of hydrogen bonds, (v) change in the rotational flexibility of the protein molecule and (vi) interactions between specific groups of the protein molecule and the polystyrene surface. In the analysis of ΔH_{ads}, it was assumed that $\Delta H_{str\ pr}$ equals the difference between ΔH_{ads} and the sum of the enthalpies due to the factors a.–e. (section 6.3.2.7.). Obviously, by this procedure, the accuracy of $\Delta H_{str\ pr}$ depends on the accuracy of the estimations of the other constituents. Moreover, $\Delta H_{str\ pr}$ also comprises possible factors that have been overlooked.

Both for HPA and RNase, positive values for ΔH_{str} (pH) are obtained. For each protein an unambiguous relationship was found to exist between $\Delta H_{str\ pr}$ (expressed per unit mass of adsorbed protein) and the adsorbed amount, $(\Gamma_p)_{max}$ (section 6.3.2.8.). This finding supports the conclusion, arrived at earlier in section 4.3.2., that variations in $(\Gamma_p)_{max}$ are due to different extents of structural changes in the protein. Considering the possible different modes of adsorption for HPA and RNase and realizing that $\Delta H_{str\ pr}$ is a compounded quantity, it is not surprising that the curves for ΔH_{str} vs. $(\Gamma_p)_{max}$ show different trends for the two proteins (see figure 6.12.).

The effect of c_{KNO_3} on ΔH_{ads} (pH) is much less for RNase than for HPA. In view of the conclusions regarding the effect of the pH of adsorption on the structure of the adsorbed protein layer (sections 4.3.2.1. and 5.3.3.2., last two paragraphs), it seems that $\Delta H_{str\ pr}$ is especially sensitive to c_{KNO_3}.

The various constituents of ΔH_{ads} are affected by the temperature in different ways. At first sight, there would seem to be a rather complex dependence of ΔH_{ads} on the temperature (figures 6.2. and 6.4.), but is has been shown that the interpretation of ΔH_{ads} is qualitatively consistent with the influence of the temperature (section 6.3.3.).

In section 6.3.4. the Gibbs free energy of adsorption, ΔG_{ads}, was considered. It was concluded that the dehydration of hydrophobic areas of the polystyrene surface favours the adsorption process. The ionic medium effect opposes protein adsorption. With latex C-3 the change in the redistribution of charge also opposes the adsorption, whereas in the case of latex L-1 this effect is only of minor importance. The contributions to ΔG_{ads} from the titration effect and the van der Waals interaction between the polystyrene and the adsorbed protein layer

TABLE 6.1. Adsorption from aqueous solution of HPA and RNase on negatively charged polystyrene surfaces. $c_{KNO_3} = 0.05$ M $T = 25°C$ Factors involved in the adsorption process.

factor	effect	relative importance	mainly influenced by
1. structural change in the adsorbing protein molecule – variation in the state of hydration – van der Waals interactions (internal and between adsorbed molecules) – disruption/formation of ion pairs – disruption/formation of hydrogen bonds – change in rotational flexibility – interactions between specific groups and specific groups of the polystyrene surface	$\Delta H > 0$ $\Delta S > 0$ $\Delta G < 0$	large	conformation and conformational stability of the protein molecule (pH, ionic strength, temperature)
2. titration	$\Delta H > 0$ $\Delta G > 0$	small	net proton charge of the protein; electric field at the polystyrene surface
3. changes in the distribution of charge	depending on the conditions		surface charge of the polystyrene
4. ionic medium effect	$\Delta H < 0$ $\Delta S < 0$ $\Delta G > 0$	large	conformational stability of the protein; electrokinetic charges of the protein and the polystyrene
5. dehydration of hydrophobic areas of the polystyrene surface	$\Delta H \lesssim 0$ $\Delta S > 0$ $\Delta G < 0$	large	hydrophobicity of the polystyrene surface
6. van der Waals interactions between the adsorbed protein layer and the polystyrene	$\Delta H < 0$ $\Delta G < 0$	negligible	

can be neglected.

On the basis of the necessary requirement of a negative value for ΔG_{ads}, it is reasoned that $\Delta G_{str\ pr}$ is also negative and, hence, favours the adsorption process. Since $\Delta H_{str\ pr}$ is positive, the entropy difference between the respective structures of the adsorbed and the dissolved protein molecule (including the changes in hydration water!) must be positive. Also, the negative Gibbs free energy of dehydration of the hydrophobic polystyrene is largely due to a positive entropy change. Thus, it appears that entropy gain is the dominant factor governing protein adsorption. Indeed, this should be the result, because for both proteins, under various conditions, ΔH_{ads} is found to be positive (figures 6.1.–6.4.). If large amounts of mobile ions are taken up from solution, for example in the case of adsorption of HPA at alkaline pH values, the ensuing reduction of entropy may substantially counteract the positive entropy from the other contributions. Then, the adsorption, is (also) favoured by a negative enthalpy (figure 6.1.).

The roles of the various factors in the adsorption of HPA and RNase are summarized in table 6.1.

This thermodynamic analysis of the systems under investigation leads to some general conclusions regarding the mechanism of protein adsorption. In this context, in section 6.3.4. some conclusions regarding the influence of various properties of the interface and of the protein molecules on their mutual affinity are stated.

SUMMARY

The adsorption from (aqueous) solution of proteins is very complex. The interfacial behaviour of proteins is determined by the properties of, and the mutual interactions between, the adsorbing interface, the protein molecules, the solvent (water) molecules and other solutes (e.g. ions). Virtually all kinds of interactions are involved, viz. electrostatic, hydrogen bonding, hydrophobic, van der Waals, etcetera.

Due to the intricate nature of the adsorption process, and also to the specificity in structure and conformational stability of protein molecules, no general theories satisfactorily describing protein adsorption have yet been developed. Furthermore, all the proposed hypotheses concerning the structure of proteins at interfaces are difficult to verify since most of the techniques that can be applied for the conformational analysis of proteins in bulk solution are not suitable for studying proteins at interfaces. Even in a qualitative sense, protein adsorption is often not well understood. The intention of this study was to gain more insight in the factors that govern the adsorption of proteins from solution.

In chapter 3 the adsorption of proteins in relation to their properties in solution was discussed on the basis of data reported in the literature. Although certain aspects of protein adsorption seem rather controversial, some general features may be recognized.

As is typical for the adsorption of macromolecules, proteins generally attach irreversibly to the adsorbent. With hydrophilic interfaces polar interactions seem to dominate, but with hydrophobic interfaces non-polar interactions appear to govern the adsorption process. As a rule, the affinity between the protein and the adsorbent surface increases with their increasing hydrophobic content. This is due primarily to the increasing entropy gain resulting from hydrophobic bonding.

The structure of a protein molecule in the adsorbed state is largely determined by its structural stability in bulk solution. The less stable the structure in solution, the more likely it is to be perturbed by the interface. The tendency of a protein molecule to change its structure on adsorption increases with increasing importance of hydrophobic interactions as a factor stabilizing the protein structure in solution. In these terms, the feature, often observed, that the plateau level of adsorption tends to a maximum in the isoelectric region of the protein in solution, may be explained.

The conformational stability on varying the pH for HPA molecules is much less than for RNase molecules. Since the hydrophobicity of HPA is greater than that of RNase, for HPA the relative contribution from intramolecular hydrophobic interactions to the stabilization of the molecular structure in solution is expected to be greater than in the case of RNase.

In chapter 2 the preparation and characterization of negatively charged polystyrene latices was described. The latices were prepared in the absence of any emulsifying agents. By this procedure 'clean' polystyrene surfaces containing no spurious materials were obtained. The charge on the polystyrene surface is essentially due to the presence of negatively charged sulphate ($-OSO_3^-$) groups. By adjusting the polymerization conditions the latex surface charge could be varied in a controlled way. Obviously, the hydrophobicity of the polystyrene surface decreases with increasing surface charge density. There are some experimental indications that oligomers of styrene containing $-OSO_3^-$ end groups are adsorbed on the polystyrene particles. However, no conclusive evidence has been obtained to ascertain whether the presence of these oligomers renders the polystyrene surface 'hairy' or smooth.

The electrophoresis of the polystyrene particles was studied in the presence of KNO_3. From the electrophoretic mobility the electrokinetic potential and electrokinetic charge density were calculated. It appears that, especially for high surface charge densities, the surface charge is to a large extent compensated by charge located within the plane of shear of the particle. This implies considerable specific adsorption of K^+ ions at the polystyrene surface.

In chapter 4 a description has been given of the determination of isotherms for the adsorption from solution of HPA and RNase onto polystyrene surfaces, under various conditions of pH (i.e. charge on the protein molecule), charge on the polystyrene surface, ionic strength (0.01 M and 0.05 M KNO_3, without adding buffers) and temperature (5°C, 22°C and 37°C).

In all cases, dilution experiments indicated that the proteins adsorb irreversibly.

The affinity between HPA and the polystyrene surface, as judged from the initial slopes of the isotherms, reflects the Coulombic interaction between the adsorbate and the adsorbent. Thus, the initial part of the isotherm is steeper, the larger the charge difference between the HPA molecules and the polystyrene surface.

The effect of temperature on the adsorption of HPA was found to be dependent on pH. Away from the isoelectric point in solution, at low degrees of coverage of the polystyrene surface, a steady increase of the amount adsorbed was observed on increasing the temperature. This suggests that, at least under these conditions, the adsorption is endothermic and, hence, that the adsorption process is driven by an entropy gain. In the isoelectric region (pH ca. 4.6 for HPA) the adsorption mechanism seems to be different. At this pH the initial adsorption isotherms, at 5°C and 22°C, are virtually identical but increasing the temperature to 37°C leads to a greater affinity between HPA and polystyrene. Moreover, it was found that the lateral repulsion between adsorbed HPA molecules tends to be maximum in the isoelectric region of the protein in solution. This argues against a conformation of the adsorbed molecules that is independent of pH.

The adsorption isotherms for RNase all show a high-affinity character.

Therefore, the effect of charge or temperature on the initial parts of the isotherms could not be measured.

Unlike for RNase, the isotherms for HPA, in some cases, show steps. This reflects transitions in the mode of adsorption at intermediate surface coverages.

For both HPA and RNase, the isotherms show plateau levels at sufficiently large concentrations in bulk solution. However, HPA and RNase differ markedly in the way the plateau levels depend on the pH of adsorption. In the case of HPA, the maximum amount adsorbed, as a function of pH, is more or less symmetrical with respect to its isoelectric point in solution, with a pronounced maximum at this pH value. With RNase the maximum adsorption is much less dependent on pH. Thus, at least for HPA, the plateau level of adsorption is predominantly determined by the net charge of the dissolved molecule. Based on a consideration of all the results, it was concluded that the reduction in the plateau level of adsorption with increasing pH beyond the isoelectric point, is due to a greater amount of structural rearrangement in the protein molecule, rather than to increased distances between the adsorbed molecules. Hence, it was assumed that the plateau level of adsorption corresponds to complete monolayers of protein molecules, structurally perturbed to varying degrees. Indeed, the influence of temperature and ionic strength on the structural stability of the protein in solution is generally reflected in the amount adsorbed.

In the case of RNase it was found that the maximum amount adsorbed decreases significantly at pH values $\gtrsim 9.5$, where this protein possesses a considerable net negative charge.

On increasing the negative charge of the polystyrene surface an increase in the adsorption of HPA and RNase was observed, even at pH values where the protein is also negatively charged. The reasons underlying this feature are not clear, but it indicates that the Coulombic interaction between the protein and the polystyrene surface is not a dominant factor in the adsorption process.

Based on the assumption of structural rearrangements in the adsorbing protein molecules, it was concluded that the fraction of the protein in actual contact with the polystyrene surface increases with decreasing amount adsorbed. It was.further argued that, after structural rearrangements, the adsorbed protein molecules retain a rather compact structure. Hence, the thickness of the adsorbed layers of HPA and RNase decreases with decreasing amount adsorbed. In the case of HPA the protein volume fraction in the adsorbed layer seems to be larger than for RNase.

The electrostatic effects, i.e. the various roles played by the charged groups of the protein and the polystyrene surface as well as by the ions in solution, have been discussed in chapter 5. This discussion refers to adsorption saturation.

Hydrogen ion titrations show that, as a result of adsorption, the dissociation of carboxyl groups in HPA and RNase molecules is suppressed. It was deduced

that in both these proteins the average position of the carboxyl groups is relatively close to the negatively charged polystyrene surface. In the case of RNase, this effect is essentially independent of the pH of adsorption, whereas for HPA this suppression of dissociation of the carboxyl groups increases the further the pH is from the isoelectric point of HPA in solution. Hence, it would seem that the structural rearrangements accompanying the adsorption process lead to a larger fraction of the carboxyl groups located close to the polystyrene surface.

In the case of RNase it was found that, after adsorption, a smaller number of positively charged groups (i.e. imidazole and amino groups) are titratable. It was assumed that this is due to the formation of strong ion pairs between these groups and the negatively charged sulphate groups at the polystyrene surface. In this respect, the experiments with HPA were not conclusive, but it is probable that the same kind of ion pairing occurs with this protein as well.

The involvement of ions in the adsorption process was investigated by electrophoresis of the polystyrene particles and the protein molecules, before and after adsorption. Calculation of the electrokinetic charges revealed that, coincident with the adsorption of either protein, a net increase in negative charge results at low pH, and a net increase in positive charge at high pH.

In order to analyze this redistribution of charge, a simple model for the protein-covered polystyrene particles was adopted. According to this model the average position of the negatively charged sulphate groups is taken to be the plane defining the polystyrene surface. The adsorbed protein layer, considered to have a rather compact structure, totally covers the adsorbent surface. The adsorbed layer is divided into three regions. In the innermost region, adjacent to the polystyrene surface, a fraction of the charged groups of the protein (e.g. carboxyl groups and positively charged groups that have formed ion pairs with negatively charged groups of the polystyrene surface), as well as specifically adsorbed ions, are located. The thickness of this region is comparable with the difference between the hydrodynamic radius of the bare polystyrene particle and the radius of the solid particle (i.e. the thickness of the shear layer). By analogy with the interior of dissolved protein molecules, the central region of the adsorbed protein layer is assumed to be electrically neutral. The outermost region, extending to the plane of shear of the covered particle, then contains the remainder of the electrokinetic charge of the protein-covered particle. For the purpose of analysis a homogeneous distribution of charge in both the innermost and the outermost regions was assumed. The permittivities of each of these three regions of the adsorbed layer were taken to be adjustable parameters.

On the basis of this model, the charge effects in the innermost and the outermost region, resulting from the transfer of ions to or from the solution phase, were calculated. It was reasoned that a net uptake of cations (i.e. K^+) from solution into the region adjacent to the polystyrene surface occurs, whereas in the outermost region of the adsorbed protein layer there is a net increase in the binding of anions (i.e. NO_3^-).

In chapter 6 a thermodynamic analysis of the adsorption process was made. The net enthalpy change, at maximum adsorption of the two proteins, was measured under various conditions. For RNase and, in most cases, for HPA this enthalpy change was found to be positive. This leads to the conclusion that the adsorption process is governed by an increase of entropy.

The experimentally obtained adsorption enthalpy was interpreted in terms of the contributions resulting from the various factors that are known to be involved in the overall adsorption process. In view of the experimental results reported in the previous chapters, the following factors were considered:

a. changes in the degree of protonation of the adsorbed and the dissolved protein molecules (especially their carboxyl groups),
b. redistribution of charge due to overlap of electric fields of the protein and the polystyrene surface,
c. changes in the medium of the ions that are transferred from the solution to the adsorbed layer,
d. van der Waals interactions between the polystyrene particle and the adsorbed protein layer,
e. dehydration of hydrophobic parts of the polystyrene surface,
f. those resulting from structural changes in the adsorbing protein molecules, including changes in the state of hydration and interactions between specific groups of the protein and the polystyrene surface.

The changes in the thermodynamic functions of state due to the factors a. – e. were estimated on the basis of the model proposed for the adsorbed layer. Due to lack of detailed knowledge concerning the nature of structural changes in the adsorbing protein molecules, the thermodynamic effects resulting from factor f. are not directly assessable. However, an estimate of the contribution made by this factor to the net adsorption enthalpy may be obtained by subtracting the sum of the calculated enthalpy changes due to the factors a. – e. from the experimental value of the adsorption enthalpy. The degree of accuracy to which the enthalpy resulting from structural changes can then, therefore, be determined, depends on the accuracy of the estimates for the other constituent terms (a.–e.) as well as on the accuracy of the experimental value; it will also contain contributions from any other factors that may have been overlooked. Nevertheless, for both HPA and RNase, the enthalpy resulting from factor f., obtained in this way, seems to show a definite relationship to the amount of protein adsorbed (i.e. to the extent of rearrangement of the protein structure). For both proteins this enthalpy effect was found always to be positive.

The mechanisms proposed for the adsorption of HPA and RNase on polystyrene are, in a qualitative sense, consistent with the effect of temperature on the overall adsorption enthalpy.

Due to the irreversibility of the process, the standard Gibbs free energy of adsorption of HPA and RNase onto polystyrene could not be established from the adsorption isotherms, but it must be negative for adsorption to occur.

It was concluded that the ionic medium effect (factor c.) opposes protein adsorption. For polystyrene latices having a large negative surface charge the

redistribution of charge (factor b.) also opposes the adsorption process, but this effect decreases with decreasing surface charge density. Dehydration of hydrophobic areas of the polystyrene surface (factor e.) favours the adsorption process primarily on account of the resulting entropy gain. The contributions from changes in the degree of protonation of the protein (factor a.) and from the van der Waals interaction between the adsorbed protein layer and the polystyrene particle (factor d.) to the Gibbs free energy of adsorption seem to be of minor importance. It was further argued that the Gibbs free energy change resulting from structural rearrangements in the protein (factor f.) is negative. Since the enthalpy change due to this factor was found to be positive, the entropy effect involved must also be positive. This entropy gain may originate e.g. from variations in the number and the kind of amino acid residues exposed to the aqueous phase, and from increased rotational freedom in the protein molecule.

Altogether, it appears that a net increase of entropy, associated with factors e. and f., dominates the adsorption from aqueous solution of HPA and RNase onto negatively charged polystyrene surfaces.

The model assumed for the adsorbed layer and the distribution of charge therein, seems to fit the experimental observations rather well; at least, the thermodynamic analysis based on this model is not incompatible with the experimental data.

Finally, the thermodynamic analysis of the adsorption processes under investigation leads to conclusions, which one may expect to be of general validity with regard to the interaction between proteins and interfaces.

SAMENVATTING

EIWITTEN AAN GRENSVLAKKEN

DE ADSORPTIE VAN MENSELIJK BLOEDPLASMA-ALBUMINE EN RUNDERPANCREAS-RIBONUCLEASE AAN POLYSTYREEN LATICES

Eiwitadsorptie is een ingewikkeld proces. Het adsorptiegedrag van eiwitten vanuit een (waterige) oplossing wordt bepaald door de eigenschappen respektievelijk de onderlinge wisselwerkingen van en tussen het adsorbensoppervlak, de eiwitmolekulen, de molekulen van het oplosmiddel (water) en die van andere opgeloste stoffen (bijv. ionen). Vele soorten wisselwerkingen zijn er bij betrokken, zoals elektrostatische, waterstofbrugvorming, hydrofobe binding en van der Waals interaktie.

Vanwege het samengestelde karakter van het adsorptieproces en ook wegens de specificiteit met betrekking tot de struktuur en konformatiestabiliteit van eiwitmolekulen, is men er nog niet in geslaagd een bevredigende theorie voor eiwitadsorptie te ontwikkelen. Bovendien is het zeer moeilijk hypothesen over de struktuur van eiwitten aan grensvlakken te toetsen, aangezien de meeste technieken die worden aangewend bij het onderzoek van de struktuur van eiwitten in oplossing niet kunnen worden toegepast. Zelfs in kwalitatieve zin wordt het mechanisme van de eiwitadsorptie veelal niet goed begrepen. De bedoeling van het hier beschreven onderzoek is meer inzicht te verschaffen in de faktoren die de adsorptie van eiwitten uit oplossing beheersen. Daarbij is uitgegaan van een reeks experimenten met goed gedefinieerde modelsystemen.

Op grond van literatuurgegevens is in hoofdstuk 3 de adsorptie van eiwitten besproken tegen de achtergrond van hun eigenschappen in oplossing. Hoewel bepaalde aspekten tegenstrijdig schijnen, kunnen er met betrekking tot eiwitadsorptie toch enkele algemene kenmerken worden aangegeven.

Eiwitmolekulen hechten zich in het algemeen irreversibel aan adsorbentia; dit is overigens typerend voor makromolekulen. In geval van hydrofiele grensvlakken schijnen polaire interakties te overheersen, terwijl aan hydrofobe grensvlakken de adsorptie door hydrofobe wisselwerkingen lijkt te worden beheerst. De affiniteit tussen het eiwit en het adsorbensoppervlak wordt, als regel, kleiner bij afnemende hydrofobiciteit van deze komponenten. Dit wordt hoofdzakelijk veroorzaakt door de afnemende entropiewinst ten gevolge van een daling in de mate van hydrofobe binding.

De struktuur van een eiwitmolekuul in geadsorbeerde toestand wordt grotendeels bepaald door de stabiliteit van haar konformatie in oplossing. Hoe labieler de konformatie in oplossing, des te waarschijnlijker is het dat deze konformatie wordt verstoord door het grensvlak. Des te meer de konformatie in oplossing wordt bepaald door hydrofobe binding, des te meer zal het eiwitmolekuul er toe neigen zijn konformatie tijdens de adsorptie te wijzigen. Op deze gronden zou

het veel voorkomende verschijnsel van een maximaal adsorptieplateau in het isoelektrisch gebied van het opgeloste eiwit verklaard kunnen worden.

De stabiliteit van de konformatie van HPA molekulen ten opzichte van wijzigingen in de pH is veel kleiner dan in geval van RNase. De hydrofobiciteit van HPA is groter dan die van RNase. Om deze reden is het te verwachten dat de relatieve bijdrage van intramolekulaire hydrofobe binding aan de stabilisering van de molekuulstruktuur in oplossing voor HPA groter is dan voor RNase.

In hoofdstuk 2 zijn de bereiding en de karakterisering van negatief geladen polystyreenlatices beschreven. De latices werden bereid zonder een emulgator te gebruiken. Volgens deze werkwijze worden 'schone' polystyreenoppervlakken verkregen, welke geen 'vreemde' komponenten bevatten. De lading op het polystyreenoppervlak wordt zo goed als geheel veroorzaakt door negatief geladen sulfaat ($-OSO_3^-$) groepen. De wandlading van het latex kan geregeld worden door het instellen van de omstandigheden waarbij de polymerisatie plaatsvindt. De hydrofobiciteit van het polystyreenoppervlak vermindert uiteraard met toenemende ladingsdichtheid. Experimentele gegevens suggereren dat oligomeren van styreen, welke $-OSO_3^-$ groepen bevatten, aan de polystyreendeeltjes geadsorbeerd zijn. Het is echter niet duidelijk of, om deze reden, het polystyreenoppervlak als 'harig' of als glad moet worden beschouwd.

Elektroforese van de polystyreenlatices werd uitgevoerd in KNO_3 oplossing. De elektrokinetische potentiaal en de elektrokinetische lading zijn berekend uit de elektroforetische beweeglijkheid. Vooral in geval van oppervlakken met grote ladingsdichtheid blijkt dat de oppervlaktelading in belangrijke mate gekompenseerd wordt door tegenlading binnen het hydrodynamische afschuifvlak van het polystyreendeeltje. Dit betekent een aanzienlijke specifieke adsorptie van K^+ ionen aan het polystyreenoppervlak.

De bepaling van isothermen voor de adsorptie van HPA en RNase uit oplossing aan polystyreenoppervlakken is beschreven in hoofdstuk 4. Adsorptieisothermen zijn bepaald als funktie van de pH (lading op het eiwitmolekuul), lading op het polystyreenoppervlak, ionsterkte (0.01 M en 0.05 M KNO_3, zonder toevoeging van buffers) en temperatuur (5°C, 22°C en 37°C).

Verdunning na adsorptie leidde in geen der gevallen tot desorptie van het eiwit, hetgeen betekent dat HPA en RNase irreversibel adsorberen.

In de affiniteit tussen een HPA molekuul en het polystyreenoppervlak, de aanvangshelling der isotherm als kriterium kiezend, wordt de Coulomb interaktie tussen deze komponenten herkend, dat wil zeggen de aanvangshellingen zijn steiler bij grotere ladingstegenstelling.

De wijze waarop de adsorptie op de temperatuur reageert is afhankelijk van de pH. Buiten het isoelektrische gebied van het opgeloste eiwit, bij lage bedekkingsgraden van het polystyreenoppervlak, heeft verhoging van de temperatuur een grotere geadsorbeerde hoeveelheid tot gevolg. Dit suggereert dat, tenminste onder genoemde omstandigheden, de adsorptie endotherm is en dat derhalve het adsorptieproces gedreven wordt door een toename van de entropie.

In het isoelektrische punt (voor HPA pH ca. 4,6) schijnt het adsorptiemechanisme anders te zijn. Bij deze pH zijn de aanvangshellingen van de isothermen bij 5 °C en 22 °C nagenoeg identiek, maar bij 37 °C wordt een grotere affiniteit tussen HPA en polystyreen waargenomen. Dit duidt op een invloed van de pH op de konformatie van de geadsorbeerde molekulen.

De adsorptieisothermen voor RNase zijn alle van het 'high affinity' type. Het is daarom in dit geval onmogelijk de invloeden van lading en temperatuur op de aanvangshellingen experimenteel vast te stellen.

In tegenstelling tot die voor RNase vertonen de isothermen voor HPA soms stappen. Dit weerspiegelt overgangen in het adsorptiegedrag van HPA molekulen bij tussenliggende bedekkingsgraden van het polystyreenoppervlak.

De isothermen van beide eiwitten vertonen duidelijke plateau-waarden bij voldoend hoge koncentraties eiwit in oplossing. De wijze waarop deze plateauwaarden afhangen van de pH waarbij de adsorptie plaats heeft, is voor de twee eiwitten echter zeer verschillend. De maximale adsorptie van RNase is veel minder afhankelijk van de pH dan die van HPA. Voor HPA geldt dat de maximale adsorptie, als funktie van de pH, symmetrisch is ten opzichte van het isoelektrische punt; bij deze pH bereikt de plateau-waarde een duidelijk maximum. De maximale adsorptie wordt dus, tenminste in geval van HPA, voornamelijk bepaald door de netto lading op het opgeloste molekuul. Alle resultaten overwegende, is gekonkludeerd dat een kleinere maximale adsorptie eerder moet worden toegeschreven aan veranderingen in de eiwitstruktuur dan aan grotere afstanden tussen de geadsorbeerde molekulen. Om deze reden is verondersteld dat bij maximale adsorptie komplete monolagen gevormd zijn van eiwitmolekulen waarvan, als gevolg van de adsorptie, de konformatie meer of minder gewijzigd is. De invloed van de temperatuur en de ionsterkte op de konformatiestabiliteit van het eiwit in oplossing korrespondeert inderdaad met de op deze wijze geïnterpreteerde geadsorbeerde hoeveelheid.

De adsorptie van RNase is veel minder gevoelig voor de pH en neemt pas duidelijk af bij $\geq$ 9,5 waar dit eiwit een aanzienlijke negatieve lading heeft.

Bij vergroting van de ladingsdichtheid op het polystyreenoppervlak wordt een toenemende adsorptie van HPA en RNase waargenomen, zelfs bij pH-waarden waarbij het eiwit eveneens negatief geladen is. De redenen voor dit verschijnsel zijn onduidelijk, maar het toont wederom aan dat niet in de eerste plaats Coulomb krachten het adsorptieproces beheersen.

Op grond van de aanname van veranderingen in de konformatie van de adsorberende eiwitmolekulen is gekonkludeerd dat bij kleinere geadsorbeerde hoeveelheid een groter deel van het eiwitmolekuul zich hecht aan het polystyreenoppervlak. Voorts werd gekonstateerd dat, nadat konformatieveranderingen hebben plaats gehad, de geadsorbeerde eiwitmolekulen een tamelijk kompakte konformatie behouden. De dikte van de geadsorbeerde lagen van HPA en RNase neemt dan af met afnemende geadsorbeerde hoeveelheid. Het is waarschijnlijk dat voor HPA de volumefraktie van het eiwit in de geadsorbeerde laag groter is dan voor RNase.

De elektrostatische effekten, dat wil zeggen de verschillende rollen die bij de adsorptie gespeeld worden door de geladen groepen van het eiwit en het polystyreenoppervlak alsmede door de ionen in oplossing, worden besproken in hoofdstuk 5. Deze behandeling beperkt zich tot omstandigheden waarbij maximale adsorptie optreedt.

Blijkens titratie-experimenten neemt, ten gevolge van de adsorptie, de dissociatiekonstante van de carboxylgroepen in zowel HPA als RNase duidelijk af. Hieruit is afgeleid dat in beide eiwitten de carboxylgroepen gemiddeld relatief dicht bij het polystyreenoppervlak geplaatst zijn. Voor RNase bleek dat na adsorptie een kleiner aantal positief geladen groepen (imidazool- en aminogroepen) getitreerd worden. Vorming van ionenparen tussen deze groepen en de negatief geladen sulfaatgroepen op het polystyreenoppervlak wordt daarvoor verantwoordelijk geacht. De experimenten met HPA lieten geen beslissing toe ten aanzien van het afschermen voor titratie van positief geladen groepen, maar de vorming van ionenparen met sulfaatgroepen van de polystyreenwand is ook voor HPA zeer wel mogelijk.

Met behulp van elektroforese van polystyreendeeltjes, opgeloste eiwitmolekulen en met eiwit bedekte polystyreendeeltjes werd de deelname van ionen aan het adsorptieproces onderzocht. Volgens de berekende elektrokinetische ladingen wordt tijdens de adsorptie van beide eiwitten bij lage pH negatieve lading opgenomen of wordt positieve lading uitgestoten, terwijl bij hoge pH opname van positieve lading of uitstoting van negatieve lading plaatsvindt.

De herverdeling van de lading is geanalyseerd op grond van een eenvoudig model voor het met eiwit bedekte polystyreendeeltje. In dit model bevindt de negatieve lading van de sulfaatgroepen zich in het vlak van de polystyreenwand. De geadsorbeerde eiwitlaag heeft een kompakte struktuur en bedekt het polystyreenoppervlak volledig. De geadsorbeerde laag is verdeeld in drie zones. De binnenste zone, grenzend aan het polystryreenoppervlak, bevat een deel van de geladen groepen van het eiwit (bijv. carboxylgroepen en positief geladen groepen welke ionenparen hebben gevormd) alsook specifiek geadsorbeerde ionen. De dikte van deze zone is vergelijkbaar met het verschil tussen de hydrodynamische straal en de werkelijke straal van het onbedekte polystyreendeeltje (dit is de dikte van de hydrodynamische afschuiflaag). De middelste zone wordt, in analogie met het binnenste gedeelte van een opgelost eiwitmolekuul, elektrisch neutraal verondersteld. De buitenste laag, welke zich uitstrekt tot het hydrodynamische afschuifvlak van het met eiwit bedekte deeltje, bevat dan het restant van de elektrokinetische lading van dit deeltje. In de binnenste en in de buitenste laag is een homogene ladingsverdeling aangenomen teneinde analyse van de ladingseffekten mogelijk te maken. De permittiviteiten in ieder van de drie lagen zijn als aanpasbare parameters gekozen.

Op basis van dit model is aannemelijk gemaakt dat bij adsorptie in de zone grenzend aan het polystyreenoppervlak een netto hoeveelheid kationen (K^+) uit de oplossing wordt opgenomen, terwijl in de buitenste zone van de geadsorbeerde eiwitlaag een netto opname van anionen (NO_3^-) plaatsvindt.

In hoofdstuk 6 wordt een thermodynamische interpretatie van het adsorptieproces gegeven. Voor beide eiwitten werd de totale enthalpieverandering voor het bereiken van maximale adsorptie onder verschillende omstandigheden gemeten. Voor RNase en, in de meeste gevallen, ook voor HPA werd een positieve adsorptie-enthalpie gevonden, hetgeen bevestigt dat het adsorptieproces verloopt dankzij een toename van de entropie.

De experimenteel bepaalde adsorptie-enthalpie is ontleed in de bijdragen van de faktoren waarvan bekend is dat ze bij het adsorptieproces betrokken zijn. Gezien de experimentele resultaten vermeld in de vorige hoofdstukken worden de volgende bijdragen in aanmerking genomen:

a. enthalpieveranderingen ten gevolge van veranderingen in de graad van protonering van de geadsorbeerde en opgeloste eiwitmolekulen (speciaal hun carboxylgroepen),
b. enthalpieveranderingen ten gevolge van herverdeling van lading ten gevolge van overlap van de elektrische velden van het eiwit en het polystyreenoppervlak,
c. enthalpieveranderingen ten gevolge van het feit dat de ionen die vanuit de oplossing naar de geadsorbeerde laag worden verplaatst in een ander medium komen,
d. enthalpieveranderingen ten gevolge van van der Waals interakties tussen het polystyreendeeltje en de geadsorbeerde eiwitlaag,
e. enthalpieveranderingen ten gevolge van dehydratatie van de hydrofobe delen van het polystyreenoppervlak,
f. enthalpieveranderingen welke het gevolg zijn van konformatieveranderingen in de eiwitmolekulen bij adsorptie (inklusief veranderingen in eiwithydratatie en interakties tussen specifieke groepen van het eiwit en het polystyreenoppervlak).

De bijdragen a. – e. zijn zo goed mogelijk geschat op grond van het voorgestelde model voor de geadsorbeerde laag. Aangezien de wijze waarop de konformatie van de adsorberende molekulen verandert onvoldoende bekend is, kan de bijdrage f. niet direct vastgesteld worden. Deze bijdrage werd daarom geschat door het gemeten totale enthalpie-effekt te verminderen met de som van de bijdragen a. – e. De nauwkeurigheid van de schatting voor de enthalpie van de konformatieveranderingen wordt dus bepaald door de nauwkeurigheden van de schattingen voor de andere termen (a. – e.) en die van de gemeten adsorptie-enthalpie. De enthalpieverandering toegeschreven aan konformatieveranderingen bevat ook bijdragen van faktoren die eventueel buiten beschouwing zijn gelaten. Niettemin vertoont, voor zowel HPA als RNase, de op deze wijze verkregen bijdrage f. een duidelijke relatie met de hoeveelheid geadsorbeerd eiwit (dat is met de mate van konformatieverandering). Voor dit enthalpie-effekt werd voor beide eiwitten onder alle omstandigheden een positieve waarde gevonden.

De invloed van de temperatuur op de totale adsorptie-enthalpie is, kwalitatief, in overeenstemming met het voorgestelde mechanisme van de adsorptie van HPA en RNase aan polystyreen.

Vanwege het irreversibele karakter van het adsorptieproces kan de standaard Gibbs energie van de adsorptie niet uit de isothermen berekend worden. Het is wel bekend dat, gezien het spontane verloop van de adsorptie, de adsorptie Gibbs energie negatief is.

Evenals de enthalpie-effekten kunnen ook de veranderingen in de entropie en derhalve in de Gibbs energie, teweeggebracht door de faktoren genoemd onder a. – e., geschat worden. Zo blijkt dat de verandering van het medium van de ionen (c.) zich verzet tegen het adsorptieproces. Ook de herverdeling van lading (b.) werkt de adsorptie tegen; de invloed neemt echter af met afnemende ladingsdichtheid op het polystyreenoppervlak. Het adsorptieproces wordt begunstigd door de dehydratatie van de hydrofobe delen van het polystyreenoppervlak (e.), voornamelijk vanwege de eruit voortvloeiende entropietoename. De veranderingen van de protonenlading van het eiwit (a.) en van de van der Waals interakties tussen de geadsorbeerde eiwitlaag en het polystyreendeeltje (d.) dragen in onbelangrijke mate bij aan de totale Gibbs energie van de adsorptie. Voorts is beredeneerd dat de konformatieveranderingen in het eiwitmolekuul (f.) de Gibbs energie verlaagt. Omdat voor de enthalpieverandering van deze faktor een positieve waarde werd gevonden, moet het entropie-effekt ervan ook positief zijn. Deze entropietoename zou het gevolg kunnen zijn van o.a. veranderingen in het aantal en de soorten aminozuren die aan het water blootgesteld zijn en van toenemende mogelijkheden tot rotaties in het eiwitmolekuul.

In alle opzichten blijkt dat toename van entropie, afkomstig van de faktoren e. en f., de adsorptie van HPA en RNase aan negatief geladen polystyreenoppervlakken beheerst.

De experimentele gegevens laten zich op redelijke wijze verklaren met behulp van het aangenomen model voor de geadsorbeerde laag en de ladingsverdeling hierin; althans is de op dit model gebaseerde thermodynamische analyse verenigbaar met de experimentele feiten.

Deze thermodynamische interpretatie van de onderzochte adsorptieprocessen leidt tenslotte tot gevolgtrekkingen waarvan verwacht mag worden dat ze algemener geldig zijn met betrekking tot de wisselwerking tussen eiwitten en grensvlakken.

ACKNOWLEDGEMENTS

Most of the experiments described in this thesis were performed in the Laboratory for Physical and Colloid Chemistry of the Agricultural University, Wageningen, The Netherlands.

The author is very much indebted to Prof. Dr. J. Lyklema for his stimulating and constructive criticism during this study.

Dr. K. Furusawa has made significant contributions to this work, especially in connection with the preparation of polystyrene latices.

Many of the electrophoretic mobilities and the adsorption isotherms for RNase were carefully determined by Mrs. E. Eikelboom-Akkerman.

The enthusiastic participation of several students was much appreciated. Experimental results of, especially, Ir. H. Stegeman and Ir. F. C. A. Vekemans (adsorption isotherms for HPA) and Ir. J. A. Pelgröm (electrophoresis of dissolved HPA and RNase) were used in this study.

Dr. B. Vincent is kindly acknowledged for correcting the English text of this thesis.

Thanks are also due to Mrs. M. Heitkamp-Rijckaert, who typed the manuscript, Mr. H. E. van Beek, who prepared the drawings and Mr. S. Maasland, who did the photographical work.

Finally, the helpfulness and friendship of the members of the Department of Physical and Colloid Chemistry is gratefully mentioned.

REFERENCES

ABRAHAM, M. H. (1973) J. Chem. Soc. Faraday Trans. I **69**, 1375.
ABRAMSON, H. A., MOYER, L. S. and GORIN, M. H. (1942) in 'Electrophoresis of proteins', Reinhold Publ. Corp., New York, Ch. 5 and Ch. 6.
ADAMS, D. J., EVANS, M. T. A., MITCHELL, J. R., PHILLIPS, M. C. and REES, P. M. (1971) J. Polym. Sci. Part C **34**, 167.
ALEXANDER, A. E. and NAPPER, D. H. (1971) in 'Progress in Polymer Science' **3**, A. D. Jenkins, ed., Pergamon Press, Oxford, p. 145.
ANDERSON, E. A. and ALBERTY, R. A. (1948) J. Phys. Colloid Chem. **52**, 1345.
ANDERSON, J. M. (1975) Nature **253**, 536.
ANDERSSON, L. (1966) Biochim. Biophys. Acta **117**, 115.
ANDERSSON, L. (1969) Biochim. Biophys. Acta **133**, 277.
AOKI, K. and FOSTER, J. F. (1957a) J. Amer. Chem. Soc. **79**, 3385.
AOKI, K. and FOSTER, J. F. (1957b) J. Amer. Chem. Soc. **79**, 3393.
ARMSTRONG, D. E. and CHESTERS, G. (1964) Soil Science **98**, 39.
ARVIDSSON, E. O. (1972) Biopolymers **11**, 2197.
BATEMAN, J. B. and ADAMS, E. D. (1957) J. Phys. Chem. **61**, 1039.
BEINTEMA, J. J. and GRUBER, M. (1967) Biochim. Biophys. Acta **147**, 612.
BENSON, E. S., HALLAWAY, B. E. and LUMRY, R. W. (1964) J. Biol. Chem. **239**, 112.
BERNAL, J. D. and FOWLER, R. H. (1933) J. Chem. Phys. **1**, 515.
BERTHELOT, D. (1898) C. R. Acad. Sci. **126**, 1703, 1857.
BIGELOW, C. C. (1967) J. Theor. Biol. **16**, 187.
BIRDI, K. S. (1973) J. Colloid Interface Sci. **43**, 545.
BOCKRIS, J. O'M., DEVANATHAN, M. A. V. and MÜLLER, K. (1963) Proc. Roy. Soc. Ser. A **274**, 55.
BODAMER, G. W. and KUNIN, R. (1953) Ind. Chem. Eng. **45**, 2577.
BOER, J. H. DE (1936) Trans. Faraday Soc. **32**, 10.
BÖHM, J. T. C. (1974) Mededelingen Landbouwhogeschool, Wageningen, the Netherlands.
BÖTTCHER, C. J. F. (1973) 'Theory of Electric Polarization', Elsevier Publ. Co., Amsterdam, p. 91.
BOVEY, F. A. and KOLTHOFF, I. M. (1950) J. Polym. Sci. **44**, 241.
BOVEY, F. A., KOLTHOFF, I. M., MEDALLIA, A. I. and MEEHAN, E. J. (1955) 'Emulsion Polymerization', Interscience, New York.
BRAAM, W. G. M. (1972) Thesis, University of Nijmegen, the Netherlands.
BRANDTS, J. F. and HUNT, L. (1967) J. Amer. Chem. Soc. **89**, 4826.
BRANDTS, J. F. (1969) in 'Biological Macromolecules' Vol. II, G. Fasman and S. N. Timasheff, eds., Marcel Dekker, New York, p. 213.
BRASH, J. L. and LYMAN, D. J. (1971) in 'The Chemistry of Biosurfaces', M. L. Hair, ed., Marcel Dekker, New York, p. 177.
BRODERSEN, R., HAUGAARD, B. J., JACOBSEN, C. and PEDERSEN, A. O. (1973) Acta Chem. Scand. **27**, 573.
BRODNYAN, J. G. and KELLEY, E. C. (1965) J. Colloid Sci. **20**, 7.
BRYAN, W. P. and NIELSEN, S. O. (1969) Biochemistry **8**, 2572.
BULL, H. B. (1956) Biochem. Biophys. Acta **19**, 464.
BULL, H. B. (1972) J. Colloid Interface Sci. **41**, 305.
BUZZELL, J. G. and TANFORD, C. (1956) J. Phys. Chem. **60**, 1204.
CARR, C. W. (1952) Arch. Biochem. Biophys. **40**, 286.
CHAPMAN, D. L. (1913) Phil. Mag. **25**, 475.
CHATTORAJ, D. K. and BULL, H. B. (1959) J. Amer. Chem. Soc. **81**, 5128.
CLINT, G. L., CLINT, J. H., CORKILL, J. M. and WALKER, T. (1973) J. Colloid Interface Sci. **44**, 121.

COOKE, D. D. and KERKER, M. (1973) J. Colloid Interface Sci. **42**, 150.
COREY, R. B. and PAULING, L. (1956) Proc. Intern. Wool Textile Research Conference Australia 1955, 249.
CREETH, J. M. (1958) J. Phys. Chem. **62**, 66.
CRESCENZI, V., QUADRIFOGLIO, F. and DELBEN, F. (1972) J. Polym. Sci. Part A-2 **10**, 357; J. Polym. Sci. Part C **39**, 241.
CRESCENZI, V., DELBEN, F., QUADRIFOGLIO, F. and DOLAR, D. (1973) J. Phys. Chem. **77**, 539.
CUMPER, C. and ALEXANDER, A. E. (1950) Trans. Faraday Soc. **46**, 235.
DANIELLI, J. F. and DAVSON, H. (1935) J. Cellular Comp. Physiol. **5**, 495.
DAVIDSON, J. A. and HALLER, H. S. (1973) 47th Natl. Colloid Symposium, Ottawa, preprint.
DELBEN, F., CRESCENZI, V. and QUADRIFOGLIO, F. (1972) Eur. Polym. J. **8**, 933.
DERJAGUIN, B. V. and LANDAU, L. (1939) Acta Physico Chim. USSR **10**, 153.
DESNUELLE, P. (1972) VIth Intern. Congress Surface Active Substances, Zürich, Proceedings I, Carl Hanser Verlag, München, p. 21.
DEŽELIĆ, N. and DEŽELIĆ, G. (1971) Croat. Chem. Acta **42**, 457.
DEŽELIĆ, G., DEŽELIĆ, N. and TELIŠMAN, Z. (1971) Eur. J. Biochem. **23**, 575.
DICKERSON, R. E. and GEIS, I. (1969) 'The Structure and Action of Proteins', Harper, New York.
DILLMAN, W. J. and MILLER, I. F. (1973) J. Colloid Interface Sci. **44**, 221.
DRIFT, A. G. M. VAN DER (1972) private communication.
DROST-HANSEN, W. (1969) Ind. Engin. Chem. **61**, 10.
DUNN, A. S. (1971) Chem. Ind. **49**, 1406.
EISENBERG, D. and KAUZMANN, W. (1969) 'The Structure and Properties of Water', Oxford University Press, Oxford.
EVANS, M. T. A., MITCHELL, J., MUSSELWHITE, P. R. and IRONS, L. (1970) in 'Surface Chemistry of Biological Systems', M. Blank, ed., Plenum Press, New York, p. 1.
EVANS, R. and NAPPER, D. H. (1973) J. Colloid Interface Sci. **45**, 138.
EVERETT, D. H. (1957) Disc. Faraday Soc. **24**, 216.
FLEER, G. J., LYKLEMA, J. and KOOPAL, L. K. (1972) Kolloid-Z. Z. Polym. **250**, 689.
FLORY, P. J. (1953) 'Principles of Polymer Chemistry' Cornell University Press, Ithaca.
FOREL, C. G., MATIJEVIĆ, E. and KRATOHVIL, J. P. (1968) Kolloid-Z. Z. Polym. **223**, 31.
FOSTER, J. F. and STERMAN, M. D. (1956) J. Amer. Chem. Soc. **78**, 3656.
FOSTER, J. F. (1960) in 'The Plasma Proteins' Vol. I, F. W. Putnam, ed., Academic Press, New York, p. 179.
FOX, S. W. and DOSE, K. (1972) 'Molecular Evolution and the Origin of Life', W. H. Freeman, San Francisco, p. 196.
FOX, U. K., ROBB, I. D. and SMITH, R. (1974) J. Chem. Soc. Faraday Trans. I **70**, 1186.
FRANK, H. S. and WEN, W. Y. (1957) Disc. Faraday Soc. **24**, 133.
FRISCH, H. L. and STILLINGER, F. H. (1962) J. Phys. Chem. **66**, 823.
FRUCHTER, R. G. and CRESTFIELD, A. M. (1965) J. Biol. Chem. **240**, 3875.
FRYLING, C. F. (1963) J. Colloid Sci. **18**, 713.
FUOSS, R. M. (1958) J. Amer. Chem. Soc. **80**, 5059.
FURUSAWA, K., NORDE, W. and LYKLEMA, J. (1972) Kolloid-Z. Z. Polym. **250**, 908.
GABLE, R. W. and STROBEL, H. A. (1956) J. Phys. Chem. **60**, 513.
GHOSH, P., CHADKA, S. C., MUKKERJEE, A. R. and PALIT, S. R. (1964) J. Polym. Sci. A **2**, 4433.
GHOSH, S. and BULL, H. B. (1963) Biochim. Biophys. Acta **66**, 150.
GILS, G. E. VAN and KRUIJT, H. R. (1936) Kolloid-Beih. **45**, 60.
GOODWIN, J. W., HEARN, J., HO, C. C. and OTTEWILL, R. H. (1973) Br. Polym. J. **5**, 347.
GOUY, G. (1910) J. Phys. **9**, 457.
GRAHAM, D. E. and PHILLIPS, M. C. (1974) S.C.I. Int. Symp. Brunel University, A. L. Smith, ed., Academic Press, New York, in press.
GRAHAM, D. E. and PHILLIPS, M. C. (1975) S.C.I. Intern. Symp. Brunel University, R. J. Akers, ed., Academic Press, New York, in press.
GREEN, D. E. and YOUNG, J. H. (1971) Amer. Sci. **59**, 92.

GURNEY, R. W. (1953) 'Ionic Processes in Solution', Mc Graw-Hill Book Co., New York, p. 248.
HAGLER, A. T., SCHERAGA, H. A. and NÉMETHY, G. (1972) J. Phys. Chem. **76**, 3229.
HAGLER, A. T., SCHERAGA, H. A. and NÉMETHY, G. (1973) Ann. N. Y. Acad. Sci. **204**, 51.
HAMAKER, H. C. (1937) Physica **4**, 1058.
HANSEN, J. and HVIDT, A. (1973) J. Chem. Soc. Faraday Trans. II **69**, 881.
HARKINS, W. D. (1947) J. Amer. Chem. Soc. **69**, 1428.
HARKINS, W. D. (1952) in 'The Physical Chemistry of Surface Films', Reinhold Publ. Corp., New York, p. 332.
HARMSEN, B. J. M. (1971) Thesis, University of Nijmegen, the Netherlands.
HARTER, R. D. and STOTZKY, G. (1971) Soil Sci. Soc. Amer. Proc. **35**, 383.
HASTED, J. B. (1973) 'Aqueous Dielectrics' Chapman and Hall, London, p. 47.
HENRY, D. C. (1931) Proc. Roy. Soc. London A **133**, 106.
HERD, J. M., HOPKINS, A. J. and HOWARD, G. J. (1971) J. Polym. Sci. Part C **34**, 211.
HERMANS JR., J. and SCHERAGA, H. A. (1961) J. Amer. Chem. Soc. **83**, 3283.
HERTZ, H. G. (1970) Angew. Chemie Internat. Edition **9**, 124.
HESSELINK, F. T. (1972) J. Electroanal. Chem. **37**, 317.
HIRS, C., MOORE, S. and STEIN, W. (1953) J. Biol. Chem. **200**, 493.
HOEVE, C. A. J. (1965) J. Chem. Phys. **43**, 3007.
HOEVE, C. A. J. (1966) J. Chem. Phys. **44**, 1505.
HOEVE, C. A. J. (1970) J. Polym. Sci. C **30**, 361.
HOEVE, C. A. J. (1971) J. Polym. Sci. C **34**, 1.
HOFF, B. M. E. VAN DER (1960) J. Polym. Sci. **44**, 241.
HOFF, B. M. E. VAN DER (1962) Advan. Chem. Ser. **34**, A. C. S., Washington, D.C.
HOFF, B. M. E. VAN DER (1967) in 'Solvent Properties of Surfactant Solutions', Vol. II, K. Shinoda, ed., Marcel Dekker, New York, p. 285.
HÜCKEL, E. (1924) Phys. Z. **25**, 204.
HUL, H. J. VAN DEN and VANDERHOFF, J. W. (1968) J. Colloid Interface Sci. **28**, 336.
HUL, H. J. VAN DEN and VANDERHOFF, J. W. (1970) Br. Polym. J. **2**, 121.
HUMMEL, J. P. and ANDERSON, B. S. (1965) Arch. Biochem. Biophys. **112**, 443.
HUNTER, R. J. and ALEXANDER, A. E. (1962) J. Colloid Sci. **17**, 781.
ITZHAKI, R. F. and GILL, D. M. (1964) Anal. Biochem. **9**, 401.
JACKSON, R. L. and HIRS, C. H. W. (1970) J. Biol. Chem. **245**, 637.
JAFFÉ, J. and RUYSSCHAERT, J. M. (1964) IVth Intern. Congres Surface Active Substances, Brussels, Proceedings II, J. T. G. Overbeek, ed., Gordon and Breach Science Publishers, London, p. 911.
JAMES, L. K. and AUGENSTEIN, L. G. (1966), Advan. Enzymology **28**, 1.
KARTHA, G., BELLO, J. and HARKER, D. (1967) Nature **213**, 862.
KAUZMANN, W. (1959) Advan. Protein Chem. **14**, 1.
KAVANAU, J. L. (1964) 'Water and Solute-Water Interactions', Holden-Day, San Francisco, p. 54.
KELLER, K. H., CANALES, E. R. and YUM, S. I. (1971) J. Phys. Chem. **75**, 379.
KENDREW, J. C. (1962) Brookhaven Symposium **15**, 216.
KHAÏAT, A. and MILLER, I. R. (1969) Biochim. Biophys. Acta **183**, 309.
KILLMANN, E. and ECKART, R. (1971) Makromolek. Chemie **144**, 45.
KLOMPÉ, M. A. M. (1941) Thesis, State University Utrecht, the Netherlands.
KLOTZ, I. M. (1953) in 'The Proteins' Vol. I, H. Neurath and K. Bailey, eds., Academic Press, New York, p. 727.
KOBAYASHI, Y. and AOMINE, S. (1967) Soil Science and Plant Nutrition **13**, 189.
KOLB, E. (1964) in'Biochemisches Taschenbuch', Teil II, H. M. Rauen, ed., Springer Verlag, Berlin, p. 330.
KOLTHOFF, I. M. and MILLER, I. K. (1951) J. Amer. Chem. Soc. **73**, 3055.
KOLTHOFF, I. M., ANASTASI, A. A., STRICKS, W., TAN, B. and DESHMUKH, G. (1957) J. Amer. Chem. Soc. **79**, 5102.

KOTERA, A., FURUSAWA, K. and TAKEDA, Y. (1970a) Kolloid-Z. Z. Polym. **239**, 677.
KOTERA, A., FURUSAWA, K. and KUDO, K. (1970b) Kolloid-Z. Z. Polym. **240**, 837.
KRESHECK, G. C. and KLOTZ, I. M. (1969) Biochemistry **8**, 8.
LAAKSONEN, J., LEBELL, J. C. and STENIUS, P. (1975) J. Electroanal. Chem. **64**, 207.
LABHART, H. and STAUB, H. (1947) Helv. Chem. Acta **30**, 1954.
LECLOUX, A., HEYNS, H. and GOBILLON, Y. (1970) Ind. Chim. Belge **35**, 1.
LEE, B. and RICHARD, F. M. (1971) J. Molec. Biol. **55**, 379.
LIJKLEMA,J. (1957) Thesis, State University Utrecht, the Netherlands.
LOEB, A. L., WIERSEMA, P. H. and OVERBEEK, J. T. G. (1961) 'The Electrical Double Layer Around a Spherical Colloidal Particle', The M.I.T. Press, Cambridge, Massachusetts.
LONGSWORTH, L. G. and MACINNES, D. A. (1940) J. Amer. Chem. Soc. **62**, 705.
LOVRIEN, R. and STURTEVANT, J. M. (1971) Biochemistry **10**, 3811.
LOWRY, O. H., ROSEBROUGH, N. J., FARR, A. C. and RANDALL, R. J. (1951) J. Biol. Chem. **193**, 265.
LUMRY, R. and BILTONEN, R. (1969) in 'Biological Macromolecules' Vol. II, G. Fasman and S. N. Timasheff, eds., Marcel Dekker, New York, p. 65.
LYKLEMA, J. and OVERBEEK, J. T. G. (1961) J. Colloid Sci. **16**, 501.
LYKLEMA, J. and NORDE, W. (1973) Croat. Chem. Acta **45**, 67.
LYMAN, D. J., BRASH, J. L., CHAIKIN, S. W., KLEIN, K. G. and CARINI, M. (1968) Trans. Amer. Soc. Artif. Internal. Organs. **14**, 250.
MACRITCHIE, F. (1972) J. Colloid Interface Sci. **38**, 1972.
MATHOT, C. and ROTHEN, A. (1969) J. Colloid Interface Sci. **31**, 51.
MAYO, F. R., GREGG, R. A. and MATHESON, M. S. (1951) J. Amer. Chem. Soc. **73**, 1691.
MAYO, F. R. (1960) IUPAC Symposium Moscow, Proceedings Vol. II, 11.
MAYO, F. R. (1968) J. Amer. Chem. Soc. **90**, 1289.
MCLAREN, A. D. (1954) J. Phys. Chem. **58**, 129.
MESSING, R. A. (1969) J. Amer. Chem. Soc. **91**, 2370.
MICHAELIS, L. (1931) Biochem. Z. **234**, 139.
MILLER, I. R. and KATCHALSKY, A. (1957) IIth Intern. Congress of Surface Activity, London, Proceedings I, J. H. Schulman, ed., Butterworths Scientific Publications, London, p. 159.
MILLER, I. R. and BACH, D. (1973) in 'Surface and Colloid Science', Vol. 6, E. Matijević, ed., Wiley-Interscience, New York, p. 185.
MILLERO, F. J. (1971) in 'Water and Aqueous Solutions', R. A. Home, ed., Wiley-Interscience, New York, p. 519.
MORRISSEY, B. W. and STROMBERG, R. R. (1974) J. Colloid Interface Sci. **46**, 152.
MOSBACH, K. (1971) Sci. Amer. **224**, 26.
MUSSELWHITE, P. R. and KITCHENER, J. A. (1967) J. Colloid Interface Sci. **24**, 80.
NANCOLLAS, G. H. (1966) 'Interactions in Electrolyte Solutions', Elsevier Publ. Co., Amsterdam, p. 121.
NÉMETHY, G. and SCHERAGA, H. A. (1962a) J. Chem. Phys. **36**, 3382.
NÉMETHY, G. and SCHERAGA, H. A. (1962b) J. Chem. Phys. **36**, 3401.
NÉMETHY, G. and SCHERAGA, H. A. (1962c) J. Phys. Chem. **66**, 1773.
NISHIKAWA, A. H. (1975) Chem. Technol. **5**, 564.
NORDE, W. and LYKLEMA, J. (1972) XXth Colloquium 'Protides of the Biological Fluids', Brugge, Proceedings, H. Peeters, ed., Pergamon Press, Oxford, p. 467.
NORDE, W., FURUSAWA, K. and LYKLEMA, J. (1972) VIth Intern. Congress Surface Active Substances, Zürich, Proceedings II-1, Carl Hanser Verlag, München, p. 209.
NORDE, W. and LYKLEMA, J. (1975) Intern. Conference on Colloid and Surface Science, Budapest, Proceedings I, E. Wolfram, ed., Akadémiai Kiadó, Budapest.
OPARIN, A. I. (1964) 'The Chemical Origin of Life', I. N. Kugelmass, ed., Charles C Thomas, Springfield, Ill, p. 42.
ORAZIO, L. A. D' and WOOD, R. H. (1963) J. Phys. Chem. **67**, 1345.
ORESKES, J. and SINGER, J. M. (1961) J. Immunology **86**, 338.

Os, G. A. J. van, Bruin, S. H. de and Janssen, L. H. M. (1972) J. Electroanal. Chem. Interfacial Electrochem. **37**, 303.
Ottewill, R. H. and Shaw, J. N. (1967a) Kolloid-Z. Z. Polym. **215**, 161.
Ottewill, R. H. and Shaw, J. N. (1967b) Kolloid-Z. Z. Polym. **218**, 34.
Ottewill, R. H. and Shaw, J. N. (1972) J. Electroanal. Chem. Interfacial Electrochemistry **37**, 133.
Overbeek, J. T. G. and Wiersema, P. H. (1967) in 'Electrophoresis', Vol. II, M. Bier, ed., Academic Press, New York, p. 1.
Overberger, C. G. and Finestone, A. B. (1956) J. Amer. Chem. Soc. **78**, 1638.
Palit, S. R. and Mandal, B. N. (1968) J. Macromol. Sci. Revs. Macromol. Chem. C **2**, 225.
Pavlovic, O. and Miller, I. R. (1971a) J. Polym. Sci. C **34**, 181.
Pavlovic, O. and Miller, I. R. (1971b) Biochemical Aspects of Electrochemistry, Experientia Suppl. **18**, 513.
Pessac, B. and Defendi, V. (1972) Science **175**, 898.
Peyser, P., Tutas, D. J. and Stromberg, R. R. (1967), J. Polym. Sci. A-1 **5**, 651.
Pflumm, M. N. and Beychok, S. (1969) J. Biol. Chem. **244**, 3973.
Phelps, R. A. and Putnam, F. W. (1960) in 'The Plasma Proteins' Vol. I, F. W. Putman, ed., Academic Press, New York, p. 143.
Phillips, M. C., Evans, M. T. A. and Hauser, H. (1972) VIth Intern. Congress Surface Active Substances, Zürich, Proceedings II-1, Carl Hanser Verlag, München, p. 381.
Pople, J. A. (1951) Proc. Roy. Soc. A **205**, 163.
Reerink, H. and Overbeek, J. T. G. (1954) Gen. Disc. Faraday Soc. **18**, 74.
Richards, F. M. and Wyckoff, H. W. (1971) in 'The Enzymes' Vol. IV, P. Boyer, ed., Academic Press, New York, p. 647.
Riddiford, C. L. and Jennings, B. R. (1966) Biochim. Biophys. Acta **126**, 71.
Roe, C. P. and Brass, P. D. (1957) J. Polym. Sci. **24**, 401.
Roe, C. P. (1968) Ind. Eng. Chem. **60**, 20.
Roozen, J. P. (1967) M. Sci. Thesis, Agricultural University, Wageningen, the Netherlands.
Rosseneu-Motreff, M., Blaton, V., Declerq, B., Vandamme, D. and Peeters, H. (1970) J. Biol. Chem. **68**, 369.
Sage, H. J. and Singer, S. J. (1962) Biochemistry **1**, 305.
Sakaki, T. and Kakihana, H. (1953) Kagaku **23**, 471; Chem. Abstr. **47**, 10951.
Salzman, E. W. (1971) Blood **38**, 509.
Scatchard, G. and Yap, W. T. (1964) J. Amer. Chem. Soc. **86**, 3434.
Schnebli, H. P. and Burger, M. M. (1972) Proc. Natl. Acad. Sci. USA **69**, 3825.
Shapira, R. (1959) Biochem. Biophys. Res. Commun. **1**, 236.
Silberberg, A. (1962a) J. Phys. Chem. **66**, 1872.
Silberberg, A. (1962b) J. Phys. Chem. **66**, 1884.
Silberberg, A. (1967) J. Chem. Phys. **46**, 1105.
Silberberg, A. (1968) J. Chem. Phys. **48**, 2835.
Singer, J. M. (1961) Amer. J. Medicine **31**, 766.
Singer, J. M. (1974) Bull. Rheumatic Diseases **24**, 762.
Singer, S. J. (1971) in 'Structure and Function of Biological Membranes', L. I. Rothfield, ed., Academic Press, New York, p. 145.
Singer, S. J. and Nicholson, G. L. (1974) Ann. Rev. Biochem. **43**, 805.
Smith, W. V. and Ewart, R. H. (1948) J. Chem. Phys. **16**, 592.
Smitham, J. B., Gibson, D. V. and Napper, D. H. (1973) J. Colloid Interface Sci. **45**, 211.
Smoluchowski, M. von (1903) Bull. Acad. Sci. Cracovie, 182.
Smyth, D. G., Stein, W. H. and Moore, S. (1963) J. Biol. Chem. **238**, 227.
Sogami, M. and Foster, J. F. (1968) Biochemistry **7**, 2172.
Spahr, P. F. and Edsall, J. T. (1964) J. Biol. Chem. **239**, 850.
Squire, P. G., Moser, P. and O'Konski, C. T. (1968) Biochem. J. **7**, 4261.
Srivastava, S. N. (1966) Z. Physik. Chemie **233**, 237.
Steinhardt, J., Krijn, J. and Leidy, J. G. (1971) Biochemistry **10**, 4005.

STONE-MASUI, J. and WATILLON, A. (1975) J. Colloid Interface Sci. **52**, 479.
STONER, G. and SRINIVASAN, S. (1970) J. Phys. Chem. **74**, 1088.
SYBESMA, C. and VREDENBERG, W. J. (1963) Biochim. Biophys. Acta **75**, 439.
SYBESMA, C. and VREDENBERG, W. J. (1964) Biochim. Biophys. Acta **88**, 205.
TANFORD, C., BUZZELL, J. G., RANDS, D. G. and SWANSON, S. A. (1955a) J. Amer. Chem. Soc. **77**, 6421.
TANFORD, C., SWANSON, S. A. and SHORE, W. S. (1955b) J. Amer. Chem. Soc. **77**, 6414.
TANFORD, C. and BUZZELL, J. G. (1956) J. Phys. Chem. **60**, 225.
TANFORD, C. and HAUENSTEIN, J. D. (1956) J. Amer. Chem. Soc. **78**, 5287.
TANFORD, C. (1967) 'Physical Chemistry of Macromolecules' John Wiley & Sons, New York, p. 508.
TANFORD, C. (1973) 'The Hydropbic Effect', Wiley-Interscience, New York.
THIES, C. (1966) J. Phys. Chem. **70**, 3783.
URNES, P. and DOTY, P. (1961) Advan. Protein Chem. **16**, 401.
VANDERHOFF, J. W., VITKUSKE, J. F., BRADFORD, E. B. and ALFREY, T. (1956) J. Polym. Sci. **20**, 225.
VERWEY, E. J. and OVERBEEK, J. T. G. (1948) 'The Theory of the Stability of Lyophobic Colloids', Elsevier Publ. Co., Amsterdam.
VIJAI, K. K. and FOSTER, J. F. (1967) Biochemistry **6**, 1152.
VINCENT, B., BIJSTERBOSCH, B. H. and LYKLEMA, J. (1971) J. Colloid Interface Sci. **37**, 171.
VISSER, J. (1972) Advan. Colloid Interface Sci. **3**, 331.
VROMAN, L. (1967) in 'Blood Clotting Enzymology', W. H. Seegers, ed., Academic Press, New York, p. 279.
WADSÖ, I. (1968) Acta Chem. Scand. **22**, 927.
WIERSEMA, P. H. (1964) Thesis, State University Utrecht, the Netherlands.
WIERSEMA, P. H., LOEB, A. L. and OVERBEEK, J. T. G. (1966) J. Colloid Interface Sci. **22**, 78.
WILKINS, D. J. (1967) J. Colloid Interface Sci. **25**, 84.
WILKINS, D. J. and MYERS, P. A. (1970) in 'Surface Chemistry of Biological Systems', M. Blank, ed., Plenum Press, New York, p. 217.
WOLMAN, M. (1970) in 'Recent Progress in Surface Science' Vol. 3, J. F. Danielli, A. C. Riddiford and M. D. Rosenberg, eds., Academic Press, New York, p. 261.
WRIGHT, M. H. and JAMES, A. M. (1973) Kolloid-Z. Z. Polym. **251**, 745.
WYCKOFF, H. W., HARDMAN, K. D., ALLEWELL, N. M., INAGAMI, T., JOHNSON, L. N. and RICHARDS, F. M. (1967) J. Biol. Chem. **242**, 3984.
WYCKOFF, H. W., TSERNOGLOV, D., HANSON, A. W., KNOK, J. R., LEE, B. and RICHARDS, F. M. (1970) J. Biol. Chem. **245**, 305.
YAMASHITA, T. and BULL, H. B. (1967) J. Colloid Interface Sci. **24**, 310.

LIST OF SYMBOLS

a	distance of closest approach between ions
A	Hamaker 'constant'
	A_{11} Hamaker constant of two bodies of material 1 in vacuum
	$A_{11(2)}$ Hamaker constant of two bodies of material 1 embedded in a medium 2
A_s	average interfacial area per attached segment of the adsorbed protein
B	second virial coefficient
c	concentration (moles per dm^3, unless otherwise stated)
c_c	coagulation concentration
c_p	concentration of protein in solution after adsorption
C	differential capacitance
	third virial coefficient (eqn. 2.5.)
C_P	heat capacity at constant pressure
	${}^{\phi}C_P$ apparent heat capacity
	C_P^{config} configurational part of the heat capacity
d	diameter (eqns. 2.1., 2.2. and 2.3.)
	d_n number-average diameter
	d_w weight-average diameter
	thickness of the shear layer around the bare polystyrene particles (eqn. 6.9.) or around the dissolved protein molecules (eqn. 6.10.)
	thickness of the adsorbed protein layer (eqns. 5.14., 5.15., 5.19., 5.20. and 6.13.)
$\vec{D}$	dielectric displacement
e	elementary charge
E	extinction coefficient
F	Faraday constant
g	gravity constant
G	Gibbs free energy
h	osmotic rise
H	enthalpy
k	Boltzmann constant
K_j	dissociation constant of the n_j groups of class j
	K_{aj} apparent dissociation constant
	K_{ij} intrinsic dissociation constant
K_{ass}	association constant
	K^0_{ass} association constant in the absence of electric interactions
K^K_H	equilibrium constant for the exchange of H^+ against K^+
m	thickness of region 1 in the model for the adsorbed protein layer (chapter 5)
M	molecular weight
	M_n number-average molecular weight
	M_s average molecular weight of the segments (= amino acid residues) of proteins
n_i	number of polystyrene particles having a diameter d_i
N_{Av}	Avogadro's number
O	surface
$\vec{O}$	surface vector
p	thickness of regions (1 + 2) in the model for the adsorbed protein layer (chapter 5)
pK_j	$-^{10}\log K_j$
P	pressure
R	gas constant
s	specific surface area
S	entropy

T absolute temperature
u electrophoretic mobility
U energy
uniformity coefficient (eqn. 2.1.)
v_1 specific volume of the solvent
V volume
x distance from the polystyrene particle wall
X strength of the electric field
z valency of an ion (sign included)
z_+ positive ion
z_- negative ion
Z number of charged groups per protein molecule
Z_H net proton charge
Z_{ek} electrokinetic charge

α_j degree of dissociation of n_j groups of class j
Γ_p amount of protein adsorbed per unit area of adsorbent
ε relative dielectric constant
ε_1, ε_2, ε_3 relative dielectric constant in regions 1, 2 and 3 respectively, in the model for the adsorbed protein layer
ε_0 permittivity of free space
ζ electrokinetic potential
θ_s fraction of the adsorbent surface occupied by the protein
$\varkappa$ reciprocal Debye length
υ_p fraction of the number of segments of the protein attached to the adsorbent
ξ ordering parameter (eqn. 6.3.)
Π osmotic pressure
ρ density (eqn. 2.3.)
space charge density (eqn. 5.12.)
σ surface charge density
σ_0 charge at the polystyrene surface
σ_m charge in the molecular condenser (Stern layer)
σ_d charge in the diffuse layer
σ_1, σ_3 charge in regions 1 and 3, respectively, in the model for the adsorbed protein layer
ϕ_p fraction of the volume of the adsorbed layer occupied by the protein
ψ electrostatic potential with respect to the bulk of the solution
ψ_0, ψ_d, ψ_m, ψ_p potentials at $x = 0$, $x = d$, $x = m$ and $x = p$, respectively

ENKELE PERSOONLIJKE GEGEVENS

De auteur werd op 16 november 1944 te Vorden geboren. Het voorbereidend wetenschappelijk onderwijs volgde hij aan het Baudartius Lyceum (afdeling HBS-B) te Zutphen. In 1962 begon hij de studie aan de Landbouwhogeschool te Wageningen. In april 1967 werd het kandidaatsexamen in de Levensmiddelentechnologie (chemisch-biologische specialisatie) afgelegd. In zijn ingenieursstudie, welke in september 1969 werd afgesloten, zijn naast het hoofdvak Levensmiddelenchemie de bijvakken Voedingsleer, Biochemie en Fysische en Kolloidchemie opgenomen. Sinds oktober 1969 is hij als wetenschappelijk medewerker verbonden aan de afdeling Fysische en Kolloidchemie van de Landbouwhogeschool te Wageningen.